# The role of Hsp90 in Rad51 mediated DNA repair A Thesis submitted to the University of Hyderabad for the award of doctor of philosophy

By
Tanvi Suhane
(11LTPH11)

Under the Supervision of Dr. Sunanda Bhattacharyya



Department of Biotechnology and Bioinformatics
School of Life Sciences
University of Hyderabad
Gachibowli

Hyderabad: 500046

Telangana, India

December 2017



## University of Hyderabad School of Life Sciences Department of Biotechnology and Bioinformatics

\_\_\_\_\_\_

### **DECLARATION**

I, Tanvi Suhane, hereby declare that this thesis entitled, "The role of Hsp90 in Rad51 mediated DNA repair" submitted by me under the guidance and supervision of Dr. Sunanda Bhattacharyya, is an original and independent research work. I also declare that it has not been submitted previously in part or in full to this University or any other University or Institution for the award of any degree or diploma.

Dr. Sunanda Bhattacharyya (Research Supervisor)

Tanvi Suhane (Research Scholar) Reg. No. 11LTPH11



### **University of Hyderabad School of Life Sciences**

### **Department of Biotechnology and Bioinformatics**

### CERTIFICATE

This is to certify that this thesis entitled, "The role of Hsp90 in Rad51 mediated DNA repair" is a record of bona fide work done by Tanvi Suhane, a research scholar for Ph.D. program in Department of Biotechnology and Bioinformatics, School of Life Sciences, University of Hyderabad under my guidance and supervision. The thesis is free from plagiarism and has not been submitted previously in part or in full to this or any other University or Institution for the award of any degree or diploma.

- **A.** Part of this work has been published in the following journals:
- 1. Suhane T, Laskar S, Advani S, Roy N, Varunan S, Bhattacharyya D, Bhattacharyya S, Bhattacharyya MK. (2015). Both the charged linker region and ATPase domain of Hsp90 are essential for Rad51- dependent DNA repair. *Eukaryotic Cell*, 14 (1):64-77
- **B.** Part of this work has been presented in the following conferences:
- 1. Keystone symposia entitled Genomic Instability and DNA Repair (Z1) held in Santa Fe, New Mexico, USA, April 2-6, 2016.
- 2. 9<sup>th</sup> International conference on Yeast Biology, Kolkata, December 9-12, 2015.

3. Gene network in chromatin/chromosome function, 5th meeting of the Asian forum of chromosome and chromatin biology-2015, organized by Jawaharlal Nehru Center for Advanced Scientific Research, Bangalore, January 15-18, 2015.

**C.** Publication from other projects:

1. Varunan, S. M., Tripathi, J., Bhattacharyya, S., Suhane, T., & Bhattacharyya, M. K. (2013).

Plasmodium falciparum origin recognition complex subunit 1 (PfOrc1) functionally

complements  $\Delta sir3$  mutant of Saccharomyces cerevisiae. *Molecular and biochemical* 

parasitology, 191(1), 28-35.

Head Department of Biotechnology Research Supervisor Dr. Sunanda Bhattacharyya Dean School of Life Sciences

and Bioinformatics

# DEDICATED TO MY BELOVED PARENTS AND BROTHERS

### Acknowledgements

......

I am grateful to my supervisor Dr. Sunanda Bhattacharyya for her constant support and encouragement during my PhD. I am highly obliged to her timely help with her valuable suggestions, which enhanced the speed of my work. Her constant guidance helped me to have patience and enthusiasm throughout my research work. I sincerely thank her for inculcating the true essence of science in me.

I thank my doctoral committee members **Prof. Kolluru VA Ramaiah** and **Prof. K. P. M. S. V. Padmasree** for all their suggestions in my work.

I am very grateful to **Prof. Mrinal Kanti Bhattacharyya** for his valuable suggestions and critical advice in my work.

I thank the Head of the Department of Biotechnology and Bioinformatics, **Prof. Anand Kumar Kondapi** and the previous heads **Prof. Niyaz Ahmed** and **Prof. Prakash Babu** for allowing me to use all the research facilities in the department.

I thank the Dean of life sciences, **Prof. P Reddanna** and the previous Deans **Prof. R. P. Sharma**, **Prof. M. Ramanadham**, and **Prof. A. S. Raghavendra** for providing all the research facilities. I sincerely thank **Dr. Dibyendu Bhattacharyya** for his guidance and support during my work and stay in Tata Memorial Centre Advanced Centre for Treatment, Research and Education in Cancer. I thank to **Dr. Achuthsankar S. Nair**, University of Kerala for his help in during my studies I thank **UGC** for the financial support throughout my research.

I thank **DBT**, **CSIR** and **UPE** funding agencies for the financial assistance.

I thank **DST-FIST**, **DBT-CREBB**, **UGC-SAP**, **DST-PURSE** funding to school and departmental facilities that aided in my research work.

I thank my current and former lab mates **Dr. Shyamasree**, **Dr. Suresh**, **Dr. Nidhi**, **Shephali**, **Nupur**, **Priyanka**, **Dr. Swati**, **Dr. Nabamita**, **Dr. Sugith**, **Dr. Shalu**, **Dr. Swati Charaborty**, **Dr.** 

Abdul Nabi, Pratap, Niranjan, Wahida, Payal and Aashesh for their help, support,

encouragement and cooperation during my research work.

I thank all the previous and present M.Sc. project students from lab of Dr. Sunanda Bhattacharyya and Prof. Mrinal Kanti Bhattacharyya for their help and cooperation.

I thank our lab assistant Mr. Ramesh for his help in lab.

I thank all the teaching and nonteaching staff members of School of Life Sciences for all their help and support.

I thank my friends Kalyani, Prateek, Nidhi, Pankaz and Angamba for making this journey memorable.

I am grateful to my parents **Mr. Umesh Chandra Suhane** and **Mrs. Urmila Suhane** for their unconditional love and support.

I extend my gratitude to my brothers **Tanmay** and **Utkarsh** for standing by my side whenever I needed help.

I am thankful to Bhavesh for his encouragement, which helped to finish my work successfully.

Finally I thank the **God almighty** with all my heart, whose blessings gave me the strength to complete this journey.

Tanvi Suhane

### **CONTENTS**

LIST OF TABLES.	V
LIST OF FIGURES	vi
ABBREVIATIONS	viii
INTRODUCTION	
1.1 Molecular chaperones: Guardian of cell proteome	1
1.2 Heat shock protein 90 (Hsp90): The chaperone which protects the cell upon s	stress1
1.2.1 Distinctive features of Hsp90	2
1.2.2 Structural domains of Hsp90.	5
1.2.3 Charged linker region: A structural component of Hsp90	7
1.2.4 Associates of Hsp90: Co chaperones	8
1.2.5 Recipients of Hsp90's services: The client	9
1.2.6 Other side of the coin: Hsp90 and progression of cancer	11
1.2.7 Mode of action by Hsp90: Chaperone cycle	13
1.2.8 Unconventional functions of Hsp90	16
1.2.8.1 Facilitating the travel of client proteins to cellular compartments	16
1.2.8.2 Assistance for the assembly of multi protein complexes	17
1.3 DNA damage: A threat for genomic stability of organism	18

1.4 Repair of damaged DNA	19
1.4.1 Homologous recombination pathway	20
1.4.2 Participants of homologous recombination	22
1.4.3 Rad52	22
1.4.4 Rad51	24
1.4.4.1 Structure of Rad51	25
1.4.4.2 Rad51 path upon DNA damage: From initiation to the destination	29
1.4.5 Importance of homologous recombination	33
1.5 Expanding wings of Hsp90: Maintaining genomic integrity	36
1.5.1 DNA repair proteins dependent on Hsp90 functions	38
1.6 Significance of the study	42
1.7 Objective of the study	44
1.8 Specific Aims of the study	45
MATERIAL AND METHODS	
2.1 MOLECULAR BIOLOGY TECHNIQUES	
2.1.1 Bacterial plasmid DNA isolation by alkaline lysis method	46
2.1.2 Bacterial competent cell preparation	47
2.1.3 Bacterial transformation.	47
2.1.4 Semi Quantitative RTPCR	47

2.1.5 Real time RTPCR	48
2.1.6 Site Directed Mutagenesis.	48
2.2 METHODS IN YEAST GENETICS	49
2.2.1 RNA isolation from yeast	49
2.2.2 Yeast competent cell preparation	49
2.2.3 Yeast transformation	51
2.2.4 Yeast genomic DNA isolation.	51
2.2.5 Protein isolation	52
2.2.6 Gene knockout.	52
2.2.7 Gene tagging.	53
2.2.8 Cellular fractionation.	53
2.3 GENETIC ASSAYS	54
2.3.1 MMS and UV sensitivity assay	54
2.3.2 Gene conversion assay	55
2.3.3 Gene targeting Assay	56
2.4 BIOCHEMICAL METHODS	58
2.4.1 Chromatin immunoprecipitation assay	58
2.4.2 Western Blot Analysis	59
2.4.3 Treatment with inhibitors	60
2.4.4 Recombinant protein purification	60
2.4.5 Surface plasmon resonance	61
SPECIFIC AIM 1- Understanding the role of Hsp90 in DNA repair	
3.1 Introduction	71

3.2.1 Individual knock out of <i>HSP82</i> or <i>HSC82</i> does not affect the cell survivability upon DNA
damage73
3.2.2 Loss of Hsp82 function results in the poor survival of the cells upon DNA damage76
3.2.3 Functional knock out of Hsp82 hampers the efficiency of homologous recombination80
3.2.4 Different mutations in Hsp82 have differential defect in the cell survivability upon DNA
damage83
3.2.5 Defect in the cell survivability of Hsp82 mutants is correlated with the deficiency in the
homologous recombination87
SPECIFIC AIM 2- Identification of homologous recombination proteins which are dependent on Hsp90 functions
4.1 Introduction
4.1 Introduction90
4.1 Introduction
4.2 Results92
4.2 Results

4.2.6 Δ211-259hsp82 mutant is defective in the efficient Rad51 foci formation upon DNA
damage
SPECIFIC AIM 3- DNA damage induced nuclear import of Rad51 is mediated by Hsp90
and Rad51 interactions
5.1 Introduction
5.2 Results
5.2.1 Molecular docking studies to predict the interaction between Hsp82 and Rad51111
5.2.2 Generation of <i>E108Lrad51</i> and <i>M142Lrad51</i>
5.2.3 Mutation at E108 <sup>th</sup> position of Rad51 sensitizes the cells to MMS and renders them
deficient in gene conversion
5.2.4 HO induced Rad51 recruitment to the broken DNA junction is severely compromised
in <i>E108Lrad51</i>
5.2.5 DNA damage fails to import Rad51 to the nucleus in <i>E108Lrad51</i> mutant
5.2.6 Rad51 <sup>E108L</sup> shows stronger association with Hsp82
DISCUSSION126
REFERENCES
APPENDIX I
APPENDIX II: SYNOPSIS
LIST OF TABLES:
<b>Table 1:</b> Known residues of Rad51 for facilitating its interaction with partner proteins
<b>Table2:</b> List of yeast strains used in the study

<b>Table3:</b> List of primers used in the study	66
Table 4: List of Plasmids used in the study	68
<b>Table 5:</b> Equilibrium dissociation constant $(K_D)$ for the interaction of Hsp82 with W	TRad51 and
rad51 mutants	125
LIST OF FIGURES:	
Figure 1: Unique nature of Hsp90	3
Figure 2: Structure of yeast Hsp90.	6
Figure 3: List of identified Hsp90 clients	12
Figure 4: ATP mediated open and closed confirmation of Hsp90.	14
Figure 5: Chaperone cycle of Hsp90.	15
Figure 6: Participants of homologous recombination	23
Figure 7: Structure of Rad51 protein	27
Figure 8: Diagrammatic representation of translocation of Rad51 in response to DNA	damage32
Figure 9: Regulatory factors of homologous recombination	35
Figure 10: Strategy for creating point mutants of <i>RAD51</i>	50
Figure 11: Gene conversion assay cassette.	57
Figure 12: Individual knock out of HSP82 and HSC82 does not hamper DNA damage	ge sensitivity
of cells	75
Figure 13: Functional knockout of Hsp82 affects DNA repair activity	78

Figure 14: Hsp82 function is essential for homologous recombination pathway	82
Figure 15: Differential effect of different Hsp82 mutants on DNA repair activity	85
Figure 16: Gene targeting efficiencies of Hsp82 point and deletion mutants	88
Figure 17: Stability of Rad51 and Rad52 are dependent on Hsp82	94
Figure 18: Stability of Rad51 and Rad52 is dependent on the ATPase activity of Hsp82	96
Figure 19: Rad51 is a client of Hsp82	98
Figure 20: Deletion of charged linker from Hsp82 does not affect Rad51 and Rad52 pr	
level	101
Figure 21: Hsp82 mutant $\Delta 211$ -259hsp82 does not alter the up-regulation of RAD51 and I	RAD52
upon DNA damage	102
Figure 22: Over expression of Rad51 partially rescue the phenotype of $\Delta 211-259 \ hsp82$	104
Figure 23: The extent of MMS-induced Rad51 focus formation is less in $\Delta 211-259hsp82$ cel	ls than
in the wild-type control.	106
Figure 24: Molecular docking studies to predict the interaction between Hsp82 and Rad51	112
Figure 25: Generation of <i>RAD51</i> mutant strains.	114
Figure 26: Mutation at E108 <sup>th</sup> position of Rad51 sensitizes the cells to MMS and render	s them
deficient in gene conversion.	117
Figure 27: HO induced Rad51 recruitment to the broken DNA junction is severely compre	omised
in F108Lrad51	119

### **ABBREVIATIONS-**

μg: Microgram

μl: Micro liter

μM: Micro molar

17-AAG: 17-N-Allylamino-17-demethoxygeldanamycin

17-DMAG: 17-Dimethylaminoethylamino-17 demethoxygeldanamycin

AA: Amyloid amyloidosis

AHR: Aryl hydrocarbon receptor

AMP-PNP: Adenylyl-imidodiphosphate

AR: Androgen receptor

ATP: Adenosine triphosphate

BER: Base excision repair

CDC: Cell-division cycle protein

CDK: Cell cycle dependent kinase

cDNA: Complementary DNA

CTD: C terminal domain

DAPI: 4',6-diamidino-2-phenylindole

DDR: DNA damage response

DEPC: Diethyl pyrocarbonate

DNA: Deoxy ribonucleic Acid

DSBR: Double strand break repair

DSBs: Double stranded breaks

dsDNA: Double stranded DNA

DTT: Dithiothreitol

EDTA: Ethylenediaminetetraacetic acid

EGCG: Epigallocatechin-3-gallate

EGFR: Epidermal growth factor receptor

EGTA: Ethylene glycol-bis(β-aminoethyl ether)-N,N,N',N'-tetraacetic acid

ER: Estrogen receptors

FANCA: Fanconi anaemia, complementation group A

FFT: Fast Fourier Transform

GC: Gene conversion

GR: Glucocorticoid receptor

GTP: Guanosine Triphosphate

HEPES: 4-(2-hydroxyethyl)-1-piperazineethanesulfonic acid

HIF: Hypoxia-inducible factor

HOP: Hsp70/Hsp90 organizing protein

HR: Homologous recombination

HSF: Heat shock factor

Hsp90: Heat shock protein 90

ICLs: Interstrand crosslinks

IPTG: Isopropyl  $\beta$ -D-1-thiogalactopyranoside

LB: Luria-Bertani

MAPK: Mitogen-activated protein kinase

MD: Middle domain

MKK: Mitogen-activated protein kinase kinase

MMS: Methyl methane sulfonate

MR: Mineralocorticoid receptor

NBN: Nijmegen breakage syndrome

NER: Nucleotide excision repair

NHEJ: Non-homologous end joining

NLS: Nuclear localization signal

NTD: N terminal domain

PARP: Poly ADP-ribose polymerase

PBS: Phosphate Buffer Saline

PCNA: Proliferating cell nuclear antigen

PCR: Polymerase chain reaction

PEG: Polyethylene glycol

PIKK: Phosphoinositide 3-kinase related kinase

PMSF: Phenylmethylsulfonyl fluoride

PPAR: Peroxisome proliferator-activated receptor

PR: Progesterone receptor

PVDF: Polyvinylidene difluoride

RNA: Ribonucleic acid

RT-PCR: Reverse transcription polymerase chain reaction

SD: Standard deviation

SDS: Sodium dodecyl sulfate

SHR: Steroid hormone receptor

siRNA: Small interfering RNA

SOE: Splice Overlap Extension

SPR: Surface plasmon resonance

SSA: Single strand annealing

SSBs: Single stranded breaks

ssDNA: Single stranded DNA

STAT: Signal transducer and activator of transcription

TBST: Tris-buffered saline

TCA: Trichloroacetic acid

TE: Tris EDTA

TIFs: Telomere dysfunction-induced foci

TLS: Translesion synthesis

TPR: Tetratricopeptide repeat

UV: Ultra Violet

YPDS: Yeast extract peptone sorbitol

YPED: Yeast extract peptone dextrose

### **INTRODUCTION**

### 1.1 Molecular chaperones: Guardian of cell proteome

Maintaining cellular protein homeostasis is one of the major tasks for the accurate cell survival, which is performed by a group of proteins called molecular chaperones. The chaperones provide functional maturation to the nascent polypeptide or denatured proteins and sort them to their required destinations and aids in the degradation of misfolded proteins (1,2). Ongoing protein synthesis and crowded cellular environment demand proper functioning of molecular chaperones, failure of which results in the aggregation of proteins (3). Diseases like Parkinson's, Huntington's, Alzheimer's, amyotrophic lateral sclerosis, type II diabetes, amyloid amyloidosis (AA), atherosclerosis, hemodialysis-related disorders and short-chain amyloidosis are associated with disfunctioning of molecular chaperones (4). Members of molecular chaperones are commonly referred as heat shock proteins (HSPs), as they get highly abundant in response to heat stress. These chaperones are distributed in various cellular compartments and hence work on a broad range of substrates (5, 6). On the basis of molecular weight, heat shock proteins are categorized into different groups; Hsp90, Hsp70, Hsp40, Hsp100 and other small molecular chaperones. Among all, heat shock protein 90 preserves special position in the cell by being distinctly different from other heat shock proteins.

### 1.2 Heat shock protein 90 (Hsp90): The chaperone which protects the cell upon stress

Hsp90, a 90 kDa protein has been extensively studied for its considerable contribution in the vast area of cellular processes. It is highly conserved among the eukaryotes and constitutes 2% of the total cellular proteins. It gets up regulated upon stress such as malignancy, variations in pH,

nutrient pressure, high temperature, hypoxia, oxidative damage. These incidents result in the highly active protein machinery, where Hsp90 actively works to ensure the proper functioning of a protein (7). Expression of Hsp90 is regulated by a transcription factor called heat shock factor (HSF1). Under normal scenario Hsp90 remians associated with HSF1 and releases it in response to stress. This released HSF1, then binds to the promoter of Hsp90 and up-regulates the expression of Hsp90. Thus, Hsp90 regulates its own transcription upon stress (8). Hsp90 is present in two isoforms called Hsp90α (expression is regulated by stress) and Hsp90β (constitutively present in the cells at basal level). These isoforms share considerable sequence identity among themself (9). Although Hsp90 is a cytoplasmic protein but its presence in the form of different isoforms is observed in several cellular compartments. In mitochondria, it is known as Hsp75/TRAP1 and in endoplasmic reticulum (ER) it is known as glucose-regulated protein 94 (Grp94) (10). It is also observed on the surface of cancer cells as well as in the secreted form in the extra cellular matrix (11). In Saccharomyces cerevisiae it is present in the form of two isoforms; Hsp82 (expressed under stress) and Hsc82 (constitutively expressed). These isoforms share 97% of sequence identity within themself and Hsp82 shares 61% sequence identity with human Hsp90 (12).

### 1.2.1 Distinctive features of Hsp90

Being a molecular chaperone, Hsp90 is known to provide conformational maturity to the variety of proteins. However, in doing so Hsp90 displays a unique nature, firstly, it delivers the final functional maturation to a specific group of proteins which are known as Hsp90 clients. Secondly, it is active at the later stages of protein folding. Unlike Hsp70 and Hsp40 which are involved in "de novo protein synthesis", Hsp90 nourishes proteins only after they cross the nascent polypeptide state and reach to a metastable confirmation (Figure 1) (13). Functions of Hsp70, Hsp40 and other

Figure 1: Unique nature of Hsp90

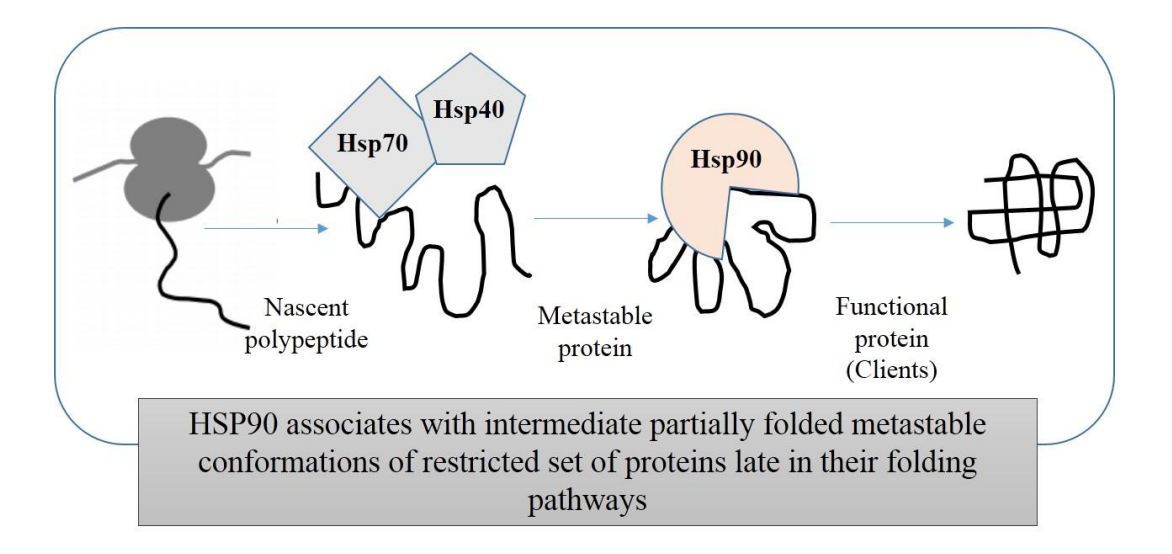


**Figure 1:** Representation of protein folding mediated by Hsp90. After protein is partially stabilized by Hsp40/Hsp70 chaperone complex, it gets transferred to Hsp90 machinery. Hsp90 facilitates proteins to attain their final functional conformation.

chaperones are devoted to fold newly synthesized polypeptides or misfolded proteins, but Hsp90 interacts even with folded proteins (14). Another example its uniqueness is seen in its clientship with Tau protiens. These proteins are associated with Hsp90, but they are always intrinsically disordered protein and never adopt folded conformation. Hence these are considered as unexpected clients of Hsp90 (15, 16). Consealing of client interaction surface is not possible with Hsp90, which is another different feature of Hsp90 than other ATP dependent chaperones. Unlike other chaperones, Hsp90 does not have common interaction surface for all the clients and it varies from client to client. Hsp90 carries extended surface for client interaction, which crosses domain boundaries. For example; Cdk4 and Tau proteins interact with the N-terminal domain (NTD) and middle domain (MD) of Hsp90 (16, 17). p53, a tumor suppressor protein has large interaction area which includes the C-terminal domain (CTD) of Hsp90 (18, 19). Mutational study of Hsp90 homolog HtpG in E. coli (Escherichia coli) signifies the presence of interaction sites on MD, CTD and on the interphase of MD and CTD. Mutations of Hsp90, in these domains disturb the interaction of Hsp90 with substrate proteins (20). Studies with middle domain point mutants of Hsp82 indicate differential effects on the activation of two well-known clients namely glucocorticoid receptor (GR) and v-Src. The W300Ahsp90 mutant results in the 10 fold increase in the cellular pool and activity of v-Src kinase although, the activity and level of GR remain unaltered. Reduced accumulation of v-Src was observed in T1011, E381K, S485Y and T525I hsp90 mutants; however GR levels were affected in T22I and E431K mutations. Reduced accumulation of v-Src was observed in T1011, E381K, S485Y and T525I mutants of Hsp90; however GR levels were affected in T22I and E431K mutants. These studies indicate, that different mutations of Hsp90 affect different client proteins, hence individual clients are regulated by different part of Hsp90 (21). In many cases, Hsp90 is associated with client proteins even after their final

maturation. This characteristic of Hsp90, again makes it unique than other chaperones. The one of the best-studied client proteins of Hsp90 is the GR. Immediately after synthesis, GR is supervised by Hsp40 and Hsp70 for acquiring the metastable confirmation. Next Hsp70/Hsp90 organizing protein (HOP) makes a sandwich by binding to the Hsp70-GR complex with Hsp90 and brings metastable steroid hormone receptor (SHR) to Hsp90 custody. This ATP bound Hsp90-GR complex is then stabilised by p23, and this process provides the maturity to GR. After providing maturity, Hsp90 remains associated with GR till the glucocorticoid hormone signal arrives. Upon hormone binding large conformational changes take place to GR, which allows it to translocate to the nucleus and where it functions as a transcription factor. It is examined that upon hormone induction, GR translocates to nucleus along with Hsp90 and releases from Hsp90 after reaching to the nucleus (22, 23).

### 1.2.2 Structural domains of Hsp90

Hsp90 sustains a highly conserved structure and is generally present in the form of a dimer. Each protomer carries three domains namely N-terminal domain, middle domain and C-terminal domain (Figure 2). Each domain has a specific assigned function that mediates the client protein folding. N-terminal domain (NTD) carries ATP binding Bergerat fold which possesses ATPase activity (24, 25). Natural products Geldanamycin and Radicicol, which are the precursors for many Hsp90 inhibitors for cancer therapy, bind to the Bergerat fold. Derivatives of Geldanamycin; 17-AAG (17-N-Allylamino-17-demethoxygeldanamycin) and 17-DMAG (17-Dimethylaminoethylamino-17 demethoxygeldanamycin) are the ATP competitors and inhibit the ATPase activity of Hsp90 (26). Middle domain (MD) is mainly recognized as a platform for co-chaperones and substrate binding. It also mediates communication with the N-terminal domain and stimulates its ATPase

Figure 2: Structure of yeast Hsp90

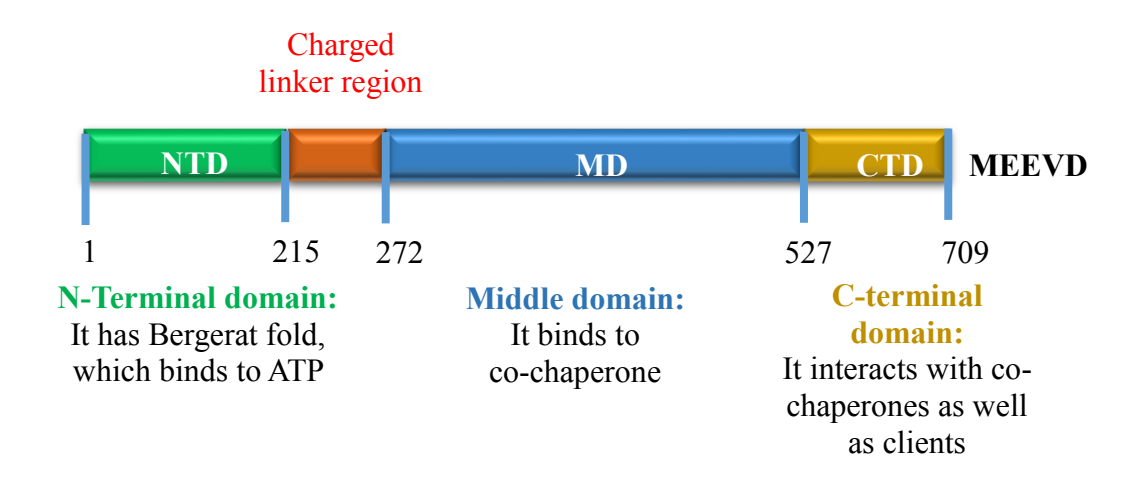


**Figure 2:** Schematic representation of different domains of yeast Hsp90 with the domain boundaries and the assigned functions for each domain

activity. Third domain is the C-terminal domain (CTD), which interacts with various substrate proteins. CTD contains a Met-Glu-Glu-Val-Asp (MEEVD) sequence at its tail which acts as an anchor for the tetratricopeptide (TPR) domain harboring co chaperones (27, 28). This domain also has another nucleotide binding site and unlike NTD it binds to both purine and pyrimidine nucleotides (ATP and GTP) (29). Hsp90 usually resides in the form of dimer and its dimerization is favored by the last few residues of CTD and partially by ATP bound NTD (30-32). Novobiocin, Cisplatin, EGCG and Taxol inhibitors are known to bind at the CTD of Hsp90 and hamper client protein functions (33). Charged linker region secures its position between NTD and MD and conserved throughout the evolution but absent in prokaryotes. This linker sequence is essential to enable flexible conformations of Hsp90. It has less complex sequence and has plentiful charged amino acids. In yeast Hsp82 includes 5 pentad repeats of the motif (D/E)(D/E)(D/E)KK (34). Crystal structure of full-length Hsp82 in the closed conformation with co chaperone Sba1 (p23 in human) and ATP analog is solved. This structure represents structural changes during dimerization and chaperone cycle of Hsp90 (35).

### 1.2.3 Charged linker region: A structural component of Hsp90

Although it is highly conserved among eukaryotes, functional basis for the charged linker region was enigmatic. Studies to understand its functions were initiated and it is observed that, its minimum length can sufficiently serve for Hsp90 activity. Later it is recognized for furnishing flexibility to Hsp90 during chaperoning cycle. In yeast Hsp90, this region is extended from residues 211 to 272 and in human Hsp90 it is a stretch of 63 amino acids. Hsp90 has divergent charged linker sequence among most eukaryotes, neither its length nor its presence, but its sequence is the defining parameter for the chaperone activity of Hsp90 (36). Essential

features of charged linker region were drawn by sequential deletion of this region, which demonstrated that, removal of (211-259) regions from yeast Hsp90 has no effect on cell growth but further deletions impart adverse effects on cell growth. These observations indicate that substantial length of the charged linker is essential for cell survivability. However, deletion of this region from Hsp90 does not affect the stability of the protein. A distinct defect in the activities of Hsp90 client proteins, such as v-Src and GR were observed upon deletion of this region. Mutant Δ211-259hsp90 shows one third activity of firefly luciferase but further trimming of this region (211–263) severely affects its activity. Deletion of (211-259) residues from Hsp90 slightly increases ATPase activity of Hsp90. However deletion of Hsp90 residues beyond (211-259), displays reduction in its characteristic ATPase activity. Co chaperones like Aha1 and p23 binding to Hsp90 is an obligatory parameter, which is hampered by the deletion of charged linker residues beyond 259 (37). Besides, charged linker region provides conformational flexibility to the N-terminal domain. Therefore deletion of this region makes Hsp90 conformationally restricted and affects N-terminal dimerization of Hsp90 which is required for client protein interaction (38).

### 1.2.4 Associates of Hsp90: Co chaperones

In the process of serving client proteins, Hsp90 employs several other proteins which accelerate Hsp90 functions. These employed proteins, which assist Hsp90 for client protein folding, are termed as co chaperones. Till date around 20 co chaperones have been identified that are engaged in different functions at the different level of client protein folding. These co chaperones interact with different domains of Hsp90, for example in yeast Cdc37, p23, SGT1 interact with the NTD, Aha1 takes its position to the middle domain and WISp39, FKBP52/ FKBP54, CYP40, PP5, TOM70 and TPR2 interact with the CTD (7). A major class of co chaperones belongs to the TPR

domain containing proteins, which interact with the MEEVD motif at the C-terminal part of Hsp90 (39). However, in many cases, exact biological functions of these co chaperones are largely ambiguous. It becomes apparent as, the set of utilized co chaperones varies from client to client and they work in organism specific manner (40). Co chaperones are further categorized on the basis of their negative or positive effect, towards ATPase activity of Hsp90. For example, few co chaperones such as Aha1 and Cpr6 (41, 42) enhance ATPase activity by accelerating favorable conformation of Hsp90 for ATP hydrolysis. Whereas Cdc37, HOP and p23 suppress ATPase activity of Hsp90. Few co chaperones have specific assigned functions for the special set of clients such as Cdc37, which helps in the loading of kinases to Hsp90 machinery (43, 44). Another chaperone p23 facilitates the multi protein complex formation with Hsp90. Co chaperones Ser/Thr phosphatase 5 has phosphatase function and immunophilin cyclophilin 40 has prolyl isomerase activity (45, 46). Although exact functions of these co chaperones are still in infancy, key features of co chaperones are as follows:

- Activate or suppress the ATPase activity of Hsp90
- Harmonize the team work of Hsp90 and other proteins
- Assemble the client protein to Hsp90
- Perform enzymatic activities like phosphatase activity and prolyl isomerase for client activation

### 1.2.5 Recipients of Hsp90's services: The client

Hsp90 machinery is dedicated to a restricted group of proteins for their final active confirmation, these are termed as clients. Hsp90 is associated with client proteins for their precise

folding, activation, degradation as well as transportation (47, 48). Demonstrating any protein as Hsp90 client, demands the following criteria to be fulfilled:

- Candidate protein must show physical association with Hsp90
- Functional loss of Hsp90 must hamper the function of candidate protein
- Irrespective of these criteria, declaring any protein as the client of Hsp90 is a challenging task because of following reasons:

Inhibition of Hsp90 should lead the protein towards proteasomal pathway for degradation

- Acknowledged clients of Hsp90 do not have any specific sequence or motif in common
- In few instances, Hsp90 client interaction is context dependent
- Nature of Hsp90-client association is poor and dynamic (49)

However solving the puzzle becomes enthralling as familiar clients sustain crucial seat in biological pathways and these clients range from transcription factors, signaling proteins, immune response proteins, DNA repair proteins, factors of epigenetic regulation etc. (Figure 3) (50, 51). Comprehensive analysis indicates that identification of clients reside in the conformation and stability of protein rather than on primary elements. For example, v-Src is a client of Hsp90 but similar protein which share 98% sequence identity c-Src is not dependent on Hsp90 functions (52-54). Recognition of clients can again be modulated by mutations in the protein, which is evident by well-studied epidermal growth factor receptor (EGFR) and B-Raf. Mutant EGFR<sup>L858R</sup> and BRAF<sup>V600E</sup> are transformed oncoproteins, which rely on Hsp90 for their stability. Analysis of these mutants reveals their stronger association with Hsp90 than their wild type counterparts (55-57). Client recognition site on Hsp90 is still undefined and it crosses domain boundaries for

varying clients (58). Most prominent clients are kinases and steroid hormone receptors (SHRs), yet continuous discoveries are expanding the list of client proteins. These findings are opening new categories of client proteins, which are unrelated to classical kinases and SHRs as mentioned in figure 3.

### 1.2.6 Other side of the coin: Hsp90 and progression of cancer

Cancer cells are reported to have higher abundance of Hsp90 than normal cells. This highly abundant Hsp90 is a common feature of both solid and liquid tumors (59). These days Hsp90 is being targeted in many types of cancers in combination with other inhibitors. It is becoming practicable because 1) Hsp90 reinforces the stability and assembly of many oncoproteins including Akt, Cdk4, mutated p53, B-Raf, EGFR, PI3K, Stat-3, GSK3β, HER-2 (60), 2) Hsp90 conquers stressed situations faced by tumor cells like hypoxia, nutrient deprivation, replication stress, proteotoxic stress etc., 3) Hsp90 from cancer cells are more susceptible to the inhibition of ATPase activity by 17-AAG than normal cells as Hsp90 derived from tumor cells has 100 fold more affinity towards 17-AAG than normal cells (63, 64). In cancer cells Hsp90 resides in the form of Hsp90-Cdc37 super chaperone complex (61, 62). Presence of Hsp90 in super complex refers cancer cells, as addicted to molecular chaperone. Hsp90 and this complex helps in tumor cell proliferation, survival, and angiogenesis. 17-AAG is the first inhibitor which entered in the clinical trial and since then various inhibitors of Hsp90 are under development, most of them disrupt the chaperone cycle by displacing ATP. These include 17DMAG, Radicicol and related oxime derivatives, cisplatin, novobiocin, CNF2024/BIIB021, MPC-3100. Debio 0932 (CUDC-305), NVP-AUY922, SNX-5422, STA-9090, KW-2478, AT13387, DS-2248 PU-H71 etc (65).

Figure 3: List of identified Hsp90 clients

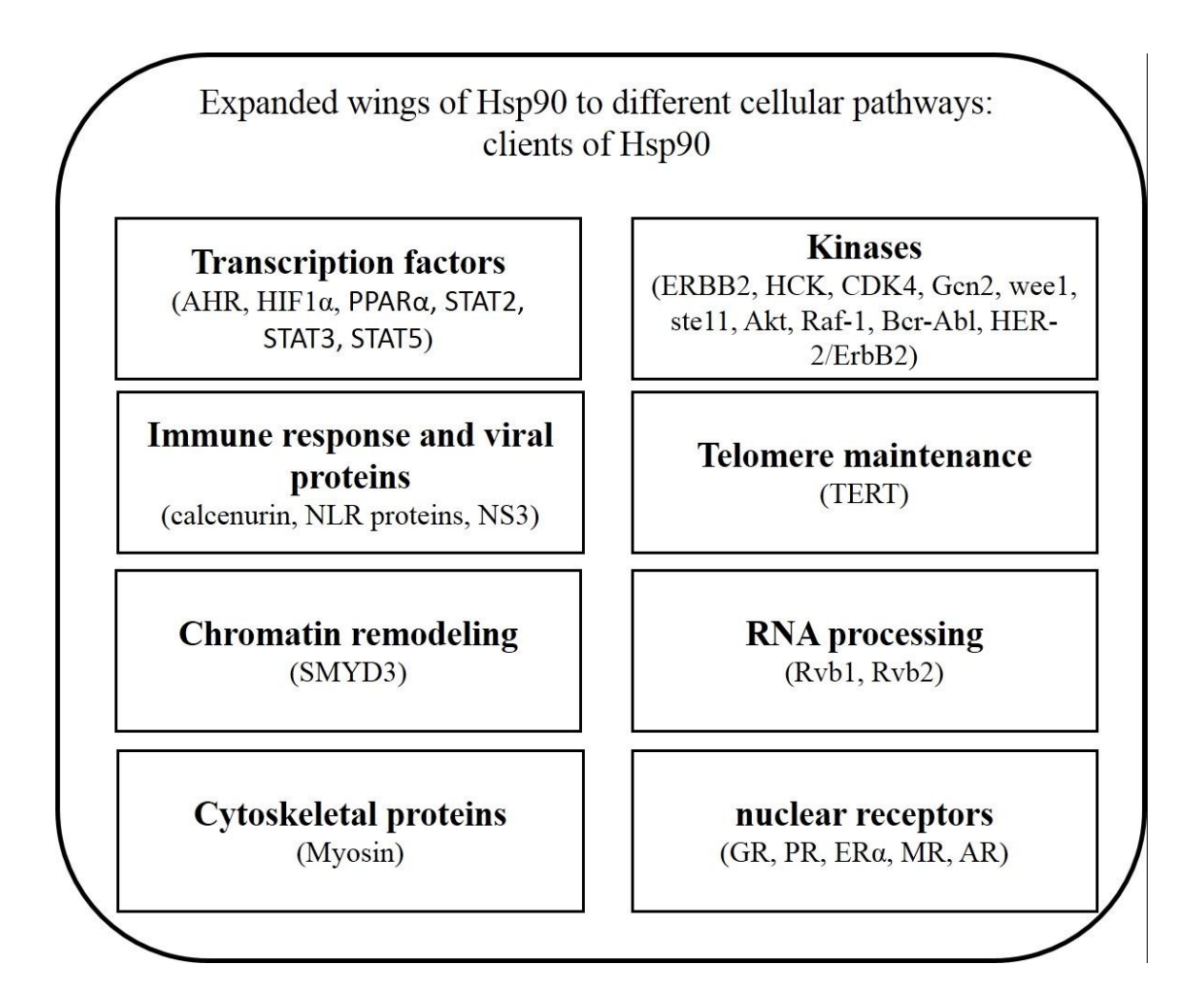
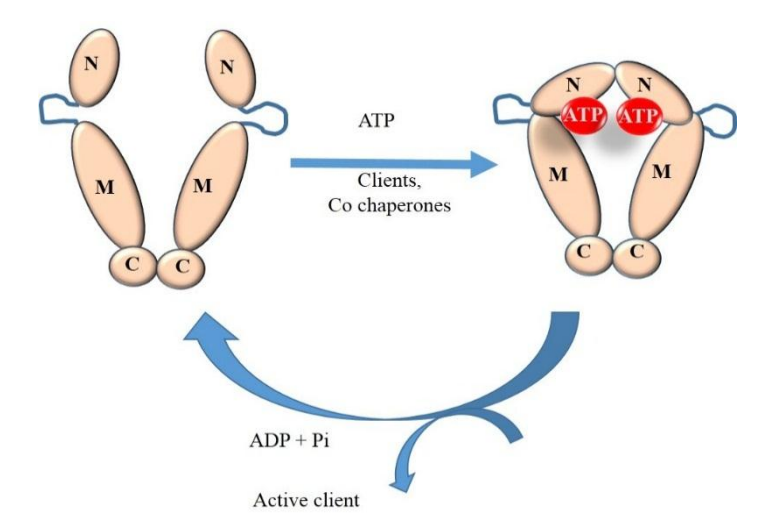


**Figure 3:** List of various known Hsp90 clients which belong to different cellular pathways

### 1.2.7 Mode of action by Hsp90: Chaperone cycle

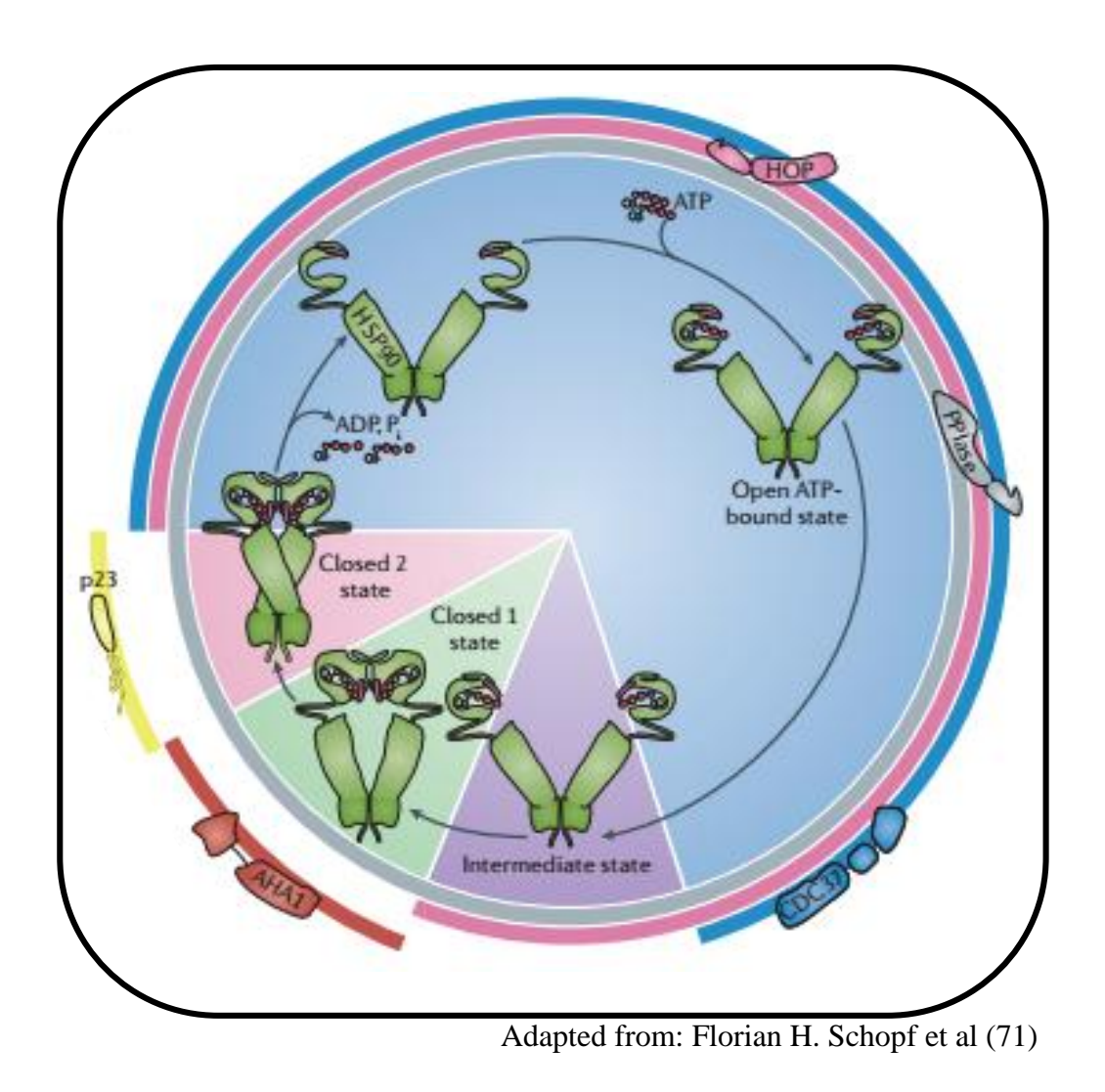
Attainment of a functionally active client is a result of the teamwork of Hsp90 with its co chaperones. This protein complex makes a dynamic multimeric network during the process of grooming the client protein. Hsp90 also uses nucleotides by its ATPase activity, which is an essential step for client folding. Before the arrival of ATP, Hsp90 remains in the V-shaped open confirmation. ATP binding to the NTD turns the rearrangement events of middle and CTD, which triggers the confirmation towards closed form (Figure 4) (66). Switching between the open and closed confirmation is governed by a lid which is constituted with the sequence of conserved amino acids at the ATP binding pocket of NTD. This lid remains open during ADP bound state of Hsp90 (33). The different stages of chaperone cycle are well studied for steroid hormone receptors. This cycle is initiated by first association of client proteins with Hsp40, which is then assisted by Hsp70 and this complex together forms an early complex. Next Hsp70-Hsp90 organizing protein (HOP/Sti1 in yeast) takes the lead and docks the early complex to Hsp90. During this docking, HOP first stabilizes Hsp90 followed by early complex and resultant complex is known as intermediate complex (67, 68). Final maturation of client protein is facilitated by the addition of ATP, p23 and PPIase accessory factors to the complex. ATP hydrolysis results in the release of active client protein from the complex and Hsp90 returns to its open confirmation for the next round of client maturation. Similar protein complex is conserved from yeast to human (69, 70) (Figure 5).

Figure 4: ATP mediated open and closed confirmation of Hsp90



**Figure 4:** ATP dependent conformational switching of Hsp90 between open inactive and closed active conformation. Red color circle represents ATP molecule bound to N-terminal domain of Hsp90.

Figure 5: Chaperone cycle of Hsp90



**Figure 5:** Schematic presentation of Hsp90 chaperone cycle: The different confirmations acquired by Hsp90 during client protein folding and its interaction with different co chaperones. HOP interacts with Hsp90 during open confirmation and intermediate confirmation while Cdc37 binding is restricted to open confirmation. PPIase remains bound throughout the chaperone cycle. Aha1 facilitates ATPase cycle by its interaction during ATP bound closed 1 state and p23 interacts with closed 2 state.

### 1.2.8 Unconventional functions of Hsp90

In recent days, Hsp90 is recognized for performing several functions other than its classical chaperone functions. This includes protein degradation, transcription, and maintenance of the protein complexes and translocation of client proteins to several compartments. Clearance of misfolded and inactivated protein is performed in CHIP mediated ubiquitin proteasome pathway of Hsp90 (72). It facilitates the transcription by several means such as;

- 1) It regulates several transcription factors such as SHRs (73)
- 2) It regulates epigenetic modifiers by connecting to Rvb1p (RuvB-like protein 1)/Rvb2p through co chaperones Tah1 and Phi1 (74)
- 3) It causes displacement of histones from the promoter (75)

### 1.2.8.1 Facilitating the travel of client proteins to cellular compartments

Hsp90 functions are not only confined to protein folding but it is also engaged in trafficking of proteins to different cellular compartments. SHRs particularly, GR, estrogen receptor (ER), Androgen receptor (AR), and progesterone receptor (PR) are Hsp90 clients and they are translocated to the nucleus to perform their activity. One of the best-understood systems is the transport of GR to the nucleus upon hormone induction. This shuttling of GR is favored by Hsp90 chaperone machinery (Hsp90, Hsp70, Hop, Hsp90-binding co-chaperone p23 and a J-domain-containing protein Hsp40). It facilitates the recruitment of TPR proteins FKBP52, FKBP51, or Cyp40 to the GR-Hsp90 complex at the last step of maturation (76, 77). This assembly keeps GR in hormone compatible state until hormone signal arrives. These TPR proteins interact with motor protein dynein and generate a link between Hsp90 and cytoskeleton which mediate the

translocation of GR to the nucleus (78). In another case, Hsp90 binds to a component of Rab GTPase cycle called rhoGdIα and manages the recycling of Rab proteins which in turn regulates membrane trafficking (79). rAB1B dependent trafficking of a neurotransmitter rAB3A is also regulated by Hsp90 from the endoplasmic reticulum to Golgi (80). AF9 is a component of gene regulation which interacts with histone H3 lysine 79 methyltransferase and is dependent on Hsp90 chaperone machinery for its nuclear distribution. Hsp90 directly interacts with AF9 with the complex of Hsp90-Hsp70-p60/Hop. Inhibition of Hsp90 with Novobiocin triggers the redistribution of AF9 from the nucleus to the cytoplasm (81).

### 1.2.8.2 Assistance for the assembly of multi protein complexes

Hsp90 supports its client proteins at the later stage of protein folding and sometimes it remains continuously associated with them. Here chaperones protect the client protein from aggregation or degradation, without being the part of a functionally matured complex. The following observations provide the glimpse of another side of Hsp90 and its importance for the stability of protein complex, other than mere helping in client proteins folding. During the assembly of box C/D snoRNP complex and processing of pre-rRNA, Pih1 is stabilized by Hsp90-Tah1. This protein further interacts with Rvb1–Rvb2 and forms a complex R2TP (82). RNA polymerase II complex which includes 12 proteins requires Hsp90 which helps in the coordination of Rpb1 with the complex. This function of Hsp90 is mediated through RNA polymerase II associated protein (RPAP3) (83). A serine threonine kinase phosphoinositide 3-kinase related kinase (PIKK) is an important regulator of cell growth in response to various stresses. Hsp90 through Tel2 protein stabilizes newly synthesized unstable PIKK and further promotes the PIKK complex assembly

formation (84, 85). In many studies, Hsp90 functions are highlighted for the stability, localization and activity of telomerase. At telomeres, Hsp90 association triggers the recruitment of telomere extension complex and shifting of capping complex away from telomere. Hsp90 does it by suppressing the binding of Cdc13 to DNA. Telomerase (TERT) owes its stability to Hsp90-p23 complex, which is essential for TERT nuclear translocation (86-88). The detachment of p23 from this complex results in the retention of TERT into the cytoplasm (89). Kinetochore assembly is also demonstrated to be stabilized by Hsp90 and its co-chaperone Sgt1. Hsp90 interacts with the complex of four proteins called CBF3 and favors the interaction of this complex with ubiquitin ligase. In this way, Hsp90 balances the turnover of this kinetochore complex (90). Repression of gene expression takes place by RNA-induced silencing complexes known as RISC complex. This complex utilizes Hsp90 for the loading of other proteins to small RNA (91). Importance of Hsp90 in 26S proteasome assembly was witnessed when Hsp90 is inhibited by GA, which results in the dissociation of 20S core and the lid component (92, 93).

## 1.3 DNA damage: A threat for genomic stability of organism

Genome is persistently attacked by numerous detrimental agents, which are either exogenous like UV, ionizing radiations and harmful chemicals or endogenous like reactive oxygen species and replication errors etc. Such phenomena result in either single stranded breaks (ssDNA breaks) or double stranded DNA breaks (dsDNA breaks) in DNA (94). Persistent assaults ultimately leave defects in the genome such as mutations and different kind of genomic rearrangements. These defects gear the cells either towards death or disease onset such as cancers, aging, neurodegenerative disorders, cardiovascular disease (95) etc. In many cases, ignored and unrepaired mutations result in the oncogenic shift of the genes which is a consequence of switching

off and switching on of a tumor suppressor gene and proto-oncogene respectively (96). Therefore, genome should always be assisted by its caretakers upon such harmful conditions. The direct guardians of the genome are the members of DDR (DNA damage response), which further coordinate with DNA repair proteins to ensure the healthy survival of cells upon DNA damage (97). During the course of development, cells have evolved multiple pathways to fix these unwanted changes in the genome. These pathways are cleverly utilized by cells on the basis of type of damage, location of breaks, and cell cycle stage.

### 1.4 Repair of damaged DNA

Mammalian cells employ non-homologous end joining (NHEJ) and homologous recombination (HR) for repairing DSBs (Double stranded breaks). Among these pathways, NHEJ is the preferred pathways over HR for repairing DSBs in case of mammals. NHEJ is active throughout cell cycle however HR is cell cycle restricted and is active only in late S and G-2 phases of cell cycle (98). During NHEJ two broken ends of DNA directly join with the help of DNA-dependent protein kinase (DNA-PK), Ku70/80 hetero dimer, XRCC4/XLF complex and the ligase IV (99-102). This event mostly produces an altered DNA product due to the loss of few base pairs near the damaged site. Although NHEJ reserves a prime position in mammalian DSBs repair, cancer cells however, represent greater efficiency of HR (103). In lower eukaryotes *Saccharomyces cerevisiae*, HR is the highly utilized pathway for DSBs repair possibly, because of the unavailability of three major NHEJ proteins namely DNA-PKcs, BRCA1, and Artemis.

# 1.4.1 Homologous recombination pathway

The repair of DSBs by homologous recombination was witnessed by Resnick in 1976, where he proposed the involvement of homologous sequence for repairing the broken junction of DNA (104). Initially, utilization of HR in the mammalian system was considered to be absent. Later, presence of HR in mammalian system was proved by "plasmid-by-chromosome recombination" experiment, which is based on the repair of DSBs of plasmid by utilizing chromosome (105). Steps of HR pathway are mostly conserved among the species with little variations in the protein components. When cells witness dsDNA breaks, different sensors, transducers and signaling proteins rush towards damaged DNA. Although, not much has been studied about sensor proteins in mammals, but possible candidate proteins include PARP (poly ADP-ribose polymerase) and DNA-PK (DNA-dependent protein kinase). Studies in yeast suggest that Rad17 (homolog of replication factor C) with Rfc2, Rfc3, Rfc4 and Rfc5 load 9-1-1 complex (Rad9, Hus1, and Rad1) to DSBs which triggers the amplification of DNA damage signal (106-109). Next, signal transducers like ATM (ataxia telangiectasia mutated) and ATR (ATM-Rad3-related) followed by checkpoint kinase 1 (Chk1) and Chk2 phosphorylate breast cancer 1 (BRCA1), Nijmegen breakage syndrome (Nbs1), 53BP1 and Cdc25. These phosphorylation events allow the arrest of cell cycle at G2/M (110-118). These signaling events initiate the recruitment of Mre11/Rad50/Nbs1 complex (MRN complex/ MRX in yeast) to DSBs and then act as a sensor protein complex for other DNA repair proteins (119). MRN complex, as an initiator of DSBs repair, coordinates with ATM and ATR kinases and gets phosphorylated at Nbs1 (120). Subsequently, MRN along with ATM recruits another set of MRN complex to the broken junction and phosphorylates this complex. The recruitment of MRN complex invites DNA repair proteins and activates them by phosphorylation (114). Subsequently, BRCA1 starts resecting the DNA 5' ends (121). Next, ATR promotes the phosphorylation of an endonuclease called CtIP (Sae2 in yeast), which helps in resection of broken DNA ends (122). After initial 5' end resection, Exo1 endonuclease participates in extensive 5' end resection by its 5' to 3' exonuclease activity. This may also happen with the help of dual helicase/nuclease activity of BLM/Exo1 (123). This process generates free 3' overhangs of broken DNA, which are avidly occupied and protected by RPA (replication protein A). Removal of RPA from ssDNA is favored by the mediator protein, which is breast cancer type 2 (BRCA2) in case of mammals (124, 125). Here BRC4 repeats of BRCA2 serves in the nucleation of Rad51 to the ssDNA by displacing RPA. BRCA2 involves in both, Rad51 filamentation onto ssDNA and stabilization of newly formed Rad51 filament (126, 127). In yeast Rad52 takes the lead role of BRCA2 where, it makes a sandwich by interacting with both Rad51 and RPA and helps in the displacement of RPA with Rad51 (128, 129).

Coating of ssDNA with Rad51 then triggers the signature step of HR, which is called strand invasion. The Rad51 bound ssDNA invades to the homologous dsDNA and acts as a primer for the synthesis of DNA, in order to repair the damage. Rad51 coated strand invasion is accelerated by another interacting partner of Rad51 called Rad54. Rad54 stabilizes Rad51 bound ssDNA and helps in the search for homology (130-131). This phenomenon is mediated by the ATPase activity of Rad51 (132, 137). Another mediator protein for the Rad51 filament stabilization is a hetero complex of Rad55/Rad57 which favors the strand invasion (138, 139). This step is known as synapsis, where Rad51 helps in the annealing of the 3' strand with the homologous template DNA which results in the structure called D-loop (140, 141). This further makes a double holiday junction which is assisted by BLM and topo-IIIα along with co factor BLAP75/Rmi1. This

structure either dissolves into a non-cross over product or resolves and results in a cross over product (142-144). These phenomena result in the accurate repair of broken DNA and hence safeguard the genomic integrity.

# 1.4.2 Participants of homologous recombination

HR is a long process and employs a series of proteins, which function at different stages. This includes several proteins, ranging from that which encounters the DNA damage to the ones which help to end HR process successfully. These proteins are mentioned in figure 6 which maintain the flow of HR process by executing their attributed activities for the pathway. Details of Rad52 and Rad51 are given below.

#### 1.4.3 Rad52

Rad52 was discovered in a genetic screen of yeast mutants, upon IR radiation induced DNA damage (145). It actively participates in all studied pathways of HR, such as double strand break repair (DSBR), synthesis dependent strand annealing (SDSA) and Rad51-independent pathway of single strand annealing (SSA) (146). Rad52 is a well-studied recombination mediator protein. Many DNA repair proteins like RAD50, RAD51, RAD54, RAD55, RAD57, RAD59, MRE11, and XRS2 are categorized under Rad52 epistatis group proteins. During HR it makes contact with RPA and takes part in the replacement of RPA with Rad51 bound to ssDNA (147). It also forms oligomeric rings and helps in strand invasion by its interaction with ssDNA and Rad51 (148). As Rad52 engrosses in the critical functions of HR, its presence in the cells becomes essential which is indicated by the severe phenotype in Rad52 deleted yeast strains. Instead of its significant contribution in HR, Rad52 knockout mice are viable. However deletion of BRCA1 and BRCA2 in Rad52 knocked out cells severely affect the cell survivability (149-151).

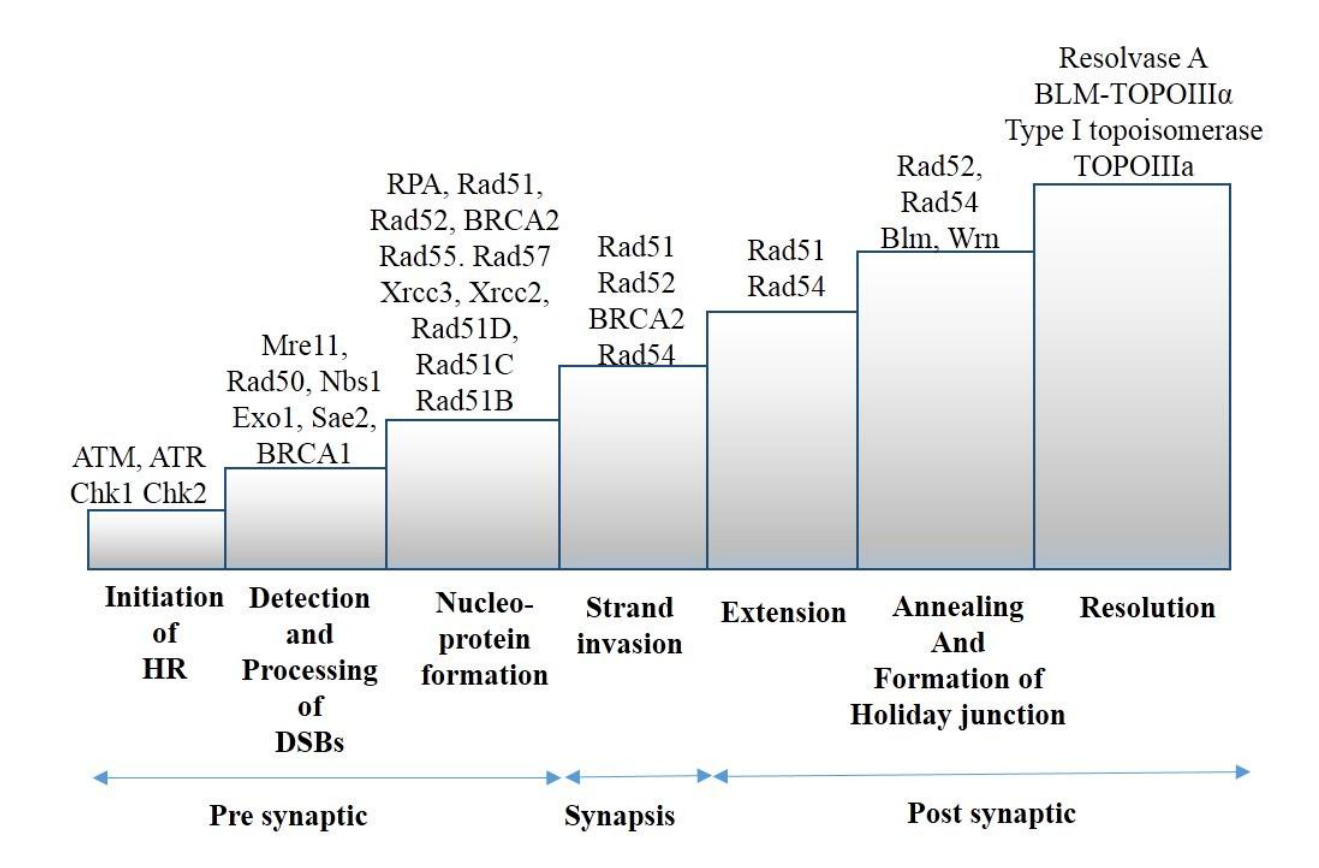


Figure 6: Participants of homologous recombination

**Figure 6:** Sequential steps of homologous recombination pathway of DSBs repair, representing the proteins involved at different steps.

#### 1.4.4 Rad51

Rad51 was initially discovered in Saccharmomyces cerevisiae as a homolog of Escherichia coli RecA. Sequence analysis reveals that Rad51 has 30% sequence identity with RecA in its core domain (136). However comparison of full length amino acid sequence of ScRad51 and RecA shows 59% sequence similarity. Later, human Rad51 was identified on the basis of homology search which share 83% sequence similarity with ScRad51 (152). The higher level of conservation in Rad51 indicates the importance and conserved functions of Rad51 throughout the evolution. Initial understanding about the functions of Rad51 was obtained by the study, where yeast null rad51 mutants were viable, but sensitive towards MMS induced DNA damage (153). In mammals, deletion of Rad51 has drastic effects as RAD51-/- in mouse, exhibits lethal phenotype during embryonic development (154). Association of this lethal phenotype with the defect in DNA repair was established from the study on blastocytes, which were isolated from rad51 knock out embryo. These blastocytes were hypersensitive towards gamma radiation induced DNA damage. Detailed understanding of Rad51 function came from the study where, Rad51 was expressed under repressible promoter. Observations of this study reveals that inhibition of Rad51 expression results in the breakage in the chromosome and cell cycle arrest (155). Another study on mammalian cells sheds light on the importance of Rad51 for DNA DSBs repair via gene conversion, which mediates sister-chromatid exchange (156, 157). In meiotic prophase, Rad51 forms chromosomal foci during meiotic recombination which is similarly observed in the DNA damaged somatic cells (158-160). These experiments establish Rad51 as an essential protein in HR. Rad51 essentially is involved in all three stages of HR, which are known as pre synaptic, synaptic and post synaptic phases. During the presynaptic phase, Rad51 occupies the ssDNA which is generated either due to 5' end resection or by replication error. These are noted as nucleo-protein filament and it comprises of six molecules of Rad51 bound to 18 nucleotide per helix (130, 161, 162). This nucleo-protein filament then undertakes the responsibility for searching the homologous sequence in the genome, with the help of Rad52 and Rad54 (163, 164). Next, Rad51 participates in the synapsis phase which is the process of communication between invaded nucleoprotein filament and homologous dsDNA molecule which results in the formation of D-loop. The last stage is called post synapsis, where invaded protein DNA complex acts as a primer and synthesizes broken DNA using homologous DNA as a template (165, 166). Rad51 generates multiple connections while accomplishing the task during homologous recombination. List of Rad51 interacting proteins is presented in table 1.

#### 1.4.4.1 Structure of Rad51

Sequence alignment of Rad51p suggests that structure of Rad51 has high degree of conservation throughout the evolution. This structure consists of three domains namely N-terminal domain, ATPase domain and C-terminal domain (Figure 7). In contrast to RecA, which has extended C-terminal domain, Human Rad51 and ScRad51 have extra stretch of amino acids at the N-terminal part. In case of human Rad51 this extended stretch of N-terminal part occupies 1<sup>st</sup> to 95<sup>th</sup> residues and is conserved among higher eukaryotes. These conserved residues have special assigned function among eukaryotes. Available reports indicate that, N-terminal part of Rad51 is essential for its interaction with DNA (167). In *Saccharomyces cerevisiae* the N-terminal domain of Rad51 is further extended and have 79 extra amino acids, which are absent in human Rad51 and RecA. N-terminal domain of Rad51 is considered to be involved in its interaction with other HR proteins during homologous recombination.

Table 1: Known residues of Rad51 for facilitating its interaction with partner proteins

S.	Protein	Significance of the	Knowledge about the interacting residues and
NO.	partners	interaction	domain on Rad51
1.	BRCA2	Helps in Rad51 filament	• E42, E59, E237 of HsRad51 (203)
		formation onto ssDNA	• Tyr205, Ser208, Ala209 and Met251 of
			HsRAD51 (204)
2.	ScRAD51	Rad51 forms homo dimer	• Initial 186 residues of N-terminal domain of
		during HR	ScRad51 (205)
3.	ScRad54	Stabilizes Rad51 filament	• G103, T146, M269, C377, A27, L310,
		and stimulates strand	S231, A248, G210, G211, L86, L99, L104
		invasion. Helps in Rad51	and Initial 150 residues of ScRad51 interact
		dissociation from	with ScRad54 (168)
		dsDNA.	• S231, Y388, G393, S231 and L119 of
			ScRAD51 (206)
4.	ScRad52	Displaces RPA from	• A320, Y388, G393, A248, G210, G211 and
		single stranded DNA and	initial 186 residues of ScRad51 (168)
		loads Rad51 onto ssDNA	• Initial 151 residues and residues after 112 <sup>th</sup>
			amino acid of ScRad51 interact ScRad52
			(205)
			• Y388, G393, S231 and L119 of ScRad51
			(206)
5.	ScRad55/	Helps in the formation of	• L86, L99, L104 and initial 150 residues of
	ScRad57	Rad51 nucleoprotein	ScRad51 (168)
		filament and facilitates	
		Rad51 recombination	
		function	

Figure 7: Structure of ScRad51 protein

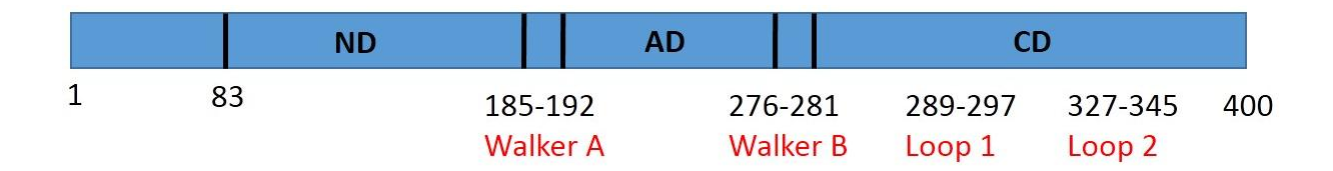


**Figure 7:** Schematic representation of *Saccharomyces cerevisiae* Rad51 protein representing different functional domains; DNA binding loop1/loop2 and Walker A/ Walker B motifs.

This understanding came from the mutational analysis of yeast Rad51, where initial 150 residues were deleted from the protein and then it was analyzed for its interaction with Rad52 epistatis group of proteins. In this analysis, this particular mutant rad51 appeared as defective for its interaction with Rad52 epistatis group proteins (168). N-terminal domain electron microscopy data indicates the formation of lobe at this region, which is essential for DNA binding during filament formation. Active or inactive conformation of Rad51 is dependent on the movement of these N-terminal lobes (169). ATPase domain is flanked by Walker A and Walker B motifs which are essential constituents for ATP binding and hydrolysis (170). Successful completion of HR is highly dependent on ATPase activity of Rad51, as strand exchange by Rad51 is mediated through its ATPase activity (171, 172). Loop 1 and loop 2 are the part of C-terminal domain in Rad51, which are present close to nucleoprotein filament axis and helps in loading of Rad51 to ssDNA (173, 174). Removal of C-terminal residues beyond 285th amino acid results in the disability of Rad51 to interact with its partner proteins from Rad52 epistatis group. This observation throws light on the importance of the C-terminal domains of Rad51 (168).

Rad51 from *Saccharomyces cerevisiae* bound to ssDNA has been crystallized by removing the extra stretch of 79 amino acids which are present at N-terminal part of yeast Rad51. Crystallization of ssDNA bound homo hexameric Rad51p was deciphered using X-ray diffraction method. This structure had a resolution of 3.25 Å and consisted of 6 chains namely A, B, C, D, E and F. Crystal structure of Rad51 has fold symmetry, as Rad51-Rad51 dimers were bound to ssDNA in hexameric form. However instead of having six-fold symmetry interphase, each dimer of hexamer is slightly different from each other. This indicates that, most probably the functional unit of ssDNA bound Rad51 is a dimeric form. According to this structure, ATPase site of the protein is placed between

the interphase of protomers. Another confirmation of crystal reveals the association of N-terminal domain of one protomer with the ATPase domain of other (162).

## 1.4.4.2 Rad51 path upon DNA damage: From initiation to the destination

DNA damage causes dramatic changes in the expressions and re-localizations of several DNA repair proteins. Contribution of Rad51 in all stages of HR is well appreciated, where it makes several contacts with different HR proteins. Considering the importance of Rad51 it becomes apparent, that its cellular levels must be properly controlled for efficient HR. Expression of Rad51 is highly dependent and regulated by cell cycle stages. Highest expression of Rad51 is observed in S/G2 phase of cell cycle, which indicates its connection with intra chromosomal recombination repair (175-180). Rad51 also gets up regulated upon DNA damage to serve its functions in HR mediated DNA repair (181-183). Up regulation of Rad51 is also witnessed in several types of tumor cells, where occurrence of unscheduled DNA breaks is observed due to excessive cell divisions. This indicates the frequent requirement of Rad51 to repair such breaks in tumor cells (184, 185). Besides, high abundance of Rad51 in tumor cells is reported to have several consequences. Like, it increases the rate of recombination which ultimately hampers the radiation mediated treatment of tumor cells. The high rate of recombination makes tumor cells resistant towards radiation induced DNA damage and cell death. Apart from up regulation, Rad51 has another layer of regulation which includes; ATM induced phosphorylation and post translational modifications (186). Tyrosine 315 of Rad51 gets phosphorylated by c-Abl and mutation in this residue makes cells sensitive towards damage (187). This phosphorylation is essential for the

association of Rad51 with dsDNA and its nuclear translocation (188). Another site of phosphorylation is observed in N-terminal domain of Rad51, which is tyrosine 54. This phosphorylation has negative impact on Rad51 functions, as it is associated with inhibition in the formation of joint molecule during DNA repair (189). Threonine 309 of Rad51 gets phosphorylated by Chk1 and this is required for the formation of Rad51 foci at broken DNA (190). Rad51 phosphorylation at serine 192 by Mec1 kinase helps in ATPase activity and DNA binding (191). Other than phosphorylation, Rad51 functions are also regulated by sumoylation by its interaction with HsUbc9. Rad51 sumoylation plays important role in the intracellular trafficking of Rad51, as this interaction allows the localization of Rad51 to synaptonemal complex (192). After reaching to the nucleus Rad51 forms active foci on damaged site, which is a hallmark of DNA repair (193). Rad51 paralogs like XRCC2, XRCC3, Rad51B and Rad51C have been extensively studied and it is believed that inappropriate expression of Rad51 paralogs result in the defective Rad51 foci formation upon genotoxic stress. Capan-1 cells, which harbor functionally defective BRCA2, show defective Rad51 foci formation upon DNA damage (194, 195). Many studies demonstrated that Rad51 translocates to the nucleus upon DNA damage and starts accumulating in the nucleus immediately after DNA damage. However, Rad51 is a 43 kDa protein and according to sequence analysis it does not carry NLS. Active NLS is considered as an essential component for the nuclear trafficking of proteins, which are larger than 20 kDa (196). Therefore, how Rad51 crosses nuclear membrane barrier upon DNA damage for participating in HR is not very clear. A tumor suppressor gene called BRCA2 interacts with Rad51 via its BRC repeats. Accumulation of Rad51 along with BRCA2 is observed in the form of foci inside the nucleus (197). However these Rad51 foci were decreased from the BRCA2 defective cells, which indicate the possible requirement of BRCA2 for Rad51 foci formation (198). This study highlights that

Rad51 is sequestered by BRCA2 in the inactive form under normal cellular conditions and it relocalizes to the site of repair upon DNA damage. Additional studies in this line revealed that, in normal Human pancreatic carcinoma cell lines (MiaPaca) Rad51 and BRCA2 were distributed evenly, between cytoplasm and nucleus. Next, Rad51 distribution was studied in Capan-1 cells, which express truncated copy of BRCA2. In these cell lines BRCA2 has a frame shift mutation due to the deletion at 6174th position, which generates stop codon and results in C-terminal truncation. When these cell lines were probed for the presence of Rad51, it was reviewed that Rad51 accumulates in the cytoplasm and only a small fraction was observed in the nucleus. Therefore, it is assumed that BRCA2 is essential for Rad51 nuclear accumulation (199). However BRCA2 independent mechanism for Rad51 nuclear clearly exists and this became apparent from another study, which has demonstrated BRCA2 independent movement of Rad51 to the nucleus. In this study, DNA damage associated Rad51 pool was increased to significant level in BRCA-2 deficient Capan-1 cells (200, 201). Another report added the important insight in the Rad51 nuclear translocation upon DNA damage. Here HeLa and HCT116 cell lines were studied for Rad51 nuclear translocation upon DNA damage. This report indicates the importance of Rad51C, which is a paralog of Rad51, for its nuclear entry. Rad51C carries functional NLS and nuclear pool of Rad51 and Rad51C were correlated in this study, which indicates the probable role of Rad51C for Rad51 movement to the nucleus. This was further evident by RNA interference-mediated depletion of Rad51C, where increment in the Rad51 levels was not co related with the DNA damage (202). However presence of Rad51 inside the nucleus was still witnessed in Rad51C siRNA treated HeLa cells, upon DNA damage. After reaching to the nucleus Rad51 then loads itself to the damaged site which gives rise to the formation of visible Rad51 foci in the nucleus (Figure 8).

Figure 8: Diagrammatic representation of translocation of Rad51 in response to DNA damage

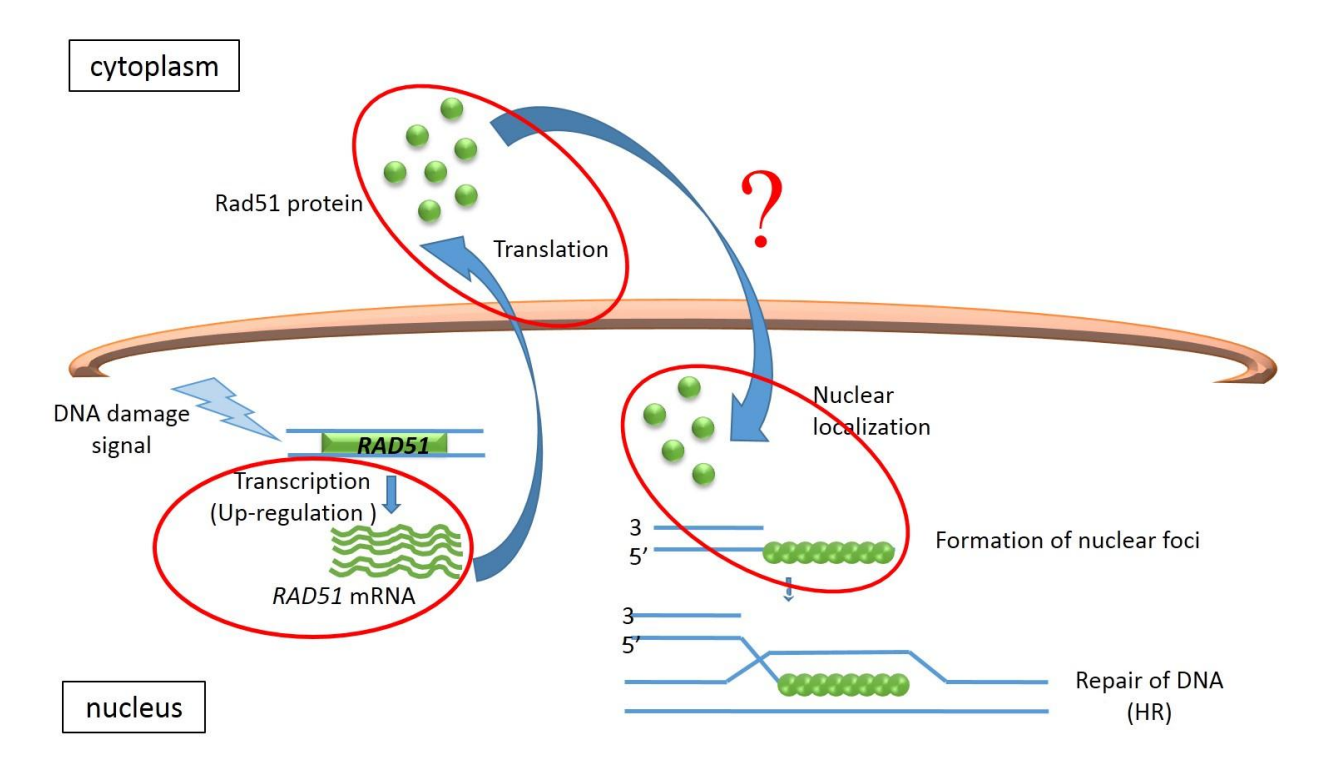


**Figure 8:** Figure showing different steps involved in Rad51 biology in response to DNA damage. First it gets up regulated upon DNA damage at transcript and protein level, which then moves to cytoplasm where post translational modifications occur upon DNA damage. Next it translocates back to the nucleus to participate in homologous recombination.

### 1.4.5 Importance of homologous recombination

HR has long been established as an essential pathway for DSBs repair however it is also recognized for providing valuable services to many other cellular processes. Mutations in key factors of HR like BRCA1 and BRCA2 are associated with deleterious effects, as these mutations cause tumor phenotype. Hence BRCA1 and BRCA2 are known as tumor suppressor gene and mutations in BRCA1 and BRCA2 result in breast, ovarian, pancreatic and prostate cancer (207-210). Defects in BRCA2 are also responsible for the occurrence of kidney, brain and hematological tumors, which are the consequences of fanconi anemia (211). Apart from these two proteins, Rad51 also comes under tumor suppressor gene category (212). Besides these observations, study on breast cancer cells manifests the higher efficiency of HR in breast cancer cells than in the normal cells. This observation suggests the importance of HR for repair of DNA in cancer cells (102). Treatment of cancer cells with anticancer drugs produces DNA lesions, which are known to get repaired by HR (213). This finding is supported by a study, which observed that mutations in BRCA1, cause sensitivity towards Mitomycin C, tirapazamine and poly (ADP-ribose) polymerase inhibitors (214, 215). This is the reason behind many recent ongoing studies, where several inhibitors such as of HR are being analyzed for the treatment of cancer (216). HR actively participates in resolving inter stand cross links and is considered as a sole pathway for repairing ICLs (interstrand crosslinks) (217). Deeper understanding of this exposes many of the HR proteins like BRCA2, Rad51 paralogs, Rad54 and Rad54B to be a part of ICLs repair mechanism (218). Rad51, a key component of HR is required for proper embryo development. This is observed, because Rad51 functional disruption is associated with the defect in the repair of replication associated DNA damage and inter stand cross links (219, 220). HR is actively involved during replication, which is marked by the co localization of Rad51 foci with replication components and increase in Rad52

foci upon inactivation of DNA polymerase alpha. Experiments on yeast and xenopus revealed that, newly synthesized DNA molecule is guarded by HR factors, immediately after replication (221). HR is also remarked for helping in, congregation and renovation of replisome machinery at dormant replication fork (222).

Additional functions of HR are witnessed at the ends of DNA, which is a structure protected by many proteins and known as telomere. Initial analysis indicates that HR usually remains suppressed at telomeres, however in recent years it is highlighted for its active participation at telomeres. Repair of DSBs at telomere takes place using HR machinery. This is unveiled from the identification of the 3' C-rich ssDNA at telomere and telomere-clustering, which is a sign for the presence of HR between sister-chromatid. This telomere clustering is withheld by the inhibition or inactivation of key HR player called Rad51 (223). HR proteins like Rad51 and Rad51 paralog Xrcc3 and Rad52 helps in the formation of telomeric D-loops, which protect the chromosome (224). Likewise HR also promotes the formation of secondary structure at telomere called T-loop, which protects the telomere ends. These observations are supported by the study, which indicates that Rad51-/- and Brca2-/- result in the occurrence of telomere dysfunction-induced foci (TIFs) (225, 226). Telomeres are the structure, which hampers the smooth movement of replication fork and result in the stalled fork. Many of the HR proteins are observed to be associated with telomere like BRCA2, Rad51, Rad51C, Rad51D and Rad54 which help to facilitate accurate replication at telomere. Disruption in the function of any of these HR proteins results in the shorten telomeres (227, 228). Preserving a prime position in many of the cellular processes, HR is reflected to be an important pathway, which needs to be regulated tightly in order to deliver proper functions. Several factors which are known till date, to regulate HR are depicted in figure 9.

**DNA Damage Response** HR targets components ATM < MRN(Ser-343,278) CtIP(Ser-664,745) Brca1(Ser-1423,1457 ATR -CtIP(Thr-859) Rad51(Thr-309) Chk1-Chk2-Brca1(Ser-988) **Cell Cycle Protein Stability** HR targets components HR targets components HSP90 Brca2 Cdk1/2 Brca2(Ser-3291) BLM **Novel Factors** RPA(Ser-13) components HR targets RBMX -Nbs1(Ser-432) SPG48 -CtIP(Ser-267) SPF45 -Rad201 Rad51 CycD1 Pso4 Rad51(Ser-14) Plk1 WNR Rad51(Ser-13) Cdc5L CK2 Psf27 Plk3 **Growth Factors** components HR targets **EGFR** Brca1 IGF1R Rad51 IRS-1 stimulation → inhibition unknown interaction

Figure 9: Regulatory factor of homologous recombination

Adapted from Małgorzata Krajewska et al 2015, review, frontiers in genetics

Figure 9: Regulation of homologous recombination with different factors.

# 1.5 Expanding wings of Hsp90: Maintaining genomic integrity

Upon stress, Hsp90 delivers the functional confirmation to the proteins that in turn maintains the protein homeostasis. However upon conditions, when Hsp90 is chemically inhibited or overloaded in the cells, it transmits deleterious effect to the cells. In recent years functional disruption of Hsp90 is related with genetic variations (229). Lesions in the genome which cannot be taken care by high fidelity DNA polymerase is repaired by translesion synthesis (TLS). One of the polymerases of this pathway, called Y-polymerase, is dependent on Hsp90 for its functions. Direct interaction of this polymerase is evident from the co-purification studies, where this polymerase is co-purified with the Hsp90. Hsp90 maintains the cellular pool of Y-polymerases and regulates its functions by targeting it to the TLS site and by aiding its interaction with PCNA (230). The function of Hsp90 in TLS is further extended by its requirement for another TLC polymerase called Rev1, which is dependent on Hsp90 functions for its stability.

Hsp90 is required for Rev1 and PCNA interaction and Hsp90 inhibition triggers UV induced mutagenesis associated with loss of Rev1 function (231). Another DNA repair protein Chk1 directly interacts with Hsp90 and has been established as a client of Hsp90 (232). Association of Hsp90 with DSBs repair pathway is also evident from several upcoming reports on cancer cells. These studies make Hsp90 as an emerging new target for the cancer therapy, which is evident from combined treatment of cancer cells with DNA damaging agents and Hsp90 inhibitors. Geldanamycin based inhibitors of Hsp90 impact radio sensitivity towards cancer cells (233, 234). 17-allylamino-17-demethoxygeldanamycin (17-AAG) which is a well-studied inhibitor of Hsp90's ATPase activity, affects the cell survival in DU145 and SQ-5 cancer cells upon radiation induced DNA damage. Detailed report of this work suggests that BRCA2 interacts with Hsp90

and inhibition of Hsp90 with 17-AAG results in the cellular clearance of this protein, which in turn hampers BRCA2 associated functions, such as Rad51 foci formation. However, contradictory finding shows that 17-AAG treatment to normal human fibroblasts (HFL III) cells does not imprint any sensitivity towards radiations (235). The effect of another Hsp90 inhibitor 17-DMAG was studied on the MiaPaCa tumor cells. This treatment signifies the defect in the DNA repair, as disappearance of H2AX foci was observed from the damaged DNA. Defect in the H2AX foci was reported to be a consequence of hampered DNA-PK activation upon Hsp90 inhibition. Hsp90 inhibition also blocks the radiation induced activation of signaling protein ATM kinase. MRN complex interacts with Hsp90 and in a condition of Hsp90 inhibition it is unable to form MRN foci to the broken DNA (236). In this direction, another inhibitor NVP-AUY922 has been tested on human head and neck squamous cell carcinoma xenograft model. This inhibition displayed delayed Rad51 foci formation upon DNA damage (237). Hsp90 at Thr-7 residue was found to be phosphorylated immediately upon DNA damage and observed in the repair foci, which indicates the importance of Hsp90 at the site of DNA repair. Detailed mechanistic understanding of Hsp90 association with DNA repair revealed the role of DNA-PK in Hsp90 phosphorylation (238). Another report showed the decrease in Rad51 proteins levels in non-small cell lung cancer cell lines A549 and H1975 upon 17-AAG treatment. Although no change was observed at mRNA level of Rad51 and this phenotype was restored upon episomal Rad51 expression (239). In a very recent report, Hsp90 inhibitor Ganetespib was used for the treatment of ovarian cancer and it suggests the dependency of fanconi anemia repair pathway (required for the repair of TLC) on Hsp90. Ganetespib causes the sensitivity to Carboplatin-induced inter strand crosslinks (ICLs). This report concludes that FancA, which is a member of TLC pathway, is a client of Hsp90 (240). In the same line, another protein of DNA repair pathway called XRCC1 is linked with Hsp90. XRCC1 is tabilized with the association on Hsp90 and this helps in the pol $\beta$  recruitment to the damaged site (241). List of DNA repair proteins which owe their folding, stability and functions to Hsp90 are mentioned here.

## 1.5.1 DNA repair proteins dependent on Hsp90 functions

BRCA1 and BRCA2: Breast cancer susceptibility genes are known as BRCA1 and BRCA2, as mutations in these genes result in the onset of breast and ovarian cancer. Both BRCA1 and BRCA2 functions are associated with the homologous recombination pathway. Upon DNA damage BRCA1 gets phosphorylated by signaling kinases like ATM, ATR and CHK2 (113). Phosphorylated BRCA1 in association with multi protein complexes helps in recognition of damaged DNA and activation of cell cycle check point (117). BRCA1 further recruits MRE11/RAD50/NBN, BRCA2, CHK1, FANCA and Rad51 to the damaged site (242, 243). The inhibition of Hsp90 by 17-AAG, leads to the ubiquitination and proteasomal degradation of BRCA1. 17-AAG treatment results in the hypersensitivity of BRCA1 deficient cells due to the defect in G2/M checkpoint activation (244). On the other hand Hsp90 directly interacts with BRCA2 and inhibition of Hsp90 with 17-AAG destabilizes BRCA2. Inhibition of Hsp90 with 17-AAG causes delayed foci formation of Rad51 on damaged DNA (235).

CHK1: CHK1 is a serine threonine kinase which is activated upon replication stress and DNA damage. Once activated by ATR mediated phosphorylation, it further promotes cell cycle arrest in G2 phase and inhibits the initiation of new replication (245). 17-AAG results in the clearance of CHK1 protein which sensitizes Gemcitabine induced, S-phase arrest in tumor cells (232). Dose dependent reduction in the CHK1 level is also observed in NVP-AUY922 treated cells (237).

**DNA-PK:** It is a nuclear serine threonine kinase, involved in the NHEJ mediated DNA repair pathway (247). In epithelial cervix carcinoma cell line, DNA-PK is established as a client of Hsp90. Radicicol mediated inhibition of Hsp90 results in the degradation of cytosolic but not nuclear DNA-PK (248). Treatment of cells with 17-DMAG hampers the IR induced activation of DNA-PK (249).

The FA Pathway: This is known as Fanconi anemia DNA repair pathway and consists of a complex of eight proteins namely FANCA, FANCB, FANCC, FANCE, FANCF, FANCG, FANCL, and FANCM. This complex recognizes DNA damage, which is induced by inter strand cross links. (250). This core complex along with ATR activated FANCD2 and FANCI interacts with BRCA1 and BRCA2 and maintains genomic integrity by the coordination of HR, NHEJ, and TLS repair pathways (251, 252). FANCA is sensitive to Hsp90 inhibitions and follows proteasomal degradation upon 17-AAG treatment. Hsp90 inhibition by 17-AAG is also associated with the defect in the DNA damage induced activation and cytoplasmic retention of FANCD2. Furthermore 17-AAG causes chromosome abnormalities and cytotoxicity due to DNA crosslinks (253, 254).

**The MRE11/RAD50/NBN Complex:** This complex is involved in the detection and signaling of DSBs and actively functions in both NHEJ and HR pathway of DSBs repair (255). Treatment of MiaPaca cells with 17-DMAG results in the defective foci formation by MRN complex to the damaged DNA. This inhibition also hampers the interaction of NBN with ATM during DNA damage (234).

**MSH2:** Being a critical component of mismatch repair pathway, MSH2 helps in the recruitment of other proteins of this pathway to the site of mismatch (256). Treatment of NSCLC (Non-small-

cell lung carcinoma) and lung adenocarcinoma cells with Pemetrexed along with 17-AAG affects the MKK3/6-p38 MAPK signal which in turn reduces MSH2 protein levels (258).

PCNA and Polymerase η: DNA polymerase η is an active player of translesion DNA synthesis (TLS), which functions to remove cyclobutane pyrimidine dimers. Polη interacts with mono ubiquitinated PCNA and accumulates in the form of nuclear foci at replication stalled site to incorporate correct base at opposite strand (259). Hsp90 functions are essential for the folding and activation of Polη. Hsp90 inhibition results in the cytotoxicity and mutagenesis, which are mediated by the inactivation of Polη. Thus Hsp90 functions are important for the regulation of TLS (230). Studies on HCT-116 (human colon cancer cell line), HNSCC-1483 (human head and neck cancer cell line) and HT-29 (human colorectal adenocarcinoma) indicate the complex formation between Hsp90 and PCNA. Hsp90 inhibition with Geldanamycin degrades PCNA hence results in impaired TLS (260).

**XRCC1:** X-ray cross complementing group 1 protein XRCC1 facilitates the DNA repair by base excision repair pathway (BER). It is also crucially important for other DNA repair pathways such as NHEJ or nucleotide excision repair (NER). BER pathway removes the DNA alteration which is caused by misincorporation of bases, oxidative damage, alkylating damage, chemical damage or spontaneous DNA damage. XRCC1 along with DNA polymerase β helps in the recruitment of other BER proteins to the damaged site. To efficiently repair SSBs, XRCC1 interacts with pol β, DNA ligase III and PARP1 (261). Hsp90 is reported as an important protein for the stability of polβ unbound XRCC1 protein. Inhibition of Hsp90 results in the degradation of XRCC1 by ubiquitin-mediated degradation pathway. Type of complex like XRCC1/Hsp90 or XRCC1/phospho-Hsp90, depends upon the type of DNA damage and cell cycle stage, which in

turn decides the BER sub pathway choice. Hsp90 phosphorylation supports the complex formation of XRCC1 with other proteins (241).

Apart from inhibitory consequences of Hsp90 on DNA damage sensitivity, over-expression of Hsp90 is also witnessed to have deleterious effects on cells upon DNA damage. One such report indicates that higher level of Hsp90 represses the signaling kinase Rad53 (homolog in human Chk1) at transcriptional level which consequently renders cells sensitive towards DNA damage. These observations highlight the importance of Hsp90 in DNA repair and indicate towards the essentiality for tight regulation of Hsp90 level in the cells (262). This made us to have deeper understanding about the structure function relationship of Hsp90 and DNA repair. However the exact role of Hsp90 in HR pathway still remains ambiguous. It is clearly evident from many studies that cancer cells have higher expressions of Hsp90 than normal cells. Cancer cells also have high demand for Hsp90 functions due to stressed condition in the tumor environment.

# 1.6 Significance of the study

Our work signifies the salient function of Hsp90 in homologous recombination (HR) pathway of DNA repair. Hsp90 being a highly conserved chaperone, keeps the central position in many cellular pathways. It is highly abundant in cancer cells than normal cells where it stabilizes many oncoproteins. According to one of the recent reports, inhibition of Hsp90 in cancer cells is related to inefficient DNA repair however; in normal cells such inhibition does not cause any changes in DNA repair efficiency. Thus, it is important to analyze whether Hsp90 is associated directly or indirectly with the DNA repair machinery. Out of the two major double strand break repair pathways, homologous recombination (HR) is majorly utilized by cancer cells whereas the normal cells show preferences towards non homologous end joining. Moreover as HR is essential for replication, telomere maintenance and other cellular processes, it is interesting to find out its regulatory elements. Our work on model organism Saccharomyces cerevisiae identified that the key player of HR Rad51, is dependent on Hsp90 for its functions. Our detailed study has revealed the requirement of ATPase domain and charged linker region of Hsp90 for this process. Our work highlighted that the charged linker region of Hsp90 is involved in DNA damage induced Rad51 foci formation in the nucleus. Rad51 is devoid of nuclear localization signal (NLS) and its nuclear translocation has not been studied in detail. Our work for the first time indicates that the dynamic association between Hsp90 with Rad51 facilitates the nuclear entry of Rad51 upon DNA damage. Thus, our study has established that Hsp90 is required for Rad51 stability and it modulates its nuclear entry upon DNA damage. This link between Hsp90 and Rad51 will be beneficial for better understanding of the DNA repair pathway which is the central component of tumor growth and maintenance. There exists a considerable similarity between the key recombination proteins

within human and *Saccharomyces cerevisiae*, so our study can be extrapolated to study the same in mammalian cell. In tumor cells HR mediated DNA repair pathway is favored over NHEJ. Thus understanding the cellular redistribution of the major recombination protein Rad51 can be exploited in targeting HR pathway in tumor cells. Further, it will be interesting to study the DNA damage induced changes in the Hsp90-Rad51 complex, which will give a better understanding about the Hsp90 mediated regulation of HR.

# 1.7 Objective of the study

We aim to study the role of Hsp90 in maintaining genomic integrity. To that end, using *Saccharomyces cerevisiae*as a model system, we have determined whether Hsp90 controls homologous recombination (HR) mediated DNA repair pathway. Rad51 is one of the major players involved in the HR mediated DNA repair in higher eukaryotes. We aimed to understand whether Rad51 stability and function is maintained via Hsp90. Using various mutants of Hsp90 we have determined the structure function relationship between Hsp90 and Rad51. Apart from providing stability to its client proteins, Hsp90 is also involved in the localization of its clients to various cellular compartments. We have asked whether DNA damage induced Rad51 translocation to the nucleus is mediated by Hsp90. Using in-silico studies we have identified the critical amino acid residues of Rad51 which are interacting strongly with Hsp90. We generated those mutants of *rad51* and our study has addressed whether those mutants result in defect in Rad51 translocation to the nucleus as well as Rad51 recruitment to the broken DNA junction upon DNA damage...

# 1.8 Specific Aims of the study

# 1. Understanding the role of Hsp90 in DNA repair

To study this, we took the advantage of well characterized temperature sensitive mutant as well as various point mutants and charged linker deletion mutants of yHsp90. Utilizing these isogenic mutant strains of yHsp90, we have determined which functional domain of yHsp90 is required for maintaining cell survivability upon DNA damage as well as required for efficient homologous recombination.

# 2. Identification of homologous recombination proteins which are dependent on Hsp90 functions

To address this question we probed the cellular level of two key HR proteins namely Rad51 and Rad52 in above mentioned Hsp90 mutant background. Our study aims to identify the functional domains of Hsp90 which are required for providing stability and DNA damage induced function of Rad51.

# 3. DNA damage induced nuclear import of Rad51 is mediated by dynamic interaction between Hsp90 and Rad51 interactions

On the basis of *in silico* studies, we have identified the strong interacting pairs of amino acids between Hsp90 and Rad51. We mutated two such important residues of *rad51* and studied the consequence of those mutants towards nuclear localization upon DNA damage and subsequently their effect on DNA damage sensitivity.

### MATERIAL AND METHODS

# 2.1 MOLECULAR BIOLOGY TECHNIQUES

## 2.1.1 Bacterial plasmid DNA isolation by alkaline lysis method:

Bacterial cells harboring required plasmid were inoculated in 10 ml of LB medium and incubated at 37°C, 200 rpm for overnight. It was then centrifuged at 4,000 rpm for 15 minutes to pellet the cells. Cell pellet was re-suspended in 400 µl of solution I (Tris 25 mM pH 8, EDTA 10 mM) and was transferred to a 1.5 ml micro-centrifuge tube. 400 µl of solution II (0.2 N NaOH, 1% SDS) was added to the tube and mixed well by inverting 4-5 times and incubated for less than 5 minutes at room temperature. Subsequently, 300 µl of ice cold solution III (3 M sodium acetate) was added to the tube and incubated on ice for 5 minutes with intermittent mixing. It was then centrifuged at 12,000 rpm for 15 minutes at room temperature and supernatant was collected in a 1.5 ml microcentrifuge tube. Supernatant was then mixed with 2.2 volume of absolute alcohol and kept at -20°C for 45 minutes for precipitation. After incubation at -20°C, the sample was centrifuged at 12,000 rpm at 4°C to precipitate the DNA. The pellet was washed with 70 % alcohol and resuspended in 50 µl of 1X Tris-EDTA buffer. For removing RNA from the sample 2-3 µl of 100 mg/ml RNase was added to the sample and incubated at 37°C for 20 minutes. Then, equal volume of phenol, chloroform, isoamyl alcohol mixture (25:24:1) was added and mixed well by vortexing for 3 minutes. Subsequently, the sample was centrifuged at 12,000 rpm for 15 minutes at room temperature and the upper aqueous layer containing DNA was taken out in micro-centrifuge tube. DNA was then precipitated by adding 2.2 volumes of 100% ethanol and 1/10<sup>th</sup> volume of solution III and incubated at -80°C for 2 hours. Plasmid was precipitated by centrifuging sample at 12,000 rpm, 4°C. Plasmid DNA was then washed with 70% alcohol by centrifuging for 5 min at 12,000 rpm, 4°C. The pellet containing plasmid was air-dried and re-suspended in 30 µl 1X TE buffer.

# 2.1.2 <u>Bacterial competent cell preparation:</u>

A single bacterial colony was inoculated in LB broth (Luria-Bertani medium) at 37°C for overnight. Next day, 500 μl of primary culture was inoculated in 25 ml of LB media and the secondary culture was incubated at 37°C till the OD<sub>600</sub> reached 0.5. Cells were then harvested by centrifuging the culture at 8,000 rpm, 4°C, for 8 minutes. The supernatant was discarded and the pellet was very gently re-suspended in 12.5 ml of ice-cold CaCl<sub>2</sub> (0.1 M) solution. The suspension was centrifuged at 8,000 rpm, 4°C for 8 minutes and the supernatant was discarded. The pellet was again re-suspended in 6.75 ml of ice-cold CaCl<sub>2</sub> (0.1 M) and incubated on ice for (4-8) hours to make cells competent. The cells were harvested by centrifuging the culture at 8,000 rpm, 4°C, for 8 minutes. The pellet was re-suspended in 1.070 ml of ice-cold CaCl<sub>2</sub> (0.1M) and 170 μl of glycerol. The cell suspension was then divided into 100 μl aliquots in pre-chilled microfuge tubes, frozen in liquid nitrogen and stored at -80°C for further use.

# 2.1.3 <u>Bacterial transformation:</u>

Around 100 ng of DNA was added on the top layer of competent cells and incubated on ice for 30 minutes. Cells were exposed to heat shock at 42°C for 30 seconds and immediately chilled on ice for 2-3 minutes. 900µl of Luria Broth was added to the cells and incubated at 37°C for 1 hour with shaking. The cells were then centrifuged at 10,000 rpm for 2 min and most of the supernatant was discarded. Pellet was re-suspended in rest of the supernatant and spread on Luria agar plate containing appropriate antibiotic. Plates were incubated at 37°C for 12-16 hours.

## 2.1.4 Semi Quantitative RTPCR:

Total RNA was isolated from yeast strains namely *iG170Dhsp82*, P82a control, *T101Ihsp82*, HH1a-p2HG/Hsp82 and HH1a-p2HG/Hsp82 (211-259). 15 μg of RNA was reverse transcribed

using oligo dT primer (Sigma Aldrich) and reverse transcriptase (Omniscript kit, Qiagen) to generate cDNA. The resulting c-DNA was then PCR amplified (27 cycles) using gene specific primers. The PCR products were run on 1.4 % ethidium bromide (Himedia) containing agarose gel. OSB16 and OSB14 primer pairs were used to amplify 307 bp of the 3' end of the *ACT1* transcript. To amplify 326 bp of the 3' end of *RAD51*, OSB44 and OSB45 primers were used. To amplify 208 bp of the 3' end of *RAD52* we used OSB133 and OSB134 primers. *ACT1* transcript of each sample was used to normalize the corresponding PCR amplified sample.

## 2.1.5 Real time RT-PCR:

For real time reverse transcription-PCR (RT-PCR), cDNA was first quantified and then diluted (1:50) to normalize. This diluted cDNA was used for PCR with an RT-PCR kit (Roche) and primer set OSB16/OSB14 for *ACT1*, OSB44/OSB45 for *RAD51* and OSB133/OSB134 for *RAD52*. The real-time analysis was carried out using an Applied Biosystems 7500 Fast Real-time PCR system. The threshold cycle (C<sub>T</sub>) value of the *ACT1* transcript of each sample was used to normalize the corresponding (C<sub>T</sub>) values of the *RAD51* and *RAD52* transcripts.

# 2.1.6 Site Directed Mutagenesis:

Point mutations were introduced in *RAD51* by using Splice Overlap Extension (SOE) PCR technique. Primer set with required mutations was designed, to incorporate mutation in *RAD51* at desired location. Yeast genomic DNA was used as a template and full length gene was amplified in two segments in order to insert point mutation (Figure 10). For amplifying first (A) and second (B) segment to generate *E108Lrad51* mutation, OSB305/OSB314 and OSB315/OSB293 primer sets were used respectively. For generating *M142Lrad51* mutation first and second segments were amplified by using OSB305/OSB322 and OSB323/OSB293 primer sets respectively. Full length of *RAD51* containing either *E108L* or *M142L* mutation was then amplified by using Segment A

and B with primer set OSB305/OSB293. Following *rad51* mutants were cloned into yeast expression vector pESC-HIS. Subsequently all *rad51* mutants were amplified using primer set OMKB90/OMKB88 and sub-cloned into *pTA* yeast expression vector. After sequencing constructs namely; *pTA/E108Lrad51* and *pTA/M142Lrad51* were transformed into yeast strain lacking native *RAD51* to create TSY17 and TSY18 strains respectively. NRY1 and NRY2 were used as a control and created by transforming empty *pTA* and *pTA/ScRAD51* respectively.

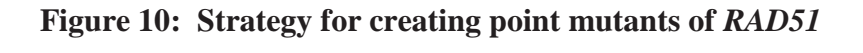
## 2.2 METHODS IN YEAST GENETICS

## 2.2.1 RNA isolation from yeast:

Yeast cells were grown in 5 ml of respective media for overnight. Next day, secondary culture was given in 10 ml media of choice using overnight culture and allowed to grow up to mid log phase. Cells were pelleted down by centrifuging at 3,000 rpm for 5 min and washed with DEPC treated water. The cell pellet was re-suspended in Tris-EDTA-SDS buffer (10 mM TrisHCl, 10 mM EDTA, 0.5% SDS). Equal volumes of phenol were added and the solution was vortexed for 10 seconds. Resulted sample was incubated at 65°C for 1 hour, with intermittent vortex. The mixture was immediately placed on ice for 5 min and centrifuged at 14,000 rpm for 10 min at 4°C. Aqueous layer was taken into new tube and RNA was precipitated by adding chilled ethanol at -80°C. Finally RNA was precipitated by centrifugation at 14,000 rpm at 4°C. The precipitate containing RNA was washed with 70% ethanol and finally re suspended in DEPC treated water.

# 2.2.2 Yeast competent cell preparation:

Desired yeast strain was grown in 5 ml of respected media at 30 °C for overnight. Next day, the secondary culture was given for final absorbance (0.6-0.8) in 40 ml medium and incubated at 30 °C till the OD<sub>600</sub> reached. The culture was then centrifuged and cell pellet was washed with 10 ml



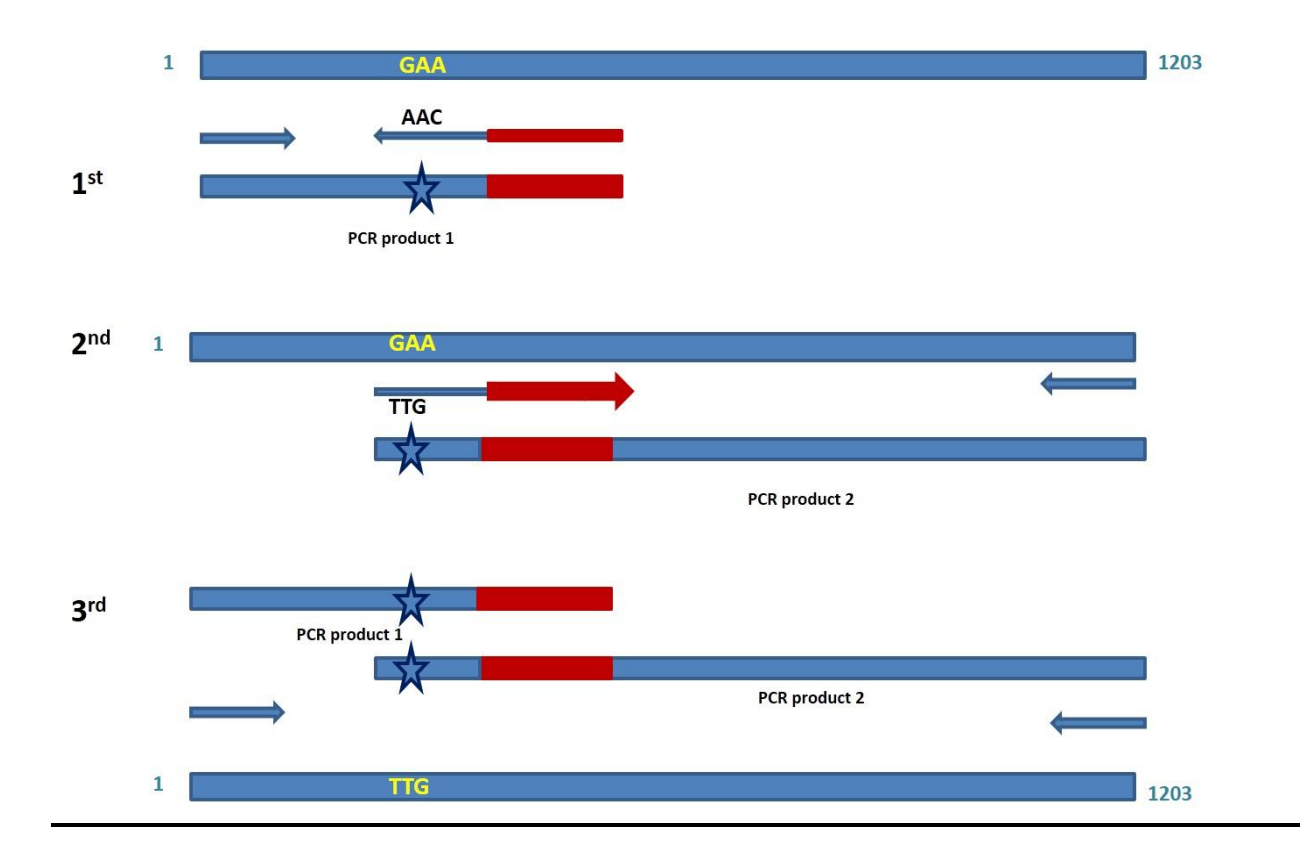


**Figure 10:** Schematic representation of the strategy used for creating *rad51* point mutants: An illustration of *E018Lrad51* mutant generation, showing three rounds of PCR amplification in order to incorporate mutation at desired location. Here GAA (codon for Glutamic acid) sequence in converted to TTG (codon for Leucine).

sterilized water. Washed cells were finally re-suspended in 300 µl Lithium solution (1X Tris-EDTA, 1X Lithium Acetate) and thus competent cells were prepared.

## 2.2.3 Yeast transformation:

(0.5-1)  $\mu g$  of DNA was mixed with 10  $\mu g$  of carrier in a tube and 200  $\mu l$  of competent yeast cells was added gently over the DNA mixture in each transformation tube. 10  $\mu g$  of carrier DNA in a tube with 200  $\mu l$  of competent cells was taken as negative control. Next, 1.2 ml of PEG solution [10X LiOAc (Sigma), 10X TE, 50% PEG 2000 (Sigma)] was added and it was incubated at 30 °C for 30 minutes with shaking. After that cells were exposed to heat shock at 42°C, 15 min followed by incubation on ice for 5 min. The cells were then collected by centrifugation at 10,000 rpm for 10 seconds. The pellet was re-suspended in 200  $\mu l$  1X Tris-EDTA buffer and then spread on appropriate plates. The plates were incubated at 30°C till transformed colonies were observed.

# 2.2.4 Yeast genomic DNA isolation:

Yeast cells were inoculated in 10 ml of media and culture was grown overnight at 30°C in shaker incubator. Overnight grown culture was centrifuged at 3,000 rpm at room temperature for 5 min. The cell pellet was washed with 500 µl of autoclaved double distilled water and centrifuged for 10 seconds. The Supernatant was removed and the pellet was re-suspended into 200 µl breaking buffer [Triton X-100 (2%) (Qualigen), SDS (1%), NaCl (0.1 M) containing glass beads (Sigma) and 200 µl of phenol/chloroform mixture. Finally this mixture was vortexed for 5 minutes. In the sample 200 µl 1X Tris-EDTA buffer (10 mM Tris-HCl, 1 mM EDTA pH 8.0) was added and mixed by vortexing followed by centrifugation at maximum speed for 5 minutes at room temperature. Supernatant was collected into a new tube and 1 ml 100% absolute ethanol was added followed by the incubation at -20°C for 30 minutes. The DNA was precipitated by centrifugation at 12,000 rpm for 5 minutes. Resulting pellet was dissolved in 400 µl of 1X Tris-EDTA buffer and RNase (10

mg/ml) (SRL) was added to remove RNA. 2.2 volume of 100% absolute ethanol and 10 μl of 4 M NH<sub>4</sub>OAc (Fisher scientific) were added and the mixture was incubated at -20°C for 1 hour to precipitate the DNA. Genomic DNA was collected by centrifuging the sample at maximum speed for 5 minutes at room temperature. Resulting pellet containing genomic DNA was washed with 70% ethanol and dissolved in 1X Tris-EDTA buffer.

# 2.2.5 <u>Protein isolation</u>:

Yeast cells were inoculated in 5 ml of appropriate medium and grown overnight at 30°C at 200 rpm. Overnight grown culture was inoculated into fresh 20 ml of appropriate media and grown till the OD<sub>600</sub> reached 0.5. Cells were harvested by centrifuging the secondary culture at 3000 rpm for 5 min. Pellet was washed in 500 µl of autoclaved water and centrifuged again to remove the residual medium. The pellet was then first washed with TCA followed by centrifugation. Resulted supernatant was discarded and the pellet was re suspended in TCA. Glass beads were then added in the sample and vortexed thoroughly. Supernatant containing protein was transferred to a new 1.5 ml microfuge tube. The mixture of cells and glass beads was washed with TCA by vortexing with intermittent cooling on ice and the supernatant was again collected into the same tube. Sample was centrifuged and the supernatant was discarded. The precipitated protein was dissolved in 60 µl 1X sample buffer (Tris-HCl, pH 6.8, 2% SDS and bromophenol blue). The sample was then boiled for 3-5 minutes and centrifuged at top speed for 5 min.

# 2.2.6 Gene knockout:

Knock out of RAD51 in NA14 strain was done by homologous recombination strategy using knockout cassette flanked with RAD51 upstream and downstream sequences. To that end, we used a  $\Delta rad51$  strain LS402, where RAD51 is replaced by LEU2 cassette. We used OSB159 and OSB320 primer pairs to amplify the cassette from LS402 strain. This cassette was then transformed

into NA14 cells to knock out RAD51. Forward primer OSB159 and reverse primer OSB313 were designed using RAD51 up stream sequence and LEU2 sequence respectively to confirm rad51 knockout. In this way we generated yeast strain (NA14 $\Delta rad51$ ).

## 2.2.7 Gene tagging:

MYC tagging at the C-terminal end of RAD52 was done by using plasmid pFA6a-13Myc-kanMX6 as a template and primers OSB68 and OSB69 were used to amplify MYC tagging cassette. PCR amplified product of 2.3-kb size was used to target the RAD52 loci of W303a, iG170Dhsp82 and T1011 mutants by homologous recombination to generate SLY47, SLY49 and MVS36 respectively. We have tagged MYC epitope to RAD52 locus in HH1a-p2HG/Hsp82 (211-259) strain by swapping HH1a-p2HG/Hsp82 (211-259) plasmid with the plasmid harboring T1011 mutation in MVS36 strain and generated the strain SLY65.

# 2.2.8 Cellular fractionation:

Strains NRY2, TSY17, TSY18 and TSY19 were inoculated in 10 ml respective medium and kept at 30°C for overnight. Next day, secondary culture was given at 30°C and cells were grown till 0.5 at OD<sub>600</sub> in selective media. Half batch of cells was then treated with 0.15% of MMS and continuously grown at 30°C for 2 hrs along with the untreated batch of cells. After 2 hrs of MMS exposure 100 OD<sub>600</sub> cells were taken and washed with PBS containing DTT and PMSF. Cells were then incubated with 4 ml spheroplast buffer (18.2% sorbitol, 1% glucose, 0.2% yeast nitrogen base, 0.2% casamino acids, 25 mM HEPES pH 7.4, 50 mM Tris, 1 mM DTT) for 15 minutes at 30°C with gentle shaking. After incubation, cells were re suspended in 4 ml of spheroplast buffer, 3 ml YPDS (YPD, 1M sorbitol) and lyticase enzyme. It was then allowed to grow at 30°C with gentle shaking for 1.5 hours. 12 ml YPDS was added into spheroplasts and spun at 4000 rpm for 10 minutes. Washing of the spheroplast was performed with ice cold 12 ml YPDS followed by

spinning at 4000 rpm for 5 minutes. Spheroplast was re-suspended in 12 ml of 1 M ice cold sorbitol and spun at 4000 rpm for 5 minutes. Ultimately the spheroplast was re suspended in 5 ml of Buffer N (25 mM K<sub>2</sub>SO<sub>4</sub>, 30 mM HEPES pH 7.6, 5 mM MgSO<sub>4</sub>, 1 mM EDTA, 10% Glycerol, 0.5% NP40, 3 mM DTT, 1% protease inhibitor cocktail) and homogenized by giving 20 strokes under chilled condition. Homogenized spheroplast was spun at 2000 rpm at 4°C for 15-20 minutes to pellet down the cell debris. We pelleted down the nuclei at 6000 rpm for 25 minutes at 4°C. This nuclear fraction was then re-suspended in 50 µl of buffer N and used for the western blotting analysis. Resulted supernatant then mixed with equal volume of 20% TCA and incubated on ice for 30 minutes to precipitate cytoplasmic fraction. Next it was centrifuged at 3500 rpm for 15 min followed by washing with chilled acetone at 3500 rpm for 5 min. The pellet was resuspended in 1X SDS loading dye (Tris-HCl, pH 6.8, 2% SDS and bromophenol blue). The sample was then boiled for 3-5 minutes and centrifuged at top speed for 5 min.

### 2.3 GENETIC ASSAYS

### 2.3.1 MMS and UV sensitivity assay:

This assay was done with SLY4, SLY5, *iG170Dhsp82*, HH1a-p2HG/Hsp82, HH1a-p2HG/Hsp82(211-259), P82a, T22I, A41V, G81S, T101I, G313S, iA587T, TSY1, TSY2, TSY3, SLY69, NRY1, NRY2, TSY17 and TSY18 yeast strains, in order to check their DNA damage sensitivity. Here TSY1 and SLY69 yeast strains were generated by transforming pTA-*ScRAD51* construct into HH1a-p2HG/Hsp82 (211-259) and *iG170Dhsp82* yeast strains respectively. For generating TSY2 and TSY3, empty pTA vector was transformed into HH1a-p2HG/Hsp82 (211-259) and *iG170Dhsp82* strains respectively. All strains were grown in respective medium (YPD broth/ TRP dropout synthetic medium) for overnight at 30°C. Next day, secondary culture was grown till 0.5 O.D<sub>600</sub> at 30°C. After O.D<sub>600</sub> reached to 0.5, the culture was divided into two sets.

One set of cells was treated with 0.03% (vol/vol) of methyl methane sulfonate (MMS) (Sigma Aldrich) and grown at 30°C for 2 hrs and another set was continuously grown at 30°C for 2 hrs without MMS. After that MMS was washed out and cells were serially diluted to 10-10 fold. Serially diluted treated and untreated cells were then spotted on normal selective media. For quantitative assessment, 1000 cells were plated on selective media and incubated at 30°C for 2-3 days. The ratio of the number of cells grown in the presence of MMS to the cells grown in the absence of MMS was multiplied by 100, which gave the value of percent survival. Each assay was repeated at least (3-4) times. In the similar manner to check sensitivity of cells towards UV induced DNA damage, cells were grown in respective medium till 0.5 OD<sub>600</sub>. After that, equal number of cells was plated in four different plates. One plate was kept as untreated and other were exposed to 50 Joules/m<sup>2</sup>, 100 Joules/m<sup>2</sup> and 150 Joules/m<sup>2</sup> and the number of viable CFU (colony forming unit) for each was determined. The required intensity of UV irradiation was carried out using Stratagene Stratalinker 1800. Plates were incubated for 3-4 days and the number of viable colonies for each indicated dosage of UV radiation was counted and the percent survivability was calculated.

### 2.3.2 Gene conversion assay:

This assay was performed in NA14 strain (6) where a cassette containing *KANMX6* flanked by two copies of *URA3* is integrated in chromosome V [as presented in Figure 11]. One mutated copy of *ura3* harbors a restriction site for *HO* endonuclease. The *HO* endonuclease is under galactose inducible promoter. Growing cells in presence of galactose triggers the expression of *HO* endonuclease and creates single double strand break (DSB) in mutated copy of *ura3* gene. The repair product of this DSB determines the choice of the pathway utilized for the repair. Yeast

strains TSY20, TSY21, TSY22 and TSY23 were created by transforming pTA (empty vector), pTAScRAD51, pTAScE108Lrad51, pTAScM142Lrad51 respectively into NA14\Delta\rad51 strain. The transformed cells were initially patched on a plate containing glycerol as a sole carbon source. Next, equal number of cells were counted and spread on two different plates, one containing glycerol and other containing galactose as a carbon source and incubated at 30°C for 3-5 days. Cells survived on galactose plates were then patched on another plate containing G418 sulfate and incubated at 30°C for 36 hours in order to determine the percentage gene conversion. Cells grown on G418 sulfate containing plates certainly utilize Rad51 mediated gene conversion pathway for the repair as they retain KANMX6. The ratio of number of cells grown on G418 sulfate plate to the cells grown on galactose plate was calculated to determine the percent gene conversion. The assay was performed more than 3 times and means values were plotted using Graphpad Prism.

### 2.3.3 Gene targeting Assay:

This assay was performed using a plasmid called pSD158. This plasmid harboring the homologous stretches of upstream and downstream sequences of *ADH4* flanking the *ADE2* gene and a *KANMX6* selectable marker upstream of the *ADH4* sequence. The plasmid was digested using SalI restriction enzyme, which results in the 7.3Kb and 3.3Kb fragments. Concentration of 7.3Kb fragment was checked and two micrograms of the DNA was transformed into each strain. Transformants were first grown on an SC-Ade plate and were subsequently replica plated on a G418 sulfate-containing plate. In each case, the Ade G418S colonies were counted. Gene-targeting efficiency was normalized by transforming an equal amount of uncut replicating plasmid into the respective strains to nullify any variation arising from the difference in competence for DNA uptake between strains. The gene-targeting efficiency, expressed as a percentage, was calculated as (number of Ade G418S colonies in each mutant)/(number of Ade G418S colonies in P82a) × 100.

Figure 11: Gene conversion assay cassette

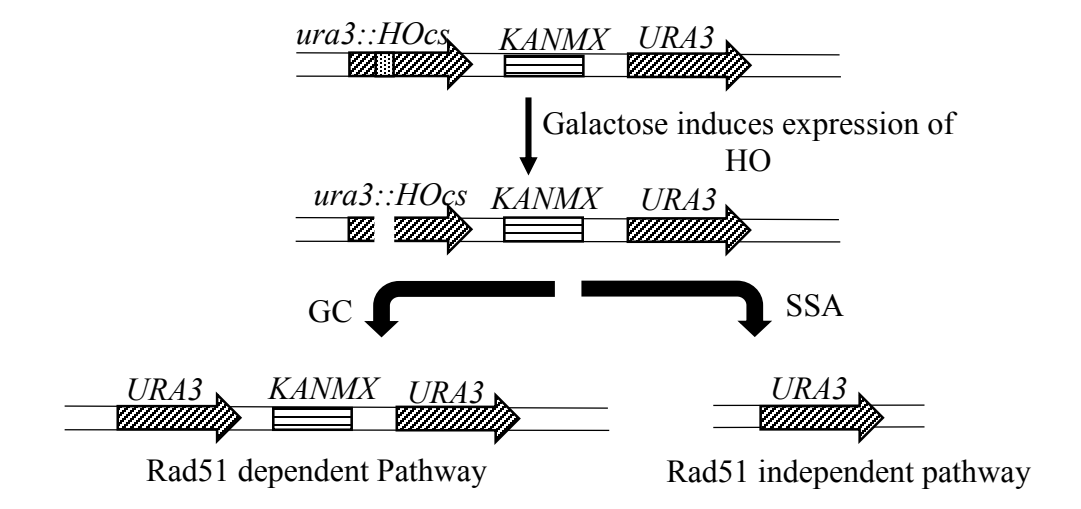


**Figure 11:** Schematic presentation of the gene conversion assay cassette: This cassette is incorporated in strain, which is used for studying gene conversion efficiency. It harbors two copies of *URA3* one of which is mutated by inserting *HO* endonuclease site. Induction with galactose created single DSBs in mutated *ura3*, repair of which takes place either by Rad51 dependent or by Rad51 independent manner. *KANMX* cassette will be retained if repair happens via Rad51 dependent manner.

### 2.4 BIOCHEMICAL METHODS

### 2.4.1 Chromatin immunoprecipitation assay:

Strains TSY20, TSY21, TSY22 and TSY23 were grown in the selective media till 0.3 at OD<sub>600</sub> in presence of 3% glycerol. Half batch of cell was then treated with 3% galactose for 3 hrs and other half batch of cell was continued to grow in glycerol media. We used cells corresponding to 60 at OD<sub>600</sub> and added 1% formaldehyde for cross-linking at 30°C for 15 minutes, at 100 rpm. Then cells were incubated with 2.5 M glycine at 30°C for 5 min. Cells were pelleted down and washed with 1X PBS buffer containing DTT and suspended in 2 ml of spheroplast buffer (18.2 % sorbitol, 1 % glucose, 0.2 % yeast nitrogen base, 0.2 % Casamino Acids, 25 mM HEPES [pH 7.4], 50 mMTris, 1 mMdithiothreitol). The lyticase enzyme was then added to the cells and incubated at 30°C for 1 hr 30 minutes to make spheroplasts. Spheroplast were then washed with 500 µl of ice cold 1XPBS (10 mM KH<sub>2</sub>PO<sub>4</sub>, 40 mM K<sub>2</sub>HPO<sub>4</sub>, 150 mM NaCl) containing PMSF. The pellet was then re-suspended in ice cold HEPES, Triton X-100 buffer (0.25% Triton X-100, 10 mM EDTA, 0.5 mM EGTA, 10 mM HEPES, pH 6.5) containing 0.5 mM PMSF and protease inhibitor cocktail (Roche) and was spun down at 7000 rpm for 7 minutes. Ultimately, the spheroplasts were resuspended in ice cold HEPES, NaCl buffer (200 mM NaCl, 1 mM EDTA, 0.5 mM EGTA, 10 mM HEPES [pH 6.5]), containing 0.5 mM PMSF and protease inhibitor cocktail and again centrifuged at 7000 rpm for 7 minutes. Finally the spheroplast was re suspended in 100 µl of SDS lysis buffer (1% SDS, 10 mM EDTA, 50 mM Tris [pH 8.1]) containing 0.5 mM PMSF and protease cocktail inhibitor and sonicated (Elma, Model-S-60H). After sonication, 1 ml of IP dilution buffer (1.1% Triton X-100, 1.2 mM EDTA, 16.7 mM Tris [pH 8.1], 167 mM NaCl, 0.5 mM PMSF and protease cocktail inhibitor) was added to the sample and left on ice for 15 minutes to form the chromatin fraction. 1 µg anti Rad51 antibody was added to the sample to precipitate

Rad51 bound DNA fragment. Recruitment of Rad51 was then monitored by PCR using primer set OSB278 and OSB279 in a reaction volume of 50 µl using the immuno precipitate and input DNA samples. Samples were subjected to electrophoresis on 1.5% agarose. For control ChIP was performed with rabbit IgG antibody. To verify whether double stranded break (DSB) was generated by HO digestion in the assay strain we used OSB289 as a forward primer which is complementary to the 20 bp upstream of HOcs and a reverse primer (KanB1) which is complementary to the *KANMX* gene. Amplification of sequence close to HO restriction site will occur only in the absence of HO endonuclease induced DSB. We amplified full length *ACTIN* using OSB14 and OSB16, which is used as a normalization control.

### 2.4.2 Western Blot Analysis:

Western blot was done to check Rad51p/Rad52p levels in *iG170Dhsp82*, SLY20, SLY47, SLY49, MVS36, SLY65, SLY69, TSY1, TSY2, TSY3, NRY1, NRY2, TSY17 and TSY18 strains. Protein samples were loaded on SDS polyacrylamide gel. Polyvinylidene difluoride (PVDF) membrane was used for the western which was pretreated with methanol for 20 seconds followed by water wash then transfer buffer (Tris buffer, glycine, SDS and methanol) for 5 minutes. Protein from gel was then transferred to pre treated PVDF membrane. Subsequently, the blot was incubated with the blocking buffer (5 % nonfat dry milk dissolved in 1X TBS-T) for 2 hours at room temperature. Blot was then incubated with the required primary antibodies for overnight at 4°C. Next day, the blot was washed with 1X TBS-T buffer (0.2 M Tris base, 9 % NaCl, pH 7.6, 0.1 % Tween-20). After washing, the, blot was incubated with appropriate secondary antibody for 2 hours at room temperature followed by washing with TBS-T buffer. The primary antibodies used, were mouse anti-Act1 antibody (Abcam), Rabbit anti-Rad51 (Promega), mouse anti-Hsp82 antibody (Calbiochem) at 1:5000 dilutions. Rabbit anti-Myc antibody (Abcam) was used at 1:8000 dilutions

Anti-Pgk1 antibody (Novus Biologicals) and mouse Anti-Nsp1 antibody (Abcam) were used at 1:3000 and 1:5000 dilutions respectively. For secondary antibodies Horseradish peroxide-conjugated anti-rabbit antibody (Promega) and anti-mouse antibody (Santa Cruz Biotechnology Inc. CA, USA) were used at 1:10,000 dilution. The western blots were developed using chemiluminescent detection system (Pierce).

### 2.4.3 Treatment with inhibitors:

For treatment with 17AAG, the cells were grown till 0.3 O.D.<sub>600</sub> at 30°C followed by addition of 17AAG at the working concentration of 40  $\mu$ M and was allowed to grow for overnight. In case of experiments which require mid-log phase cells, a secondary inoculum was given in the next day in the presence of 17AAG and the cells were grown till the required O.D. was reached. For treatment with MG132, wild type strain ( $\Delta pdr5$ ) was grown at 37°C overnight in the presence of MG132 at the working concentration of 50  $\mu$ M.

### 2.4.4 Recombinant protein purification:

*RAD51*, *E108Lrad51* and *M142Lrad51* were cloned in pET22b vector (annexure I) with C-terminal 6xHIS tag using primer set OSB305/OSB293. For Hsp90 purification, cloned *HSP90* in pET28a with N-terminal 6xHIS tag was utilized. These clones were transformed into *Escherichia coli* BL-21 DE3\* cells. Transformants were patched and single colonies of each clone were inoculated into LB media containing ampicillin for pET22b-Sc*RAD51*, pET22b-Sc*E108Lrad51 and pET22b-ScM142Lrad51*. Similarly LB media containing kanamycin was used for selection of *pET28a-HSP90* clones. Secondary culture was grown till OD<sub>600</sub> 0.6-0.7, then 1 mM IPTG was added and cells were grown for 4 hrs at 37°C. For Hsp82 protein purification cells were pelleted down and re suspended in lysis buffer (50 mM NaH<sub>2</sub>PO<sub>4</sub>, 1M NaCl, 20 mM imidazole, 50% Glycerol, 20 mM β-mercaptoethanol) containing PMSF. Cells were lysed using sonicator (SONICS Vibram

Cell TM) by giving 15-16 bursts at 200 W for 40 sec with intermittent cooling keeping on ice for every 5 min interval. Cell lysate was collected by centrifugation at 10,000g for 45 min at 4°C and kept for binding with 50% Ni-NTA agarose (Qiagen) for 1hr. The loading flow through (LFT) was collected and column was washed with 8 column volume of wash buffer (50 mM NaH<sub>2</sub>PO<sub>4</sub>, 300 mM NaCl, 20 mM imidazole, 50% Glycerol, 20 mM β-mercaptoethanol, 2% Tween 20). Column was also washed with two more wash buffers (8 column volumes) containing 50 mM imidazole and other having 100 mM imidazole. Elution was performed with 4 column volumes of elution buffer (50 mM NaH<sub>2</sub>PO<sub>4</sub>, 300 mM NaCl, 150 mM imidazole, 50% Glycerol, 20 mM βmercaptoethanol, 2% Tween 20), finally two more elution buffers were used one containing 250 mM imidazole and the other containing 400 mM imidazole. We observed fairly purified protein in last few fractions, which were eluted with 400 mM imidazole buffer. These fractions were dialyzed and purified protein was stored for further use. Similar protocol was followed to purify ScRad51,  $Scrad51^{E108L}$  and  $rad51^{M142L}$  with little modifications in buffer composition. In this case, the lysis buffer (50 mM NaH<sub>2</sub>PO<sub>4</sub>, 300mM NaCl, 10mM imidazole, 50% Glycerol, 20 mM βmercaptoethanol) composition was modified. We used the same composition of three wash buffers as mentioned earlier. Protein of interest was eluted with elution buffer containing 250 mM imidazole and 400 mM imidazole. Eluted fractions were loaded on 10% SDS-PAGE visualized by using Coomassie brilliant blue G-250 (Bio-Rad). Eluted fractions which have purified Hsp90, ScRad51, Scrad51<sup>E108L</sup> and rad51<sup>M142L</sup> were pooled individually for each protein and dialyzed against 20 mM TrisHCl (pH = 8), 1 mM dithiothretol (DTT), for SPR analysis.

#### 2.4.5 Surface plasmon resonance:

SPR experiments were performed on a Biacore T200 (GE Healthcare). Purified Hsp90 (1.83  $\mu$ M) was immobilized on a series CM5 chip (GE Healthcare) with amine coupling. Immobilization was

done with 10 mM sodium acetate pH 4.0 (Immobilization buffer). For washing of chip, 50 mM NaOH was used as wash solution at 25 °C according to manufacturer's protocol. Reference cell was treated with same buffers without protein immobilization. Final Response 265.8 RU was observed after surface activation with Hsp82. Binding experiments were performed at 25°C in buffer HBS-EP pH 7.4 [(0.1 M HEPES, 1 M NaCl, 30 mM EDTA, 0.5% v/v surfactant P20) (GE Healthcare Life Sciences)] with flow rate 30 μL/min, contact time 180 s and dissociation time 120 second. Column was regenerated after flow of each concentration with Glycine-HCl pH 2.5, with flow rate 30 μL/min. Sensogram was plotted taking RU (response unit) at y-axis and time at x-axis and kinetic parameters were calculated using SPR Biacore T200 Evaluation software version 2.0 (GE Healthcare). We repeated this experiment with fresh immobilization of Hsp90, where after surface activation we observed the final response as 288.6 RU. This second set of experiment was performed using same buffers and same experimental conditions with same concentrations of analytes.

Table2: List of yeast strains used in the study

Strains	Genotype	Source
iG170Dhsp82	MATacan1-100 ade2-1 his3-11,15 leu2-3,112 trp1-1 ura3-1	D. Picard
mutant	hsp82::LEU2 hsc82::LEU2HIS3::HSP82G170D	(270)
P82a (control)	MATacan1-100 ade2-1 his3-11,15 leu2-3,112 trp1 ura3-1	S. Lindquist
	hsp82::LEU2 hsc82::LEU2 CEN pTGPD/P82	(269)
T101I mutant	MATacan1-100 ade2-1 his3-11,15 leu2-3,112 trp1 ura3-1	S. Lindquist
	hsp82::LEU2 hsc82::LEU2 CENpTGPD/T3-138	(269)
НН1а-	MATahsp82::LEU2 hsc82::LEU2 ade2 his3 leu2 trp1 ura3	D. Picard
p2HG/Hsp82	HSP82-2-HIS (p2HG/Hsp82)	(270)
HH1a-p2HG/	MATahsp82::LEU2 hsc82::LEU2 ade2 his3 leu2 trp1 ura3	D. Picard
Hsp82(211-259)	HSP82(211-259)-2-HIS[p2HG/Hsp82(211-259)]	(270)
NRY1	MATa leu2-3,112 trp1-1 can1-100 ura3-1 ade2-1 his3-11,15	This study
	[phi+]RAD51::LEU2 pTA	
NRY2	MATa leu2-3,112 trp1-1 can1-100 ura3-1 ade2-1 his3-11,15	This study
	[phi+]RAD51::LEU2 pTA/ScRAD51	
TSY17	MATa leu2-3,112 trp1-1 can1-100 ura3-1 ade2-1 his3-11,15	This study
	[phi+]RAD51::LEU2 pTA/Scrad51(E108L)	
TSY18	MATa leu2-3,112 trp1-1 can1-100 ura3-1 ade2-1 his3-11,15	This study
	[phi+]RAD51::LEU2 pTA/Scrad51(M142L)	
LS402	MATa leu2-3,112 trp1-1, can1-100, ura3-1, his 3-11, ade2-1, RAD51::LEU2	This study

NA14	NA14 MATa -inc ura3-HOcs lys2::ura3-HOcs-inc ade3:: GALHO	Agmon et
	ade2-1 leu2-3,112 his3-11,15 trp1-1 can1-100	al. (289)
NA14	MATa-inc ura3-HOcs lys2::ura3-HOcs-inc ade3::GALHO ade2-1	This study
(∆rad51)	leu2-3,112 his3-11,15 trp1-1 can1-100 RAD51::LEU2	
SLY47	MATaleu2-3,112 trp1 ura3-1 ade2-1 his3-11,15 VIIL::ADE2 Rad52-13MYC-KANMX6	This study
SLY49	MATacan1-100 ade2-1 his3-11,15 leu2-3,112 trp1 ura3-1	This study
	hsp82::LEU2 hsc82::LEU2 HIS3::HSP82G170DRad52-13MYC-	
	KANMX6	
MVS36	MATacan1-100 ade2-1 his3-11,15 leu2-3,112 trp1 ura3-1	This study
	hsp82::LEU2 hsc82::LEU2 CEN pTGPD/T3-138 Rad52-13MYC-	
	KANMX6	
SLY65	MATacan1-100 ade2-1 his3-11,15 leu2-3,112, trp1 ura3-1	This study
	hsp82::LEU2 hsc82::LEU2pRS313hsp82(211-259) Rad52-	
	13MYC-KANMX6	
SLY4	MATaleu2-3,112 trp1 ura3-1 ade2-1 his3-11,15 VIIL::ADE2	Lskar et al.
	hsc82:: KAN <sup>r</sup>	(51)
SLY5	MATaleu2-3,112 trp1 ura3-1 ade2-1 his3-11,15 VIIL::ADE2	Laskar <i>et al</i> .
	hsp82:: KAN <sup>r</sup>	(51)
T22I	MATacan1-100 ade2-1 his3-11,15 leu2-3,112 trp1 ura3-1	S. Lindquist
mutant	hsp82::LEU2 hsc82::LEU2 CENpTGPD/T3-142	(269)
A41V	MATacan1-100 ade2-1 his3-11,15 leu2-3,112 trp1 ura3-1	S. Lindquist
mutant	hsp82::LEU2 hsc82::LEU2 CEN pTGPD/T1-40	(269)
G81S	MATacan1-100 ade2-1 his3-11,15 leu2-3,112 trp1 ura3-1	S. Lindquist
mutant	hsp82::LEU2 hsc82::LEU2 CEN pTGPD/T1-15	(269)
T101I	MATacan1-100 ade2-1 his3-11,15 leu2-3,112 trp1 ura3-1	S. Lindquist
mutant	hsp82::LEU2 hsc82::LEU2 CENpTGPD/T3-138	(269)

G313S	MATacan1-100 ade2-1 his3-11,15 leu2-3,112 trp1 ura3-1	S. Lindquist
mutant	hsp82::LEU2 hsc82::LEU2 CEN pTGPD/T4-47	(269)
iA587T	MATacan1-100 ade2-1 his3-11,15 leu2-3,112 trp1 ura3-1	S. Lindquist
mutant	hsp82::LEU2 hsc82::LEU2 hsp82 A587T::HIS3	(269)
	piHGPD/A587T	
TSY1	MATa hsp82::LEU2 hsc82::LEU2 ade2 his3 leu2 trp1 ura3	This study
	HSP82(211-259)-2-HIS [p2HG/Hsp82(211-259)]2μ(pTAScRad51)	
TSY2	MATa hsp82::LEU2 hsc82::LEU2 ade2 his3 leu2 trp1 ura3	This study
	HSP82(211-259)-2-HIS [p2HG/Hsp82(211-259)] 2μ-pTA	
TSY3	MATa can1-100 ade2-1 his3-11,15 leu2-3,112 trp1 ura3-1	This study
	hsp82::LEU2 hsc82::LEU2 HIS3::HSP82G170D 2μ-pTA	
TSY20	MATa-inc ura3-HOcs lys2::ura3-HOcs-inc ade3::GALHO ade2-1	This study
	leu2-3,112 his3-11,15 trp1-1 can1-100 RAD51::LEU2 pTA	
TSY21	MATa-inc ura3-HOcs lys2::ura3-HOcs-inc ade3::GALHO ade2-1	This study
	leu2-3,112 his3-11,15 trp1-1 can1-100 RAD51::LEU2	
	pTAScRAD51	
TSY22	MATa-inc ura3-HOcs lys2::ura3-HOcs-inc ade3::GALHO ade2-1	This study
	leu2-3,112 his3-11,15 trp1-1 can1-100 RAD51::LEU2 pTA	
	Scrad51(E108L)	
TSY23	MATa-inc ura3-HOcs lys2::ura3-HOcs-inc ade3::GALHO ade2-1	This study
	leu2-3,112 his3-11,15 trp1-1 can1-100 RAD51::LEU2 pTA	
	Scrad51(M142L)	
SLY20	MATaleu2-3,112 trp1 ura3-1 ade2-1 his3-11,15 VIIL::ADE2	Laskar <i>et al</i> .
		(51)
SLY69	MATacan1-100 ade2-1 his3-11,15 leu2-3,112 trp1 ura3-1	This study
	hsp82::LEU2 hsc82::LEU2 HIS3::HSP82G170D	
	2 pTAScRAD51	
	1	<u> </u>

Table3: List of primers used in the study

Primer	Sequence	Purpose
OSB16	5' TGA CCA AAC TAC TTA CAA CTC C	Forwards primer used to amplify
	3'	ACT1 for semi quantitative PCR
OSB14	5' TTA GAA ACA CTT GTG GTG AAC G	Reverse primer used to amplify
	3'	ACT1 for semi quantitative PCR
OSB 44	5' GTG GTG AAC TAA GCG CAA G 3'	Forwards primer used to amplify
		<i>RAD51</i> for semi quantitative PCR
OSB 45	5' CTA CTC GTC TTC TTC TCT GG 3'	Reverse primer used to amplify
		<i>RAD51</i> for semi quantitative PCR
OSB 133	5' TGG GAA TCA AGT ACC GCG TG 3'	Forwards primer used to amplify
		RAD52 for semi quantitative PCR
OSB 134	5' TCA AGT AGG CTT GCG TGC ATG 3'	Reverse primer used to amplify
		RAD52 for semi quantitative PCR
OSB305	5' CTC GGA TCC ATG TCT CAA GTT	Forward primer used to amplify
	CAA GAA CAA C 3'	full length <i>rad51</i> mutants
OSB293	5' GTC GTC GAC CTC GTC TTC TTC	Reverse primer used to amplify
	TCT GGG G 3'	full length <i>rad51</i> mutants
OSB315	5' AGT GGG CTT CAC ACT GCT TTG	Forward primer to create
	GCG GTA GCA 3'	E108Lrad51 mutation
OSB314	5' TCT GGG AGC ATA TGC TAC CGC	Reverse primer to create
	CAA AGC AGT G 3'	E108Lrad51 mutation
OSB323	5' GCG GCA AGG CTA GTG CCT TTG	Forward primer to create
	GGA TTT GTC 3'	M142Lrad51 mutation
OSB322	5'ATC AGC AGC CGT GAC AAA TCC	Reverse primer to create
	CAA AGG CAC TAG 3'	M142Lrad51 mutation

OMKB88	5' CTG CAG CTA CTC GTC TTC TC	Reverse primer to amplify full
	3'	length RAD51
OMKB90	5'GGA TCC TGT CTC AAG TTC AAG	Forward primer to amplify full
	AAC 3'	length RAD51
OSB159	5' TAC AGT ACG CGT GGT GGG 3'	Forward primer to amplify
		RAD51 knock out cassette
OSB320	5'CGA AGA CAA GGA AAT TCA TTG 3'	Reverse primer to amplify
		RAD51 knock out cassette
OSB313	5' ACG AAG TCA GTA CCT TTA GC 3'	Reverse primer to amplify <i>LEU2</i>
OSB68	5' AAG ACC AAA GAT CAA TCC CCT	Forward primer to MYC tag
	GCA TGC ACG CAA GCC TAC TCG	RAD52
	GAT CCC CGG GTT AAT TAA 3'	
OSB69	5' ATA ATG ATG CAA ATT TTT TAT	Reverse primer to MYC tag
	TTG TTT CGG CCA GGA AGC	RAD52
	GGAATTCGAGCTCGTTTA AAC 3'	
OSB278	5' CAT GCA AGG GCT CCC TAG C 3'	Forward primer used to amplify
		URA3 region for ChIP
OSB279	5' CAA CCA ATC GTA ACC TTC ATC T	Reverse primer used to amplify
	3'	URA3 region for ChIP
OSB289	5' GTT AGT TGA AGC ATT AGG TCC 3'	Forward primer used to confirm
		HO digestion
KanB1	5' TGT ACG GGC GAC AGT CAC AT 3'	Reverse primer used to confirm
		HO digestion

Table 4: List of Plasmids used in the study

Name of Plasmid	Brief description
pFA6a-KanMX6	It is utilized for gene knock out and carries ampicillin resistance
	gene as bacterial selectable marker.
pFA6a-13MYC-KanMX6	It is utilized for MYC tagging and carries ampicillin resistance
	gene as bacterial selectable marker.
pRS313/Δ211-259hsp82	It is CEN/ARS plasmid and harbors \( \Delta 211-259hsp82 \) mutant
	copy of <i>HSP82</i> under the control of GPD promoter. It has HIS
	marker and ampicillin resistance gene.
piHGpd/G170D	It carries mutated copy of <i>HSP82</i> , which has glycine to aspartic
	acid substitution at 170 <sup>th</sup> position under the control of GPD
	promoter. It is a multi-copy plasmid and carries HIS marker and
	ampicillin resistance gene.
pBEVYT-ScRAD51,	It is a 2μ plasmid and harbors either <i>WTRAD51</i> or mutant copy
pBEVYT-ScE108Lrad51,	of rad51 under GPD promoter. It has TRP marker and
pBEVYT-ScM142Lrad51	ampicillin resistance gene.
pET22b-ScRAD51,	Used for the expression of recombinant C-terminal His tagged
pET22b-ScE108Lrad51,	protein in bacterial system. It has ampicillin resistance gene and
pET22b-ScM142Lrad51	IPTG inducible promoter.

Used for the expression of recombinant N-terminal His tagged
protein in bacterial system. It has kanamycin resistance gene
and IPTG inducible promoter.
Used for the gene targeting assay. This plasmid have the <i>ADH4</i>
flanking the ADE2 gene and a KANMX6 selectable marker
upstream of the ADH4 sequence.

### **SPECIFIC AIM 1**

Understanding the role of Hsp82 in DNA repair

### 3.1 INTRODUCTION

Molecular chaperones are the key regulator of proteome homeostasis in the cell. Among all chaperones, Hsp90 is remarkably versatile, most abundant and highly conserved chaperone. In recent years, Hsp90 gained tremendous importance for providing its services to various cellular pathways like chromatin remodeling, transcription, RNA processing, DNA replication, telomere maintenance, translocation of proteins, signaling etc (263, 264). Apart from the balanced proteome, error free genome is a key for accurate cell survival, which is a result of accurate DNA repair. Studies on cancer cells indicate the possible connection of Hsp90 with DNA repair. However, because of the presence of contradictory reports, the exact role of Hsp90 in DNA repair still remained undefined. For example, 17-AAG (Hsp90 inhibitor) treated DU145 and SQ-5 human tumor cell lines become sensitive towards IR induced DNA damage, however similar treatment does not impart any defect to normal cells (235). Among different double stranded break repair pathways, mammalian cells employ specifically non homologous end joining (NHEJ) pathway (265). However, it is reported that, the efficiency of HR is elevated to significant level in sporadic breast cancer cells and NHEJ remains same as normal cells (103). This study signifies the importance of HR in cancer cells therefore altogether, this made us motivated to study in detail about the importance of Hsp90 in HR mediated DNA repair.

Hsp90 comprises of three functional domains namely; N-terminal domain (NTD), middle domain (MD) and C-terminal domain (CTD). The NTD has a binding pocket for ATP, which is required for the client protein maturation. The MD helps in client protein and co chaperone binding and CTD facilitates the dimerization of Hsp90 (266, 267). A long, flexible charged linker resides

between the NTD and MD, which has pentad repeat of the motif (D/E)(D/E)(D/E)KK and is absent from prokaryotic Hsp90 (37, 268). Charged linker mediates the contact between NTD and MD, hence affects the flexibility of Hsp90 (36, 38). Functions of Hsp90 are dependent on the ATP hydrolysis and the usage of different co chaperones. These co chaperones secure their binding site to specific domains of Hsp90 and function in client specific manner.

On the basis of these reports, we aimed to study the involvement of Hsp90 in HR under normal cellular condition and tried to uncover the essential domains of Hsp90 for DNA repair. To accomplish this task we used *Saccharomyces cerevisiae* as a model system, where HR is the predominant pathway of double strand break repair. Hsp90 has two paralogs in yeast; one is Hsp82 (which is expressed under stressed condition) and Hsc82 (which is constitutively expressed). Our study demonstrates that Hsp82 functions are important for the homologous recombination pathway of DNA repair. Detailed analysis with various well characterized mutants of Hsp82, unveils the importance of ATPase domain and charged linker region of Hsp82 for efficient DNA repair (269, 270).

### 3.2 RESULTS

## 3.2.1 Individual knock out of *HSP82* or *HSC82* does not affect the cell survivability upon DNA damage

In earlier studies, it is recognized that tumor cell lines (DU145 and SQ-5) become defective in radiation-induced DSB repair if prior treated with Hsp90 inhibitor 17-AAG. However, similar treatment does not impart any defect to normal cell lines. To explore whether Hsp90 is directly or indirectly linked to such phenotype we aimed to probe it in yeast as a model system where genetic manipulations can be achieved easily. Also, the HR machinery is highly conserved in Saccharomyces cerevisiae. We investigated the sensitivities of single mutant hsp82 and hsc82 towards DNA-damaging agents, such as MMS and UV radiation, which causes DNA damage via distinct mechanisms. Both the wild-type strain (SLY20) and the single mutants were exposed to 0.03% MMS for 2 h and were then returned to growth. Serial dilutions of treated and untreated cells were spotted onto the normal plates and incubated at 30°C for 2-3 days. Since defect in repairing damaged DNA in single cellular organism results in cell death, the accountability of cell survival can be a direct measure of the efficiency of DNA repair. After exposure to DNA damage we compared the growth of each strain treated and untreated with DNA damaging agents. We observed that the mutants  $\Delta hsp82$  (SLY5) and  $\Delta hsc82$  (SLY4) did not show significant difference in the survival upon MMS exposure than wild type cells (Fig. 12A). To have quantitative understanding after MMS treatment, we calculated equal number of treated and untreated cells of individual strains and then plated them on normal media for return to growth. Counting of the fractions of MMS-treated cells versus untreated cells reveals 85% cell survival of single knock out strains as compared to the wild type cells (Fig. 12B). These single mutants were also studied for

their sensitivity towards UV induced DNA damage. Equal number of  $\Delta hsp82$  and  $\Delta hsc82$  along with wild type cells were exposed to different doses of UV radiation. Percent viability was calculated in case of each strain by counting the number of survived colonies on treated and untreated plates. Our results show no significant difference among the survival of both single mutant compared to the wild type cells (Fig. 12C). These results suggest that the two paralogs HSP82 and HSC82 are redundant to each other towards DNA damage sensitivity.

Figure: 12

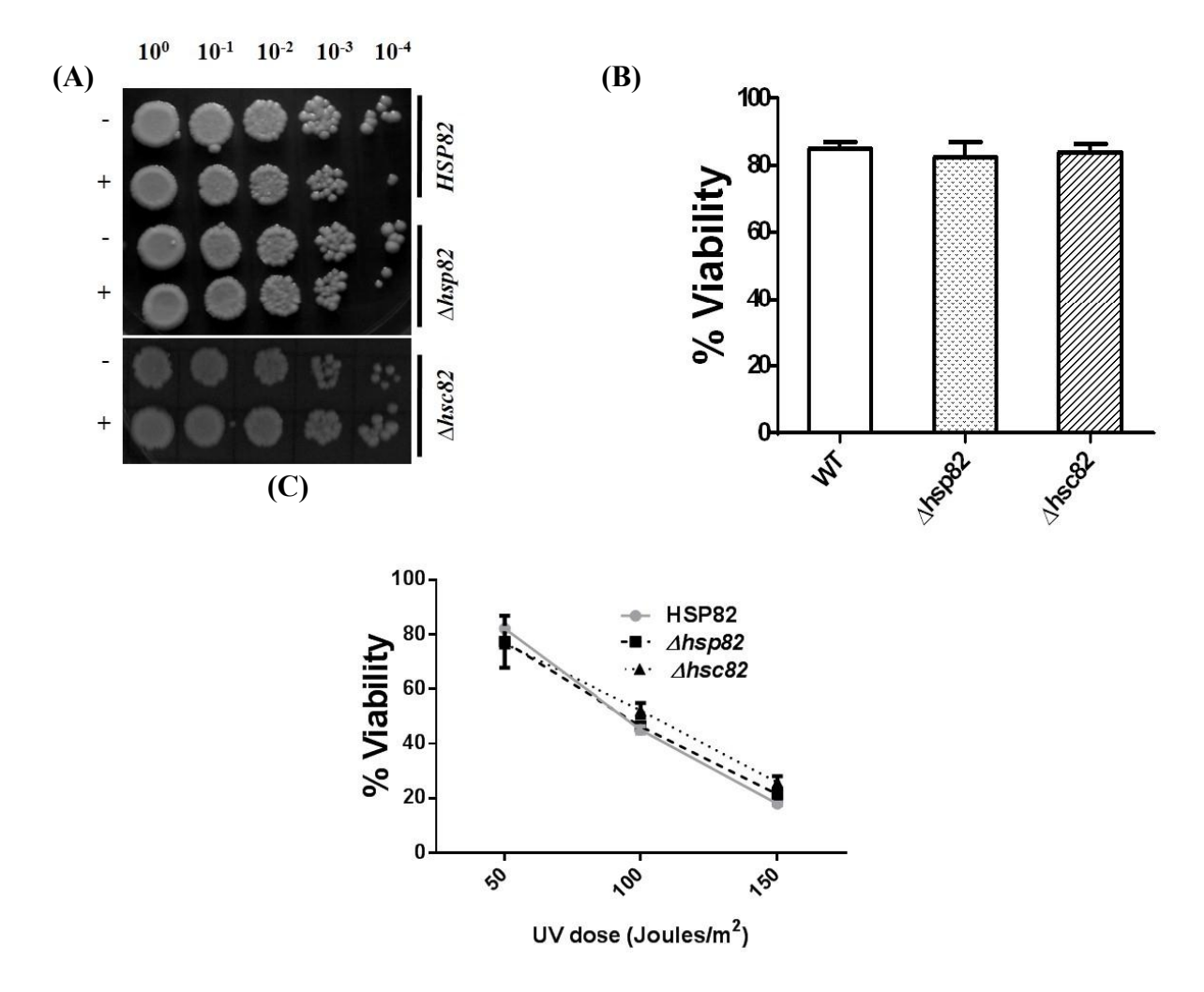


**Figure 12:** Individual knock out of *HSP82* and *HSC82* does not hamper DNA damage sensitivity of cells: (A) Return-to-growth experiments were performed with single mutant (*hsp82* or *hsc82*) strains and with their isogenic wild-type (*HSP82*) control. For each strain, the upper row represents serial dilutions of untreated cells (-) and the lower row represents serial dilutions of cells treated with 0.03% MMS (+). (B) Percentages of survivability upon MMS treatment were plotted as the plating efficiencies of MMS-treated cells relative to that of untreated cells. Each treatment was repeated three times, and the mean value (SD) was plotted. (C) Wild-type (*HSP82*), *hsp82*, and *hsc82* cells were irradiated with increasing doses of UV radiation. Percentages of viability were plotted as the plating efficiencies of irradiated cells relative to that of control cells. Mean values (SD) from three independent experiments were plotted.

### 3.2.2 Loss of Hsp82 function results in the poor survival of the cells upon DNA damage

We observed that individual deletion of either HSC82 or HSP82 does not affect the sensitivity of the cells upon DNA damage. In order to investigate the effect of double knock out of hsc82 and hsp82 in DNA repair, we used the strain that is devoid of both Hsc82 and Hsp82. Hsp82 is an essential protein and deletion of both the Hsc82 and Hsp82 copies, imparts lethal effect on the yeast cell survivability. Therefore to answer the question, whether Hsp82 has any role in DNA repair we took advantage of a mutant called iG170Dhsp82. In this mutant, the endogenous HSP82 and HSC82 are deleted and cells are surviving only on mutated copy iG170Dhsp82. This mutation renders Hsp82 nonfunctional at 37°C, as glycine at 170<sup>th</sup> position held conformationally restricted position and its switching with aspartic acid (G170D) destabilizes Hsp82 at higher temperature (37°C). Therefore we have used the *iG170Dhsp82* strain to investigate the effect of the abrogation of both Hsp82 and Hsc82 functions on DNA damage sensitivity. We allowed iG170Dhsp82 strain to grow at 25°C (permissive temperature) as well as at 37°C (restrictive temperature) for 2 h and 4 h prior to the treatment with 0.03% of MMS. When iG170Dhsp82 was incubated at 37°C for short time duration (2 h) we observed significant reduction in the growth upon DNA damage compared to that at 25°C. Further, extended incubation of iG170Dhsp82 at 37°C for 4 h makes cells hypersensitive to MMS induced DNA damage. However, the sensitivity towards MMS was not as severe as that of the *∆rad51* strain (Fig 13A). Quantitative measurement of the survivability of iG170Dhsp82 strain upon MMS treatment displayed a 62% decrement when grown at 37°C for 4 h compared to cells grown at 25°C (Fig 13B). In similar way incubation of iG170Dhsp82 at 37°C for 4 h followed by exposure to different doses of UV imparts more drastic effect on survivability than the strain grown at 25°C (Fig 13C). In order to establish that the growth defect in *iG170Dhsp82* strain is solely due to inactivation of Hsp82 and not because of the exposure to an

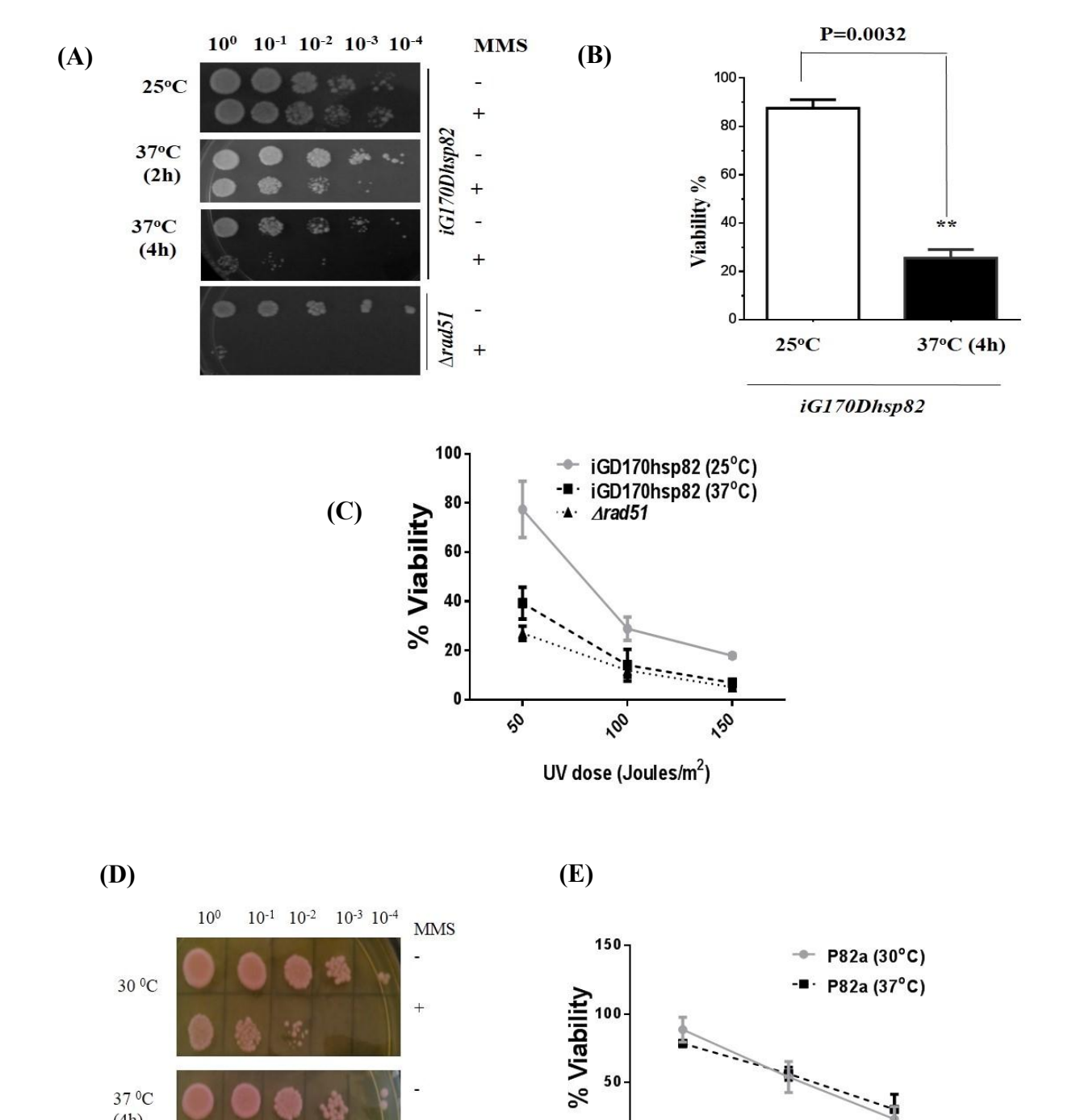
increased temperature, the MMS sensitivity of the isogenic wild-type cells (P82a) was monitored at 37°C. We incubated P82a cells at 37°C for 4 h prior to MMS exposure. We noticed that such conditions were well tolerated by P82a strain and no significant difference in the viability was observed upon MMS exposure compared to the cells grown at normal temperature 30°C (Fig 13D). Similarly sensitivity to UV was also monitored for P82a strain after pre-incubation at 37°C (for 4 h) and compared with the cells grown at 30°C. Similar trend was observed in the percent survivability between P82a grown at two various temperatures 37°C and 30°C (Fig 13E). Our experimental data explains that the sensitivity of *iG170Dhsp82* cells towards MMS and UV induced DNA damage is directly associated with the loss of Hsp82 function. It also indicates the importance of the presence of at least one of the paralogs of Hsp82 for cell survivability upon UV and MMS induced DNA damage.

150

UV dose (Joules/m²)

50

Figure: 13



37 °C (4h)

P82a

Figure 13: Functional knockout of Hsp82 affects DNA repair activity: (A) The *iG170Dhsp82* strain at a permissive (25°C) or a restrictive (37°C) temperature (duration, 2 h or 4 h) was treated with 0.03% MMS, and return-to-growth analysis was performed. A *rad51* strain served as a negative control. (B) Percentages of survivability upon MMS treatment were plotted for the *iG170Dhsp82* strain grown at 25°C or 37°C for 4hr. *P* values were calculated as 0.0032 using the two-tailed Student *t* test. (C) *iG170Dhsp82* cells were grown at 25°C or 37°C for 4 h and were then exposed to increasing doses of UV radiation. Percentages of viability were calculated as described above. The experiment was repeated three times and the mean values (SD) were plotted. (D) Return to growth assay with P82a strain after exposing to 0.03% of MMS for 4 hrs followed by spotting the serially diluted cells to normal media. Top row in each panel represents the untreated cells and bottom row represents treated cell. (E) Cell survivability assay upon UV induced DNA damage. Graph represents the percent viability of cells grown at 30°C and 37°C and exposed to different UV doses. Viability was calculated with respect to the untreated cells of respective temperatures and mean value of three individual experiment is plotted.

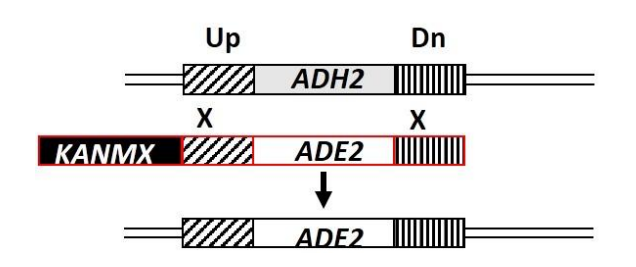
### 3.2.3 Functional knock out of Hsp82 hampers the efficiency of homologous recombination

Measurement of cell survivability upon MMS and UV induced DNA damage points towards the overall DNA repair activity of cells. However our aim was to assess the activity of homologous recombination upon Hsp90 inhibition. DNA damaging agents used in our analysis have different modes of action. MMS first creates single stranded breaks (SSBs) which are subsequently converted to DSBs during S phase. UV radiation causes random DSBs and these are not restricted to any specific phase of cell cycle. Hence to prove the involvement of Hsp82 in homologous recombination we relied on gene targeting assay which utilizes homologous-recombination machinery and can be a direct measure of homologous recombination efficiency. We followed our study by constructing a cassette have ADE2 gene flanked by ADH4 up-stream and down-stream sequences. We allowed to target this cassette to the ADH4 locus of chromosome VII-L. This cassette also harbors a copy of KANMX gene, which allows cells to grow on G418 sulphate containing plates. The targeted integration of this cassette to the genome causes the cells sensitive towards G418 sulphate, whereas random integration of the cassette causes them resistant towards that chemical. We transformed equal amount of this cassette to the wild type and the Hsp82inactivated mutant (the iG170Dhsp82 strain) at 37°C in order to determine the efficiency of HR. Obtained transformants were patched on G418 sulphate containing plates (Fig 14A). For calculation of gene targeting efficiency we used following formula; % gene targeting efficiency = (number of Ade<sup>+</sup> G418<sup>S</sup> colonies in each mutant) / (number of Ade<sup>+</sup> G418<sup>S</sup> colonies in P82a) X 100. To rule out the possibility for any variation in transformation capabilities of these mutants we normalized gene targeting efficiencies by transforming equal amounts of an uncut replicating plasmid into each strain. Our observation of this assay suggests that iG170Dhsp82 temperaturesensitive mutant when grown at restrictive temperature (37°C) is defective in performing gene targeting. We conclude that the inappropriate homologous recombination occurs at 37°C compared to that grown at the permissive temperature (25°C) (Fig 14B). To rule out the possibility that the reduction in gene targeting efficiency is not a consequence of exposing cells to high temperature, we included P82a as a positive control for this assay and scored the gene-targeting efficiency of this strain after prior incubation at 37°C for 4 h. We did not observe any significant reduction in the gene targeting of this strain when incubated at the high temperature (37°C) (Fig 14B). Overall we conclude that functions of Hsp82 in mandatory for homologous recombination pathway of DNA repair.

Figure: 14

(A) Targeted integration:

#### Random integration:





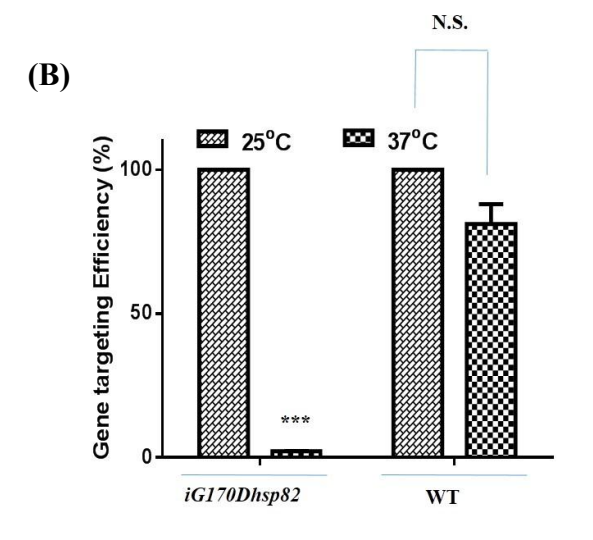


**Figure 14:** Hsp82 function is essential for homologous recombination pathway (A) Schematic diagram of cassette and principal behind gene targeting assay. First part depicts the targeted integration of cassette into the genome at *ADH2* locus by utilizing the flanking upstream and downstream sequences of *ADH2* in the cassette, this event loses *KANMX* gene. Second part of diagram represents random integration event into the genome which retains the *KANMX* cassette. (B) Plots showing the percentage of gene-targeting efficiency for the *iG170Dhsp82* strain at 25°C and 37°C. As a control, the gene-targeting efficiency of the isogenic wild-type (P82a) strain was measured at 25°C and 37°C. Gene-targeting efficiency was normalized by transforming an equal amount of an uncut replicating plasmid into the strain grown at 25°C and 37°C to nullify the difference in competence for DNA uptake between strains.

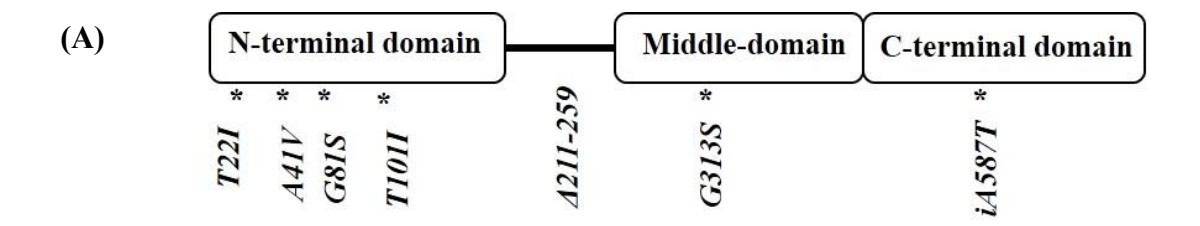
# 3.2.4 Different mutations in Hsp82 have differential defect in the cell survivability upon DNA damage

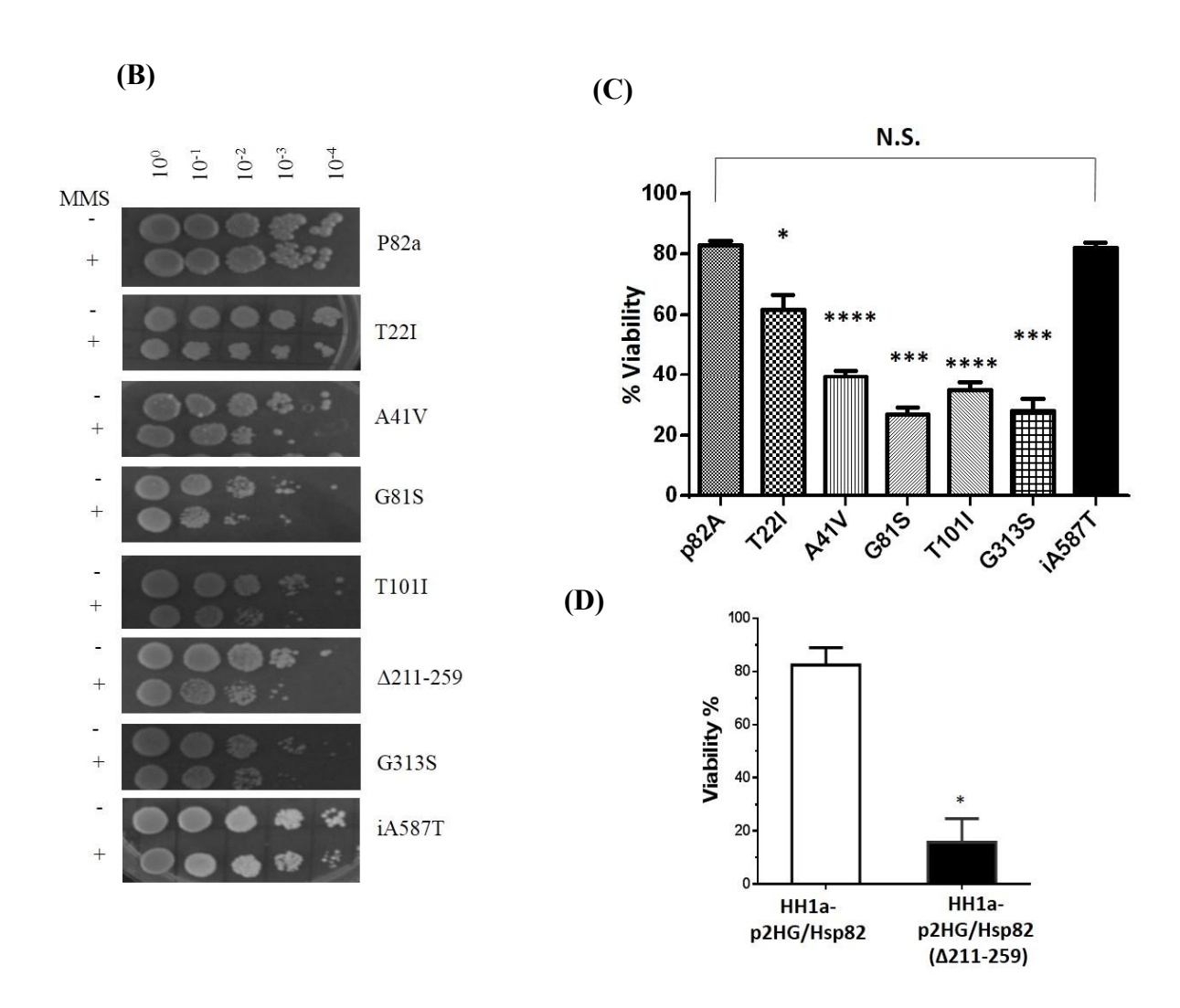
To explore the role of Hsp82 in detail we extended our interest to understand, which domain of Hsp82 serves important role in DNA repair. Hsp82 has a highly conserved structure which comprises of three domains. We employed six HSP82 point mutants (T22I, A41V, G81S, T101I, G313S, and iA587T) spanning its three domains. We also included one charged linker deletion mutant HH1a-p2HG/Hsp82 (211-259) in our study (271). Considering the importance of ATPase activity for Hsp82 chaperone cycle, we included T101I mutant in our study as it is well reported to have less than 5% ATPase activity compared to the wild type Hsp82. iA587T mutant is included as a positive control because its ATPase activity is similar to wild type Hsp82. The charged linker region connects the N-terminal domain with the middle domain and known to be essential for providing flexibility to Hsp82 (Fig 15A). Above mentioned mutants were monitored for their cell survivability after DNA damage resulted by MMS treatment. We performed the return to growth assay for all these mutants upon exposure to 0.03% MMS for 2 hrs. Subsequently treated and untreated cells were spotted onto YPD plates after serial dilution. P82a was taken as an isogenic positive control. Our experimental data suggest that five mutants, namely, the A41V, G81S, T101I, G313S, and hsp82 (211-259) were hypersensitive to MMS treatment, since they displayed 2-logunit differences in their growth (Fig 15B). To acquire quantitative comparisons between these mutants, we performed fluctuation analysis where after MMS treatment we counted equal number of treated and untreated cells and then spread on normal media. Our results displayed 88% reduction in cell viability in the charged linker deletion mutant HH1a-p2HG/Hsp82 (211-259) relative to the isogenic positive control. Three ATPase domain point mutants, the A41V, G81S

and T101I mutants, showed dramatic reductions in cell viability upon MMS treatment, indicating the importance of the ATPase domain in DNA repair. The G313S middle-domain mutant also displayed about a 50% reduction in survivability upon MMS treatment, whereas the *iA587T* mutant shows no sensitivity towards MMS. The T22I mutant showed only a 10% decrease in survivability from that of the wild type (P82a). We conclude from here that N-terminal ATPase domain of Hsp82 is important for DNA repair. This study also brings out the requirement of evolutionarily conserved charged linker region of Hsp82 for DNA repair (Fig 15C and 15D).

To understand whether the observed phenotype of all Hsp82 mutants is specific to MMS or it is a generalized phenomenon upon any kind of DNA damage. We included UV as a DNA damaging agent in our study, where all mutants were exposed to increasing doses of UV radiation. After exposure to different doses of UV, equal number of cells were counted and spread on normal plates. Number of survived cells after UV treatment, were counted on the treated and untreated plates and the percentage of survivability was analyzed. It was observed that the iA587T and T22I point mutants were marginally different in UV survivability from the control strain, while the G313S mutant was hypersensitive. On the other hand, the A41V, G81S, and T101I point mutants were significantly sensitive to UV treatment, reinforcing the importance of the ATPase domain in repairing UV mediated DNA damage (Fig 15E). Also, the ability of the charged linker deletion mutant HH1a-p2HG/Hsp8 (211-259) to survive after UV-induced damage was significantly different from that of its isogenic control (Fig 15F). Thus, these results suggested that the charged linker region and residues A41, G81, T101, and G313 of Hsp82 are important for cell survival upon UV-induced DNA damage. This outcome matches with our MMS sensitivity assay data, which divulges the importance of ATPase activity and charged linker region of Hsp82 for its activity in DNA repair.

Figure: 15





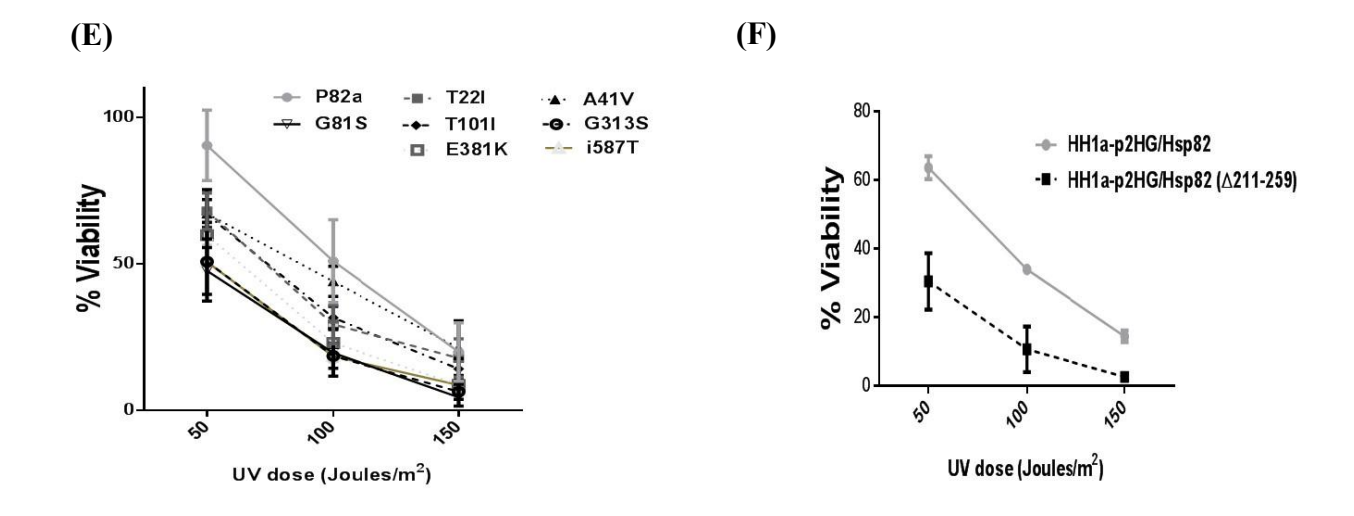
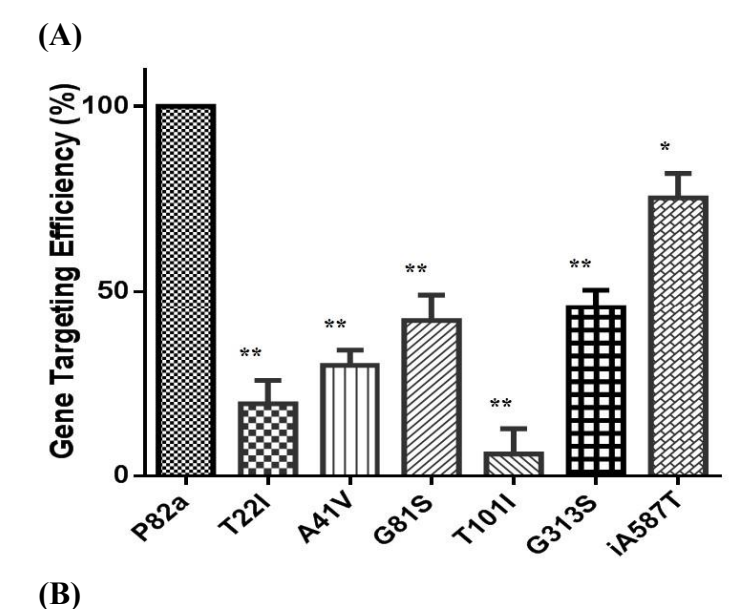


Figure 15: Differential effect of different Hsp82 mutants on DNA repair activity: (A) Diagrammatic representation of Hsp82 structure illustrating different mutated residues. All these mutants are used in our study to carry out the mutational analysis. (B) MMS sensitivity assay performed with all the mutants along with isogenic wild type strain P82a. After treatment with 0.03% MMS for 2 hrs, serially diluted cells were spotted into normal media. Upper row in each panel is the representation of untreated cells and bottom row is the representation of treated cells. (C) Bar diagram showing the quantitative measure of DNA repair activity of different point mutants. Mean percent viability calculated from three independent set of experiments in case of each point mutant is plotted. \*\*\*\*, P 0.0001; \*\*\*, P 0.001; \*\*, P 0.01; \*, P 0.05; N.S., not significant. (D) Quantitative measure of cell survivability of charged linker deletion mutant along with its isogenic wild type strain, plotted by calculation mean value of three independent experiments. (E) Percentages of viability of six hsp82 point mutant strains and their isogenic wildtype control, P82a, after exposure to increasing doses of UV radiation. The experiment was repeated three times and the mean values (SD) are plotted. (F) Percentages of viability of wildtype (HH1a-p2HG/Hsp82) and charged linker deletion mutant [HH1a-p2HG/Hsp82 (211-259)] strains after exposure to increasing doses of UV radiation. The experiment was repeated three times and the mean values (SD) are plotted.

## 3.2.5 Defect in the cell survivability of Hsp82 mutants is correlated with the deficiency in the homologous recombination

Our initial analysis demonstrates the requirement of Hsp82 in homologous recombination pathway of DNA repair. After witnessing the DNA damage sensitivity of different Hsp82 mutants, we were keen to explore the HR efficiency of these mutants. We determined the gene-targeting efficiencies of all mutants and compared their homologous-recombination efficiencies as a read out of this assay. Gene-targeting efficiencies were found to be affected to various degrees by the mutations. Based on their DNA damage sensitivities and gene-targeting efficiencies, we categorized the mutants into three groups. Group A consisted of the iA587T mutant, which had little effect on gene targeting efficiency (75% of activity retained). This correlates well with the previous result showing a negligible effect on MMS and UV survivability. Group B includes the A41V, T22I, G81S, and G313S mutants, which showed moderate effects on gene targeting (about a 66% reduction). Group C is comprised of the mutants that were severely defective in gene targeting. In our study the T1011 mutant, the charged linker deletion mutant, and the HSP82 temperaturesensitive mutant iG170Dhsp82 at the non-permissive temperature fall into this category (Fig 16A and 16B). Thus, mutational analysis identified the specific regions of Hsp82 that were vital for the proper functioning of HR-mediated gene targeting.





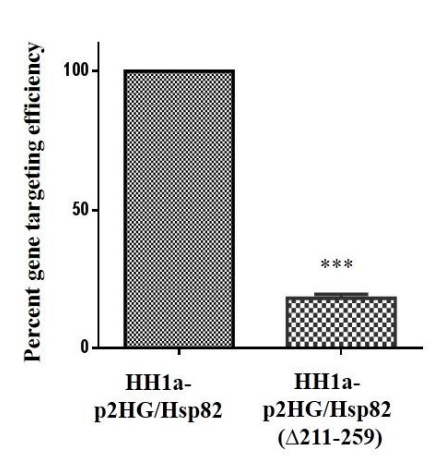


**Figure 16:** Gene targeting efficiencies of Hsp82 point and deletion mutants (A) Bar diagram representing the calculated gene targeting efficiencies of Hsp82 point mutants. Mean value of at least three independent set of experiment in case of each mutant were plotted. Error bars indicate SD; n 3. P values were calculated using the two-tailed Student t test (\*\*, P 0.01; \*, P 0.05). (B) Gene targeting efficiency of charged linker deleted mutant with respect to isogenic wild type strain. Error bars indicate SD; n=3. P values were calculated as 0.0010 (\*\*\*) using the two-tailed Student t test.

### **SPECIFIC AIM 2**

Identification of homologous recombination proteins which are dependent on Hsp90 functions

#### 4.1 INTRODUCTION

Hsp90 is a highly conserved molecular chaperone, which helps in the post-translational folding, stabilization, maturation and activation of specific group of proteins, known as Hsp90 clients. Unlike other chaperones, Hsp90 assists only metastable conformation of the proteins, which have crossed nascent polypeptide state. Well known Hsp90 clients include transcription factors, signaling proteins, immune response proteins, DNA repair proteins, factors of epigenetic regulation etc. (50, 51). These clients of Hsp90 do not share any defining sequence or motif, hence it is hard to predict any protein as Hsp90 client from their structure (272). However, a protein must fulfill following criteria in order to get entitled as Hsp90 client; 1) there should be a physical interaction between Hsp90 and the candidate protein, 2) protein functions should be lost under Hsp90 inactivated condition, and 3) protein should undergo proteasomal degradation pathway upon Hsp90 inactivation. Client protein folding is accelerated by the ATPase activity of Hsp90 and failing to it affects the stability of client proteins (8). In the process of client folding, Hsp90 makes use of several co chaperones like Cdc37, p23, Aha1, TPR2 etc., which interact with different domains of Hsp90 and function in client specific manner (273). Moreover client recognition site on Hsp90 is still undefined as it crosses domain boundaries for varying clients (58).

As our previous results indicate the importance of Hsp82 (Human Hsp90) for the homologous recombination (HR), next we sought to determine if it is essential for the functions of any HR protein. HR starts with the resection of broken end and thus generation of single-stranded DNA (ssDNA) overhangs, which form the binding site for Rad51. Rad51 then searches for the homologous templates and invades similar sequences by utilizing its ATPase activity. Rad51, Rad52, Rad54, and replication protein A (RPA) are the key proteins involved in the HR-mediated

break repair pathway (274). In *Saccharomyces cerevisiae*, Rad52 facilitates the formation of a hexameric Rad51-bound ssDNA complex at the broken junction in the presence of RPA. Rad52p plays a central role in HR, and *rad52* mutation abolishes all recombination events in yeast (275). Rad51 and Rad52 are highly conserved which suggests conserved function of these proteins during evolution. As Rad51 and Rad52 take part in the signature steps of HR, we were interested to understand if their stability is dependent on Hsp82.

For this purpose, we analyzed Hsp82 mutants, which showed differential defect in HR efficiency in our previous study. Our results suggest that mutations in Hsp82 affect the stability of Rad51 and Rad52. Next we found that, Rad51 physically interacts with Hsp82 and follows proteasomal pathway upon Hsp82 inactivation. This set of experiments established Rad51 as a client of Hsp82. Our work highlighted charged linker region of Hsp82, as an important element for DNA repair. Residues (211-259) of charged linker, which neither affects the ATPase activity of Hsp82 nor the stability of protein, were immerged to be important for the DNA repair in our work. We did not observe any difference in the Rad51 and Rad52 protein levels in  $\Delta 211-259hsp82$  mutant. However removal of this region affects the efficiency of Rad51 foci formation which makes this mutant as defective in HR.

#### 4.2 RESULTS

### 4.2.1 Steady state of Rad51 and Rad52 proteins is affected in non-functional mutant *iG170Dhsp82*

Indications from our previous study suggest that Hsp82 functions are important for homologous recombination pathway, which is evident from our gene targeting assay. We next examined the mechanism behind such significant reduction in gene-targeting efficiency in the Hsp82 mutant cells. We have monitored the consequences of Hsp82 mutation on two key players of HR namely Rad51 and Rad52. Firstly, we determined the cellular pool of Rad51 and Rad52 under Hsp82 nonfunctional background. Western blot shows slight reduction in the levels of Rad51 and Rad52 upon exposure of iG170Dhsp82 at 37°C for 4 h. On the other hand, extreme reduction in both the Rad51 and Rad52 protein levels were observed upon overnight exposure of cells at 37°C (Fig 17A). We quantified the level of Rad51 and Rad52 from three independent batches of experiments and it shows about 20% reduction in the Rad52 level after 4 hour incubation at 37°C, a condition which inactivates Hsp82. However, after overnight incubation at 37°C we could hardly detect Rad52 in the cell. Similarly, the Rad51p levels were also decreased by at least 80% after overnight incubation (Fig 17B). We further verified that, the sole cause of Rad51 and Rad52 reduction is the mutation in Hsp82 but not the exposure of cells to high temperature. To this end, we probed for the presence of Rad51 and Rad52 in wild-type strain by exposing them at 37°C (Fig 17A). We do not observe any change in the level of Rad51 and Rad52 in the wild-type strain after incubating it at 37°C for 4 hrs. This suggests that non functionality of Hsp82 affects the stability of Rad51 and Rad52.

Hsp82 is a molecular chaperone and accomplishes its functions only at proteins level. Here we tried to understand, whether the decline in endogenous pool of Rad51 and Rad52 was due to the direct consequence of Hsp82 inactivation or was due to the result of a large transcriptional shift. To this end, we estimated the transcript levels of *RAD51* and *RAD52* in the *iG170Dhsp82* strain at both the permissive (25°C) and restrictive (overnight incubation at 37°C) temperatures. We isolated RNA from the strains grown at permissive and non-permissive temperatures. Our real-time analysis data displayed no significant change in the relative mRNA levels of the *RAD51* or *RAD52* transcript under those conditions (Fig 17C). Thus, our work reveals that Hsp82 is involved in the maturation and stability of Rad52 and Rad51.

Figure: 17

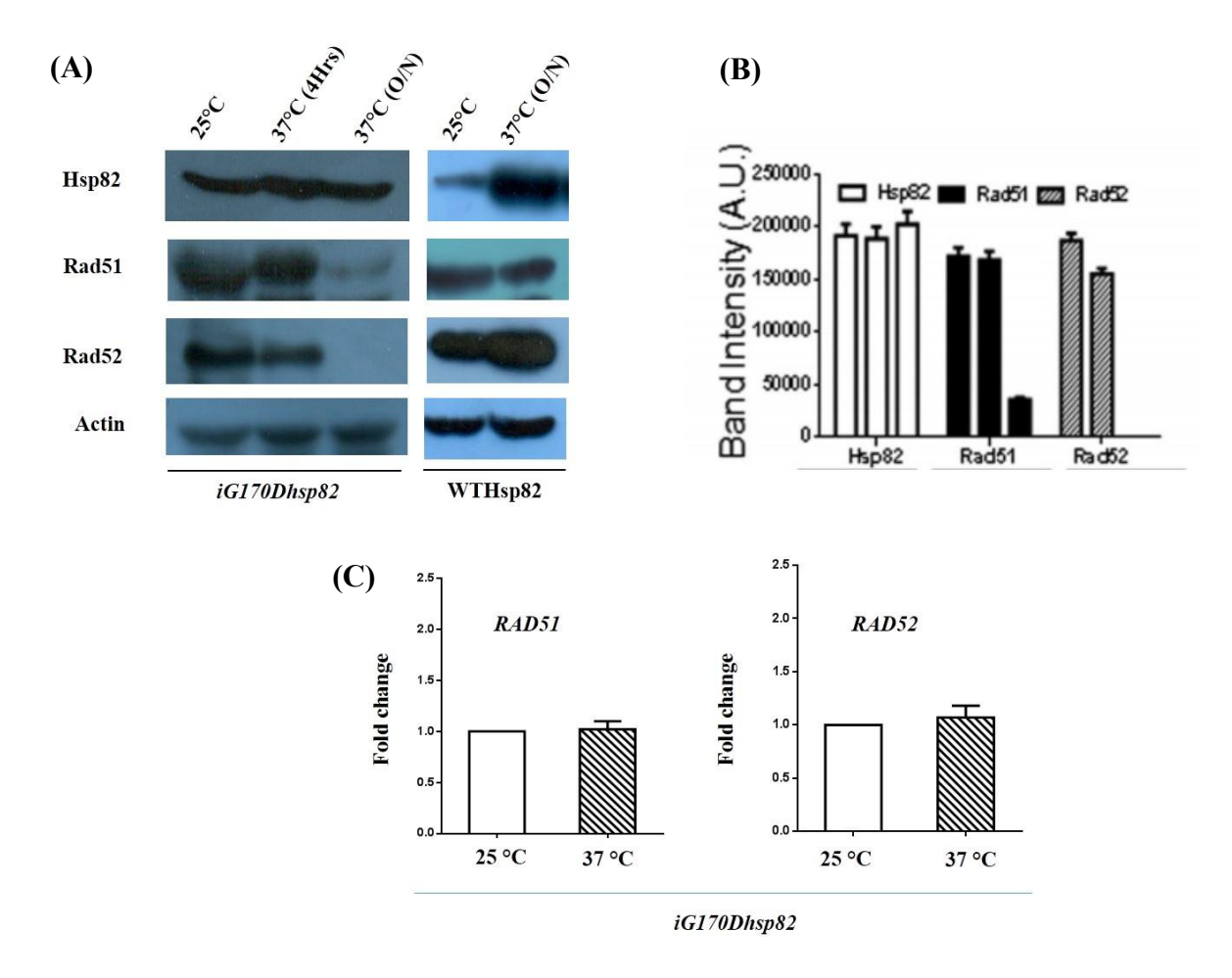


**Figure 17:** Stability of Rad51 and Rad52 are dependent on Hsp82: (A) Western blot was done to probe the steady state levels of Hsp82, Rad51 and Rad52 in *iG170Dhsp82* mutant grown at permissive (30°C) and non-permissive temperature (37°C) for 4 hrs and overnight. As a control steady state level of these proteins were checked in the wild type strain grown at 30°C and 37°C for overnight. Actin was used as a loading control (B) Quantification of western blot by calculating the band intensities. Rad51 shows 4 fold reduction in the cells incubated at non permissive temperature for O/N however Rad52 completely diminished form the cells upon O/N incubation. (C) Relative abundance of *RAD51* and *RAD52* transcripts in the *iG170Dhsp82* grown at permissive (25°C) and non-permissive (37°C) temperatures. Real time PCR was performed to calculate the abundance of RNA in these strain background.

#### 4.2.2 Stability of Rad51 and Rad52 is dependent on the ATPase activity of Hsp82

T1011hsp82 mutant is an ATPase dead mutant of Hsp82 and reported to have less than 5 % of ATPase activity as compared to wild type Hsp82 (276). To investigate the mechanism underlying the poor HR function in T1011hsp82 mutant as observed in our previous study, we intend to study the endogenous pool of Rad51 and Rad52 in this mutant. To do so, we tagged the C-terminal end of RAD52 in this strain to make its detection possible for our analysis. Next we probed for the presence of Rad51 and Rad52 in this mutant. Western blot performed with this mutant showed that the amount of Rad51 and Rad52 were significantly decreased in the T1011hsp82 mutant, which demonstrates the importance of ATPase domain for the maturation of Rad51 and Rad52 (Fig 18A). Quantification of band intensities showed a 4-fold reduction in the Rad51 level and a 2-fold reduction in the Rad52 level in the T1011 mutant (Fig 18B). Taken together, our result indicates that the loss of gene-targeting efficiency in the ATPase-dead mutant is a consequence of lower endogenous levels of Rad51 and Rad52.

ATPase activity of Hsp82 is required for protein folding by Hsp82 chaperone machinery. We were interested to know whether the observed phenotype of *T101Ihsp82* mutant is a direct consequence of Hsp82 on Rad51 and Rad52 proteins or it is an indirect effect. For this purpose, we isolated RNA from *T101Ihsp82* and wild-type strains and performed semi quantitative analysis. Our results suggest no marked difference in the pool of transcript levels among wild-type and *T101Ihsp82* mutant. We further analyzed these samples by real-time RT-PCR analysis which showed no change in the steady-state levels of *RAD51* and *RAD52* transcripts in the *T101Ihsp82* mutant background (Fig 18C).

Figure: 18

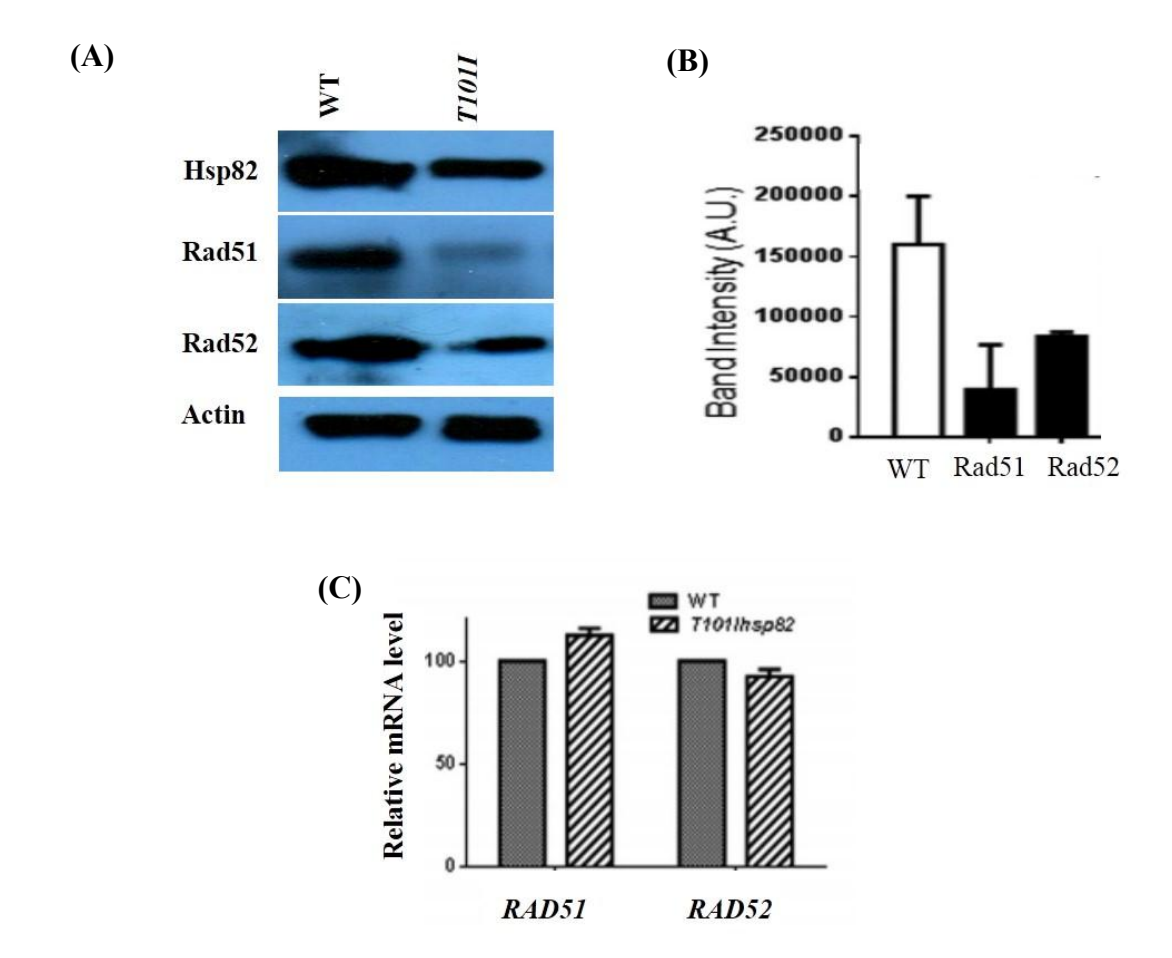


**Figure 18:** Stability of Rad51 and Rad52 is dependent on the ATPase activity of Hsp82: (A) Western blot showing the cellular pool of Hsp82, Rad51 and Rad52 in wild type and *T101Ihsp82* mutant. Actin used as a loading control. (B) Band intensities of western blot were calculated to quantify the levels of Rad51 and Rad52 in WT and T101I mutant. Rad51 and Rad52 both proteins were reduced in *T101Ihsp82* mutant. (C) Quantification of *RAD51* and *RAD52* transcript levels in *T101Ihsp82* mutant along with its isogenic wild type strain by real time PCR.

#### 4.2.3 Rad51 is a client of Hsp82

To date, there has been no report that establishes Rad51 as a client of Hsp82. One of the primary requisites for clientage is a physical interaction between Hsp82 and its client. A genome wide chemical genetic screen had identified Rad51 as a putative interactive partner of Hsp82 (74). However, a physical interaction between Rad51 and Hsp82 had never been established. We performed a co-immuno precipitation experiment that showed strong association between Rad51 and Hsp82. The fraction that was immune precipitated using IgG did not cross-react with the anti-Rad51 antibody (Fig 19A). Additionally, the anti-Hsp82 antibody did not cross-react with Rad51 on a Western blot (data not shown), suggesting that such an interaction is specific in nature. Also, the control strain lacking rad51 showed no detectable background, although Hsp82 was immune precipitated from the cellular extract. It had been demonstrated earlier that degradation of Hsp90 clients upon treatment with 17-AAG is mediated via proteasomal pathway (277). We were interested in exploring whether Rad51 undergoes proteasome-mediated degradation in conditions of Hsp82 inhibition. For this purpose, we treated a wild-type strain with 40 µM 17-AAG, which functionally inactivates HSP82. We used a  $\Delta pdr5$  strain, since deletion of the PDR5 gene, which codes for a membrane-associated drug export pump, ensures the optimal entry of drugs (278). A fraction of that culture was supplemented with 50µM MG132 (a proteasome inhibitor) along with 17-AAG. Total protein was isolated from those strains and was probed with anti-Rad51 antibody. Consequences of these inhibitors on Hsp90 client are presented in Figure 19B. Western blot analysis showed that treatment with 17-AAG led to a considerable reduction in the Rad51 level, while MG132 treatment resulted in the restoration of Rad51p abundance (Fig 19C and 19D). This experiment reveals that under conditions of Hsp82 inhibition, Rad51 is processed via proteasomal degradation, supporting the conclusion that Rad51 is a direct client of Hsp82.



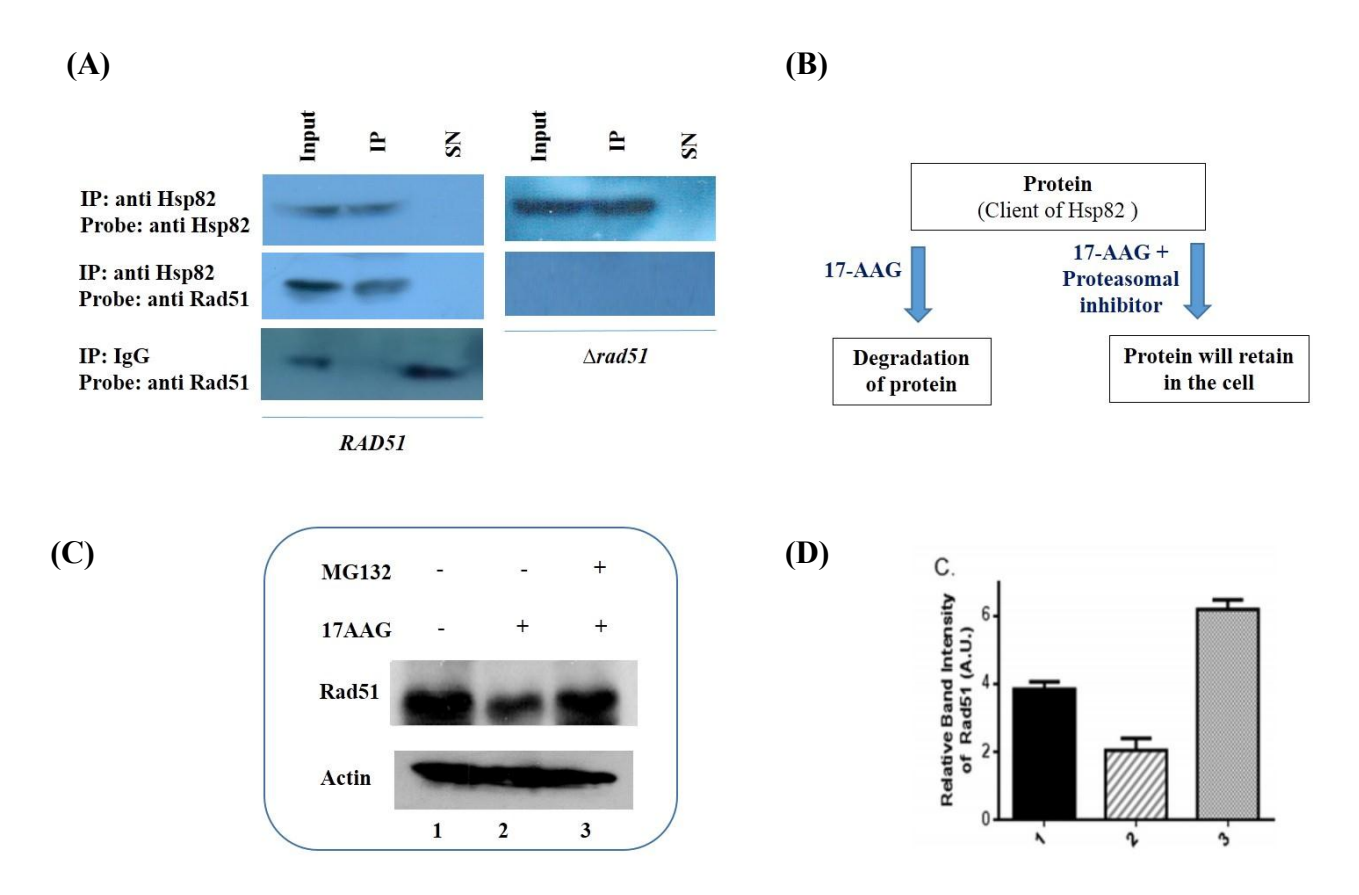


**Figure 19:** Rad51 is a client of Hsp82: (A) Coimmuno-precipitation was performed using anti Hsp82 antibody and non-specific IgG antibody using wild type and null Rad51 strains ( $\Delta rad51$ ). Samples were probed with anti-Hsp82 and anti-rad51 antibodies for western blot analysis. Input: whole cell extract, IP: immuno precipitate, SN: supernatant (B) Outline potraying strategy behind the assay (C) Western blot showing the levels of Rad51p in wild-type untreated cells (lane 1), in cells treated with 40 μM 17-AAG for 16 h (lane 2), and in cells treated with 40 μM 17-AAG and 50 μM MG132 for 16 h (lane 3). Actin is used as a loading control (D) Band intensities calculated for given western blot showing the relative abundance of protein in lane 1, 2 and 3 corresponds to western blot in B.

### 4.2.4 Charged linker region does not affect the abundance of Rad51 and Rad52 proteins in the cell

Charged linker region of Hsp82 is a pentad repeat of (D/E)(D/E)(D/E)KK, and conserved among eukaryotes (279). Despite of its high conservation exact function of this region remained elusive. Initially it is considered to be important for mere providing flexibility to Hsp82 (280, 281). In our work we observed that deletion of this region makes cells defective in HR mediated DNA repair. In order to understand the mechanism underlying the loss of HR function in charged linker deleted mutant, we determined the endogenous levels of Rad51 and Rad52 in the  $\Delta 211-259hsp82$  mutant. To this end, for the detection of Rad52, we attempted to tag the C-terminal end of RAD52 in  $\Delta 211$ -259hsp82 strain. Inspite of several attempts, we failed to Myc tag RAD52 gene in  $\Delta 211-259hsp82$ strain, by using recombination based strategy. This firmly confirms that this mutant is really defective in homologous recombination. Hence in order to Myc tag RAD52, we followed another strategy where we swapped the  $\Delta 211-259hsp82$  plasmid in the T101Ihsp82 point mutant (which was RAD52-MYC tagged at the chromosomal locus) to create the RAD52-MYC tagged △211-259hsp82 strain SLY65. Western blot analysis we found that the levels of Rad51 and Rad52 were unaltered in the \(\Delta 211-259hsp82\) mutant (Fig 20A). Quantification of band intensities does not show any significant changes in the Rad51 and Rad52 in this mutant (Fig 20B). Thus, the apparent lack of correlation between HR function and the abundance of recombinase proteins in the charged linker deletion mutant implies a complex interplay between the chaperone and these clients.

Further to explore the mechanism behind the drastic reduction in HR efficiency in the  $\Delta 211$ -259hsp82 mutant, we studied the MMS-induced up regulation of Rad51 and Rad52. Wild-type and  $\Delta 211$ -259hsp82 strains were grown upto an OD of 0.6 and were then separated into

two groups, one of which was grown in the presence of MMS while the other was grown in its absence. Western blotting showed that the induction of Rad51 and Rad52 in the mutant strain was similar to that observed in the wild-type strain (Fig 20C). Quantification of Rad51 from three independent harvests of cells showed a 4-fold induction of Rad51 in the wild type and a 2-fold induction in the charged linker deletion mutant (Fig 20D). Next, we aimed to understand if charged linker region have any effect on controlling the transcription up-regulation of RAD51 and RAD52 upon MMS treatment. For that purpose, we isolated the total RNAs of the wild-type and  $\Delta 211$ - $\Delta 259hsp82$  strains that had been left untreated or treated with MMS and measured the relative abundances of the RAD51 and RAD52 transcripts. Semi quantitative RT-PCR showed up regulation of RAD51 and RAD52 upon MMS treatment in both strains (Fig 21A). Real-time RT-PCR quantification showed almost equal induction (4.7-fold) of RAD51 and RAD52 transcripts (2-fold) in MMS treated and untreated samples in the wild type as well as in the  $\Delta 211$ - $\Delta 259hsp82$  mutant (Fig 21B and 21C). Thus, our results revealed that the MMS-induced transcriptional up regulation of BAD51 and BAD52 was unaltered in the charged linker deletion mutant.



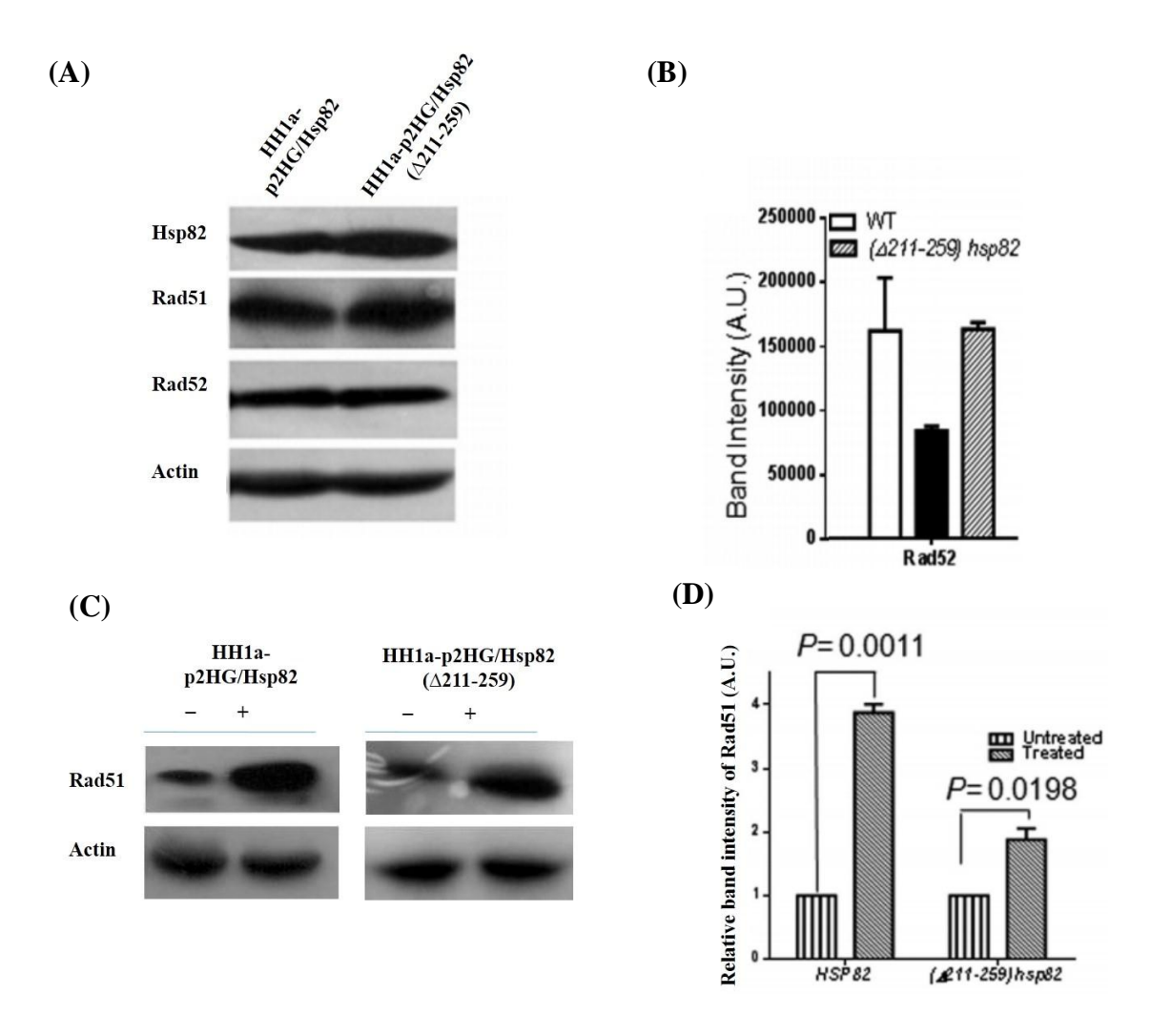
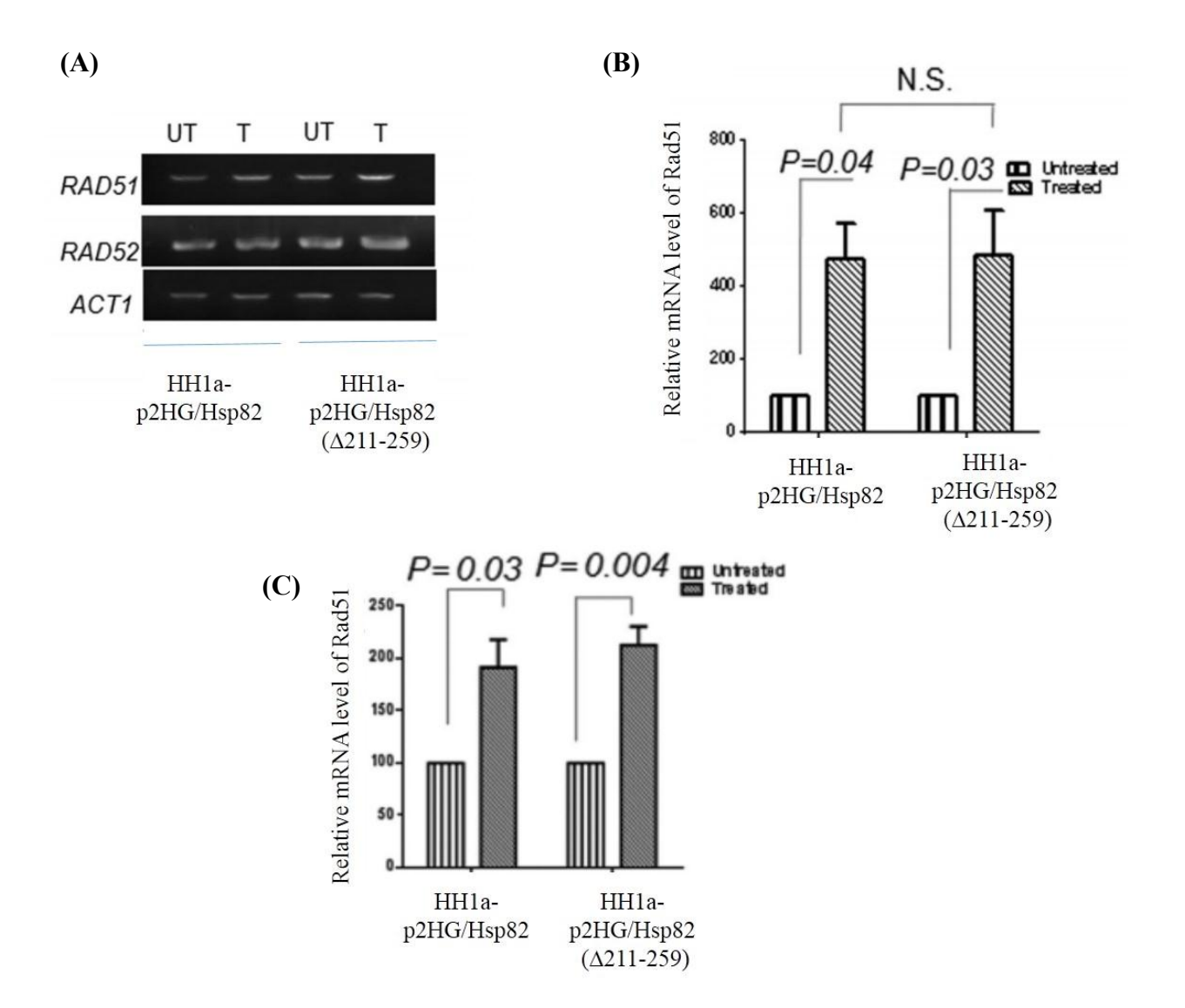


Figure 20: Deletion of charged linker from Hsp82 does not affect Rad51 and Rad52 proteins level (A) Western blot done using protein samples isolated from  $\Delta 211$ -259hsp82 mutant and its isogenic wild type cells. Samples were probed with anti-Hsp82, anti-Rad51, anti-Rad52 antibodies. Actin was used as a loading control. (B) Quantification of western blot by calculating the band intensities represent no significant change in the Rad51 and Rad52 with respect to wild type cells. (C) Western blot indicating the up regulation of Rad51p and Rad52p upon 0.03% MMS treatment in wild type and  $\Delta 211$ -259hsp82 mutant. (D) Quantification of Western blots from three independent experiments shows significant induction of Rad51p upon MMS treatment in both wild-type and mutant strains. The band intensity for each strain calculated by taking the mean densities of western blots and SD are plotted. The *P* values were calculated using the Student *t* test.

Figure: 21



**Figure 21:** Hsp82 mutant  $\Delta 211$ -259hsp82 does not alter the up-regulation of RAD51 and RAD52 upon DNA damage: (A) Gel image of semi quantitative PCR showing the transcript level of RAD51 and RAD52 in  $\Delta 211$ -259hsp82 and wild type strains. T: treated with 0.03% MMS, UT: untreated. Actin used as a loading control. (B) Quantification of relative mRNA of RAD51 in wild type and  $\Delta 211$ -259hsp82 mutant. (C) Quantification of relative mRNA of RAD52 in wild type and  $\Delta 211$ -259hsp82 mutant.

### 4.2.5 Over-expression of Rad51 in \( \Delta 211-259 hsp82 \) mutant partially rescues the phenotype of the mutant strain

From Western blot analysis, it was apparent that the amount of Rad51 in the charged linker deletion mutant was similar to that in the wild type. However, the amount of active Rad51 may be limited, leading to decreased gene-targeting efficiency and increased MMS sensitivity. To establish it further, we over-expressed Rad51 in the mutant strain and investigated whether it could rescue MMS hypersensitivity and overcome the defect in gene-targeting efficiency. To this end, we transformed a  $2\mu$  expression vector harboring S. cerevisiae RAD51 into the  $\Delta 211$ -259hsp82 and iG170Dhsp82 strains to generate strains TSY1 and SLY69, respectively. We exposed the cells to 0.03% MMS for 2 h and calculated the percentages of cell viability. We compared the viability of the strains with and without Rad51 over-expression (Fig. 22A) and observed a significant difference between the two alleles. In the iG170Dhsp82 strain grown at 37°C, over-expression of Rad51 could not rescue MMS sensitivity, as evident by the fact that the temperature-sensitive mutant at the restrictive temperature was unable to chaperone Rad51 folding. However, in the  $\Delta 211$ -259hsp82 strain, over-expression of Rad51 can partially rescue MMS sensitivity. Our results showed that the percentage of cell viability increased 5-fold with Rad51 over-expression, but it was still 20% less than that of the wild type. In another assay, we studied the gene-targeting efficiency of mutant cells carrying pRAD51 and compared it with that of mutant cells carrying an empty vector. We observed that Rad51 over-expression resulted in 2.3-fold increased gene-targeting efficiency in the  $\Delta 211$ -259hsp82 strain; however, this level of efficiency was still significantly less than that of the wild type (Fig 22B). Western blotting confirmed the over-expression of Rad51 in these mutant strains (Fig 22C).



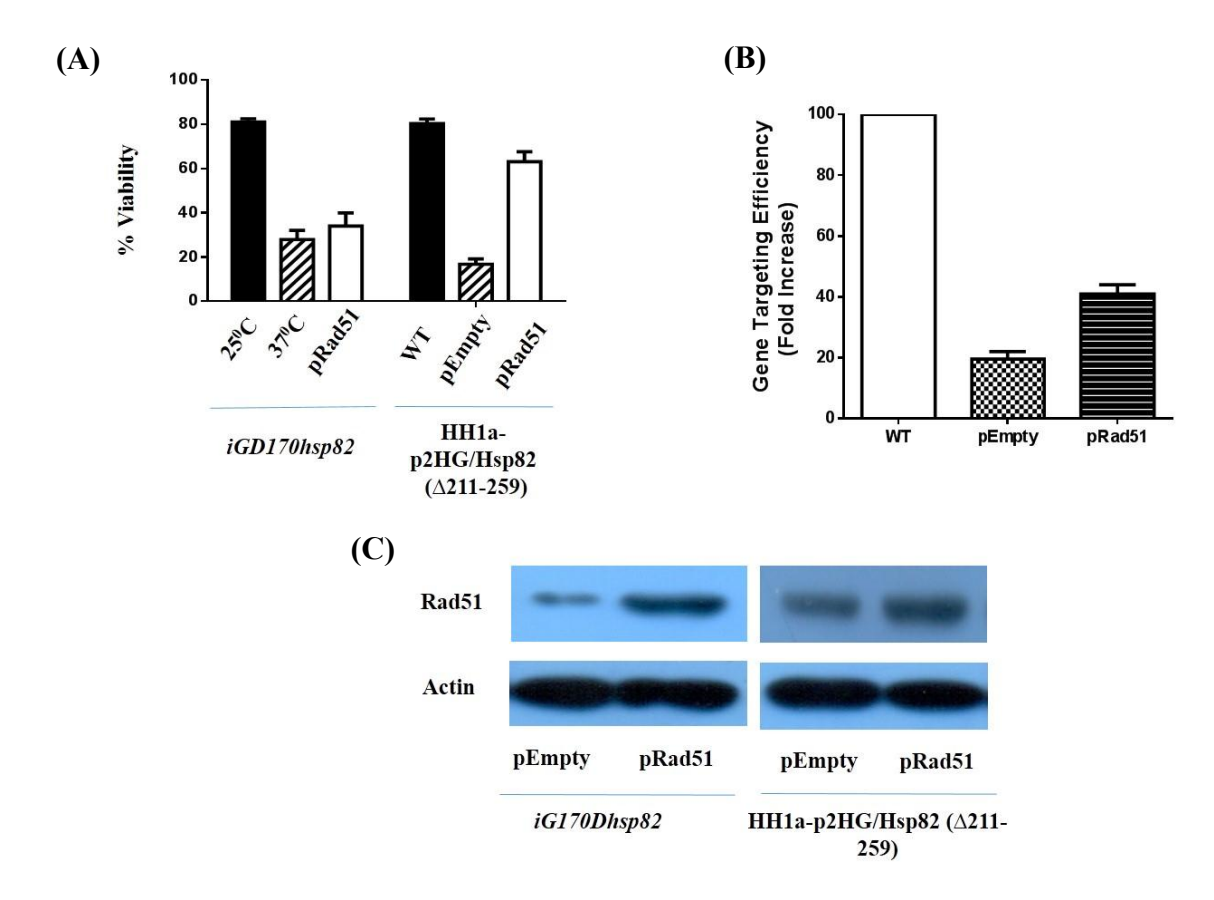


Figure 22: Over expression of Rad51 partially rescue the phenotype of  $\Delta 211$ -259hsp82: (A) Over-expression of Rad51 partially rescues the MMS sensitivity and gene-targeting efficiency of the  $\Delta 211$ -259hsp82 mutant. (A) The difference in the survivability of the iG170Dhsp82 strain treated with 0.03% MMS between 25°C and 37°C remained unaltered with Rad51p over-expression. However, the percentage of survivability of the  $\Delta 211$ -259hsp82 mutant treated with MMS was partially rescued in the presence of Rad51p over-expression. Graphs show mean densities SD from five independent experiments \*\*\*\*, P 0.0001; \*\*\*, P 0.001. (B) The Rad51 over-expression plasmid and an empty expression vector were transformed individually into  $\Delta 211$ -259hsp82 mutant cells. Gene-targeting efficiency was normalized by transforming equal amounts of an uncut replicating plasmid into both strains to nullify the difference in competence for DNA uptake between strains. Each bar represents the mean (SD) for three independent experiments. Asterisks indicate values significantly different from that for the control (\*\*\*\*, P 0.0001; \*\*\*, P 0.001; \*\*\*, P 0.01). (C) Immunoblot showing over-expression of Rad51p in the iG170Dhsp82 and  $\Delta 211$ -259hsp82 strains. Actin serves as a loading control

# 4.2.6 \( \alpha 211-259 hsp 82 \) mutant is defective in the efficient Rad51 foci formation upon DNA damage

Since MMS induced Rad51p up regulation is unaffected in the  $\Delta 211-259hsp82$  mutant, we sought to investigate whether the downstream function of Rad51 is affected in this mutant strain. For that purpose, we used an indirect immunofluorescence assay to investigate the ability to form MMS-induced Rad51 foci. We observed very bright fluorescent foci that were enriched with Rad51 in MMS-treated cells but not in untreated cells (Fig 23A). We counted about 1,500 nuclei in each of the three independent harvests of cells in order to calculate the percentage of nuclei that had Rad51 foci. Our results demonstrated a 20% reduction in Rad51 focus formation in  $\Delta 211$ -259hsp82 cells from that in wild-type cells upon DNA damage (Fig 23B). Next, we analyzed the distribution of foci in each nucleus. After analyzing a total of 4,500 MMS-treated nuclei of wildtype and mutant cells, we observed a striking, statistically significant difference in the distribution of foci. Our analysis revealed that mutant cells possessed primarily 1 focus per nucleus, and the total number was comparable to that for wild-type cells. However, the percentage of nuclei containing more than 1 focus was drastically lower in mutant cells than in wild-type cells. Our study showed 33% fewer nuclei with 2 foci, 42% fewer nuclei with 3 foci, and 77% fewer nuclei with 4 foci in mutant cells than in wild-type cells (Fig 23C). Thus, we came to the conclusion that in the charged linker deletion mutant, the level of Rad51 foci formation, which is a prerequisite for repairing breaks in DNA, is significantly lower than that in the wild type, leading to greater MMS sensitivity.



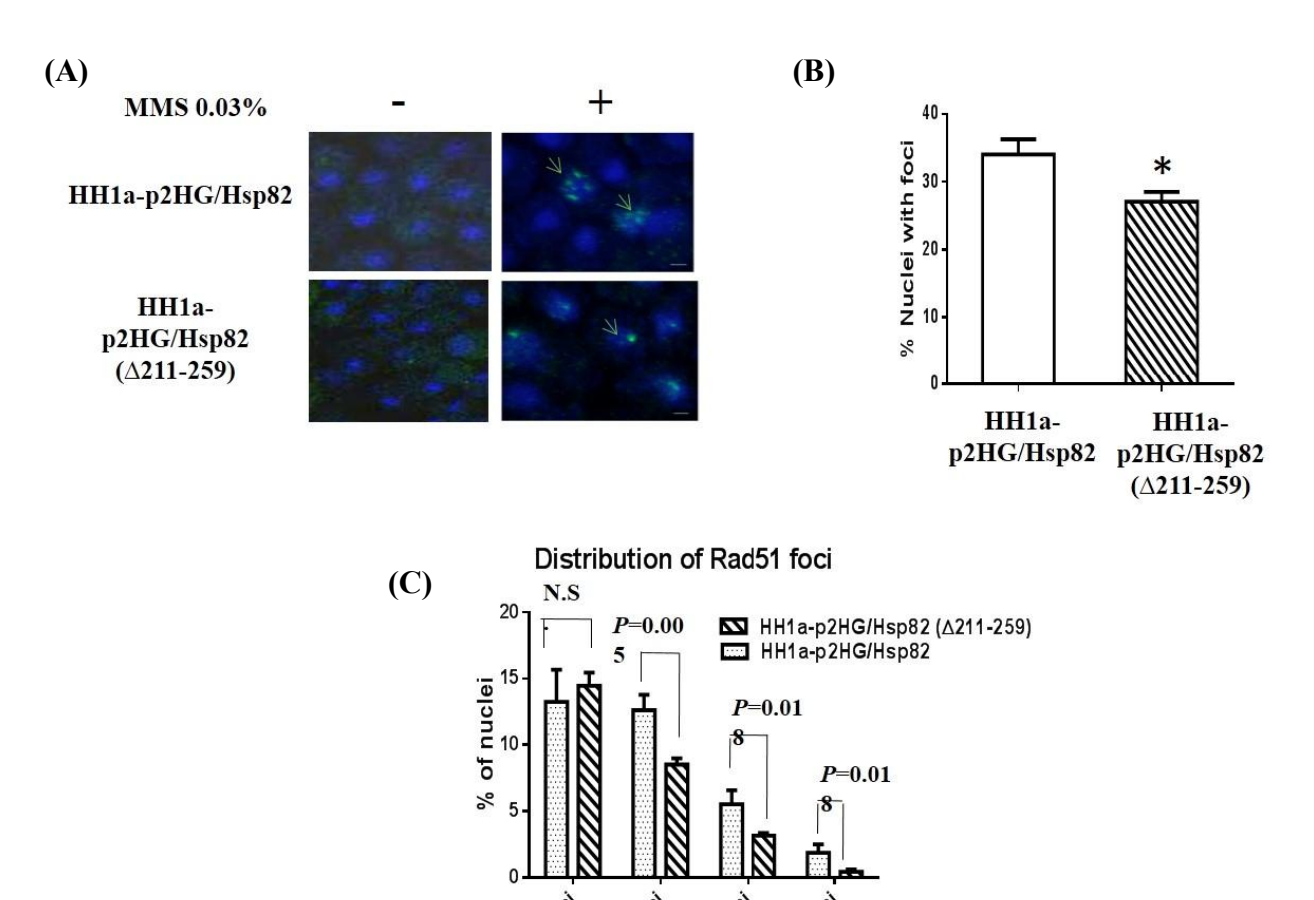


Figure 23: The extent of MMS-induced Rad51 focus formation is less in  $\Delta 211$ -259hsp82 cells than in the wild-type control. (A) Wild-type (HH1a-p2HG/Hsp82) and mutant (HH1a-p2HG/Hsp82 (211-259) cells were treated with 0.03% MMS, and an indirect immunofluorescence assay was performed with anti-Rad51 to locate Rad51 foci. Nuclei were stained with DAPI. The arrows indicate Rad51 foci. The experiment was repeated three times, and representative data from one replicate are presented. (B) About 1,500 nuclei in each case were analyzed for the presence of Rad51 foci, and the percentages of nuclei with Rad51 foci were calculated for mutant and wild-type cells. The experiment was performed with three independent harvests of cells. The P value was calculated as 0.0103 using the two-tailed Student t test. (C) Image J software was used to analyze the image of each nucleus and to count the number of foci in it. A total of 4,500 wild-type and 4,500 mutant nuclei with 1, 2, 3, and 4 foci were counted, and the percentages of nuclei having 1, 2, 3, and 4 Rad51 foci were plotted for wild-type and mutant cells. An unpaired t test was performed using GraphPad Prism software, version 6. P values are indicated.

### **SPECIFIC AIM 3**

DNA damage induced nuclear import of Rad51 is mediated by dynamic interaction between Hsp90 and Rad51

#### **5.1 INTRODUCTION**

Whenever cells are exposed to DNA damaging agents, the family of DNA repair proteins must relocate to various cellular compartments to ensure efficient signaling and repair of damaged DNA (282). These groups of proteins include DNA damage signaling proteins (ATM, ATR, and DNA-PKcs), cell cycle checkpoint effectors (Chk1, Chk2) and DNA processing enzymes (Rad51, Rad52, Rad54, BRCA1/2, BLM, NBS1 etc.). Proteins larger than 20 kDa need to have NLS (nuclear localization signal) for nuclear import (283). Rad51, a 43 kDa protein is devoid of NLS and needs to cross nuclear membrane barrier in order to participate in HR. Inappropriate translocation of Rad51 can lead to the development of diseases such as cancer as HR efficiency is substantially more in cancer cells. Presently, not much information is available about its translocation upon DNA damage. Earlier reports demonstrated that BRCA-2 is associated with the nuclear entry of Rad51 upon DNA damage (199). However BRCA-2 independent mechanism for Rad51 nuclear entry clearly exists, as DNA damage associated Rad51 pool was significantly increased in BRCA-2 deficient Capan-1 cell lines (200, 201). Another report indicates the requirement of Rad51C, a paralog of Rad51 for its nuclear entry (284). However in this study, Rad51 is present inside the nucleus even in the absence of Rad51C. Also, BRCA-2 and Rad51C are absent in the lower eukaryotes like Saccharomyces cerevisiae where HR is the predominant pathway. Hence, in lower eukaryotes alternative pathways must be present for nuclear import of Rad51. Alternatively, it is possible to have an unidentified evolutionary conserved pathway among all eukaryotes which is responsible for DNA damage dependent nuclear entry of Rad51.

Our previous part of work reveals that Rad51 is a direct client of Hsp82 (Human Hsp90) and is dependent on Hsp82 for its maturity and activity. Apart from mere providing maturity to the client

proteins, Hsp90 also assists in the translocation of its clients to different cellular compartments (285). Steroid hormone receptors (SHRs), particularly glucocorticoid receptor (GR), estrogen receptor (ER), androgen receptor (AR), and progesterone receptor (PR) are Hsp90 clients and they need to translocate to the nucleus to activate transcription of the targeted gene. Hsp90 upholds SHRs in a hormone responsive state and modulates their nuclear entry upon hormone signal (14). Hsp90 chaperone machinery (Hsp90, Hsp70, Hop, p23 and Hsp40) along with FKBP52, FKBP51 and Cyp40 help in the nuclear translocation of SHRs (286). Nuclear transport of GR is well studied where Hsp90 remains bound to the receptor until hormone signal arises and helps GR to bind to the nuclear pore complex, thus facilitating its transport into the nucleus. These evidences highlight the functional relationship of Hsp90 with few of its client proteins other than mere helping in their maturation (73).

In this part of work we have examined whether the nuclear translocation of Rad51 is controlled by Hsp90. Our earlier study demonstrated that the charged linker deletion mutant of Hsp82 ( $\Delta 211$ -259hsp82) inhibits effective Rad51 foci formation in the nucleus upon DNA damage. This finding was positively correlated with severe MMS sensitivity (comparable to  $\Delta rad51$ ) and complete absence of Rad51 specific gene targeting function in that strain background. We demonstrated that ( $\Delta 211$ -259hsp82) mutant strain is strikingly different than the wild type strain in the distribution of Rad51 foci upon MMS treatment. Explicitly, although there were only 20% overall reduction in Rad51 foci formation however, the nuclei having multiple foci was significantly reduced in the mutant strain compared to the wild type. It clearly indicates that in mutant nuclei effective Rad51 level may be low. As the charged linker region is responsible for providing structural flexibility between amino and carboxyl terminal domain of Hsp82, the optimum interaction between Rad51 and Hsp82 might be lacking in that mutant. Hence, we hypothesize that effective Hsp82 and Rad51

interaction may be crucial for nuclear function of Rad51. Using *in-silico* approaches involving Hsp82 and Rad51 protein docking we have identified two strong interacting partners, namely; Hsp82<sup>R670</sup>-Rad51<sup>E108</sup> (salt-bridge) and Hsp82<sup>K637</sup>-Rad51<sup>M142</sup> (H-bond). In order to understand the importance of these interaction, we have generated two mutants of rad51 (E108L and M142L) where the corresponding amino acid residues are replaced by a hydrophobic residue leucine. Our analysis reveals that between the two mutants of rad51 the single mutant E108L is extremely sensitive towards DNA damaging agents and completely defective in gene conversion, a signature function of Rad51. Our study reveals that Rad51<sup>E108L</sup> being strongly associated with Hsp82 becomes defective to redistribute itself to the nucleus upon DNA damage. Our study thus identifies a critical transition state in translocation of Rad51 from cytoplasm to nucleus. We conclude that Hsp82 regulates the entry of Rad51 to the nucleus upon DNA damage signal through reversible protein-protein interaction. In the case of Rad51<sup>E108L</sup>, the interaction between Hsp82 and mutant Rad51 becomes irreversible due to stronger association, and hence even in the presence of DNA damaging condition, the mutant Rad51 protein remains probably locked within Hsp82 in the cytoplasm. Hence, such condition manifests complete loss of function of Rad51.

#### **5.2 RESULTS**

#### 5.2.1 Molecular docking studies to predict the interaction between Hsp82 and Rad51

The 3D structure of Rad51 (PDB ID: 1SZP) and Hsp82 (PDB ID: 2CG9) were retrieved from RCSB Protein Data Bank. Rad51 protein (1SZP) is a homo hexamer containing chains A, B, C, D, E, and F with sulphate ion bound to each chain. Hsp82 protein (2CG9) is a homo dimer containing chains A and B and is complexed with co chaperone Sba1 comprising chains X and Y. Proteinprotein docking was done in collaboration with the laboratory of Dr. Achuthsankar S. Nair, University of Kerala. The docking study was performed for varying combinations of monomers, dimers and hexamers using fully automated web-based program ClusPro 2.0 (287) which employs improved Fast Fourier Transform (FFT) based rigid docking program PIPER (288). 30 models of the protein-protein complex were generated in each docking for each of the four types of interactions namely; Balanced, Electrostatic favored, Hydrophobic favored and Van der Waals + Electrostatic favored. The hydrophobic-favored interaction showed lowest energy values and corresponding protein complex model with maximum members in the largest cluster were chosen. The surface view of three dimensional structure of Rad51 displays a characteristic pocket in each of the monomer into which the Hsp82 is found to dock. The docked complex models showed formation of several salt bridge and hydrogen bonds implying strong interaction between the proteins. Close analysis showed that the critical amino acids involved in the interaction of the two proteins were C-terminal residues of Hsp82 A chain - Arg670, Lys637, Thr649 and N-terminal residues of Rad51 E chain - Glu108, Met142 and Glu156 respectively. We focused our analysis on two such pairs which are having shortest bond distance within themselves. We observed that there exists a salt bridge between Hsp82<sup>R670</sup> and Rad51<sup>E108</sup> with a bond distance of 1.88 Å and hydrogen bonding between Hsp82<sup>K637</sup> and Rad51<sup>M142</sup> having a bond distance of 1.7 Å (Fig 24).

Figure: 24

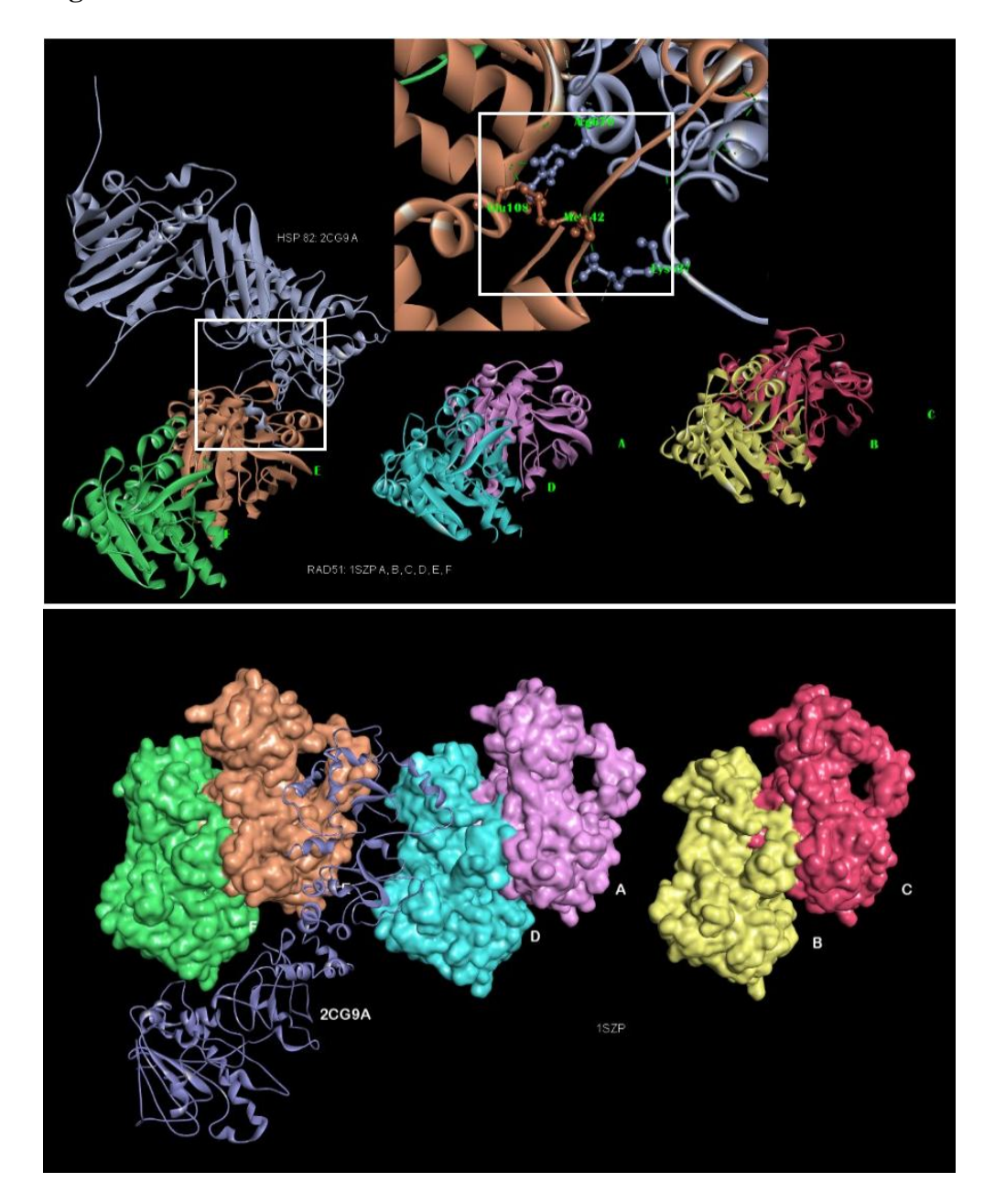


**Figure 24:** Molecular docking studies to predict the interaction between Hsp82 and Rad51: Docked complex of Hsp82A chain with Rad51 hexamer EF-AD-BC shows interaction in E chain. Inset is the magnified view of the interacting residues Glu108 and Met142 of Rad51 with Arg670 and Arg637 of Hsp82.

#### 5.2.2 Generation of *E108Lrad51* and *M142Lrad51* mutants

To understand the importance of the identified residues in our in silico analysis, we planned to incorporate the mutation on the Rad51. As E108 and M142 residues of Rad51 are predicted to have strongest interaction with Hsp82, we initiated the analysis by mutating these residues on Rad51. Two point mutants of Rad51 were generated using Splice Overlap Extension (SOE) as mentioned in material and method section. We have done the multiple sequence alignment of Hsp82 and Rad51 and found that these pairs of amino acids in Rad51 and Hsp82 are evolutionary conserved (Fig 25A and 25B). In Hsp82, these residues reside in the C-terminal domain of Hsp82 (33). In Rad51, both the amino acids E108 and M142 are present in the N-terminal domain of Rad51 which is outside its catalytic domain (Fig 25C). To evaluate the functional roles of these amino acids we have mutated glutamic acid (Glu) at 108<sup>th</sup> and methionine (Met) at 142<sup>nd</sup> position with the hydrophobic amino acid leucine. We speculate that the change in the amino acids of Rad51 would disturb the interaction through salt bridge/H-bonds with the corresponding residues on Hsp82. The mutants were subsequently cloned into yeast 2µ expression vector (pTA) and confirmed by DNA sequencing. As Rad51 and Hsp82 interaction is essential for the stability of Rad51, we have determined the stability of rad51 mutant proteins by western blot analysis. For this, we generated yeast strains as listed in table 2 by transforming individually pTA (empty), pTA-RAD51, pTAE108Lrad51, and pTAM142Lrad51 vectors into null rad51 yeast strain. We isolated protein from NRY1, NRY2, TSY17 and TSY18 strains and probed with anti-Rad51 antibody. The endogenous levels of mutant rad51 were found to be comparable to that of the wild type. Hence we conclude that rad51 mutant proteins are stably maintained in the cell (Fig 25D).



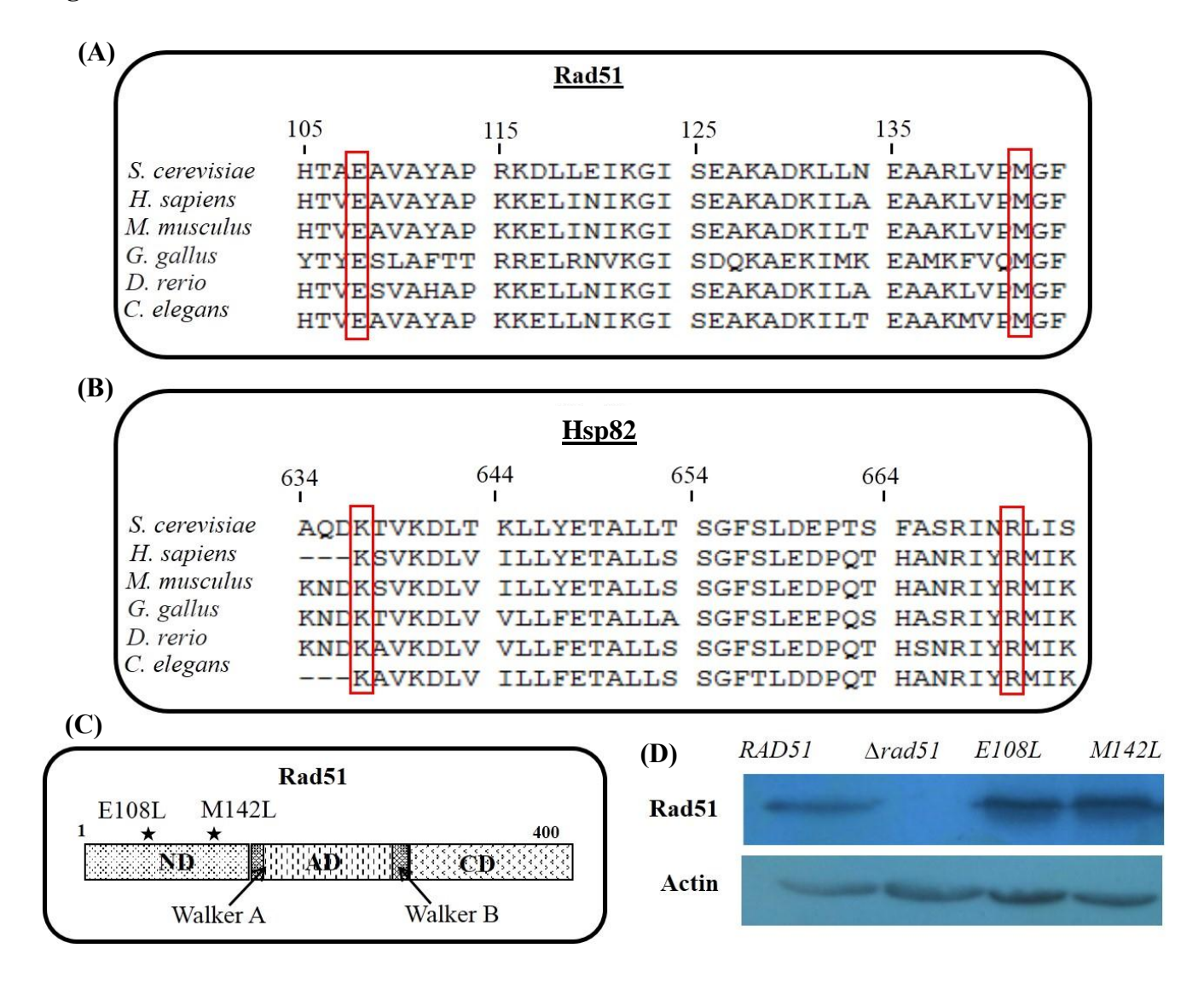


**Figure 25:** Generation of *RAD51* mutant strains: (A) Multiple sequence alignment of Rad51 (Nterminal domain) and (B) Hsp82 (C-terminal domain) protein sequences of *S. cerevisiae* (yeast) with *M. musculus* (mouse), Homo sapiens (human), C. elegance (caeel), *D. rario* (Zebrafish), *S. pombe* (schpo). The highlighted amino acids in red color box represent the identified residues in our docking analysis. (C) Schematic representation of Rad51 domains demonstrating boundaries of N-terminal, ATPase (AD) and C-terminal domain along with the Walker A, Walker B motif. (D) Western blot performed using protein extracts of strains expressing Rad51, Rad51<sup>E108L</sup> and Rad51<sup>M142L</sup>. Actin used as a loading control.

## 5.2.3 Mutation at E108<sup>th</sup> position of Rad51 sensitizes the cells to MMS and renders them deficient in gene conversion

In Saccharomyces cereviseae, homologous recombination is the preferred pathway for repairing DSBs and Rad51 occupies the crucial position in the pathway. To understand the effect of rad51 mutation, we first performed the return to growth cell survivability assayupon DNA damage. This was implemented by exposing NRY1, NRY2, TSY17 and TSY18 cells to 0.03% of MMS (methyl methane sulphonate) for 2 hrs. Subsequently treated and untreated cells were spotted on normal selective medium after serial dilution (Fig 26A). We observed that E108Lrad51 cells are highly sensitive to MMS induced DNA damage, similar to that observed in  $\Delta rad51$  cells. However M142Lrad51 mutant does not display significant effect on cell survivability upon DNA damage. Mechanism of homologous recombination involves repairing the DSBs by utilizing homologous sequence from the genome. This process involves the gene conversion which is mediated by Rad51. Therefore any inadequacy in Rad51 function will result in defective gene conversion and reduced HR efficiency. Our previous experiment displays sensitivity of one of the rad51 mutants towards MMS, which indicates the intriguing possibility of defect in Rad51 function. To gain insight about the exact effect of rad51 mutations on HR, we performed gene conversion assay by employing a yeast strain called NA14 (289). This strain has a cassette having two copies of URA3, separated by 3 Kb, out of which one *ura3* copy is inactivated by the insertion of HO endonuclease restriction site. The KANMX gene is incorporated within the two URA3 genes. HO endonuclease is expressed in the strain by a galactose inducible promoter. Upon galactose treatment, HO endonuclease is expressed and it creates DSB in the first *ura3* gene as depicted in the Figure 26B. The DSB can be repaired by any of the two HR pathways; one is Rad51 independent single strand annealing (SSA), which is an error prone repair pathway that results complete loss of intermediate KANMX gene, the other one is Rad51 dependent error free repair pathway known as gene conversion which allows the retention of the KANMX cassette (Fig 26B) (13). To score the effect of mutant rad51 on gene conversion, we modified the NA14 strain and generated strains where native RAD51 is knocked out and in that background the empty plasmid, wild-type RAD51 and each of the two mutant rad51(s) were transformed respectively. Hence we generated strains TSY20, TSY21, TSY22 and TSY23 as mentioned in material and method section. The percent gene conversion was scored by growing cells on G418 sulfate containing plates after galactose induction. Our experimental data indicates that there is no significant change in the gene conversion (GC) efficiency of wild type and M142Lrad51 both being near 40%. However, the GC score for the E108Lrad51 mutant (10.5%) is comparable to that of  $\Delta rad51$  (7%) (Fig 26C). Overall we conclude from our experimental data that E108L mutant behave as complete loss of function mutant of Rad51 and the M142L mutant behaves as the wild type strain in our assay.



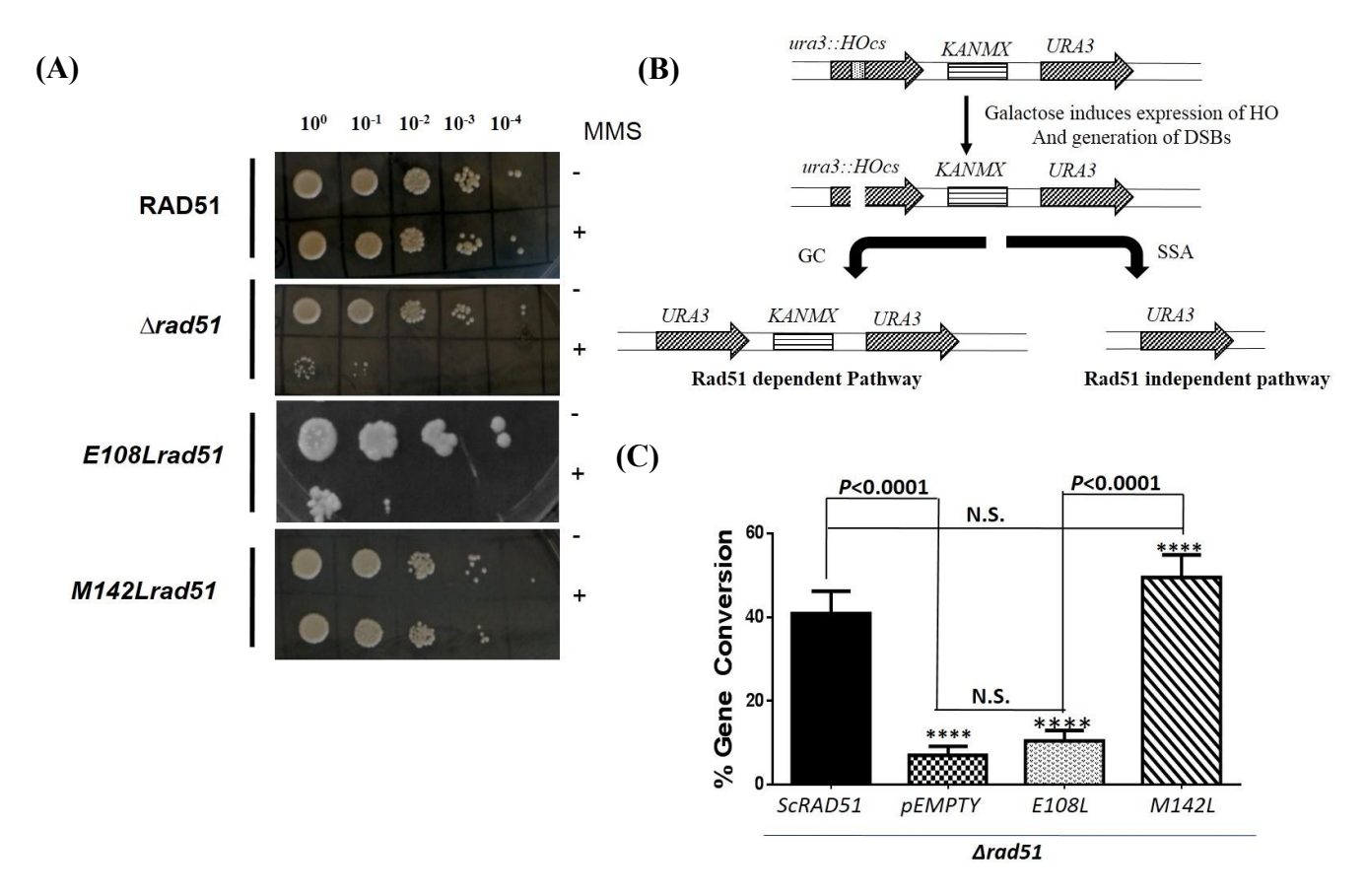


**Figure 26:** Mutation at E108<sup>th</sup> position of Rad51 sensitizes the cells to MMS and renders them deficient in gene conversion: (A) Pictorial representation of return to growth assay upon MMS treatment. Cells were spotted after serial dilution of treated and untreated cells for each mutant. First lane in case of each mutant shows untreated and second lane shows treated cells (B) Schematic diagram of a cassette incorporated in the strain used for studying gene conversion efficiency. It harbors two copies of *URA3* one of which is mutated by the insertion of HO endonuclease site. Induction with galactose creates single DSB in the mutated *ura3*, repair of which takes place either by Rad51 dependent or by Rad51 independent manner. *KANMX* cassette will be retained only if repair happens *via* Rad51 dependent manner. (C) Graph showing the percentage of gene conversion. Cells were spread on galactose containing plates and subsequently obtained colonies were patched on G418 sulphate plates. Percentage is determined by calculating the number of colonies grown on G418 sulphate plate versus number of colonies obtained on galactose plate. Error bars indicate SD; n = 3 (\*\*\*\*\*, P< 0.0001; P values were calculated using the two-tailed Student t test).

### 5.2.4~HO induced Rad51 recruitment to the broken DNA junction is severely compromised in E108Lrad51

During the repair of damaged DNA through HR, Rad51 is loaded to the ssDNA and facilitates the repair by performing strand exchange. This recruitment of Rad51 to the broken junction is a hallmark of DNA repair (130). Our previous observations suggest that rad51 mutants are defective in cell survivability and gene conversion upon DNA damage. This defect may be a defect in inadequate localization of rad51 mutants to the nucleus, upon DNA damage. To probe that, we investigated the recruitment of rad51 to the DSBs. We used chromatin immuno-precipitation to study the recruitment of rad51 to the damaged site. We used the strains which were used earlier for scoring gene conversion efficiency. Using the anti-Rad51 antibody (as described in material method section) we pulled down the Rad51 bound DNA segments. The Rad51 recruitment was quantified using URA3 specific primer set OSB278 and OSB279. Quantification of amplified DNA indicates the defective recruitment of rad51 mutants to the DSB as compared to the wild type Rad51. To confirm the specificity of Rad51 recruitment to the DSB, we performed ChIP with IgG, which does not give any amplification with the precipitated sample. We have estimated that the recruitment of Rad51<sup>E108L</sup> is 50% however there is no significant difference in the recruitment of rad51<sup>M142L</sup> to the broken DNA compared to that of the wild type (Fig 27A and 27B). To exclude the possibility that, the defect in the mutant rad51 recruitment to the DSB is not due to the inefficiency of galactose induced DSB, we performed a control experiment. For this purpose, we isolated genomic DNA from galactose treated and un-treated cells of each strain and performed the PCR using a forward primer, which is 20 bp upstream to the HO site and KanB1 reverse primers. We observed very less amplification in case of galactose treated samples as compared to untreated samples, indicating the successful generation of DSB in all the strains (Fig 27C). Overall from this set of data we conclude that rad51<sup>E108L</sup> is defective in the recruitment to DSBs.

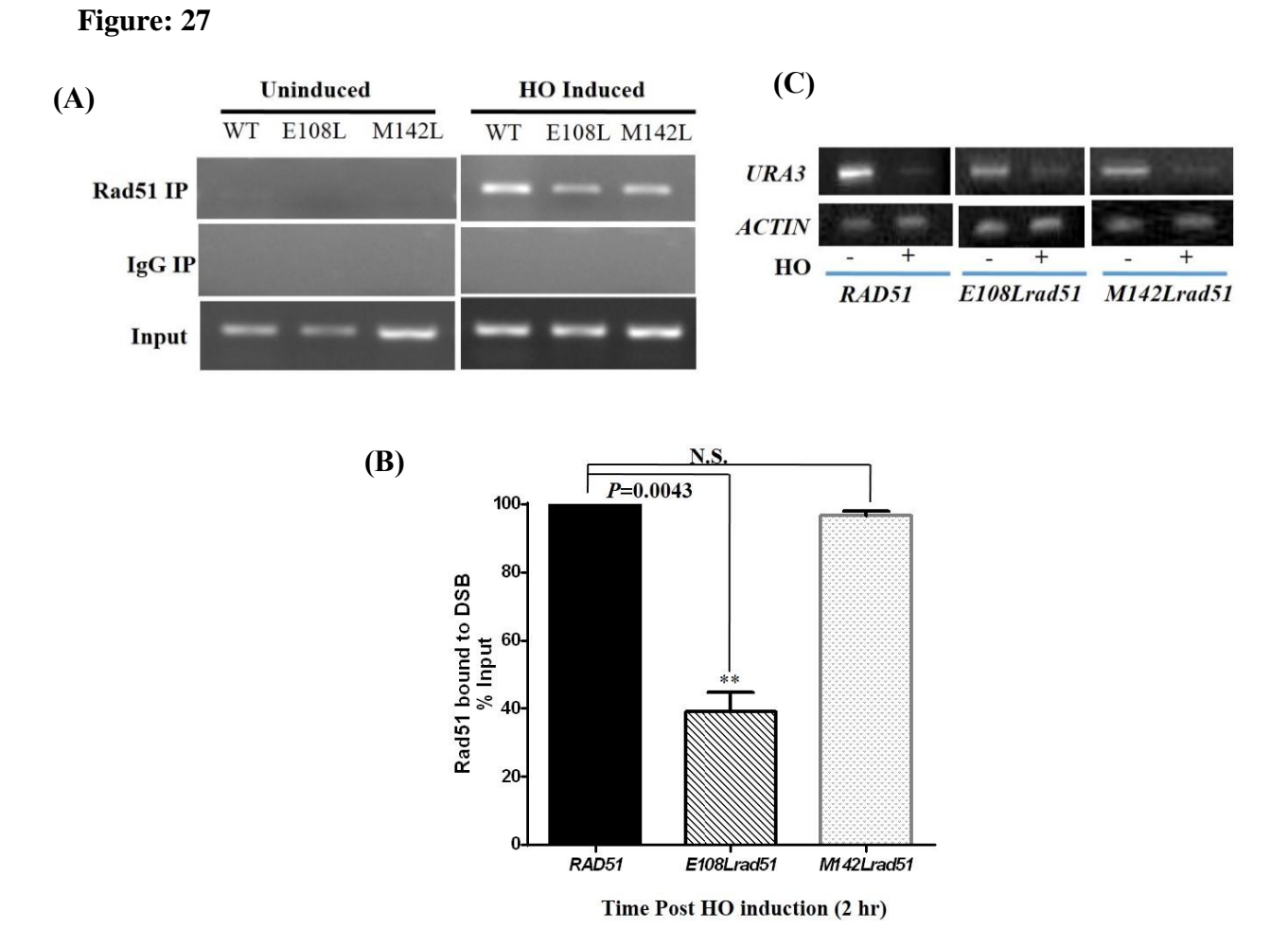
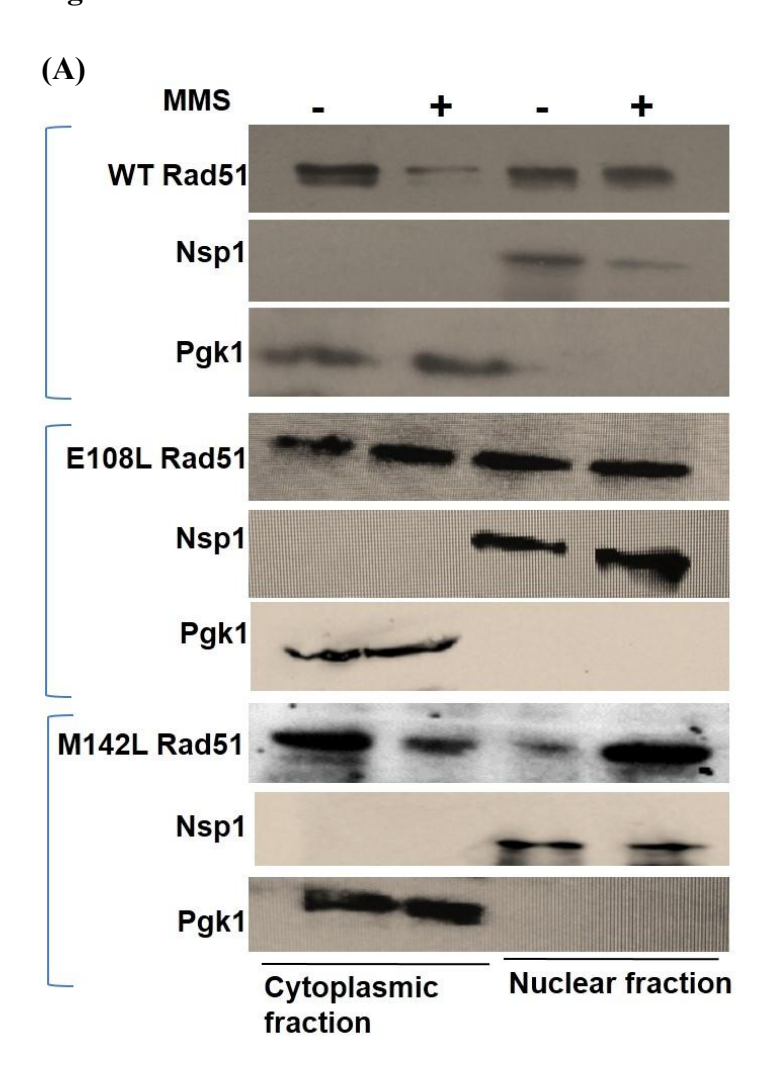


**Figure 27:** *HO* induced Rad51 recruitment to the broken DNA junction is severely compromised in *E108Lrad51*: (A) chromatin immunoprecipitation (ChIP) of strains expressing wild type Rad51, *E108Lrad51* and *M142Lrad51*. Gel image showing the one of the representatives PCR product of input and precipitated samples using *URA3* donor specific primer. Immunoprecipitation was performed using anti-Rad51 and IgG antibodies. Input represents the total amount of DNA in the sample. (B) Each set was repeated three times and the band intensities of the recruited samples upon HO induction were quantified using image J software and comparative recruitment of Rad51 and mutants are plotted with respect to the input. Error bars indicate SD; n = 3 (*P* values were calculated using the two-tailed Student t test, \*\*\*, *P*< 0.01, NS= non significant). (C) Semi quantitative RT-PCR, representing the amplification of DNA around DSB site in *URA3*, before and after HO endonuclease induction. Lower intensity of band in HO induced sample indicates the DSB generation in strains having WTRad51, *E108Lrad51* and *M142Lrad51*. Actin was used as a loading control.

#### 5.2.5 DNA damage fails to import Rad51 to the nucleus in E108Lrad51 mutant

Earlier experimental result shows that upon double strand break, the recruitment of mutant rad51 to the broken DNA junction is significantly less compared to the wild type Rad51. This may be due to the defect in the translocation of rad51 to the nucleus upon DNA damage. To examine that we used the strains NRY2, TSY17 and TSY18 that are harboring episomal copy of RAD51, E108Lrad51 and M142Lrad51 respectively. In each strain Rad51 is expressed from the constitutive promoter GPD. Hence the expression levels of Rad51/rad51 mutants are not induced upon DNA damage. We subjected the strains with 0.15% MMS for 2 hr. We used sub-cellular fractionation to isolate the nuclear and cytoplasmic fraction and subjected them to western blot using anti Rad51 antibody. We used the nuclear maker Nsp1 and cytoplasmic marker PGK1 as a loading control. Our study shows that even in absence of MMS some residual amount of Rad51 is already present to the nucleus. However, in post MMS treatment, there occurs 4 folds increment in the levels of Rad51 in the nucleus in case of wild type and M142Lrad51 mutant (Fig 28A and 28B) compared to the cytoplasm. However there occurs no increment in E108Lrad51 in the nucleus upon DNA damage (Fig 28A). This result emphasizes that importance of Rad51<sup>E108</sup> towards the DNA damage induced nuclear import of Rad51.

Figure: 28



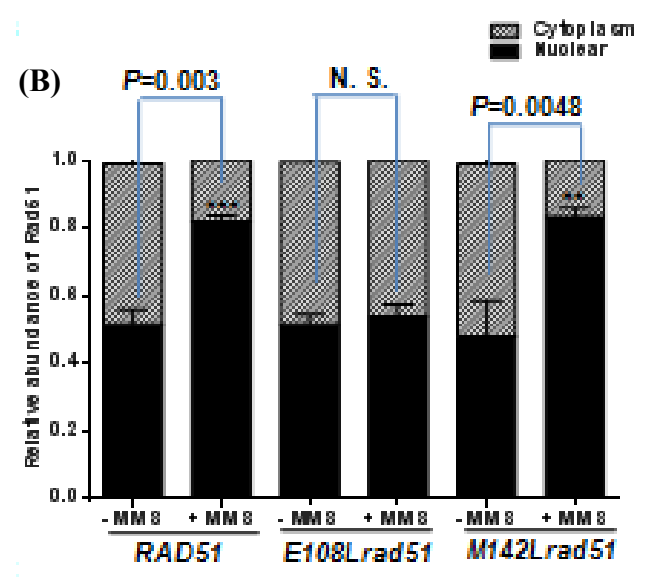


**Figure 28:** DNA damage fails to import Rad51 to the nucleus in *E108Lrad51* mutants: (A) Western blot showing the nuclear fraction and cytoplasmic fraction of strains harboring WTRad51, *E108Lrad51* and *M142Lrad51*. Samples are probed with anti-Rad51 antibody before and after 2 hrs of MMS induction. Nuclear fraction is normalized with Nsp1 and cytoplasmic fraction is normalized with Pgk1. (B) Quantification of band intensities of above western blot. Average intensities of at least three western blots were quantified of each strain and mean values were plotted. Relative abundance of wild type and mutant Rad51 in the nuclear fraction upon MMS treatment is compared to that of untreated nuclear fraction. Error bar shows the mean standard deviation (SD); n=3; *P* values were represented, NS means not significant.

### 5.2.6 Rad51<sup>E108</sup> shows stronger association with Hsp82

In order to quantitatively measure the interaction of Rad51 with Hsp82, we analyzed the interaction between wild type and mutant Rad51(s) and Hsp82 using SPR (surface plasmon resonance) spectroscopy. To this end, we cloned RAD51, E108Lrad51 and M142Lrad51 into pET22b expression vector and HSP82 into pET28a vector. After successful cloning, we expressed Rad51, Rad51<sup>E108L</sup> and Rad51<sup>M142L</sup> into Rossetta E. coli bacterial expression system and Hsp82 into BL-21DE3\* E coli. expression system (Fig 29A, 29B, 29C and 29D) as mentioned in material and method section. Expressed proteins were purified using Ni-NTA column using protocol described in material method section and used for further studies (Fig 29E). We immobilized purified Hsp82 (ligand) on CM-5 sensor chip. The analytes (Rad51) were taken in varied concentrations and we observed increase in the relative response with increasing concentration which establishes the accurate interaction of analyte with ligand. Interaction between ligand and the analyte was quantified and the equilibrium dissociation constant  $(K_D)$  was measured. To determine the  $K_D$ values, three independent set of experiments were performed with wild type and each of the Rad51 mutants and average  $K_D$  was calculated. We determined the dissociation constant of (0.9176 $\pm$ 0.5) μM and (12.85±3.6) μM for the wild type Rad51-Hsp82 and Rad51<sup>M142L</sup>-Hsp82 complex respectively. However, we find that for Rad $51^{E108L}$ -Hsp82 interaction, the  $K_D$  value was  $(1.24\pm0.7)$ nM, which is 1000 folds lesser than the wild type complex. The equilibrium dissociation constant is inversely proportional to the strength of interaction between proteins. Thus our analysis indicates 1000 folds stronger association between Rad51<sup>E108L</sup> and Hsp82. However, the association between Rad51<sup>M142L</sup> and Hsp82 is 10 folds less compared to the wild type interactions (Table 5).

Figure: 29

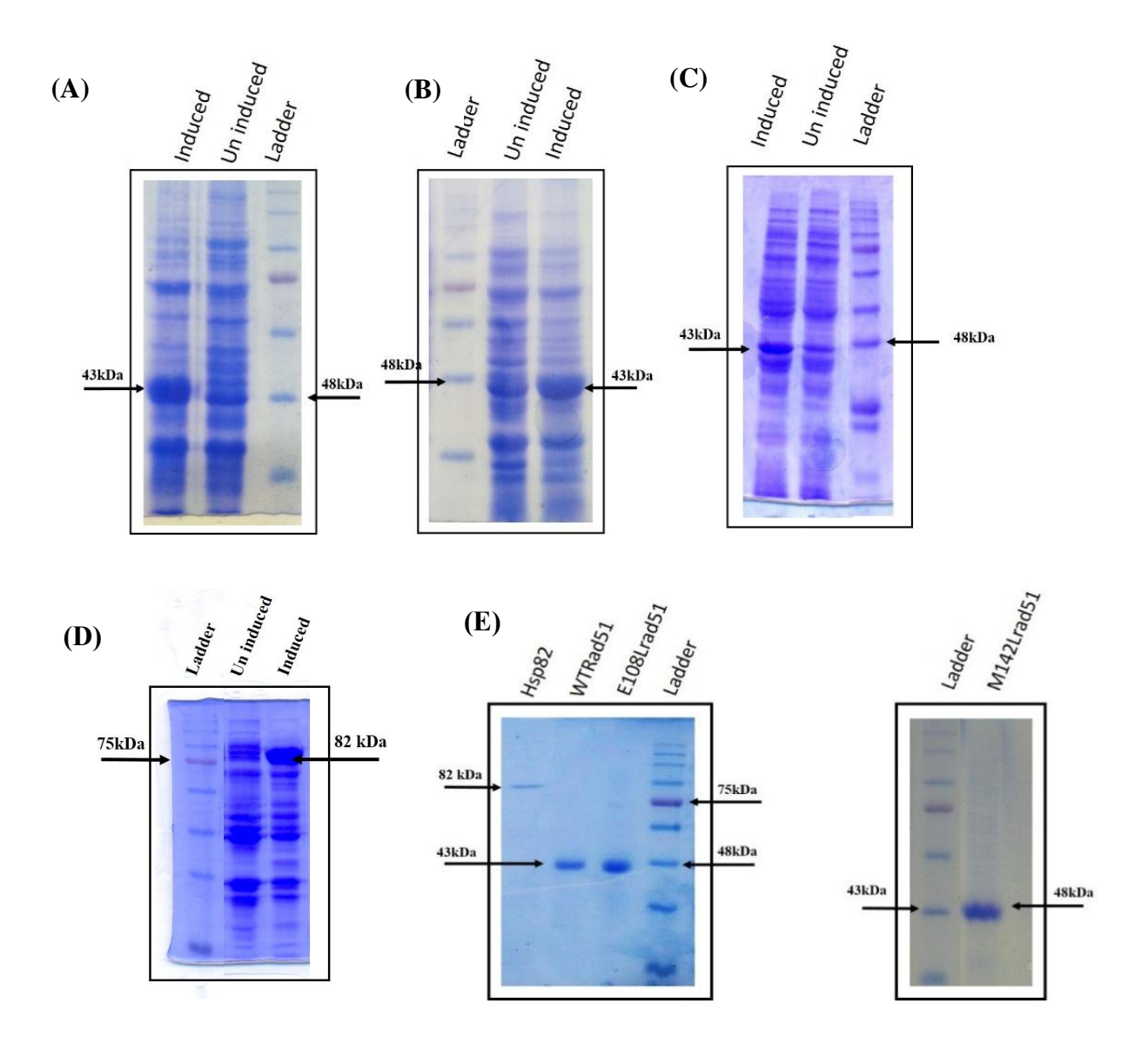


**Figure 29:** (A) SDS gel image showing the expression of recombinant WT Rad51 protein (B) SDS gel showing the expression of recombinant Rad51<sup>E108L</sup> (C) SDS gel showing the expression of recombinant Rad51<sup>M142L</sup> mutant protein. In figures A, B and C: Induced samples collected after 4hrs of IPTG inductions (D) SDS gel showing the expression of recombinant Hsp82 (E) SDS gel displaying the purified Hsp82, Rad51, Rad51<sup>E108L</sup> and Rad51<sup>M142L</sup> proteins.

Table 5: Equilibrium dissociation constant ( $K_D$ ) for the interaction of Hsp82 with wild type Rad51 and rad51 mutant proteins

S. NO	proteins	K <sub>D</sub> value
1	Hsp82-Rad51	0.9176±05 μM
2	Hsp82-Rad51 <sup>E108L</sup>	1.24±0.7 nM
3	Hsp82-Rad51 <sup>M142L</sup>	12.85±3.6 μM

## **DISCUSSION**

In the first part of our work we have established that Hsp90 controls the homologous recombination pathway of DNA repair by providing stability to Rad51. In the second part of our study we demonstrated that Hsp90 regulates the nuclear translocation of Rad51 upon DNA damage. Initial knowledge in this field indicated that, the inhibition of Hsp90 leads to deficiency in DNA repair. However, due to the presence of contradictory reports, it was not clear, whether Hsp90 is directly or indirectly linked with DNA repair (235). Thus, we aim to explore in detail about the regulation of HR by Hsp90. Using *Saccharomyces cerevisiae* as a model, where HR is the predominant DNA repair pathway, we explored the effect of Hsp90 (yeast Hsp82) inhibition on DNA repair. Our results with temperature sensitive mutant (*iG170Dhsp82*) depict that Hsp90 function is essential for the cell survival upon MMS and UV induced DNA damage. Since MMS and UV sensitivity cannot be directly correlated with the HR efficiency, we measured the gene targeting efficiency of this mutant and scored the HR efficiency. This analysis reveals the importance of Hsp90 specifically for HR mediated DNA repair.

Hsp90 has a highly conserved structure where different domain contributes to different functions by having domain specific interactions with several co chaperones. We included various Hsp90 mutants, which are expanded through different domains of Hsp90. Our work indicates the differential defect in HR efficiency with various Hsp90 mutants across the three domains. Our work demonstrates that N-terminal mutants of Hsp90 are severely defective in the cell survival and gene targeting upon DNA damage. As N-terminal domain is involved in ATP binding and

hydrolysis, it is not surprising to observe the necessity of ATPase activity of Hsp90 for HR. This is proved by the experiments with ATPase dead mutant *T1011hsp82*, which possesses only 5% ATPase activity as compared to wild type Hsp90 (276). Dramatic decrease in the cell survival as well as gene targeting was observed in *T1011hsp82* mutant, which supports the requirement of ATPase activity for DNA repair. Dependency of DNA repair on ATPase activity of Hsp90 is also confirmed by iA587T C-terminal Hsp82 mutant. This mutant possesses ATPase activity and binds to AMP-PNP with similar affinity like wild type Hsp82 and in our study this mutant does not show any defect in DNA repair pathway. Another mutant T22I holds 6 times more ATPase activity than the wild-type however its affinity for AMP-PNP is less than that of the wild type (276). This mutant results in the significant reduction in the HR efficiency. On the other hand, the A41V point mutant, with a mutation located at the rear end of the nucleotide binding pocket, also shows reduced affinity for AMP-PNP, which accounts for its moderate phenotype in HR efficiency of these mutants. These set of observations clearly signify the differential effect of Hsp90 domains on DNA repair, where N-terminal domain is critical for the DNA repair.

ATPase activity of Hsp90 triggers its conformational switching and helps in the maturation of client proteins. High-throughput *in vitro* study reveals the interaction of HR player Rad52 with Hsp90 N-terminal domain by tandem affinity but no direct interaction of Hsp90 with Rad51 (key contributor in HR) has been reported (74). In the present study, we described that both Rad52 and Rad51 are destabilized in the cells upon Hsp90 functional knockout. The co-immuno precipitation data reveals the direct physical interaction between Hsp90 and Rad51 and establishes Rad51 as a client of Hsp90. *T1011hsp82* also displays significant reduction in the Rad51 protein level, which correlates well with high MMS sensitivity of this mutant. The charged linker deletion mutant (Δ211-259hsp82) presents an interesting scenario. It is the only mutant that shows 8-fold reduction

in cell survivability upon MMS treatment as well as 80 % reduction in gene-targeting efficiency even though the levels of Rad51 and Rad52 remain unchanged. This mutant is so severely defective in HR function that it remains refractory to gene tagging and gene knockout despite several attempts. Previously, it was reported that the hsp82(211-259) mutant did not affect nucleotide binding to the N-terminal domain of Hsp90 and that its ATPase activity was also slightly higher (0.6 min<sup>-1</sup>) than that of the wild type (0.5 min<sup>-1</sup>) (280). Our work indicates that though the structural stabilities of Rad51 and Rad52 in this mutant probably remain unaltered, but Rad51-mediated gene-targeting activity is drastically reduced. To account for this discrepancy, we propose that the ATPase activity of Hsp82 is necessary but not sufficient for the activity of Rad51. Our hypothesis is supported by the significant reduction in the number of Rad51 foci formation, specially the nuclei containing more than 1 focus was drastically low in this mutant, which accounts for the enormous reduction in cell viability. Thus, it is likely that in the absence of the charged linker region, only a fraction of the total Rad51 is active. We propose that a dynamic equilibrium might exist between the active and inactive forms of Rad51 in the cell. In the charged linker deletion mutant, the equilibrium is probably shifted toward the inactive state of Rad51. Based on this hypothesis, one may predict that if the amount of Rad51 were increased artificially, the abundance of active Rad51 would increase, and this might rescue the phenotype. Our work showing a partial rescue of MMS sensitivity and gene-targeting efficiency supports this hypothesis.

Charged linker region maintains the flexibility of Hsp90, which is required for client protein interaction (36, 38). As DNA damage induced foci formation is inefficient in charged linker deletion mutant, we hypothesize that there may be a correlation between the extent of Rad51-Hsp90 interaction and optimum Rad51 functions upon DNA damage. To that end, we proceeded to map this interaction and identified the residues involved in this interaction. N-terminal domain

(NTD) residues of Rad51 namely; glutamic acid 108th and methionine 142nd, were predicted for participating in stronger interaction with Hsp90. The two residues of Rad51 (E108 and M142) that are closely linked with Hsp90 (through salt bridges/H-bonding) reside outside the ATPase domain of Rad51 and are evolutionary conserved. Although both the mutations are present in the Nterminal domain, however they were not previously identified as the essential amino acids required for the interaction with RAD52 epistatis group (168). To understand the role of these residues, we followed the mutational approach to incorporate mutations on these two residues and created two point mutants; E108Lrad51 and M142Lrad51. The rationale behind our analysis was to perceive the correlation between the Rad51-Hsp90 interactions and the Rad51 function upon DNA damage. Although Hsp90 interaction points were mutated on Rad51, we find that it does not alter the stability of the mutants. However in spite of holding the stability, E108Lrad51 was highly sensitive towards DNA damaging agents, but the phenotype of M142Lrad51 was comparable to wild type. During homologous recombination Rad51 participates in the homology search and this is mediated by gene conversion (131, 132). We find that the rad51<sup>E108L</sup> mutant is also defective in gene conversion efficiency, a signature function of Rad51. This made us curious to understand the reason behind the insufficiency of this rad51 mutant for their functions. We observed that changing 108th glutamic acid with leucine, results in 1000 folds stronger association between Rad51<sup>E108L</sup> and Hsp90 compared to wild type Rad51 and Hsp90. This could be possible due to the changes in the conformation of Rad51<sup>E108L</sup>, which exposes several new contacts residues for interactions with Hsp90.

This is supported by the bioinformatics docking analysis of Hsp90 and mutant rad51<sup>E108L</sup>. We observed increase in cluster size in mutant complex compared to the wild type. It is known that Hsp90 shows variable degree of association with its clients. Hsp90 clients like kinases are primarily associated with Hsp90 through transient interaction and once chaperoned they are readily

released from Hsp90 as a functional protein. However, clients like steroid hormone receptors, heat shock factor 1 (HSF1) etc. remain associated with Hsp90 to maintain their functional form. Also, the extent of association between Hsp90 and its client can alter the cellular function of its client. It was earlier reported that recognition of clients can be modulated by the single mutation in the protein. As for example, EGFR<sup>L858R</sup> and BRAF<sup>V600E</sup> are transformed oncoproteins and rely on Hsp90 for their stability however their wild type counterparts do not show such relation. It is observed that single amino acid change leads to the increased association between EGFR<sup>L858R</sup> / BRAF<sup>V600E</sup> and Hsp90 as compared to the respective wild type proteins. In a typical experiment it was observed that BRAFV600E as well as EGFRL858R were detected in the form of complex with Hsp90 and co chaperone Cdc37 by co immune precipitation analysis (55-57), however the association of their wild type counterparts are transient with Hsp90. Thus it is apparent that single substitution in the protein can alter its association towards Hsp90. Stronger association between mutant Rad51<sup>E108L</sup> and Hsp90 makes it difficult to explain the cause behind the extreme sensitivity of this mutant towards DNA damaging agent. We postulate that the dynamic interaction between Hsp90 and Rad51 is required to facilitate the proper functioning of client protein Rad51. Consequently, the defect in dynamic nature in client chaperone interaction may hamper the release of Rad51 upon DNA damage. If this hypothesis is true, we would see the inadequacy in DNA damage induced mutant rad51 accumulation in the nucleus. Alternatively, it is possible to have an unidentified evolutionary conserved pathway among all eukaryotes which is responsible for DNA damage dependent nuclear entry of Rad51. There are many evidences which demonstrate that Hsp90 assists the client proteins for their translocation to different cellular compartments. One such example is steroid hormone receptors (SHR), which remains in the cytoplasm in the complex form with Hsp90 and upon hormone signal Hsp90 facilitates its nuclear entry (290, 291). We probed the level of rad51mutant proteins in the nucleus and cytoplasm upon DNA damage. Our

analysis reveals that Rad51<sup>E108L</sup> fails to relocate to the nucleus upon DNA damage and major amount of Rad51<sup>E108L</sup> remains in the cytoplasm. Reduced availability of Rad51<sup>E108L</sup> mutants in the nucleus ultimately reflects the defective recruitment of Rad51<sup>E108L</sup> mutants to the broken junction. This observation combining with our previous observations indicate the requirement of dynamic nature of Rad51-Hsp90 association. This is further confirmed by another mutant Rad51<sup>M142L</sup> which has 10 folds less association with Hsp90 as compared to the wild type Rad51. This mutant has no sensitivity towards MMS and possesses gene conversion efficiency similar to that of WTRad51. Besides it, the quantitative measurement reveals that the Rad51<sup>E108L</sup> recruitment to the broken double stranded DNA is 50% less than the wild type, while the recruitment of Rad51<sup>M142L</sup> is comparable to that of the wild type. In our sub-cellular fractionation study, we observe some basal levels of Rad51 remaining in the nucleus even in absence of MMS treatment. This is supported by our CHIP analysis which shows 30% recruitment of Rad51<sup>E108L</sup> to the broken DNA, although this strain is completely deficient in gene targeting. We speculate this 30% of Rad51<sup>E108L</sup> protein has been recruited to the DNA, which was already present in the nucleus before HO induction and this may not be sufficient for effective gene conversion. Hence it is evident that, the probable cause behind defective functions of Rad51<sup>E108L</sup> is inappropriate translocation of this mutant to the nucleus, which is linked to the loss in dynamic nature of Rad51 and Hsp90 interaction. Collectively our work establishes the importance of Hsp90 in homologous recombination pathway, where it appears to regulate the stability and functions of Rad51. Increasing line of upcoming evidences connects several DNA repair proteins like BRCA1, BRCA2, CHK1, DNA-PKcs, FANCA, and the MRE11/RAD50/NBN as dependent on Hsp90(292). Recent report shows that over-expression of Hsp90 leads to genomic instability by negative regulation of the check point kinase RAD53 (262). Our work along with these reports embarks the knowledge about the relationship of Hsp90 with DNA repair. Currently DNA repair along with the Hsp90 inhibitor is

being targeted in many cancer studies (216, 293). Understanding the detailed regulation of HR will be beneficial for further knowledge in the field. Hence in our proposed model, Hsp90 provides the functional maturity to Rad51 and also facilitates the DNA damage induced nuclear translocation of Rad51 either directly or indirectly. However detail analysis need to be done, in order to reach to a conclusive mechanistic involvement of Hsp90 in Rad51 mediated DNA repair.

## **References:**

- 1. Hipp, M. S., Park, S. H., & Hartl, F. U. (2014). Proteostasis impairment in protein-misfolding and-aggregation diseases. *Trends in cell biology*, 24(9), 506-514.
- 2. Bukau, B., Weissman, J., & Horwich, A. (2006). Molecular chaperones and protein quality control. *Cell*, 125(3), 443-451.
- 3. Dobson, C. M., Šali, A., & Karplus, M. (1998). Protein folding: a perspective from theory and experiment. *Angewandte Chemie International Edition*, *37*(7), 868-893.
- 4. Knowles, T. P., Vendruscolo, M., & Dobson, C. M. (2014). The amyloid state and its association with protein misfolding diseases. *Nature reviews. Molecular cell biology*, 15(6), 384.
- 5. Langer, T., Rosmus, S., & Fasold, H. (2003). Intracellular localization of the 90 kDA heat shock protein (HSP90α) determined by expression of a EGFP–HSP90α-fusion protein in unstressed and heat stressed 3T3 cells. *Cell biology international*, 27(1), 47-52.
- Tsutsumi, S., & Neckers, L. (2007). Extracellular heat shock protein 90: a role for a molecular chaperone in cell motility and cancer metastasis. *Cancer science*, 98(10), 1536-1539.
- 7. Taipale, M., Jarosz, D. F., & Lindquist, S. (2010). HSP90 at the hub of protein homeostasis: emerging mechanistic insights. *Nature reviews. Molecular cell biology*, *11*(7), 515.
- 8. Nadeau, K., Das, A., & Walsh, C. T. (1993). Hsp90 chaperonins possess ATPase activity and bind heat shock transcription factors and peptidyl prolyl isomerases. *Journal of Biological Chemistry*, 268(2), 1479-1487.

- 9. Subbarao Sreedhar, A., Kalmár, É., Csermely, P., & Shen, Y. F. (2004). Hsp90 isoforms: functions, expression and clinical importance. *FEBS letters*, *562*(1-3), 11-15.
- 10. Sorger, P. K., & Pelham, H. R. (1987). The glucose-regulated protein grp94 is related to heat shock protein hsp90. *Journal of molecular biology*, 194(2), 341-344.
- 11. Eustace, B. K., & Jay, D. G. (2004). Extracellular roles for the molecular chaperone, hsp90. *Cell cycle*, *3*(9), 1096-1098.
- 12. https://blast.ncbi.nlm.nih.gov/Blast.cgi
- 13. Young JC, Moarefi I&Hartl FU. (2001). Hsp90: a specialized but essential protein-folding tool. The journal of cell biology 23;154(2):267-73
- 14. Echeverria, P. C., & Picard, D. (2010). Molecular chaperones, essential partners of steroid hormone receptors for activity and mobility. *Biochimica et Biophysica Acta (BBA)-Molecular Cell Research*, 1803(6), 641-649.
- Van Der Lee, R., Buljan, M., Lang, B., Weatheritt, R. J., Daughdrill, G. W., Dunker, A. K., ... & Kim, P. M. (2014). Classification of intrinsically disordered regions and proteins. *Chemical reviews*, 114(13), 6589-6631.
- Karagöz, G. E., Duarte, A. M., Akoury, E., Ippel, H., Biernat, J., Luengo, T. M., Dickey,
   C. A. (2014). Hsp90-Tau complex reveals molecular basis for specificity in chaperone action. *Cell*, 156(5), 963-974.
- 17. Taipale, M., Krykbaeva, I., Koeva, M., Kayatekin, C., Westover, K. D., Karras, G. I., & Lindquist, S. (2012). Quantitative analysis of HSP90-client interactions reveals principles of substrate recognition. *Cell*, *150*(5), 987-1001.
- 18. Hagn, F., Lagleder, S., Retzlaff, M., Rohrberg, J., Demmer, O., Richter, K., & Kessler, H. (2011). Structural analysis of the interaction between Hsp90 and the tumor suppressor protein p53. *Nature structural & molecular biology*, *18*(10), 1086-1093.

- 19. Park, S. J., Kostic, M., & Dyson, H. J. (2011). Dynamic interaction of Hsp90 with its client protein p53. *Journal of molecular biology*, 411(1), 158-173.
- 20. Genest, O., Reidy, M., Street, T. O., Hoskins, J. R., Camberg, J. L., Agard, D. A.,& Wickner, S. (2013). Uncovering a region of heat shock protein 90 important for client binding in E. coli and chaperone function in yeast. *Molecular cell*, 49(3), 464-473.
- 21. Hawle, P., Siepmann, M., Harst, A., Siderius, M., Reusch, H. P., & Obermann, W. M. (2006). The middle domain of Hsp90 acts as a discriminator between different types of client proteins. *Molecular and cellular biology*, 26(22), 8385-8395.
- 22. Morishima, Y., Kanelakis, K. C., Murphy, P. J., Lowe, E. R., Jenkins, G. J., Osawa, Y.,& Pratt, W. B. (2003). The hsp90 cochaperone p23 is the limiting component of the multiprotein hsp90/hsp70-based chaperone system in vivo where it acts to stabilize the client protein hsp90 complex. *Journal of Biological Chemistry*, 278(49), 48754-48763.
- 23. Grad, I., & Picard, D. (2007). The glucocorticoid responses are shaped by molecular chaperones. *Molecular and cellular endocrinology*, 275(1), 2-12.
- 24. Bergerat, A., de Massy, B., Gadelle, D., & Varoutas, P. C. (1997). An atypical topoisomerase II from Archaea with implications for meiotic recombination. *Nature*, *386*(6623), 414.
- 25. Panaretou, B., Prodromou, C., Roe, S. M., O'Brien, R., Ladbury, J. E., Piper, P. W., & Pearl, L. H. (1998). ATP binding and hydrolysis are essential to the function of the Hsp90 molecular chaperone in vivo. *The EMBO journal*, *17*(16), 4829-4836.
- Gorska, M., Popowska, U., Sielicka-Dudzin, A., Kuban-Jankowska, A., Sawczuk, W., Knap, N., & Wozniak, F. (2012). Geldanamycin and its derivatives as Hsp90 inhibitors. *Front Biosci*, 17(2269), 77.

- 27. Prodromou, C., Siligardi, G., O'Brien, R., Woolfson, D. N., Regan, L., Panaretou, B., & Pearl, L. H. (1999). Regulation of Hsp90 ATPase activity by tetratricopeptide repeat (TPR)-domain co-chaperones. *The EMBO journal*, *18*(3), 754-762.
- 28. Scheufler, C., Brinker, A., Bourenkov, G., Pegoraro, S., Moroder, L., Bartunik, H., & Moarefi, I. (2000). Structure of TPR domain–peptide complexes: critical elements in the assembly of the Hsp70–Hsp90 multichaperone machine. *Cell*, *101*(2), 199-210.
- 29. Donnelly, A., & Blagg, B. S. (2008). Novobiocin and additional inhibitors of the Hsp90 C-terminal nucleotide-binding pocket. *Current medicinal chemistry*, *15*(26), 2702-2717.
- 30. Richter, K., Reinstein, J., & Buchner, J. (2002). N-terminal residues regulate the catalytic efficiency of the Hsp90 ATPase cycle. *Journal of Biological Chemistry*, 277(47), 44905-44910.
- 31. Obermann, W. M., Sondermann, H., Russo, A. A., Pavletich, N. P., & Hartl, F. U. (1998). In vivo function of Hsp90 is dependent on ATP binding and ATP hydrolysis. *The Journal of cell biology*, *143*(4), 901-910.
- 32. Sato, S., Fujita, N., & Tsuruo, T. (2000). Modulation of Akt kinase activity by binding to Hsp90. *Proceedings of the National Academy of Sciences*, 97(20), 10832-10837.
- 33. Ali, M. M., Roe, S. M., Vaughan, C. K., Meyer, P., Panaretou, B., Piper, P. W.& Pearl, L. H. (2006). Crystal structure of an Hsp90-nucleotide-p23/Sba1 closed chaperone complex. *Nature*, 440(7087), 1013.
- 34. Donnelly, A., & Blagg, B. S. (2008). Novobiocin and additional inhibitors of the Hsp90 C-terminal nucleotide-binding pocket. *Current medicinal chemistry*, *15*(26), 2702-2717.
- 35. Farrelly, F. W., & Finkelstein, D. B. (1984). Complete sequence of the heat shock-inducible HSP90 gene of Saccharomyces cerevisiae. *Journal of Biological Chemistry*, 259(9), 5745-5751.

- 36. Tsutsumi, S., Mollapour, M., Prodromou, C., Lee, C. T., Panaretou, B., Yoshida, S., & Neckers, L. M. (2012). Charged linker sequence modulates eukaryotic heat shock protein 90 (Hsp90) chaperone activity. *Proceedings of the National Academy of Sciences*, 109(8), 2937-2942.
- 37. Hainzl, O., Lapina, M. C., Buchner, J., & Richter, K. (2009). The charged linker region is an important regulator of Hsp90 function. *Journal of Biological Chemistry*, 284(34), 22559-22567.
- 38. Jahn, M., Rehn, A., Pelz, B., Hellenkamp, B., Richter, K., Rief, M.,& Hugel, T. (2014). The charged linker of the molecular chaperone Hsp90 modulates domain contacts and biological function. *Proceedings of the National Academy of Sciences*, 111(50), 17881-17886.
- 39. Young, J. C., Obermann, W. M., & Hartl, F. U. (1998). Specific binding of tetratricopeptide repeat proteins to the C-terminal 12-kDa domain of hsp90. *Journal of Biological Chemistry*, 273(29), 18007-18010.
- 40. Johnson, J. L., & Brown, C. (2009). Plasticity of the Hsp90 chaperone machine in divergent eukaryotic organisms. *Cell Stress and Chaperones*, *14*(1), 83-94.
- 41. Panaretou, B., Siligardi, G., Meyer, P., Maloney, A., Sullivan, J. K., Singh, S. & Cramer, R. (2002). Activation of the ATPase activity of hsp90 by the stress-regulated cochaperone aha1. *Molecular cell*, 10(6), 1307-1318.
- 42. McLaughlin, S. H., Smith, H. W., & Jackson, S. E. (2002). Stimulation of the weak ATPase activity of human hsp90 by a client protein. *Journal of molecular biology*, 315(4), 787-798.

- 43. Siligardi, G., Panaretou, B., Meyer, P., Singh, S., Woolfson, D. N., Piper, P. W. & Prodromou, C. (2002). Regulation of Hsp90 ATPase activity by the co-chaperone Cdc37p/p50 cdc37. *Journal of Biological Chemistry*, 277(23), 20151-20159.
- 44. Prodromou, C., Siligardi, G., O'Brien, R., Woolfson, D. N., Regan, L., Panaretou, B.& Pearl, L. H. (1999). Regulation of Hsp90 ATPase activity by tetratricopeptide repeat (TPR)-domain co-chaperones. *The EMBO journal*, *18*(3), 754-762.
- 45. Smith, D. F., Sullivan, W. P., Marion, T. N., Zaitsu, K. I. Y. O. S. H. I., Madden, B., McCormick, D. J., & Toft, D. O. (1993). Identification of a 60-kilodalton stress-related protein, p60, which interacts with hsp90 and hsp70. *Molecular and cellular biology*, *13*(2), 869-876.
- 46. Silverstein, A. M., Galigniana, M. D., Chen, M. S., Owens-Grillo, J. K., Chinkers, M., & Pratt, W. B. (1997). Protein phosphatase 5 is a major component of glucocorticoid receptor-hsp90 complexes with properties of an FK506-binding immunophilin. *Journal of Biological Chemistry*, 272(26), 16224-16230.
- 47. Pratt, W. B., Morishima, Y., Peng, H. M., & Osawa, Y. (2010). Proposal for a role of the Hsp90/Hsp70-based chaperone machinery in making triage decisions when proteins undergo oxidative and toxic damage. *Experimental Biology and Medicine*, 235(3), 278-289.
- 48. Whittier, J. E., Xiong, Y., Rechsteiner, M. C., & Squier, T. C. (2004). Hsp90 enhances degradation of oxidized calmodulin by the 20 S proteasome. *Journal of Biological Chemistry*, 279(44), 46135-46142.
- 49. McClellan, A. J., Xia, Y., Deutschbauer, A. M., Davis, R. W., Gerstein, M., & Frydman, J. (2007). Diverse cellular functions of the Hsp90 molecular chaperone uncovered using systems approaches. *Cell*, *131*(1), 121-135

- 50. Echeverría, P. C., Bernthaler, A., Dupuis, P., Mayer, B., & Picard, D. (2011). An interaction network predicted from public data as a discovery tool: application to the Hsp90 molecular chaperone machine. *PloS one*, *6*(10), e26044.
- 51. Laskar, S., Bhattacharyya, M. K., Shankar, R., & Bhattacharyya, S. (2011). HSP90 controls SIR2 mediated gene silencing. *PLoS One*, *6*(8), e23406.
- 52. Xu, Y., & Lindquist, S. (1993). Heat-shock protein hsp90 governs the activity of pp60v-src kinase. *Proceedings of the National Academy of Sciences*, 90(15), 7074-7078.
- 53. Brugge, J. S. (1986). Interaction of the Rous sarcoma virus protein pp60 src with the cellular proteins pp50 and pp90. In *Retroviruses 4* (pp. 1-22). Springer Berlin Heidelberg.
- 54. Xu, Y., Singer, M. A., & Lindquist, S. (1999). Maturation of the tyrosine kinase c-src as a kinase and as a substrate depends on the molecular chaperone Hsp90. *Proceedings of the National Academy of Sciences*, 96(1), 109-114.
- 55. Shimamura, T., Lowell, A. M., Engelman, J. A., & Shapiro, G. I. (2005). Epidermal growth factor receptors harboring kinase domain mutations associate with the heat shock protein 90 chaperone and are destabilized following exposure to geldanamycins. *Cancer research*, 65(14), 6401-6408.
- 56. da Rocha Dias, S., Friedlos, F., Light, Y., Springer, C., Workman, P., & Marais, R. (2005).

  Activated B-RAF is an Hsp90 client protein that is targeted by the anticancer drug 17-allylamino-17-demethoxygelda
- 57. Grbovic, O. M., Basso, A. D., Sawai, A., Ye, Q., Friedlander, P., Solit, D., & Rosen, N. (2006). V600E B-Raf requires the Hsp90 chaperone for stability and is degraded in response to Hsp90 inhibitors. *Proceedings of the National Academy of Sciences of the United States of America*, 103(1), 57-62.

- 58. Buchner, J. (2010). Bacterial Hsp90–desperately seeking clients. *Molecular microbiology*, 76(3), 540-544.
- 59. Whitesell, L., & Lindquist, S. L. (2005). HSP90 and the chaperoning of cancer. *Nature reviews. Cancer*, 5(10), 761.
- 60. Sreedhar, A. S., So, C., & Csermely, P. (2004). Inhibition of Hsp90: a new strategy for inhibiting protein kinases. *Biochimica et Biophysica Acta (BBA)-Proteins and Proteomics*, 1697(1), 233-242.
- 61. Scheibel, T., Weikl, T., & Buchner, J. (1998). Two chaperone sites in Hsp90 differing in substrate specificity and ATP dependence. *Proceedings of the National Academy of Sciences*, 95(4), 1495-1499.
- 62. Chiosis, G., & Neckers, L. (2006). Tumor selectivity of Hsp90 inhibitors: the explanation remains elusive.
- 63. Kamal, A., Thao, L., Sensintaffar, J., & Zhang, L. (2003). A high-affinity conformation of Hsp90 confers tumour selectivity on Hsp90 inhibitors. *Nature*, *425*(6956), 407.
- 64. Kamal, A., Boehm, M. F., & Burrows, F. J. (2004). Therapeutic and diagnostic implications of Hsp90 activation. *Trends in molecular medicine*, *10*(6), 283-290
- 65. Sidera, K., & Patsavoudi, E. (2014). HSP90 inhibitors: current development and potential in cancer therapy. *Recent patents on anti-cancer drug discovery*, 9(1), 1-20.
- 66. Shiau, A. K., Harris, S. F., Southworth, D. R., & Agard, D. A. (2006). Structural analysis of E. coli hsp90 reveals dramatic nucleotide-dependent conformational rearrangements. *Cell*, *127*(2), 329-340.
- 67. Chen, S., & Smith, D. F. (1998). Hop as an adaptor in the heat shock protein 70 (Hsp70) and hsp90 chaperone machinery. *Journal of Biological Chemistry*, 273(52), 35194-35200.

- 68. Johnson, B. D., Schumacher, R. J., Ross, E. D., & Toft, D. O. (1998). Hop modulates Hsp70/Hsp90 interactions in protein folding. *Journal of Biological Chemistry*, 273(6), 3679-3686.
- 69. Freeman, B. C., Felts, S. J., Toft, D. O., & Yamamoto, K. R. (2000). The p23 molecular chaperones act at a late step in intracellular receptor action to differentially affect ligand efficacies. *Genes & development*, 14(4), 422-434.
- 70. McLaughlin, S. H., Sobott, F., Yao, Z. P., Zhang, W., Nielsen, P. R., Grossmann, J. G., & Jackson, S. E. (2006). The co-chaperone p23 arrests the Hsp90 ATPase cycle to trap client proteins. *Journal of molecular biology*, *356*(3), 746-758.
- 71. Wandinger, S. K., Richter, K., & Buchner, J. (2008). The Hsp90 chaperone machinery. *Journal of Biological Chemistry*, 283(27), 18473-18477.
- Connell, P., Ballinger, C. A., Jiang, J., Wu, Y., Thompson, L. J., Höhfeld, J., & Patterson,
   C. (2001). The co-chaperone CHIP regulates protein triage decisions mediated by heat-shock proteins. *Nature cell biology*, 3(1), 93.
- 73. Pratt, W. B., & Toft, D. O. (2003). Regulation of Signaling Protein Function and Trafficking by the hsp90/hsp70-Based Chaperone Machinery 1. *Experimental biology and medicine*, 228(2), 111-133.
- 74. Zhao, R., Davey, M., Hsu, Y. C., Kaplanek, P., Tong, A., Parsons, A. B. & Boone, C. (2005). Navigating the chaperone network: an integrative map of physical and genetic interactions mediated by the hsp90 chaperone. *Cell*, 120(5), 715-727.
- 75. Zhao, J., Herrera-Diaz, J., & Gross, D. S. (2005). Domain-wide displacement of histones by activated heat shock factor occurs independently of Swi/Snf and is not correlated with RNA polymerase II density. *Molecular and cellular biology*, 25(20), 8985-8999.

- 76. Chen, S., Sullivan, W. P., Toft, D. O., & Smith, D. F. (1998). Differential interactions of p23 and the TPR-containing proteins Hop, Cyp40, FKBP52 and FKBP51 with Hsp90 mutants. *Cell stress & chaperones*, *3*(2), 118.
- 77. Warth, R., Briand, P. A., & Picard, D. (1997). Functional analysis of the yeast 40 kDa cyclophilin Cyp40 and its role for viability and steroid receptor regulation. *Biological chemistry*, 378(5), 381-392.
- 78. Pratt, W. B., Silverstein, A. M., & Galigniana, M. D. (1999). A model for the cytoplasmic trafficking of signalling proteins involving the hsp90-binding immunophilins and p50cdc37. *Cellular signalling*, 11(12), 839-851.
- 79. Chen, C. Y., & Balch, W. E. (2006). The Hsp90 chaperone complex regulates GDI-dependent Rab recycling. *Molecular biology of the cell*, *17*(8), 3494-3507.
- 80. Lotz, G. P., Brychzy, A., Heinz, S., & Obermann, W. M. (2008). A novel HSP90 chaperone complex regulates intracellular vesicle transport. *J Cell Sci*, 121(5), 717-723.
- 81. Lin, J. J., & Hemenway, C. S. (2010). Hsp90 directly modulates the spatial distribution of AF9/MLLT3 and affects target gene expression. *Journal of Biological Chemistry*, 285(16), 11966-11973.
- 82. Massenet, S., Bertrand, E., & Verheggen, C. (2016). Assembly and trafficking of box C/D and H/ACA snoRNPs. *RNA biology*, 1-13.
- 83. Boulon, S., Pradet-Balade, B., Verheggen, C., Molle, D., Boireau, S., Georgieva, M. & Lamond, A. I. (2010). HSP90 and its R2TP/Prefoldin-like cochaperone are involved in the cytoplasmic assembly of RNA polymerase II. *Molecular cell*, *39*(6), 912-924.
- 84. Takai, H., Xie, Y., de Lange, T., & Pavletich, N. P. (2010). Tel2 structure and function in the Hsp90-dependent maturation of mTOR and ATR complexes. *Genes & development*, 24(18), 2019-2030.

- 85. Takai, H., Wang, R. C., Takai, K. K., Yang, H., & de Lange, T. (2007). Tel2 regulates the stability of PI3K-related protein kinases. *Cell*, *131*(7), 1248-1259.
- 86. Woo, S. H., An, S., Lee, H. C., Jin, H. O., Seo, S. K., Yoo, D. H., & Park, I. C. (2009). A truncated form of p23 down-regulates telomerase activity via disruption of Hsp90 function. *Journal of Biological Chemistry*, 284(45), 30871-30880.
- 87. Lee, J. H., & Chung, I. K. (2010). Curcumin inhibits nuclear localization of telomerase by dissociating the Hsp90 co-chaperone p23 from hTERT. *Cancer letters*, 290(1), 76-86.
- 88. Chiu, W. T., Shen, S. C., Yang, L. Y., Chow, J. M., Wu, C. Y., & Chen, Y. C. (2011). Inhibition of HSP90-dependent telomerase activity in amyloid β-induced apoptosis of cerebral endothelial cells. *Journal of cellular physiology*, 226(8), 2041-2051.
- 89. Lee, J. H., & Chung, I. K. (2010). Curcumin inhibits nuclear localization of telomerase by dissociating the Hsp90 co-chaperone p23 from hTERT. *Cancer letters*, 290(1), 76-86
- 90. Zhang, M., Botër, M., Li, K., Kadota, Y., Panaretou, B., Prodromou, C., & Pearl, L. H. (2008). Structural and functional coupling of Hsp90-and Sgt1-centred multi-protein complexes. *The EMBO journal*, 27(20), 2789-2798.
- 91. Iwasaki, S., Kobayashi, M., Yoda, M., Sakaguchi, Y., Katsuma, S., Suzuki, T., & Tomari, Y. (2010). Hsc70/Hsp90 chaperone machinery mediates ATP-dependent RISC loading of small RNA duplexes. *Molecular cell*, *39*(2), 292-299.
- 92. Imai, J., Maruya, M., Yashiroda, H., Yahara, I., & Tanaka, K. (2003). The molecular chaperone Hsp90 plays a role in the assembly and maintenance of the 26S proteasome. *The EMBO journal*, 22(14), 3557-3567.
- 93. Yamano, T., Mizukami, S., Murata, S., Chiba, T., Tanaka, K., & Udono, H. (2008). Hsp90-mediated assembly of the 26 S proteasome is involved in major histocompatibility complex class I antigen processing. *Journal of Biological Chemistry*, 283(42), 28060-28065.

- 94. Lindahl, T. (1993). Instability and decay of the primary structure of DNA. *nature*, 362(6422), 709-715.
- 95. Hoeijmakers, J. H. (2009). DNA damage, aging, and cancer. *New England Journal of Medicine*, 361(15), 1475-1485.
- 96. Loeb, L. A. (1991). Perspectives in Cancer Research Mutator Phenotype May Be Required for Multistage Carcinogenesis 1. *Cancer research*, *51*, 3075-3079.
- 97. Gavande, N. S., VanderVere-Carozza, P. S., Hinshaw, H. D., Jalal, S. I., Sears, C. R., Pawelczak, K. S., & Turchi, J. J. (2016). DNA repair targeted therapy: the past or future of cancer treatment? *Pharmacology & therapeutics*, *160*, 65-83.
- 98. Mao, Z., Bozzella, M., Seluanov, A., & Gorbunova, V. (2008). DNA repair by nonhomologous end joining and homologous recombination during cell cycle in human cells. *Cell cycle*, 7(18), 2902-2906.
- 99. Uematsu, N., Weterings, E., Yano, K. I., Morotomi-Yano, K., Jakob, B., Taucher-Scholz, G. & Chen, D. J. (2007). Autophosphorylation of DNA-PKCS regulates its dynamics at DNA double-strand breaks. *The Journal of cell biology*, 177(2), 219-229.
- 100. Mari, P. O., Florea, B. I., Persengiev, S. P., Verkaik, N. S., Brüggenwirth, H. T., Modesti, M.& Houtsmuller, A. B. (2006). Dynamic assembly of end-joining complexes requires interaction between Ku70/80 and XRCC4. *Proceedings of the National Academy of Sciences*, 103(49), 18597-18602.
- 101. Wu, Q., Ochi, T., Matak-Vinkovic, D., Robinson, C. V., Chirgadze, D. Y., & Blundell, T.L. (2011). Non-homologous end-joining partners in a helical dance: structural studies of XLF–XRCC4 interactions.

- 102. Costantini, S., Woodbine, L., Andreoli, L., Jeggo, P. A., & Vindigni, A. (2007). Interaction of the Ku heterodimer with the DNA ligase IV/Xrcc4 complex and its regulation by DNA-PK. *DNA repair*, 6(6), 712-722.
- 103. Mao, Z., Jiang, Y., Liu, X., Seluanov, A., & Gorbunova, V. (2009). DNA repair by homologous recombination, but not by nonhomologous end joining, is elevated in breast cancer cells. *Neoplasia*, *11*(7), 683IN3-691.
- 104. Resnick, M. A. (1976). The repair of double-strand breaks in DNA: a model involving recombination. *Journal of Theoretical Biology*, 59(1), 97-106.
- 105. Jasin, M., de Villiers, J., Weber, F., & Schaffner, W. (1985). High frequency of homologous recombination in mammalian cells between endogenous and introduced SV40 genomes. *Cell*, *43*(3), 695-703.
- 106. O'Connell, M. J., Walworth, N. C., & Carr, A. M. (2000). The G2-phase DNA-damage checkpoint. *Trends in cell biology*, *10*(7), 296-303.
- 107. Lindsey-Boltz, L. A., Bermudez, V. P., Hurwitz, J., & Sancar, A. (2001). Purification and characterization of human DNA damage checkpoint Rad complexes. *Proceedings of the National Academy of Sciences*, 98(20), 11236-11241.
- 108. Lydall, D., & Weinert, T. (1995). Yeast checkpoint genes in DNA damage processing: implications for repair and arrest. *Science*, 270(5241), 1488.
- 109. Parker, A. E., Van de Weyer, I., Laus, M. C., Oostveen, I., Yon, J., Verhasselt, P., & Luyten, W. H. (1998). A human homologue of the Schizosaccharomyces pombe rad1+ checkpoint gene encodes an exonuclease. *Journal of Biological Chemistry*, 273(29), 18332-18339.

- 110. Chaturvedi, P., Eng, W. K., Zhu, Y., Mattern, M. R., Mishra, R., Hurle, M. R. & Scott, G. F. (1999). Mammalian Chk2 is a downstream effector of the ATM-dependent DNA damage checkpoint pathway. *Oncogene*, 18(28)
- 111. Elledge, S. J. (1996). Cell cycle checkpoints: preventing an identity crisis. *Science*, 274(5293), 1664.
- 112. Matsuoka, S., Huang, M., & Elledge, S. J. (1998). Linkage of ATM to cell cycle regulation by the Chk2 protein kinase. *Science*, 282(5395), 1893-1897.
- 113. Sanchez, Y., Wong, C., Thoma, R. S., Richman, R., Wu, Z., Piwnica-Worms, H., & Elledge, S. J. (1997). Conservation of the Chk1 checkpoint pathway in mammals: linkage of DNA damage to Cdk regulation through Cdc25. *Science*, 277(5331), 1497-1501.
- 114. Cortez, D., Wang, Y., Qin, J., & Elledge, S. J. (1999). Requirement of ATM-dependent phosphorylation of brca1 in the DNA damage response to double-strand breaks. *Science*, 286(5442), 1162-1166.
- 115. Jong-Soo, L., Collins, K. M., Brown, A. L., Chang-Hun, L., & Chung, J. H. (2000). hCds1 mediated phosphorylation of BRCA1 regulates the DNA damage response. *Nature*, 404(6774), 201.
- 116. Tibbetts, R. S., Cortez, D., Brumbaugh, K. M., Scully, R., Livingston, D., Elledge, S. J., & Abraham, R. T. (2000). Functional interactions between BRCA1 and the checkpoint kinase ATR during genotoxic stress. *Genes & development*, *14*(23), 2989-3002.
- 117. Emili, A. (1998). MEC1-dependent phosphorylation of Rad9p in response to DNA damage. *Molecular cell*, 2(2), 183-189.
- 118. Yarden, R. I., Pardo-Reoyo, S., Sgagias, M., Cowan, K. H., & Brody, L. C. (2002). BRCA1 regulates the G2/M checkpoint by activating Chk1 kinase upon DNA damage. *Nature genetics*, 30(3), 285.

- 119. Chamankhah, M., & Xiao, W. (1999). Formation of the yeast Mre11-Rad50-Xrs2 complex is correlated with DNA repair and telomere maintenance. *Nucleic acids research*, 27(10), 2072-2079.
- 120. Lim, D. S., Seong-Tae, K., Xu, B., & Maser, R. S. (2000). ATM phosphorylates p95/nbs1 in an S-phrase checkpoint pathway. *Nature*, 404(6778), 613.
- 121. Kozlov, S. V., Graham, M. E., Jakob, B., Tobias, F., Kijas, A. W., Tanuji, M. & So, S. (2011). Autophosphorylation and atm activation additional sites add to the complexity. *Journal of Biological Chemistry*, 286(11), 9107-9119.
- 122. Wang, H., Shi, L. Z., Wong, C. C., Han, X., Hwang, P. Y. H., Truong, L. N. & Yates III, J. R. (2013). The Interaction of CtIP and Nbs1 Connects CDK and ATM to Regulate HR—Mediated Double-Strand Break Repair. *PLoS genetics*, 9(2), e1003277.
- 123. Nimonkar, A. V., Genschel, J., Kinoshita, E., Polaczek, P., Campbell, J. L., Wyman, C.& Kowalczykowski, S. C. (2011). BLM–DNA2–RPA–MRN and EXO1–BLM–RPA–MRN constitute two DNA end resection machineries for human DNA break repair. *Genes & development*, 25(4), 350-362.
- 124. Fanning, E., Klimovich, V., & Nager, A. R. (2006). A dynamic model for replication protein A (RPA) function in DNA processing pathways. *Nucleic acids research*, *34*(15), 4126-4137.
- 125. Pellegrini, L., David, S. Y., Lo, T., & Anand, S. (2002). Insights into DNA recombination from the structure of a RAD51-BRCA2 complex. *Nature*, *420*(6913), 287.
- 126. Davies, O. R., & Pellegrini, L. (2007). Interaction with the BRCA2 C-terminus Protects

  RAD51–DNA Filaments from Disassembly by BRC Repeats. *Nature structural* & molecular biology, 14(6), 475.

- 127. Esashi, F., Galkin, V. E., Xiong, Y., Egelman, E. H., & West, S. C. (2007). Stabilization of RAD51 nucleoprotein filaments by the C-terminal region of BRCA2. *Nature structural & molecular biology*, *14*(6), 468.
- 128. Hays, S. L., Firmenich, A. A., Massey, P., Banerjee, R., & Berg, P. (1998). Studies of the interaction between Rad52 protein and the yeast single-stranded DNA binding protein RPA. *Molecular and cellular biology*, *18*(7), 4400-4406.
- 129. Sugiyama, T., & Kowalczykowski, S. C. (2002). Rad52 protein associates with replication protein A (RPA)-single-stranded DNA to accelerate Rad51-mediated displacement of RPA and presynaptic complex formation. *Journal of Biological Chemistry*, 277(35), 31663-31672.
- 130. Sung, P., & Robberson, D. L. (1995). DNA strand exchange mediated by a RAD51-ssDNA nucleoprotein filament with polarity opposite to that of RecA. *Cell*, 82(3), 453-461.
- 131. Sung, P. (1994). Catalysis of ATP-dependent homologous DNA pairing and strand exchange by yeast RAD51 protein. *Science*, 265(5176), 1241-1244.
- 132. Baumann, P., Benson, F. E., & West, S. C. (1996). Human Rad51 protein promotes ATP-dependent homologous pairing and strand transfer reactions in vitro. *Cell*, 87(4), 757-766.
- 133. A Rad51 Presynaptic Filament Is Sufficient to Capture Nucleosomal Homology during Recombinational Repair of a DNA Double-Strand Break
- 134. Heyer, W. D., Li, X., Rolfsmeier, M., & Zhang, X. P. (2006). Rad54: the Swiss Army knife of homologous recombination?. *Nucleic acids research*, *34*(15), 4115-4125.
- 135. Petukhova, G., Stratton, S., & Sung, P. (1998). Catalysis of homologous DNA pairing by yeast Rad51 and Rad54 proteins. *Nature*, *393*(6680), 91.
- 136. Shinohara, A., Ogawa, H., & Ogawa, T. (1992). Rad51 protein involved in repair and recombination in S. cerevisiae is a RecA-like protein. *Cell*, 69(3), 457-470.

- 137. Sung, P. (1994). Catalysis of ATP-dependent homologous DNA pairing and strand exchange by yeast RAD51 protein. *Science*, 265(5176), 1241-1244.
- 138. Gasior, S. L., Wong, A. K., Kora, Y., Shinohara, A., & Bishop, D. K. (1998). Rad52 associates with RPA and functions with Rad55 and Rad57 to assemble meiotic recombination complexes. *Genes & development*, *12*(14), 2208-2221.
- 139. Sugawara, N., Wang, X., & Haber, J. E. (2003). In vivo roles of Rad52, Rad54, and Rad55 proteins in Rad51-mediated recombination. *Molecular cell*, *12*(1), 209-219.
- 140. Sugiyama, T., New, J. H., & Kowalczykowski, S. C. (1998). DNA annealing by RAD52 protein is stimulated by specific interaction with the complex of replication protein A and single-stranded DNA. *Proceedings of the National Academy of Sciences*, 95(11), 6049-6054.
- 141. Sugiyama, T., Kantake, N., Wu, Y., & Kowalczykowski, S. C. (2006). Rad52-mediated DNA annealing after Rad51-mediated DNA strand exchange promotes second ssDNA capture. *The EMBO journal*, 25(23), 5539-5548.
- 142. Wu, L., & Hickson, I. D. (2003). The Bloom's syndrome helicase suppresses crossing over during homologous recombination. *Nature*, *426*(6968), 870.
- 143. Plank, J. L., Wu, J., & Hsieh, T. S. (2006). Topoisomerase IIIα and Bloom's helicase can resolve a mobile double Holliday junction substrate through convergent branch migration. *Proceedings of the National Academy of Sciences*, *103*(30), 11118-11123.
- 144. Holliday, R. (1964). A mechanism for gene conversion in fungi. *Genetics Research*, 5(2), 282-304.
- 145. Game, J. C., & Mortimer, R. K. (1974). A genetic study of X-ray sensitive mutants in yeast. *Mutation Research/Fundamental and Molecular Mechanisms of Mutagenesis*, 24(3), 281-292.

- 146. San Filippo, J., Sung, P., & Klein, H. (2008). Mechanism of eukaryotic homologous recombination. *Annu. Rev. Biochem.*, 77, 229-257.
- 147. Symington, L. S. (2002). Role of RAD52 epistasis group genes in homologous recombination and double-strand break repair. *Microbiology and molecular biology reviews*, 66(4), 630-670.
- 148. Milne, G. T., & Weaver, D. T. (1993). Dominant negative alleles of RAD52 reveal a DNA repair/recombination complex including Rad51 and Rad52. *Genes & Development*, 7(9), 1755-1765.
- 149. Yamaguchi-Iwai, Y., Sonoda, E., Buerstedde, J. M., Bezzubova, O., Morrison, C., Takata, M., & Takeda, S. (1998). Homologous recombination, but not DNA repair, is reduced in vertebrate cells deficient in RAD52. *Molecular and Cellular Biology*, 18(11), 6430-6435.
- 150. Feng, Z., Scott, S. P., Bussen, W., Sharma, G. G., Guo, G., Pandita, T. K., & Powell, S. N. (2011). Rad52 inactivation is synthetically lethal with BRCA2 deficiency. *Proceedings of the National Academy of Sciences*, 108(2), 686-691.
- 151. Rijkers, T., Van Den Ouweland, J., Morolli, B., Rolink, A. G., Baarends, W. M., Van Sloun, P. P., & Pastink, A. (1998). Targeted inactivation of mouse RAD52reduces homologous recombination but not resistance to ionizing radiation. *Molecular and cellular biology*, 18(11), 6423-6429.
- 152. Baumann, P., & West, S. C. (1998). Role of the human RAD51 protein in homologous recombination and double-stranded-break repair. *Trends in biochemical sciences*, 23(7), 247-251.
- 153. Shinohara, A., Ogawa, H., & Ogawa, T. (1992). Rad51 protein involved in repair and recombination in S. cerevisiae is a RecA-like protein. *Cell*, 69(3), 457-470.

- 154. Lim, D. S., & Hasty, P. (1996). A mutation in mouse rad51 results in an early embryonic lethal that is suppressed by a mutation in p53. *Molecular and cellular biology*, 16(12), 7133-7143
- 155. Sonoda, E., Sasaki, M. S., Buerstedde, J. M., Bezzubova, O., Shinohara, A., Ogawa, H.& Takeda, S. (1998). Rad51-deficient vertebrate cells accumulate chromosomal breaks prior to cell death. *The EMBO journal*, *17*(2), 598-608.
- 156. Lambert, S., & Lopez, B. S. (2000). Characterization of mammalian RAD51 double strand break repair using non-lethal dominant-negative forms. *The EMBO journal*, *19*(12), 3090-3099.
- 157. Lambert, S., & Lopez, B. S. (2001). Role of RAD51 in sister-chromatid exchanges in mammalian cells. *Oncogene*, 20(45), 6627.
- 158. Haaf, T., Golub, E. I., Reddy, G., Radding, C. M., & Ward, D. C. (1995). Nuclear foci of mammalian Rad51 recombination protein in somatic cells after DNA damage and its localization in synaptonemal complexes. *Proceedings of the National Academy of Sciences*, 92(6), 2298-2302.
- 159.Li, M. J., Peakman, M. C., Golub, E. I., Reddy, G., Ward, D. C., Radding, C. M., & Maizels, N. (1996). Rad51 expression and localization in B cells carrying out class switch recombination. *Proceedings of the National Academy of Sciences*, *93*(19), 10222-10227.
- 160. Barlow, A. L., Benson, F. E., West, S. C., & Hultén, M. A. (1997). Distribution of the Rad51 recombinase in human and mouse spermatocytes. *The EMBO Journal*, *16*(17), 5207-5215.
- 161. Ogawa, T., Yu, X., Shinohara, A., & Egelman, E. H. (1993). Similarity of the yeast RAD51 filament to the bacterial RecA filament. *SCIENCE-NEW YORK THEN WASHINGTON*, 259, 1896-1896.

- 162. Conway, A. B., Lynch, T. W., Zhang, Y., Fortin, G. S., Fung, C. W., Symington, L. S., & Rice, P. A. (2004). Crystal structure of a Rad51 filament. *Nature structural & molecular biology*, 11(8), 791.
- 163.Li, X., & Heyer, W. D. (2008). RAD54 controls access to the invading 3'-OH end after RAD51-mediated DNA strand invasion in homologous recombination in Saccharomyces cerevisiae. *Nucleic acids research*, 37(2), 638-646.
- 164. Alexiadis, V., & Kadonaga, J. T. (2002). Strand pairing by Rad54 and Rad51 is enhanced by chromatin. *Genes & development*, 16(21), 2767-2771.
- 165. Jaskelioff, M., Van Komen, S., Krebs, J. E., Sung, P., & Peterson, C. L. (2003). Rad54p is a chromatin remodeling enzyme required for heteroduplex DNA joint formation with chromatin. *Journal of Biological Chemistry*, 278(11), 9212-9218.
- 166. Rothenberg, E., Grimme, J. M., Spies, M., & Ha, T. (2008). Human Rad52-mediated homology search and annealing occurs by continuous interactions between overlapping nucleoprotein complexes. *Proceedings of the National Academy of Sciences*, 105(51), 20274-20279.
- 167. Aihara, H., Ito, Y., Kurumizaka, H., Yokoyama, S., & Shibata, T. (1999). The N-terminal domain of the human Rad51 protein binds DNA: structure and a DNA binding surface as revealed by NMR. *Journal of molecular biology*, 290(2), 495-504.
- 168. Krejci, L., Damborsky, J., Thomsen, B., Duno, M., & Bendixen, C. (2001). Molecular dissection of interactions between Rad51 and members of the recombination-repair group. *Molecular and cellular biology*, 21(3), 966-976.
- 169. Yu, X., Jacobs, S. A., West, S. C., Ogawa, T., & Egelman, E. H. (2001). Domain structure and dynamics in the helical filaments formed by RecA and Rad51 on DNA. *Proceedings of the National Academy of Sciences*, 98(15), 8419-8424.

- 170. Egelman, E. H., & Yu, X. (1989). The location of DNA in RecA-DNA helical filaments. *Science*, 245(4916), 404-407.
- 171. Namsaraev, E. A., & Berg, P. (1998). Binding of Rad51p to DNA INTERACTION OF Rad51p WITH SINGLE-AND DOUBLE-STRANDED DNA. *Journal of Biological Chemistry*, 273(11), 6177-6182.
- 172. Rice, K. P., Eggler, A. L., Sung, P., & Cox, M. M. (2001). DNA pairing and strand exchange by the Escherichia coli RecA and yeast Rad51 proteins without ATP hydrolysis on the importance of not getting stuck. *Journal of Biological Chemistry*, 276(42), 38570-38581.
- 173. Zhang, X. P., Galkin, V. E., Yu, X., Egelman, E. H., & Heyer, W. D. (2008). Loop 2 in Saccharomyces cerevisiae Rad51 protein regulates filament formation and ATPase activity. *Nucleic acids research*, *37*(1), 158-171.
- 174. Matsuo, Y., Sakane, I., Takizawa, Y., Takahashi, M., & Kurumizaka, H. (2006). Roles of the human Rad51 L1 and L2 loops in DNA binding. *The FEBS journal*, 273(14), 3148-3159.
- 175. Flygare, J., Benson, F., & Hellgren, D. (1996). Expression of the human RAD51 gene during the cell cycle in primary human peripheral blood lymphocytes. *Biochimica et Biophysica Acta (BBA)-Molecular Cell Research*, *1312*(3), 231-236.
- 176. Yamamoto, A., Yagi, H., Habu, T., Yoshimura, Y., Matsushiro, A., Nishimune, Y., & Yamamoto, K. (1996). Cell cycle-dependent expression of the mouseRad51 gene in proliferating cells. *Molecular and General Genetics MGG*, 251(1), 1-12.
- 177. Hannay, J. A., Liu, J., Zhu, Q. S., Bolshakov, S. V., Li, L., Pisters, P. W., & Lev, D. (2007).

  Rad51 overexpression contributes to chemoresistance in human soft tissue sarcoma cells: a

- role for p53/activator protein 2 transcriptional regulation. *Molecular cancer therapeutics*, 6(5), 1650-1660.
- 178. Iwanaga, R., Komori, H., & Ohtani, K. (2004). Differential regulation of expression of the mammalian DNA repair genes by growth stimulation. *Oncogene*, 23(53), 8581.
- 179. Hasselbach, L., Haase, S., Fischer, D., Kolberg, H. C., & Stürzbecher, H. W. (2005). Characterisation of the promoter region of the human DNA-repair gene Rad51. *European journal of gynaecological oncology*, 26(6), 589-598.
- 180. Arias-Lopez, C., Lazaro-Trueba, I., Kerr, P., Lord, C. J., Dexter, T., Iravani, M. & Silva, A. (2006). p53 modulates homologous recombination by transcriptional regulation of the RAD51 gene. *EMBO reports*, 7(2), 219-224.
- 181. Cohen, Y., Dardalhon, M., & Averbeck, D. (2002). Homologous recombination is essential for RAD51 up-regulation in Saccharomyces cerevisiae following DNA crosslinking damage. *Nucleic acids research*, *30*(5), 1224-1232.
- 182. Basile, G., Aker, M., & Mortimer, R. K. (1992). Nucleotide sequence and transcriptional regulation of the yeast recombinational repair gene RAD51. *Molecular and cellular biology*, 12(7), 3235-3246.
- 183. Averbeck, D., & Averbeck, S. (1998). DNA Photodamage, Repair, Gene Induction and Genotoxicity Following Exposures to 254 nm UV and 8-Methoxypsoralen Plus UVA in a Eukaryotic Cell System. *Photochemistry and photobiology*, 68(3), 289-295.
- 184. Xia, S. J., Shammas, M. A., & Reis, R. S. (1997). Elevated recombination in immortal human cells is mediated by HsRAD51 recombinase. *Molecular and cellular biology*, *17*(12), 7151-7158.

- 185. Raderschall, E., Stout, K., Freier, S., Suckow, V., Schweiger, S., & Haaf, T. (2002). Elevated levels of Rad51 recombination protein in tumor cells. *Cancer research*, 62(1), 219-225.
- 186. Shafman, T., Khanna, K. K., Kedar, P., Spring, K., Kozlov, S., Yen, T. & Egerton, M. (1997). Interaction between ATM protein and c-Abl in response to DNA damage. *Nature*, 387(6632), 520-523.
- 187. Conilleau, S., Takizawa, Y., Tachiwana, H., Fleury, F., Kurumizaka, H., & Takahashi, M. (2004). Location of tyrosine 315, a target for phosphorylation by cAbl tyrosine kinase, at the edge of the subunit–subunit interface of the human Rad51 filament. *Journal of molecular biology*, 339(4), 797-804.
- 188. Takizawa, Y., Kinebuchi, T., Kagawa, W., Yokoyama, S., Shibata, T., & Kurumizaka, H. (2004). Mutational analyses of the human Rad51-Tyr315 residue, a site for phosphorylation in leukaemia cells. *Genes to Cells*, *9*(9), 781-790
- 189. Yuan, Z. M., Huang, Y., Ishiko, T., Nakada, S., Utsugisawa, T., Kharbanda, S., & Kufe,
  D. (1998). Regulation of Rad51 function by c-Abl in response to DNA damage. *Journal of Biological Chemistry*, 273(7), 3799-3802.
- 190. Sørensen, C. S., Hansen, L. T., Dziegielewski, J., Syljuåsen, R. G., Lundin, C., Bartek, J.,& Helleday, T. (2005). The cell-cycle checkpoint kinase Chk1 is required for mammalian homologous recombination repair. *Nature cell biology*, 7(2)
- 191. Flott, S., Kwon, Y., Pigli, Y. Z., Rice, P. A., Sung, P., & Jackson, S. P. (2011). Regulation of Rad51 function by phosphorylation. *EMBO reports*, *12*(8), 833-839.
- 192. Kovalenko, O. V., Plug, A. W., Haaf, T., Gonda, D. K., Ashley, T., Ward, D. C., & Golub, E. I. (1996). Mammalian ubiquitin-conjugating enzyme Ubc9 interacts with Rad51

- recombination protein and localizes in synaptonemal complexes. *Proceedings of the National Academy of Sciences*, 93(7), 2958-2963.
- 193. Haaf, T., Raderschall, E., Reddy, G., Ward, D. C., Radding, C. M., & Golub, E. I. (1999).

  Sequestration of mammalian Rad51-recombination protein into micronuclei. *The Journal of cell biology*, *144*(1), 11-20.
- 194. Takata, M., Sasaki, M. S., Tachiiri, S., Fukushima, T., Sonoda, E., Schild, D., & Takeda, S. (2001). Chromosome instability and defective recombinational repair in knockout mutants of the five Rad51 paralogs. *Molecular and cellular biology*, 21(8), 2858-2866.
- 195. Nomme, J., Takizawa, Y., Martinez, S. F., Renodon-Cornière, A., Fleury, F., Weigel, P., & Takahashi, M. (2008). Inhibition of filament formation of human Rad51 protein by a small peptide derived from the BRC-motif of the BRCA2 protein. *Genes to Cells*, 13(5), 471-481.
- 196. Adam, S. A., Marr, R. S., & Gerace, L. (1990). Nuclear protein import in permeabilized mammalian cells requires soluble cytoplasmic factors. *The Journal of Cell Biology*, 111(3), 807-816.
- 197. Chen, J., Silver, D. P., Walpita, D., Cantor, S. B., Gazdar, A. F., Tomlinson, G., & Scully, R. (1998). Stable interaction between the products of the BRCA1 and BRCA2 tumor suppressor genes in mitotic and meiotic cells. *Molecular cell*, 2(3), 317-328.
- 198. Yuan, S. S. F., Lee, S. Y., Chen, G., Song, M., Tomlinson, G. E., & Lee, E. Y. P. (1999).

  BRCA2 is required for ionizing radiation-induced assembly of Rad51 complex in vivo. *Cancer research*, 59(15), 3547-3551.
- 199. Davies, A. A., Masson, J. Y., McIlwraith, M. J., Stasiak, A. Z., Stasiak, A., Venkitaraman, A. R., & West, S. C. (2001). Role of BRCA2 in control of the RAD51 recombination and DNA repair protein. *Molecular cell*, 7(2), 273-282.

- 200. Ayoub, N., Rajendra, E., Su, X., Jeyasekharan, A. D., Mahen, R., & Venkitaraman, A. R. (2009). The carboxyl terminus of Brca2 links the disassembly of Rad51 complexes to mitotic entry. *Current Biology*, *19*(13), 1075-1085.
- 201. Tarsounas, M., Davies, D., & West, S. C. (2003). BRCA2-dependent and independent formation of RAD51 nuclear foci. *Oncogene*, 22(8), 1115.
- 202. Gildemeister, O. S., Sage, J. M., & Knight, K. L. (2009). Cellular Redistribution of Rad51 in Response to DNA Damage NOVEL ROLE FOR Rad51C. *Journal of Biological Chemistry*, 284(46), 31945-31952.
- 203. Subramanyam, S., Jones, W. T., Spies, M., & Spies, M. A. (2013). Contributions of the RAD51 N-terminal domain to BRCA2-RAD51 interaction. *Nucleic acids research*, *41*(19), 9020-9032.
- 204. Shin, D. S., Pellegrini, L., Daniels, D. S., Yelent, B., Craig, L., Bates, D., & Volkmann, N. (2003). Full-length archaeal Rad51 structure and mutants: mechanisms for RAD51 assembly and control by BRCA2. *The EMBO journal*, 22(17), 4566-4576.
- 205. Donovan, J. W., Milne, G. T., & Weaver, D. T. (1994). Homotypic and heterotypic protein associations control Rad51 function in double-strand break repair. *Genes & development*, 8(21), 2552-2562.
- 206. Fortin, G. S., & Symington, L. S. (2002). Mutations in yeast Rad51 that partially bypass the requirement for Rad55 and Rad57 in DNA repair by increasing the stability of Rad51–DNA complexes. *The EMBO journal*, 21(12), 3160-3170.
- 207. King, M. C., Marks, J. H., & Mandell, J. B. (2003). Breast and ovarian cancer risks due to inherited mutations in BRCA1 and BRCA2. *Science*, 302(5645), 643-646.

- 208. Metcalfe, K., Gershman, S., Lynch, H. T., Ghadirian, P., Tung, N., Kim-Sing, C., & Foulkes, W. D. (2011). Predictors of contralateral breast cancer in BRCA1 and BRCA2 mutation carriers. *British journal of cancer*, *104*(9), 1384.
- 209. Wooster, R., Bignell, G., Lancaster, J., & Swift, S. (1995). Identification of the breast cancer susceptibility gene BRCA2. *Nature*, *378*(6559), 789.
- 210. Tavtigian, S. V., Simard, J., Rommens, J., Couch, F., Shattuck-Eidens, D., Neuhausen, S.
  & Belanger, C. (1996). The complete BRCA2 gene and mutations in chromosome 13q-linked kindreds. *Nature genetics*, 12(3), 333-337.
- 211. Howlett, N. G., Taniguchi, T., Olson, S., Cox, B., Waisfisz, Q., de Die-Smulders, C., & Ikeda, H. (2002). Biallelic inactivation of BRCA2 in Fanconi anemia. *Science*, 297(5581), 606-609.
- 212. Carling, T., Imanishi, Y., Gaz, R. D., & Arnold, A. (1999). RAD51 as a candidate parathyroid tumour suppressor gene on chromosome 15q: absence of somatic mutations. *Clinical endocrinology*, *51*(4), 403-407.
- 213. Evans, J. W., Chernikova, S. B., Kachnic, L. A., Banath, J. P., Sordet, O., Delahoussaye, Y. M. & Wilson, W. R. (2008). Homologous recombination is the principal pathway for the repair of DNA damage induced by tirapazamine in mammalian cells. *Cancer Research*, 68(1), 257-265.
- 214. Moynahan, M. E., Cui, T. Y., & Jasin, M. (2001). Homology-directed dna repair, mitomycin-c resistance, and chromosome stability is restored with correction of a Brca1 mutation. *Cancer research*, 61(12), 4842-4850.
- 215. Bryant, H. E., Schultz, N., Thomas, H. D., & Parker, K. M. (2005). Specific killing of BRCA2-deficient tumours with inhibitors of poly (ADP-ribose) polymerase. *Nature*, 434(7035), 913.

- 216. Chernikova, S. B., Game, J. C., & Brown, J. M. (2012). Inhibiting homologous recombination for cancer therapy. *Cancer biology & therapy*, *13*(2), 61-68.
- 217. De Silva, I. U., McHugh, P. J., Clingen, P. H., & Hartley, J. A. (2000). Defining the roles of nucleotide excision repair and recombination in the repair of DNA interstrand cross-links in mammalian cells. *Molecular and cellular biology*, 20(21), 7980-7990.
- 218. Wesoly, J., Agarwal, S., Sigurdsson, S., Bussen, W., Van Komen, S., Qin, J., & Ghazvini, M. (2006). Differential contributions of mammalian Rad54 paralogs to recombination, DNA damage repair, and meiosis. *Molecular and cellular biology*, 26(3), 976-989.
- 219. Lim, D. S., & Hasty, P. (1996). A mutation in mouse rad51 results in an early embryonic lethal that is suppressed by a mutation in p53. *Molecular and cellular biology*, 16(12), 7133-7143.
- 220. TsUZUKI, T. E. R. U. H. I. S. A., FuJII, Y., Sakumi, K., Tominaga, Y., Nakao, K., Sekiguchi, M., ... & Yoshimura, Y. (1996). Targeted disruption of the Rad51 gene leads to lethality in embryonic mice. *Proceedings of the National Academy of Sciences*, 93(13), 6236-6240.
- 221. Costanzo, V. (2011). Brca2, Rad51 and Mre11: performing balancing acts on replication forks. *DNA repair*, *10*(10), 1060-1065.
- 222. Michel, B., Boubakri, H., Baharoglu, Z., LeMasson, M., & Lestini, R. (2007). Recombination proteins and rescue of arrested replication forks. *DNA repair*, 6(7), 967-980.
- 223. Mao, P., Liu, J., Zhang, Z., Zhang, H., Liu, H., Gao, S.& Zhao, Y. (2016). Homologous recombination-dependent repair of telomeric DSBs in proliferating human cells. *Nature communications*, 7.

- 224. Verdun, R. E., & Karlseder, J. (2006). The DNA damage machinery and homologous recombination pathway act consecutively to protect human telomeres. *Cell*, *127*(4), 709-720.
- 225. Tarsounas, M., Muñoz, P., Claas, A., Smiraldo, P. G., Pittman, D. L., Blasco, M. A., & West, S. C. (2004). Telomere maintenance requires the RAD51D recombination/repair protein. *Cell*, *117*(3), 337-347.
- 226. Badie, S., Escandell, J. M., Bouwman, P., Carlos, A. R., Thanasoula, M., Gallardo, M. M. & Blasco, M. A. (2010). BRCA2 acts as a RAD51 loader to facilitate telomere replication and capping. *Nature structural & molecular biology*, 17(12), 1461-1469.
- 227. Badie, S., Escandell, J. M., Bouwman, P., Carlos, A. R., Thanasoula, M., Gallardo, M. M. & Blasco, M. A. (2010). BRCA2 acts as a RAD51 loader to facilitate telomere replication and capping. *Nature structural & molecular biology*, 17(12), 1461-1469.
- 228. Jaco, I., Muñoz, P., Goytisolo, F., Wesoly, J., Bailey, S., Taccioli, G., & Blasco, M. A. (2003). Role of mammalian Rad54 in telomere length maintenance. *Molecular and cellular biology*, 23(16), 5572-5580.
- 229. Sangster, T. A., Salathia, N., Undurraga, S., Milo, R., Schellenberg, K., Lindquist, S., & Queitsch, C. (2008). HSP90 affects the expression of genetic variation and developmental stability in quantitative traits. *Proceedings of the National Academy of Sciences*, 105(8), 2963-2968.
- 230. Sekimoto, T., Oda, T., Pozo, F. M., Murakumo, Y., Masutani, C., Hanaoka, F., & Yamashita, T. (2010). The molecular chaperone Hsp90 regulates accumulation of DNA polymerase η at replication stalling sites in UV-irradiated cells. *Molecular cell*, *37*(1), 79-89.

- 231. Pozo, F. M., Oda, T., Sekimoto, T., Murakumo, Y., Masutani, C., Hanaoka, F., & Yamashita, T. (2011). Molecular chaperone Hsp90 regulates REV1-mediated mutagenesis. *Molecular and cellular biology*, *31*(16), 3396-3409.
- 232. Arlander, S. J., Eapen, A. K., Vroman, B. T., McDonald, R. J., Toft, D. O., & Karnitz, L. M. (2003). Hsp90 inhibition depletes Chk1 and sensitizes tumor cells to replication stress. *Journal of Biological Chemistry*, 278(52), 52572-52577.
- 233. Miyata, Y. (2005). Hsp90 inhibitor geldanamycin and its derivatives as novel cancer chemotherapeutic agents. *Current pharmaceutical design*, 11(9), 1131-1138.
- 234. Dote, H., Burgan, W. E., Camphausen, K., & Tofilon, P. J. (2006). Inhibition of hsp90 compromises the DNA damage response to radiation. *Cancer research*, 66(18), 9211-9220.
- 235. Noguchi, M., Yu, D., Hirayama, R., Ninomiya, Y., Sekine, E., Kubota, N. & Okayasu, R. (2006). Inhibition of homologous recombination repair in irradiated tumor cells pretreated with Hsp90 inhibitor 17-allylamino-17-demethoxygeldanamycin. *Biochemical and biophysical research communications*, *351*(3), 658-663.
- 236. Dote, H., Burgan, W. E., Camphausen, K., & Tofilon, P. J. (2006). Inhibition of hsp90 compromises the DNA damage response to radiation. *Cancer research*, 66(18), 9211-9220.
- 237. Zaidi, S., McLaughlin, M., Bhide, S. A., Eccles, S. A., Workman, P., Nutting, C. M. & Harrington, K. J. (2012). The HSP90 inhibitor NVP-AUY922 radiosensitizes by abrogation of homologous recombination resulting in mitotic entry with unresolved DNA damage. *PloS one*, 7(4), e35436.
- 238. Quanz, M., Herbette, A., Sayarath, M., de Koning, L., Dubois, T., Sun, J. S., & Dutreix,
  M. (2012). Heat shock protein 90α (Hsp90α) is phosphorylated in response to DNA

- damage and accumulates in repair foci. *Journal of Biological Chemistry*, 287(12), 8803-8815.
- 239. Ko, J. C., Chen, H. J., Huang, Y. C., Tseng, S. C., Weng, S. H., Wo, T. Y., & Lin, Y. W. (2012). HSP90 inhibition induces cytotoxicity via down-regulation of Rad51 expression and DNA repair capacity in non-small cell lung cancer cells. *Regulatory Toxicology and Pharmacology*, 64(3), 415-424.
- 240. Kramer, D., Stark, N., Schulz-Heddergott, R., Erytch, N., Edmunds, S., Roßmann, L., & Dobbelstein, M. (2017). Strong antitumor synergy between DNA crosslinking and HSP90 inhibition causes massive premitotic DNA fragmentation in ovarian cancer cells. *Cell Death & Differentiation*, 24(2), 300-316.
- 241. Fang, Q., Inanc, B., Schamus, S., Wang, X. H., Wei, L., Brown, A. R. & Yates, N. A. (2014). HSP90 regulates DNA repair via the interaction between XRCC1 and DNA polymerase β. *Nature communications*, 5, 5513.
- 242. Chen, L., Nievera, C. J., Lee, A. Y. L., & Wu, X. (2008). Cell cycle-dependent complex formation of BRCA1· CtIP· MRN is important for DNA double-strand break repair. *Journal of Biological Chemistry*, 283(12), 7713-7720.
- 243. Zhong, Q., Chen, C. F., Li, S., Chen, Y., Wang, C. C., Xiao, J. & Lee, W. H. (1999). Association of BRCA1 with the hRad50-hMre11-p95 complex and the DNA damage response. *science*, 285(5428), 747-750.
- 244. Stecklein, S. R., Kumaraswamy, E., Behbod, F., Wang, W., Chaguturu, V., Harlan-Williams, L. M., & Jensen, R. A. (2012). BRCA1 and HSP90 cooperate in homologous and non-homologous DNA double-strand-break repair and G2/M checkpoint activation. *Proceedings of the National Academy of Sciences*, 109(34), 13650-13655.

- 245. Bartek, J., & Lukas, J. (2003). Chk1 and Chk2 kinases in checkpoint control and cancer. *Cancer cell*, *3*(5), 421-429.
- 246. Arlander, S. J., Eapen, A. K., Vroman, B. T., McDonald, R. J., Toft, D. O., & Karnitz, L.
   M. (2003). Hsp90 inhibition depletes Chk1 and sensitizes tumor cells to replication stress. *Journal of Biological Chemistry*, 278(52), 52572-52577.
- 247. Davis, A. J., Chi, L., So, S., Lee, K. J., Mori, E., Fattah, K. & Chen, D. J. (2014). BRCA1 modulates the autophosphorylation status of DNA-PKcs in S phase of the cell cycle. *Nucleic acids research*, 42(18), 11487-11501.
- 248. Falsone, S. F., Gesslbauer, B., Tirk, F., Piccinini, A. M., & Kungl, A. J. (2005). A proteomic snapshot of the human heat shock protein 90 interactome. *FEBS letters*, *579*(28), 6350-6354.
- 249. Mittelman, D., Sykoudis, K., Hersh, M., Lin, Y., & Wilson, J. H. (2010). Hsp90 modulates CAG repeat instability in human cells. *Cell Stress and Chaperones*, *15*(5), 753-759.
- 250. Walden, H., & Deans, A. J. (2014). The Fanconi anemia DNA repair pathway: structural and functional insights into a complex disorder. *Annual review of biophysics*, 43, 257-278.
- 251. Nakanishi, K., Yang, Y. G., Pierce, A. J., Taniguchi, T., Digweed, M., D'Andrea, A. D. & Jasin, M. (2005). Human Fanconi anemia monoubiquitination pathway promotes homologous DNA repair. *Proceedings of the National Academy of Sciences of the United States of America*, 102(4), 1110-1115.
- 252. Yamamoto, K., Ishiai, M., Matsushita, N., Arakawa, H., Lamerdin, J. E., Buerstedde, J. M. & Takata, M. (2003). Fanconi anemia FANCG protein in mitigating radiation-and enzyme-induced DNA double-strand breaks by homologous recombination in vertebrate cells. *Molecular and Cellular Biology*, 23(15), 5421-5430.

- 253. Oda, T., Hayano, T., Miyaso, H., Takahashi, N., & Yamashita, T. (2007). Hsp90 regulates the Fanconi anemia DNA damage response pathway. *Blood*, *109*(11), 5016-5026.
- 254. Yamashita, T., Oda, T., & Sekimoto, T. (2007). Hsp90 and the Fanconi anemia pathway: a molecular link between protein quality control and the DNA damage response. *Cell Cycle*, *6*(18), 2232-2235.
- 255. Lamarche, B. J., Orazio, N. I., & Weitzman, M. D. (2010). The MRN complex in double-strand break repair and telomere maintenance. *FEBS letters*, *584*(17), 3682-3695.
- 256. Jiricny, J. (2013). Postreplicative mismatch repair. *Cold Spring Harbor perspectives in biology*, 5(4), a012633.
- 257. Tung, H. Y., Plunkett, B., Huang, S. K., & Zhou, Y. (2014). Murine mast cells secrete and respond to interleukin-33. *Journal of Interferon & Cytokine Research*, 34(3), 141-147.
- 258. Ko, J. C., Chiu, H. C., Syu, J. J., Chen, C. Y., Jian, Y. T., Huang, Y. J. & Lin, Y. W. (2015). Down-regulation of MSH2 expression by Hsp90 inhibition enhances cytotoxicity affected by tamoxifen in human lung cancer cells. *Biochemical and biophysical research communications*, 456(1), 506-512.
- 259. Strzalka, W., & Ziemienowicz, A. (2010). Proliferating cell nuclear antigen (PCNA): a key factor in DNA replication and cell cycle regulation. *Annals of botany*, 107(7), 1127-1140.
- 260. Wang, X., Heuvelman, D. M., Carroll, J. A., Dufield, D. R., & Masferrer, J. L. (2010). Geldanamycin-induced PCNA degradation in isolated Hsp90 complex from cancer cells. *Cancer investigation*, 28(6), 635-641.
- 261. Kirby, T. W., Gassman, N. R., Smith, C. E., Pedersen, L. C., Gabel, S. A., Sobhany, M. & London, R. E. (2015). Nuclear localization of the DNA repair scaffold XRCC1: uncovering the functional role of a bipartite NLS. *Scientific reports*, 5.

- 262. Khurana, N., Laskar, S., Bhattacharyya, M. K., & Bhattacharyya, S. (2016). Hsp90 induces increased genomic instability toward DNA-damaging agents by tuning down RAD53 transcription. *Molecular biology of the cell*, 27(15), 2463-2478.
- 263. Echtenkamp, F. J., Zelin, E., Oxelmark, E., Woo, J. I., Andrews, B. J., Garabedian, M., & Freeman, B. C. (2011). Global functional map of the p23 molecular chaperone reveals an extensive cellular network. *Molecular cell*, 43(2), 229-241.
- 264. DeZwaan, D. C., & Freeman, B. C. (2008). HSP90: the Rosetta stone for cellular protein dynamics?. *Cell Cycle*, 7(8), 1006-1012.
- 265. Mao, Z., Bozzella, M., Seluanov, A., & Gorbunova, V. (2008). Comparison of nonhomologous end joining and homologous recombination in human cells. *DNA repair*, 7(10), 1765-1771.
- 266. Prodromou, C., Roe, S. M., Piper, P. W., & Pearl, L. H. (1997). A molecular clamp in the crystal structure of the N-terminal domain of the yeast Hsp90 chaperone. *Nature Structural & Molecular Biology*, *4*(6), 477-482.
- 267. Prodromou, C., Roe, S. M., O'Brien, R., Ladbury, J. E., Piper, P. W., & Pearl, L. H. (1997). Identification and structural characterization of the ATP/ADP-binding site in the Hsp90 molecular chaperone. *Cell*, *90*(1), 65-75.
- 268. Tsutsumi, S., Mollapour, M., Graf, C., Lee, C. T., Scroggins, B. T., Xu, W., & Panaretou, B. (2009). Hsp90 charged-linker truncation reverses the functional consequences of weakened hydrophobic contacts in the N domain. *Nature structural & molecular biology*, *16*(11), 1141-1147.
- 269. Nathan, D. F., & Lindquist, S. (1995). Mutational analysis of Hsp90 function: interactions with a steroid receptor and a protein kinase. *Molecular and Cellular Biology*, *15*(7), 3917-3925.

- 270. Louvion, J. F., Warth, R., & Picard, D. (1996). Two eukaryote-specific regions of Hsp82 are dispensable for its viability and signal transduction functions in yeast. *Proceedings of the National Academy of Sciences*, *93*(24), 13937-13942.
- 271. Nathan, D. F., & Lindquist, S. (1995). Mutational analysis of Hsp90 function: interactions with a steroid receptor and a protein kinase. *Molecular and Cellular Biology*, *15*(7), 3917-3925.
- 272. Buchner, J. (1996). Supervising the fold: functional principles of molecular chaperones. *The FASEB journal*, *10*(1), 10-19.
- 273. Riggs, D. L., Cox, M. B., Cheung-Flynn, J., Prapapanich, V., Carrigan, P. E., & Smith, D. F. (2004). Functional specificity of co-chaperone interactions with Hsp90 client proteins. *Critical reviews in biochemistry and molecular biology*, *39*(5-6), 279-295.
- 274. Baumann, P., & West, S. C. (1998). Role of the human RAD51 protein in homologous recombination and double-stranded-break repair. *Trends in biochemical sciences*, 23(7), 247-251.
- 275. Lok, B. H., & Powell, S. N. (2012). Molecular pathways: understanding the role of Rad52 in homologous recombination for therapeutic advancement. *Clinical cancer research*, 18(23), 6400-6406.
- 276. Prodromou, C., Panaretou, B., Chohan, S., Siligardi, G., O'Brien, R., Ladbury, J. E., & Pearl, L. H. (2000). The ATPase cycle of Hsp90 drives a molecular 'clamp'via transient dimerization of the N-terminal domains. *The EMBO journal*, *19*(16), 4383-4392.
- 277. Mimnaugh, E. G., Xu, W., Vos, M., Yuan, X., Isaacs, J. S., Bisht, K. S., & Neckers, L. (2004). Simultaneous inhibition of hsp 90 and the proteasome promotes protein ubiquitination, causes endoplasmic reticulum-derived cytosolic vacuolization, and enhances antitumor activity. *Molecular Cancer Therapeutics*, *3*(5), 551-566.

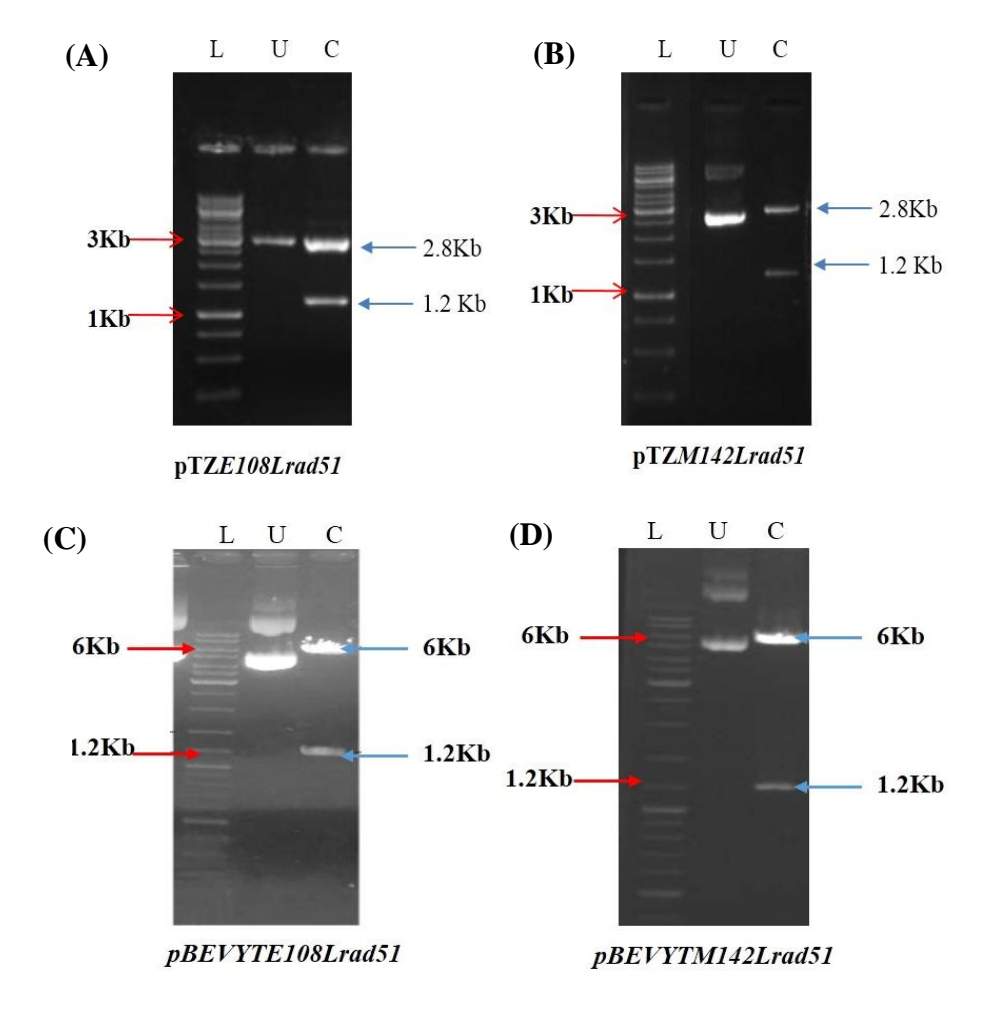
- 278. Ravid, T., & Hochstrasser, M. (2007). Autoregulation of an E2 enzyme by ubiquitin-chain assembly on its catalytic residue. *Nature cell biology*, *9*(4), 422-427.
- 279. Farrelly, F. W., & Finkelstein, D. B. (1984). Complete sequence of the heat shock-inducible HSP90 gene of Saccharomyces cerevisiae. *Journal of Biological Chemistry*, 259(9), 5745-5751.
- 280. Hainzl, O., Lapina, M. C., Buchner, J., & Richter, K. (2009). The charged linker region is an important regulator of Hsp90 function. *Journal of Biological Chemistry*, 284(34), 22559-22567.
- 281. Krukenberg, K. A., Street, T. O., Lavery, L. A., & Agard, D. A. (2011). Conformational dynamics of the molecular chaperone Hsp90. *Quarterly reviews of biophysics*, 44(2), 229-255.
- 282. Tembe, V., & Henderson, B. R. (2007). Protein trafficking in response to DNA damage. *Cellular signalling*, 19(6), 1113-1120.
- 283. Adam, S. A., Marr, R. S., & Gerace, L. (1990). Nuclear protein import in permeabilized mammalian cells requires soluble cytoplasmic factors. *The Journal of Cell Biology*, *111*(3), 807-816.
- 284. Gildemeister, O. S., Sage, J. M., & Knight, K. L. (2009). Cellular Redistribution of Rad51 in Response to DNA Damage NOVEL ROLE FOR Rad51C. *Journal of Biological Chemistry*, 284(46), 31945-31952.
- 285. Echeverria, P. C., & Picard, D. (2010). Molecular chaperones, essential partners of steroid hormone receptors for activity and mobility. *Biochimica et Biophysica Acta (BBA)-Molecular Cell Research*, 1803(6), 641-649.
- 286. Carrello, A., Ingley, E., Minchin, R. F., Tsai, S., & Ratajczak, T. (1999). The common tetratricopeptide repeat acceptor site for steroid receptor-associated immunophilins and

- hop is located in the dimerization domain of Hsp90. *Journal of Biological Chemistry*, 274(5), 2682-2689.
- 287. Comeau, S. R., Gatchell, D. W., Vajda, S., & Camacho, C. J. (2004). ClusPro: a fully automated algorithm for protein–protein docking. *Nucleic acids research*, 32(suppl\_2), W96-W99.
- 288. Kozakov, D., Brenke, R., Comeau, S. R., & Vajda, S. (2006). PIPER: an FFT-based protein docking program with pairwise potentials. *Proteins: Structure, Function, and Bioinformatics*, 65(2), 392-406.
- 289. Agmon, N., Pur, S., Liefshitz, B., & Kupiec, M. (2009). Analysis of repair mechanism choice during homologous recombination. *Nucleic acids research*, *37*(15), 5081-5092.
- 290. Pratt, W. B., Gehring, U., & Toft, D. O. (1996). Molecular chaperoning of steroid hormone receptors. In *Stress-inducible cellular responses* (pp. 79-95). Birkhäuser Basel.
- 291. Pratt, W. B., Galigniana, M. D., Morishima, Y., & Murphy, P. J. (2004). Role of molecular chaperones in steroid receptor action. *Essays in biochemistry*, 40, 41-58.
- 292. Pennisi, R., Ascenzi, P., & di Masi, A. (2015). Hsp90: a new player in DNA repair? *Biomolecules*, 5(4), 2589-2618.
- 293. Solit, D. B., & Rosen, N. (2006). Hsp90: a novel target for cancer therapy. *Current topics in medicinal chemistry*, 6(11), 1205-1214.
- 294. Felts, S. J., Karnitz, L. M., & Toft, D. O. (2007). Functioning of the Hsp90 machine in chaperoning checkpoint kinase 1 (Chk1) and the progesterone receptor (PR). *Cell stress* & *chaperones*, 12(4), 353-363.
- 295. Borkovich, K. A., Farrelly, F. W., Finkelstein, D. B., Taulien, J., & Lindquist, S. (1989). Hsp82 is an essential protein that is required in higher concentrations for growth of cells at higher temperatures. *Molecular and cellular biology*, *9*(9), 3919-3930.

# APPENDIX I

# Cloning of wild type RAD51 and rad51 mutants into pBEVYT yeast expression vector

After incorporating mutations in *RAD51* full length *E108Lrad51* and *M142Lrad51* were amplified using primer set OMKB88 and OMKB90. Full length 1.2 Kb PCR product was then cloned into TA cloning vector *pTZ57R/T*. After confirming the clones namely *pTZ-E108Lrad51* and *pTZ-M142Lrad51*, inserted gene was extracted by digestion with BamH1 and Pst1 restriction enzymes. These digested products were further sub cloned into 6Kb *pBEVYT* vector.



A1: Cloning of wild type *RAD51* and *rad51* mutants into *pBEVYT* yeast expression vector (A) Clone confirmation of *pTZE108Lrad51* (B) Clone confirmation of *pTZM142Lrad51*. In figures (A) and (B) agarose gel images showing the release of 1.2 Kb insert by double digestion with BamHI and PstI confirms the successful cloning of mutant *rad51* in *pTZ* vector. (C) Clone confirmation of *pBEVYTE108Lrad51* (D) Clone confirmation of *pBEVYTM142Lrad51*. In figures (C) and (D) agarose gel images showing the release of 1.2 Kb insert by double digestion with BamHI and PstI confirms the successful cloning of mutant *rad51* in *pBEVYT* vector. In all gel images L: DNA ladder, U: uncut, C: (cut) digested DNA with given restriction enzymes

# Cloning of E108Lrad51 and M142Lrad51 into pET22b bacterial expression vector

E108Lrad51 and M142Lrad51 were amplified using primer set OSB305/OSB293. Sequence confirmed full length point mutants E108Lrad51 and M142Lrad51 were extracted from clones pESCHIS-E108Lrad51 and pESCHIS-M142Lrad51 by BamHI and SalI digestion. These extracted 1.2 Kb genes were then sub cloned into 5493 bp long vector pET22b bacterial expression vector.

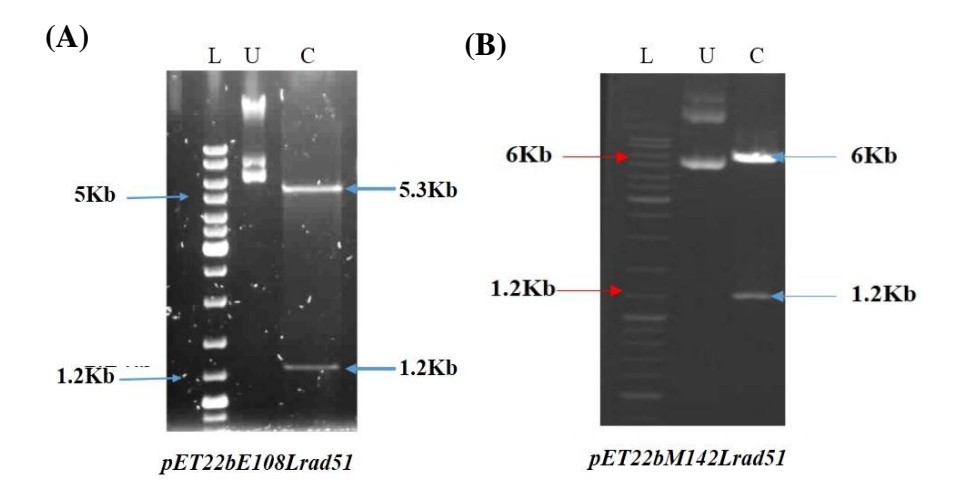


Figure A2: Cloning of *E108Lrad51* and *M142Lrad51* into pET22b bacterial expression vector (A) Clone conformation of *pET22bE108Lrad51*, agarose gel images showing the release of 1.2 Kb insert by double digestion with BamHI and SalI confirms the successful cloning of mutant *E108Lrad51* in *pET22b* vector. (B) Clone conformation of *pET22bM142Lrad51* agarose gel images showing the release of 1.2 Kb insert by double digestion with BamHI and SalI confirms the successful cloning of mutant *M142Lrad51* in *pET22b* vector.

# **Synopsis:**

Cells rely on a special set of proteins for maintenance of their proteome and these proteins are termed as molecular chaperones. Many such molecular chaperones get up-regulated upon heat stress, which are known as heat shock proteins. Hsp90 resides at the core of these heat shock proteins, which is essential and highly conserved throughout all kingdoms of life. In mammals, Hsp90 has two isoforms; Hsp90β, which is constitutively expressed and Hsp90α which expressed only upon stress. Hsp90 is highly abundant protein, constitutes 2% of total cellular proteins and its level increases up to 10% upon heat shock (1). Hsp90 remains associated with broad spectrum of proteins, known as Hsp90 clients and contributes to client protein maturation. Several co chaperones like Cdc37, p23, Aha1, HOP, CHIP, TRP2 etc., have been reported to participate in chaperone cycle by their interaction with different domains of Hsp90. These co chaperones function in client specific manner, as folding of different clients is dependent on different set of co chaperones (2). Although a long list of Hsp90 clients is available, it still remains ambiguous how Hsp90 selects its client proteins as they do not share any common sequence or motif. These diverse but restricted set of Hsp90 clients majorly keep central position in different biological functions like telomere maintenance, signal transduction, RNA processing, tumorogenesis, muscle contraction, cell motility. Majority of Hsp90 clients belongs to kinases and transcription factors (3, 4). Variable degree of association is reported between Hsp90 and its client proteins. Kinases are transiently associated with Hsp90 and once they are chaperoned they release from Hsp90 as a stable protein. However, in case of other clients such as steroid hormone receptors, it remains continuously associated to maintain its functional form (5-7). In recent years, molecular chaperones gained tremendous impact for assisting cells well beyond the stress tolerance. Although Hsp90 is a cytosolic chaperone, it is observed to assist many nuclear functions

like telomere silencing by regulating Sir2 abundance in the cells (8). This indicates that the Hsp90 engages in diverse cellular functions and takes central positions in many pathways.

One such pathway which is important for accurate survival and maintenance of genomic integrity is the DNA repair pathway. Several earlier studies on cancer cells indicated the possible connection between DNA repair and Hsp90. It was reported that in cancer cell line MRC-5 (transformed human fibroblast) Hsp90 immediately gets phosphorylated upon DNA damage at Thr-7 residue and forms repair foci into the nucleus (9). Inhibition of Hsp90 with 17-(dimethylaminoethylamino)-17-demethoxygeldanamycin (17-DMAG) results in reduced phosphorylation of DNA-PKcs, which is an important component of NHEJ (non-homologous end joining) mediated double-strand break repair (10). Another potent inhibitor of Hsp90, 17-AAG (17-allylamino-17-demethoxygeldanamycin), inhibits DSB repair in DU145 and SQ-5 cancer cell lines by BRCA2 degradation. Inhibition of Hsp90 with 17-AAG is reported to make DU145 and SQ-5 sensitive towards IR induced DNA damage, however similar treatment does not impact any difference in normal cell survival (11). These contradictory findings provoke us to ask whether Hsp90 is directly linked with the DNA repair pathway. Eukaryotes employ two independent DNA double strand break repair pathways; non homologous end joining (NHEJ) and homologous recombination (HR), where NHEJ is predominantly used by mammalian cells (12). The study on breast cancer cells displayed significant increase in HR efficiency. This indicates the dependency of cancer cells more on the HR for repairing breaks in the genome (13).

In our study, we address whether Hsp90 is directly linked with HR mediated DNA repair pathway and whether any protein of HR pathway is a direct client of Hsp90. To address these questions we utilized *Saccharomyces cerevisiae* (yeast) as a model system. It has two isoforms of Hsp90; Hsp82 which is expressed under stress and Hsc82 which is constitutively expressed in the cells (14). We created individual knockouts of these isoforms in yeast and studied

their behavior towards MMS and UV induced DNA damaging agents. Our results indicate that individual knockouts of these isoforms are redundant and they do not hamper cell growth upon DNA damage. Next, we wanted to determine whether inhibition of both the isoforms affects DNA damage sensitivity. To that end, we used a temperature sensitive strain *iG170Dhsp82*, in which the endogenous *HSP82* and *HSC82* are deleted and cells are surviving only on mutated copy *iG170Dhsp82*. This mutation renders Hsp82 nonfunctional at 37°C, as glycine at 170<sup>th</sup> position helds conformationally restricted position and its switching with aspartic acid (G170D) destabilizes Hsp82 at higher temperature (15, 16). When cells were pre-incubated at 37°C for 4 hrs and then subjected to MMS (0.03%), there occurs 62% reduction in the cell survivability. Similarly, treatment with UV makes the temperature sensitive (ts) mutant very sensitive at the restrictive temperature. This indicates the requirement of functional Hsp82 for the cell survivability upon DNA damage.

To investigate whether this observed phenomenon is specifically due to the defect in HR pathway of DNA repair we performed gene targeting assay which relies exclusively on HR. We used a cassette harboring *ADE2* marker flanked by *ADH4* upstream and downstream regions, additionally, it has another marker *KANMX* which is upstream of the *ADH4* sequence. Targeted and random integration events of this cassette can be scored by the loss or presence of *KANMX* marker. To this end, we transformed equal amount of this cassette in the *iG107Dhsp82* cells grown at permissive and restricted temperatures. We observe that the cells grown at restrictive temperature were drastically defective for gene targeting which is the indication of a defect in HR pathway.

Hsp82 is highly conserved and composed of three domains; N-terminal domain (NTD), middle domain (MD) and C-terminal domain (CTD). N-terminal domain is connected to the middle domain through a negatively charged linker region which is conserved among the

eukaryotes. Charged linker region is a flexible structure and assists during the coordinated movement between three domains which is required for client protein folding (17). Hsp82 functions as a dimer and its N-terminal domain possesses ATPase activity which facilitates client protein folding. Knowing the fact that different domains of Hsp82 carry different functions our interest was to perform mutational analysis of Hsp82 in order to understand the structure function relation of Hsp82 towards DNA repair. We took the advantage of well-studied Hsp82 mutants (generated by Professor Susan Lindquist) and analyzed their DNA repair activity. To this end, we included 4 mutants T22I, A41V, G81S and T101I from N-terminal domain, G313S from the middle domain and iA587T from C terminal domain. Among these mutants, T101I has ATPase activity less than 5% of the wild type cells while ATPase activity of iA587T is very close to the wild type cells (18). Activity of a well characterized Hsp90 client, glucocorticoid receptor is observed to be compromised in T101Ihsp82 mutant. We also included a deletion mutant of Hsp82 called charged linker deletion mutant, HH1a-p2HG/Hsp82 (211-259). Charged linker region of Hsp82 is evolutionarily conserved, however its exact role was undefined. According to previous reports, compromised chaperone activity of charged linker deleted Hsp90 mutant was reported towards glucocorticoid receptor and v-Src. Removal of this region does not however, affects nucleotide binding to the N-terminal domain of Hsp90. Also, its ATPase activity is slightly higher  $(0.6 \text{ min}^{-1})$  than that of the wild type  $(0.5 \text{ min}^{-1})$  (19).

In our study cell survivability of these mutants was studied as a measure of DNA repair activity in presence of MMS as well as UV induced DNA damage. Mutants which belong to the N-terminal (A41V, G81S and T101I) domain showed dramatic decrease in the cell survivability upon UV and MMS induced DNA damage. Middle domain mutant G313S also displayed 50% reduction in the cell survivability although iA587T did not show the significant defect in survivability. Deletion mutant of charged linker region (Δ211-259hsp82) of Hsp82 led to

88% reduction in the cell survivability upon MMS and UV induced DNA damage. These results indicate the importance of NTD residues and charged linker region for repairing the UV and MMS induced DSBs. We further explored these mutants and studied their effect on homologous recombination by performing gene targeting assay as mentioned earlier. On the basis of this analysis, we observed that A41V, T22I, G81S, and G313S mutants were moderately defective in gene targeting. However, T101Ihsp82 and charged linker deletion mutants were severely defective in performing gene targeting. In conclusion, the mutational analysis of Hsp82 revealed the importance of NTD (T1011hsp82) and charged linker region for DNA repair. It is illustrated that ATPase activity of Hsp82 is an essential step in the client folding and maturation (20). Keeping this fact in mind, we next tried to understand whether any of the DNA repair proteins is dependent on Hsp82 chaperone machinery for their final maturation. HR being error free pathway appoints series of proteins like Rad51, Rad52, Rad54, replication protein A (RPA) to preserve genomic integrity (21). Rad51, a homolog of RecA in Escherichia coli, is crucial for HR, which is recruited to 3' end of ssDNA with the help of Rad52 and forms hexameric nucleo-protein filament on the broken DNA junction (22). These Rad51 nuclear filaments, known as Rad51 foci, are the hallmark of DNA damage and perform homology search in order to explicitly repair the DNA. To study the steady state levels of Rad51 and Rad52 under Hsp82 mutant conditions, we probed the steady state level of these proteins in HR dead mutants namely; iG170Dhsp82, T101Ihsp82 and Δ211-259hsp82. Rad51 and Rad52 were drastically reduced in the ts mutant iG170Dhsp82 when grown at restrictive temperature for 2 hrs, and absent completely when grown at 37°C for overnight. Similarly, Rad51 and Rad52 were significantly reduced in ATPase dead mutant T101Ihsp82, which suggests the requirement of ATPase activity of Hsp82 for their stability. We also monitored Rad51 and Rad52 levels in  $\Delta 211$ -259hsp82 which was also a HR deficient strain. Surprisingly, in this mutant, we did not observe any difference in Rad51 and Rad52 levels. Our results indicate

that Rad51 and Rad52 likely share the client-ship with Hsp82. Being a chaperone, Hsp82 modulates its clients only at protein level without getting involved at the transcript level. Hence to pave the path towards understanding the client-ship, we checked the transcript levels of *RAD51* and *RAD52* in *hsp82* mutant conditions. Our real time data display no difference at *RAD51* and *RAD52* transcript levels when Hsp82 is nonfunctional. This data suggest, that destabilization of Rad51 and Rad52 is likely the major mechanism for the sensitivity of Hsp82 mutants towards DNA damage.

Our experiments indicate towards the possible client ship of Hsp90 with Rad51 and Rad52. For getting recognized as a client of Hsp82, candidate protein must fulfill following criteria; firstly, it should have physical interaction with Hsp82 and secondly, it should follow proteasomal pathway of degradation upon Hsp82 inhibition. Rad52 is previously reported to have interaction with Hsp82 through TAP-tag affinity chromatography and is not an essential protein in mammalian system as that of Rad51 (23). We continued our analysis only with Rad51 to establish client ship with Hsp82. To check the physical interaction of Rad51 with Hsp82 we performed coimmunoprecipitation and our data signifies strong association between Hsp82 and Rad51. Next, to explore the pathway for Rad51 degradation upon Hsp90 inactivated condition, we treated wild type cells with MG132, (proteasome inhibitor) in presence and absence of 17-AAG (Hsp82 inhibitor which inhibits the ATPase activity of Hsp82) and monitored the endogenous level of Rad51. We observe that 17-AAG treatment causes destabilization of Rad51 and targets it towards protesomal degradation. In presence of proteasomal inhibitor MG132, Rad51 level is increased even in presence of 17-AAG. Collectively, our data has established Rad51 as a direct client of Hsp82.

In mutant  $\Delta 211$ -259hsp82 we observed a decrease in HR efficiency without any change in Rad51 and Rad52 levels. This made us curious to study the mechanism behind HR

deficiency in  $\Delta 211$ -259hsp82. It is established that in response to DNA damage, Rad51 gets transcriptionally up regulated and translocates to the nucleus. Upon reaching to nucleus, Rad51 is recruited to the broken junction of DNA and forms foci, which is the hallmark of DNA repair (24). To check all these subsequent steps, we treated WT and  $\Delta 211$ -259hsp82 cells with 0.03% of MMS for 2 hrs and isolated RNA and protein from these cells. We did not observe any change in the upregulation of the *RAD51* transcript as well as Rad51 proteins level in  $\Delta 211$ -259hsp82 mutant upon DNA damage. We then studied the recruitment of Rad51 to the broken junction by performing indirect immuno-fluorescence assay upon DNA damage. Our experiment showed around 20% reduction in Rad51 foci formation as compared to the wild type cells. We analyzed the distribution of foci in each nucleus. After analyzing a total of 4,500 MMS-treated nuclei of wild-type and mutant cells, we observed a striking, statistically significant difference in the distribution of foci. Our analysis revealed that mutant cells possessed primarily 1 focus per nucleus, and the total number was comparable to that for wild-type cells. However, the percentage of nuclei containing more than 1 focus was drastically lower in mutant cells than in wild-type cells.

Charged linker region of Hsp82 maintains the flexible state of Hsp82 which is essential for client protein interaction and folding (25, 26). Our study indicates that the charged linker deletion mutant causes inefficient translocation of Rad51 to the nucleus. Hence we hypothesize that Hsp82-Rad51 interaction is important for optimum translocation of Rad51 to the nucleus upon DNA damage. To that end, we wanted to understand whether there exists any correlation between the extent of interaction between Hsp82 and Rad51 and the optimum Rad51 function upon DNA damage. To this end, we planned to map residues on Rad51 which interacts with Hsp82. As a collaborative measure, we mapped the interaction between Hsp82 and Rad51 using *in-silico* analysis and this analysis predicted several residues of Rad51, which interact strongly with Hsp82. Reported interactions in this analysis, are favored by the formation of several

contacts with bond distance less than 2 Å, implying the strong interaction between Hsp82 and Rad51. Our study described that out of all contacts, two residues; Glu108 and Met142 of Rad51 displayed the strongest interaction with Arg670 and Lys637 of Hsp82 respectively. These amino acid residues are evolutionary conserved and does not belong to the catalytic domain (ATPase domain) of Rad51. To analyze the importance of these residues in Rad51 function, we planned to generate rad51 mutants by replacing Glutamic acid at 108th position and Methionine at 142th position with hydrophobic residue Leucine that would disrupt the salt bridge/H-bonds with corresponding residues of Hsp82. The site directed mutants were created by splice overlap extension (SOE). We created three point mutants namely E108Lrad51, M142Lrad51 and one double mutant E108L/M142Lrad51, which were further confirmed by sequencing. They were individually cloned into yeast expression vector and transformed into  $\Delta rad51$ . The stability of mutant rad51 proteins was found to be comparable with that of wild type. We first intended to study and compare the interaction between mutant and wild type Rad51 with Hsp82. In order to do so, we expressed wild type Rad51, E108Lrad51, M142Lrad51 and Hsp82 as histidine tagged protein using bacterial expression system and further purified all these proteins using affinity chromatography. Later we determined the extent of association between Rad51 and Hsp82 using Surface Plasmon Resonance (SPR) analysis. During this analysis, Hsp82 was immobilized on CM5 chip and wild type Rad51, E108Lrad51 and M142Lrad51 mutants were injected to check their interaction with Hsp82. We measured the average equilibrium dissociation constant (K<sub>D</sub>) of each of the mutant rad51(s) and wild type Rad51. Our study shows that, while the K<sub>D</sub> value for wild type Rad51 was 46.22 µM, it was about 1000 times less in case of the mutant E108Lrad51 (K<sub>D</sub> being 69.235 nM). The other mutant M142Lrad51 however, showed comparable K<sub>D</sub> value (23.33 µM) with that of wild type Rad51. The kinetic parameters from our SPR analysis demonstrated that the association of E108Lrad51 and Hsp82 is 1000 folds stronger than the wild

type Rad51 and Hsp82. We aimed to understand whether such strong interaction between mutant rad51 and Hsp82 affects the function of Rad51 under DNA damaging condition. We measured the MMS induced survivability of the strains harboring RAD51, E108Lrad51, M142Lrad51 and double mutant E108L/M142Lrad51. We observed a drastic reduction in the survivability of strains harboring E108Lrad51 and E108L/M142Lrad51, while M142Lrad51 was moderately affected by DNA damage. During repair through HR, Rad51 gets recruited to the damaged DNA and performs gene conversion, which is a signature function of Rad51. To score the function of mutant rad51, we used an assay strain NA14. In this strain, a cassette is introduced into the genome which has a KANMX gene flanked by two URA3 copies, out of which one ura3 copy is mutated by the insertion of HO endonuclease restriction site. HO endonuclease is expressed upon galactose induction and creates a single DSB in the mutated version of ura3. Cells retain KANMX gene (G418 sulfate resistance), only if repair of this break takes place in Rad51 dependent manner. The percent gene conversion can be calculated by growing cells on G418 sulfate containing plates. To score the effect of mutant rad51 on gene conversion, we modified the NA14 strain where native RAD51 is knocked out and in that background either wild-type RAD51 or each of the three mutant rad51(s) were individually transformed. We calculated percent gene conversion of RAD51, E108Lrad51, M142Lrad51 and double mutant E108L/M142Lrad51. According to our analysis, E018Lrad51 and E108L/M142Lrad51 mutants have the drastic reduction in gene conversion efficiency.

To understand the phenomenon behind reduced cells survivability and gene conversion efficiency of rad51 mutants, we checked upstream functions of Rad51 upon DNA damage. These include the up regulation of rad51 mutant, translocation of rad51p to the nucleus and recruitment of rad51p to the damaged site. In our analysis, Rad51 and rad51 mutants are constitutively expressed under the GPD promoter hence; their expression levels remain unaffected upon DNA damage. We directly checked the translocation of rad51p to the nucleus. To estimate

the fraction of rad51 which is translocated to the nucleus upon DNA damage, we performed sub cellular fractionation in presence and absence of DNA damaging agent and measured the ratio of rad51 in the nucleus and the cytoplasm. Our analysis indicates that, *E108Lrad51* and *E108L/M142Lrad51* are defective in DNA damage induced translocation of Rad51 to the nucleus compared to the wild type. We took another approach to study Rad51 nuclear translocation, which is the recruitment of rad51 to the DSB. We performed the chromatin immuno-precipitation (ChIP) in the strain which was used for gene conversion assay. Rad51 recruitment was estimated by amplifying the DNA sequence using *URA3* specific donor primers. We observe that there exists a defect in the recruitment of mutant *rad51* to the damaged DNA, as compared to the wild type Rad51. We reason that the deficiency in the translocation of mutant rad51 protein is responsible for the defect in Rad51 function. This is supported by the strongest association of the mutant rad51 with Hsp82. Hence it is concluded that the mutant rad51 is locked in the Hsp82 chaperone machinery and hence unable to move to the nucleus upon DNA damage resulting a severely low Rad51 dependent gene conversion efficiency.

In conclusion, our work shows the importance of Hsp82 in HR pathway of DNA repair. Firstly, our work establishes that Hsp90 provides functional maturity to Rad51 and hence shares a client ship with it. Secondly; we demonstrate that the dynamic interaction between Hsp82 and Rad51 modulates nuclear entry of Rad51 upon DNA damage. Nuclear entry of Rad51 is an essential step for its functions in DNA repair, however it does not carry functional nuclear localization signal (NLS). The nuclear entry of Rad51 seems to be supported by other proteins. BRCA2 and Rad51C are two proteins, individually reported in two independent studies for assisting Rad51 translocation to the nucleus (27, 28). However contradictory reports indicate the presence of Rad51 in the nucleus even in the absence of these proteins (29-32). Besides, in lower eukaryotes like *Saccharomyces cerevisiae*, these two proteins are absent. Hence, there should be

some evolutionary conserved mechanism for Rad51 translocation to the nucleus. Our present work indicates that Hsp82 controls the dynamic association of Rad51 with itself and thereby regulates the entry of Rad51 to the nucleus and thereby directly controls the DNA repair pathway. However, future studies involving the DNA damage induced conformational changes in the Hsp82 and Rad51 complex is required, to understand this complex process. As HR efficiency is significantly elevated in several cancer cells, understanding the regulation of HR is an important concern. Besides, combined inhibition of Hsp90 along with other proteins is an emerging research area for cancer therapy. Thus comprehensive knowledge of HR regulation by Hsp90 will aid in understanding the mechanism behind the effects of Hsp90 inhibition on cancer cells.



# Both the Charged Linker Region and ATPase Domain of Hsp90 Are Essential for Rad51-Dependent DNA Repair

Tanvi Suhane, <sup>b</sup> Shyamasree Laskar, <sup>b</sup> Siddheshwari Advani, <sup>a</sup> Nabamita Roy, <sup>a</sup> Shalu Varunan, <sup>a</sup> Dibyendu Bhattacharyya, <sup>c</sup> Sunanda Bhattacharyya, <sup>b</sup> Mrinal Kanti Bhattacharyya <sup>a</sup>

Department of Biochemistry, School of Life Sciences, University of Hyderabad, Hyderabad, Hyderabad, India<sup>a</sup>; Department of Biotechnology and Bioinformatics, School of Life Sciences, University of Hyderabad, Hyderabad, India<sup>b</sup>; Tata Memorial Centre, ACTREC, Mumbai, India<sup>c</sup>

The inhibition of Hsp90 in cancerous cells has been correlated with the reduction in double-strand break (DSB repair) activity. However, the precise effect of Hsp90 on the DSB repair pathway in normal cells has remained enigmatic. Our results show that the Hsp82 chaperone, the ortholog of mammalian Hsp90, is indispensable for homologous-recombination (HR)-mediated DNA repair in the budding yeast *Saccharomyces cerevisiae*. A considerable reduction in cell viability is observed in an Hsp82-inactivated mutant upon methyl methanesulfonate (MMS) treatment as well as upon UV treatment. The loss of Hsp82 function results in a dramatic decrease in gene-targeting efficiency and a marked decrease in the endogenous levels of the key recombination proteins Rad51 and Rad52 without any notable change in the levels of *RAD51* or *RAD52* transcripts. Our results establish Rad51 as a client of Hsp82, since they interact physically *in vivo*, and also show that when Hsp82 is inhibited by 17-AAG, Rad51 undergoes proteasomal degradation. By analyzing a number of point mutants with mutations in different domains of Hsp82, we observe a strong association between the sensitivity of an ATPase mutant of Hsp82 to DNA damage and the decreases in the amounts of Rad51 and Rad52 proteins. The most significant observations include the dramatic abrogation of HR activity and the marked decrease in Rad51 focus formation in the charged linker deletion mutant of Hsp82 upon MMS treatment. The charged linker region of Hsp82 is evolutionarily conserved in all eukaryotes, but until now, no biological significance has been assigned to it. Our findings elucidate the importance of this region in DNA repair for the first time.

When cells are exposed to any DNA double-strand break (DSB)-inducing agent, a plethora of proteins are activated and recruited at the broken junction in order to repair the damage. Failure to repair such DNA lesions leads to cell death, loss of genetic information, and malignancy. In eukaryotes, DSBs can be repaired primarily by two pathways: homologous recombination (HR) and nonhomologous end joining (NHEJ) (1, 2). In higher eukaryotes, NHEJ, which does not rely on any homology, is the predominant break repair mechanism. This process often leads to the deletion of a small portion of the genome. The key proteins associated with this pathway include Mre11, Ku70, Ku80, the DNA-dependent protein kinase catalytic subunit (DNA-PKcs), Artemis, and XRCC4 (3). Most of the lower eukaryotic microbes primarily use HR as the major repair pathway.

HR involves resection of the broken end and thus generation of single-stranded DNA (ssDNA) overhangs, which form the binding site for Rad51p. Rad51p, with its ATPase activity, searches for the homologous templates and invades similar sequences. Rad51, Rad52, Rad54, and replication protein A (RPA) are the key proteins involved in the HR-mediated break repair pathway (4, 5). In *Saccharomyces cerevisiae*, Rad52p facilitates the formation of a hexameric Rad51p-bound ssDNA complex at the broken junction in the presence of RPA. Rad52p plays a central role in HR, and *rad52* mutation abolishes all recombination events in yeast (6).

Hsp90 is an important cellular chaperone that is evolutionarily conserved from bacteria to mammals. It is abundantly present (~1 to 2% of total cellular proteins) in cytosol and is involved in the maturation and stability of a special class of client proteins (7, 8, 9, 10). *In vitro* experiments have shown that Hsp90 cannot refold completely denatured protein. However, it assists in the folding of client proteins where considerable amounts of secondary structures are retained (11). Hsp90 is not a general chaperone

like Hsp70, and how it selectively chooses a special class of clients has remained enigmatic. In the budding yeast *S. cerevisiae*, Hsp90 exists in two isoforms: Hsc82, which is constitutively expressed in the cell, and a paralog, Hsp82, which is induced under stress conditions (12). Hsc82 and Hsp82 are 97% identical in their amino acid sequences, and at least one of them is essential for yeast viability. In recent years, Hsp90 has shown tremendous potential as an anticancer target (13), and thus it is important to gain a better understanding of Hsp90 functions.

Hsp90 functions as a dimer, and the protein folding is mediated by the participation of different cochaperones and the ATPase activity of the chaperone (14, 15). Hsp82 is an 82-kDa protein with three distinct domains. The amino-terminal domain (amino acids 1 to 220) has an ATP binding pocket that gives rise to the Bergerat fold. A recent crystal structure of Hsp90 revealed that the function of Hsp82 is dependent on its binding and the hydrolysis of ATP (16, 17, 18). The N-terminal domain is linked to the middle domain (amino acids 273 to 525) through a charged linker

Received 2 July 2014 Accepted 27 October 2014

Accepted manuscript posted online 7 November 2014

Citation Suhane T, Laskar S, Advani S, Roy N, Varunan S, Bhattacharyya D, Bhattacharyya S, Bhattacharyya MK. 2015. Both the charged linker region and ATPase domain of Hsp90 are essential for Rad51-dependent DNA repair. Eukaryot Cell 14:64–77. doi:10.1128/EC.00159-14.

Address correspondence to Sunanda Bhattacharyya, sbtsl@uohyd.ernet.in, or Mrinal Kanti Bhattacharyya, mkbsl@uohyd.ernet.in.

T.S. and S.L. contributed equally to this article.

Copyright © 2015, American Society for Microbiology. All Rights Reserved. doi:10.1128/EC.00159-14

region, which is an important regulator of Hsp90 function. The charged linker region contains s pentad repeat of the motif (D/ E)(D/E)(D/E)KK and is absent from prokaryotic Hsp90. Previously, it was shown that this domain is dispensable for steroid hormone receptor regulation and the pheromone signaling pathway (19). However, a more recent study has demonstrated that deletion of the linker has a distinctive effect on client activation

A study of the crystal structure revealed that the cochaperone Aha1 interacts with the middle and N-terminal domains of Hsp90 and facilitates the binding of a subset of clients (21, 22, 23). The carboxy-terminal domain of Hsp90 has a dimerization domain (24). It has a conserved MEEVD motif at the extreme end, which is the binding site for a special class of cochaperones that contain multiple copies of a tetratricopeptide repeat (TPR) (25, 26). Because the interaction between the chaperone and its clients is very transient, it is very challenging to identify the interactome of Hsp90. Different high-throughput studies aimed at finding out the genomewide interactors of HSP82 have identified some of the key proteins involved in the DNA damage repair pathway (27, 28). However, due to the lack of any detailed study, it remains ambiguous whether Hsp90 plays any role in the DNA repair pathway under normal cellular conditions. A potent Hsp90 inhibitor, 17-(dimethylaminoethylamino)-17-demethoxygeldanamycin (17-DMAG), has been found to inhibit radiation-induced double-strand break repair in tumor cells by reducing the phosphorylation of DNA-PKcs (29). Also in tumor cells, Hsp90 phosphorylation has been found to be correlated with DNA damage (30), and Rad51 focus formation at the damaged sites has been found to be delayed by NVP-AUY922, an inhibitor of Hsp90 (31). Another study has demonstrated that 17-allylamino-17-demethoxygeldanamycin (17-AAG) inhibits DSB repair in tumor cells by BRCA2 degradation; however, it has no effect in normal cells (32).

So far, no detailed work has been carried out to investigate whether Hsp90 plays any role in the DNA repair pathway in lower eukaryotes. In order to understand whether the DSB repair phenotypes, observed in tumor cell lines upon treatment with Hsp90 inhibitors, stem from direct or an indirect involvement of Hsp90, we have examined the role of yeast Hsp82 in the DSB repair pathway by employing well-characterized S. cerevisiae mutant strains. This is the first report which demonstrates that in lower eukaryotes, Hsp82 is indispensable for the homologous-recombination mechanism and that Rad51 is a direct client of Hsp82. Our findings reveal that in an Hsp82-inactivated background ( $\Delta hsp82$  $\Delta hsc82$ ), the endogenous levels of Rad51p and Rad52p are drastically reduced and HR-mediated DSB repair is severely compromised. Structure-function correlation studies have revealed differential effects of several Hsp82 mutants on gene-targeting efficiency, which is well correlated with endogenous levels of Rad51p and Rad52p. Our study shows that the deletion of a charged linker region causes a pronounced defect in gene targeting and Rad51 focus formation upon treatment with methyl methanesulfonate (MMS).

## **MATERIALS AND METHODS**

Yeast strains. The strains used in this study are listed in Table 1. The iG170Dhsp82 strain, HH1a-p2HG/Hsp82, and HH1a-p2HG/Hsp82(Δ211-259) were kindly provided by Didier Picard (33, 34). The hsp82 T22I, A41V, G81S, T101I, G313S, and iA587T point mutants and the control strain P82a were provided by Susan Lindquist (35). The yeast expression vector (2µ plasmid) harboring ScRad51 (36) was transformed into

HH1a-p2HG/Hsp82( $\Delta$ 211-259) and the *iG170Dhsp82* strain to generate strains TSY1 and SLY69, respectively. The blank vector was transformed into the iG170Dhsp82 strain and HH1a-p2HG/Hsp82( $\Delta$ 211-259) to generate strains TSY3 and TSY2, respectively.

Construction of epitope-tagged RAD52 in various strain backgrounds. In order to tag the MYC epitope at the C-terminal end of RAD52, we used plasmid pFA6a-13Myc-kanMX6 (37) as a template and primers OSB68 (5' AAG ACC AAA GAT CAA TCC CCT GCA TGC ACG CAA GCC TAC TCG GAT CCC CGG GTT AAT TAA 3') and OSB69 (5' ATA ATG ATG CAA ATT TTT TAT TTG TTT CGG CCA GGA AGC GGA ATT CGA GCT CGT TTA AAC 3'), with upstream and downstream sequences of RAD52. The 2.3-kb PCR product was used to target the RAD52 loci of W303α and the iG170Dhsp82 and T101I mutants by homologous recombination to generate SLY47, SLY49, and MVS36, respectively. In order to tag the *RAD52* locus of strain HH1a-p2HG/Hsp82( $\Delta$ 211-259) with Myc, we first isolated the plasmid from this mutant strain. The  $hsp82(\Delta 211$ -259) gene was PCR amplified and was cloned into the pRS313 yeast expression vector (CEN plasmid). The recombinant plasmid with the HIS marker was transformed into the RAD52 MYC-tagged T101I strain (MVS36), and the transformants were selected on a SC-His (synthetic medium without histidine) plate. Thus, we generated strain SLY65 by plasmid swapping to create the RAD52 MYC-tagged  $hsp82(\Delta 211-259)$ 

MMS and UV sensitivity assays. In order to perform the return-togrowth assay in the presence of the DNA-damaging agent methyl methanesulfonate (MMS), fresh yeast cells were grown in yeast extract-peptone-dextrose (YPD) at 25°C to an optical density (OD) of 0.5. The cells were then divided into two parts with equal volumes. One part of the cells was exposed to 0.03% (vol/vol) MMS (Sigma-Aldrich) for 2 h, followed by plating on YPD medium at the required temperature (either 25°C or 37°C) after a 10-fold serial dilution. The other batch was grown in the absence of MMS for 2 h; its growth was then normalized to that of the MMS-treated cells, and it was subsequently plated at the required temperature. The plates were incubated for 36 h, and the growth of the two batches was compared.

In order to determine the difference in MMS sensitivity more quantitatively, we did a viability assay. Briefly, about 1,000 cells (as estimated from optical density) from MMS-treated or mock-treated cultures were plated and allowed to grow. The ratio of the number of colonies observed from the MMS-treated cells to the mock-treated cells was multiplied by 100, which gave the percentage of survival. We repeated each assay at least 3 to 4 times before plotting the values.

For the UV sensitivity assay, cells of each strain were grown in YPD medium to an OD of 0.5. Then they were diluted, and 1,000 cells were spread on YPD medium and were exposed to the doses of UV radiation indicated in Fig. 1 and 4. UV irradiation was carried out using Stratagene Stratalinker 1800. The plates were then incubated for 4 days; the number of viable colonies for each dosage of UV radiation was counted; and the percentage of survivability was calculated by considering the growth of each strain without UV irradiation to be 100%.

**Gene-targeting assay.** The ADE2 gene was knocked out at the ADH4 loci of P82a, the hsp82 T22I, A41V, G81S, T101I, G313S, G170D, and iA587T point mutants, and the  $hsp82(\Delta 211-259)$  strain. The targeting cassette (36) contained the homologous stretches of upstream and downstream sequences of ADH4 flanking the ADE2 gene and a KANMX6 selectable marker upstream of the ADH4 sequence. Two micrograms of the DNA was transformed into each strain. Transformants were first grown on an SC-Ade plate and were subsequently replica plated on a G418 sulfate-containing plate. In each case, the Ade<sup>+</sup> G418<sup>S</sup> colonies were counted. Gene-targeting efficiency was normalized by transforming an equal amount of uncut replicating plasmid into the respective strains to nullify any variation arising from the difference in competence for DNA uptake between strains. The gene-targeting efficiency, expressed as a percentage, was calculated as (number of Ade + G418 colonies in each mutant)/(number of Ade<sup>+</sup> G418<sup>S</sup> colonies in P82a)  $\times$  100.

TABLE 1 Yeast strains used in this study

Strain	Genotype	Source
SLY20	MATa leu2-3,112 trp1 ura3-1 ade2-1 his3-11,15 VIIL::ADE2	Laskar et al. (38)
SLY47	MATa leu2-3,112 trp1 ura3-1 ade2-1 his3-11,15 VIIL::ADE2 Rad52-13MYC-KANMX6	This study
SLY4	MATa leu2-3,112 trp1 ura3-1 ade2-1 his3-11,15 VIIL::ADE2 hsc82::KAN <sup>r</sup>	Laskar et al. (38)
SLY5	MAT <b>a</b> leu2-3,112 trp1 ura3-1 ade2-1 his3-11,15 VIIL::ADE2 hsp82::KAN <sup>r</sup>	Laskar et al. (38)
iG170Dhsp82 mutant	MATa can1-100 ade2-1 his3-11,15 leu2-3,112 trp1-1 ura3-1 hsp82::LEU2 hsc82::LEU2 HIS3::HSP82G170D	D. Picard
HH1a-p2HG/Hsp82	MATa hsp82::LEU2 hsc82::LEU2 ade2 his3 leu2 trp1 ura3 HSP82-2µ-HIS (p2HG/Hsp82)	D. Picard (34)
HH1a-p2HG/Hsp82(Δ211-259)	MATa hsp82::LEU2 hsc82::LEU2 ade2 his3 leu2 trp1 ura3 HSP82(Δ211-259)-2μ-HIS [p2HG/Hsp82(Δ211-259)]	D. Picard (34)
DP533	Δhsc82::kanMx4 Δhsp82::kanMx4/2μ-HSC82-URA3 [YEplac195] Δpdr::loxP-leu2-loxP trp1-289 leu2-3,112 his3-Δ200 URA3-52 ade2-101Δc lys2-801	D. Picard (34)
SLY49	MATa can1-100 ade2-1 his3-11,15 leu2-3,112 trp1 ura3-1 hsp82::LEU2 hsc82::LEU2 HIS3::HSP82G170D Rad52-13MYC-KANMX6	This study
MVS36	MATa can1-100 ade2-1 his3-11,15 leu2-3,112 trp1 ura3-1 hsp82::LEU2 hsc82::LEU2 CEN pTGPD/T3- 138 Rad52-13MYC-KANMX6	This study
SLY65	MATa can1-100 ade2-1 his3-11,15 leu2-3,112, trp1 ura3-1 hsp82::LEU2 hsc82::LEU2 pRS313hsp82( $\Delta$ 211-259) Rad52-13MYC-KANMX6	This study
SLY69	MATa can1-100 ade2-1 his3-11,15 leu2-3,112 trp1 ura3-1 hsp82::LEU2 hsc82::LEU2 HIS3::HSP82G170D 2μ pTAScRAD51	This study
TSY1	MATa hsp82::LEU2 hsc82::LEU2 ade2 his3 leu2 trp1 ura3 HSP82(Δ211-259)-2μ-HIS [p2HG/ Hsp82(Δ211-259)] 2μ (pTAScRad51)	This study
TSY2	MATa hsp82::LEU2 hsc82::LEU2 ade2 his3 leu2 trp1 ura3 HSP82(Δ211-259)-2μ-HIS [p2HG/ Hsp82(Δ211-259)] 2μ-pTA	This study
TSY3	MATa can1-100 ade2-1 his3-11,15 leu2-3,112 trp1 ura3-1 hsp82::LEU2 hsc82::LEU2 HIS3::HSP82G170D 2μ-pTA	This study
P82a (control)	MAT <b>a</b> can1-100 ade2-1 his3-11,15 leu2-3,112 trp1 ura3-1 hsp82::LEU2 hsc82::LEU2 CEN pTGPD/P82	S. Lindquist (35)
T22I mutant	MATa can1-100 ade2-1 his3-11,15 leu2-3,112 trp1 ura3-1 hsp82::LEU2 hsc82::LEU2 CEN pTGPD/T3-142	S. Lindquist (35)
A41V mutant	MATa can1-100 ade2-1 his3-11,15 leu2-3,112 trp1 ura3-1 hsp82::LEU2 hsc82::LEU2 CEN pTGPD/T1-40	S. Lindquist (35)
G81S mutant	MATa can1-100 ade2-1 his3-11,15 leu2-3,112 trp1 ura3-1 hsp82::LEU2 hsc82::LEU2 CEN pTGPD/T1-15	S. Lindquist (35)
T101I mutant	MATa can1-100 ade2-1 his3-11,15 leu2-3,112 trp1 ura3-1 hsp82::LEU2 hsc82::LEU2 CEN pTGPD/T3-138	S. Lindquist (35)
G313S mutant	MATa can1-100 ade2-1 his3-11,15 leu2-3,112 trp1 ura3-1 hsp82::LEU2 hsc82::LEU2 CEN pTGPD/T4-47	S. Lindquist (35)
iA587T mutant	MATa can1-100 ade2-1 his3-11,15 leu2-3,112 trp1 ura3-1 hsp82::LEU2 hsc82::LEU2 hsp82 A587T::HIS3 piHGPD/A587T	S. Lindquist (35)

Western blotting. For the estimation of levels of Rad51 and 13-Myctagged Rad52 proteins, we grew SLY47, the iG170Dhsp82 strain, SLY49, MVS36, SLY65, SLY69, TSY1, TSY2, and TSY3 overnight at 25°C. Next morning, the overnight cultures were diluted at a 1:100 ratio and were grown again for 3 to 4 h at 25°C until the OD at 600 nm (OD<sub>600</sub>) reached 0.5. For the temperature-sensitive strains, the cells were divided into two groups; one part was incubated at 25°C for 4 h, and another part was incubated at 37°C overnight. After that, equal numbers of cells were taken and precipitated, and protein was isolated from them by the trichloroacetic acid (TCA) method, followed by Western blotting (38). A rabbit anti-Rad51 antibody (Promega), a mouse anti-Hsp82 antibody (Calbiochem), and a mouse anti-Act1 antibody (Abcam) were used at a 1:5,000 dilution. A rabbit anti-Myc antibody (Abcam) was used at a 1:8,000 dilution. A horseradish peroxidase-conjugated anti-rabbit secondary antibody (Promega) and a horseradish peroxidase-conjugated anti-mouse secondary antibody (Santa Cruz Biotechnology Inc., Santa Cruz, CA, USA) were used at a 1:10,000 dilution. The Western blots were developed using a chemiluminescent detection system (Pierce). The bands on the gel were quantified using GeneTools (Syngene), and the relative densities thus obtained were plotted using GraphPad Prism software. The mean values from four independent experiments were plotted with standard deviations (SD). All blots were normalized against actin.

**Real-time RT-PCR.** Total RNA was isolated from the *iG170Dhsp82* strain after growth at 25°C and at 37°C for 4 h. In another assay, wild-type strain HH1a-p2HG/Hsp82 and the charged linker deletion mutant, as

well as P82a and the hsp82 T101I point mutant, were either left untreated or exposed to 0.03% MMS for 2 h, and by using the acid phenol method as described previously (38), we isolated RNA from these strains. We synthesized cDNA exactly as described in reference 38. We used OSB16 (5' TGA CCA AAC TAC TTA CAA CTC C 3') and OSB14 (5' TTA GAA ACA CTT GTG GTG AAC G 3') to amplify 307 bp at the 3' end of the ACT1 transcript. To amplify 326 bp of the 3' end of RAD51, we used primers OSB44 (5' GTG GTG AAC TAA GCG CAA G 3') and OSB45 (5' CTA CTC GTC TTC TCT GG 3'), and to amplify 208 bp of the 3' end of RAD52, we used primers OSB133 (5' TGG GAA TCA AGT ACC GCG TG 3') and OSB134 (5' TCA AGT AGG CTT GCG TGC ATG 3'). For realtime reverse transcription-PCR (RT-PCR), cDNA was diluted (1:50) and was used for PCR with an RT-PCR kit (Roche). The real-time analysis was carried out using an Applied Biosystems 7500 Fast Real-Time PCR system. The threshold cycle  $(C_T)$  value of the *ACT1* transcript of each sample was used to normalize the corresponding  $C_T$  values of the RAD51 and *RAD52* transcripts. The normalized  $C_T$  values of *RAD51* and *RAD52* from different samples were compared to obtain  $\Delta C_T$  values. The relative levels of mRNA were deduced from the following equation: change in mRNA level =  $2^{\Delta CT}$ . The mean values ( $\pm$ SD) from three independent experiments were plotted using GraphPad Prism software, version 6.

Indirect immunofluorescence. The wild-type strain HH1a-p2HG/Hsp82 and the charged linker deletion mutant HH1a-p2HG/Hsp82( $\Delta$ 211-259) were grown at 30°C to an OD of 0.5 and were then divided into two parts. One part was allowed to grow under the same conditions, and the

other part was treated with 0.03% MMS for 2 h, followed by an indirect immunofluorescence assay. Cells were briefly fixed with 4% paraformal-dehyde for 2 h, washed with 0.1 M potassium phosphate buffer and 1 mM MgCl<sub>2</sub>, and permeabilized with yeast Lyticase enzyme. Spheroplasts were fixed on a coverslip with poly-L-lysine (Sigma). Samples were blocked with 1% dry milk in phosphate-buffered saline (PBS) for 30 min, incubated with anti-Rad51 (Promega) at a 1:200 dilution for 1 h at room temperature, and washed with PBS 10 to 12 times. Incubation with an Alexa Fluor 488-conjugated anti-goat antibody (Molecular Probes; Life Technologies) at a 1:200 dilution and 4′,6-diamidino-2-phenylindole (DAPI) at a 1:2,000 dilution was carried out for 30 min in the dark. The samples were then washed 10 to 12 times with PBS. Slides were then covered with a mounting solution and were used for confocal microscopy with a Zeiss LSM 510 Meta confocal microscope.

**Coimmunoprecipitation.** Wild-type and  $\Delta rad51$  cells were grown to an OD of 0.5. Ten milliliters of each culture was harvested, resuspended in 1 ml spheroplast buffer (50 mM Tris-HCl [pH 8], 25 mM HEPES [pH 7.4], 0.2% Casamino Acids, 0.2% yeast nitrogen base [YNB], 1% glucose, 18.2% sorbitol) containing dithiothreitol (DTT) and Lyticase, and incubated at 30°C for 90 min. Two milliliters of piperazine-N,N'-bis(2-ethanesulfonic acid) (PIPES) buffer was added to the cells, and they were centrifuged at 5,000 rpm for 5 min. The cells were then resuspended in 2 ml ice-cold EBC buffer (50 mM Tris-HCl [pH 8], 120 mM NaCl, 0.5% [vol/vol] NP-40) containing protease inhibitor (Roche), left on ice for 1 h, and subsequently centrifuged at 12,000 rpm and 4°C. An anti-Hsp82 antibody was added to the supernatant for overnight incubation at 4°C. Protein A Agarose (25%; Calbiochem) was added, and the mixture was incubated for 2 h at room temperature. The beads were then spun down for 15 s at 1,000 rpm, and the pellet was washed 3 times with NETNS buffer (20 mM Tris-HCl [pH 8], 1 mM EDTA, 1 M NaCl, 0.5% [vol/vol] NP-40 with protease inhibitor) and twice with NETN buffer (20 mM Tris-HCl [pH 8], 1 mM EDTA, 100 mM NaCl, 0.5% [vol/vol] NP-40 with protease inhibitor). The proteins were eluted with 2× Laemmli buffer by boiling for 10 min and were spun down, and the supernatants were collected and used for Western blotting.

## **RESULTS**

Loss of Hsp82 function affects DSB repair activity. Previous findings revealed that 17-AAG, a potent inhibitor of Hsp90, causes a drastic reduction in radiation-induced DSB repair in tumor cell lines (DU145 and SQ-5). However, no such effect on DSB repair activity was observed in normal cell lines in the presence of an Hsp90 inhibitor (32). In order to investigate the role of HSP82 in the DNA repair pathway, we used S. cerevisiae as a model system. To this end we have used  $\Delta hsp82$  or  $\Delta hsc82$  single mutants as well as a temperature-sensitive mutant (iG170Dhsp82) in which the activities of both Hsp82 and Hsc82 are abrogated. We investigated the sensitivities of these mutants to DNA-damaging agents, such as MMS and UV radiation. These agents cause DNA damage via distinct mechanisms. Both the wild-type strain (SLY20) and the single mutants were exposed to 0.03% MMS for 2 h and were then returned to growth without MMS. Serial dilutions of cells were spotted onto the plates for comparison of the growth of different strains after DNA damage. Since failure to repair damaged DNA leads to the death of the cells, the survival of cells is directly proportional to the efficiency of DNA repair. We observed that the single mutants SLY5 ( $\Delta hsp82$ ) and SLY4 ( $\Delta hsc82$ ) did not show significantly more sensitivity to MMS in the plate assay than wildtype cells (Fig. 1A). The fractions of MMS-treated cells that survived in the return-to-growth experiment were measured, and the growth of single mutants was found to be about 85% that of the wild type (Fig. 1B). The sensitivities of single mutants to UV radiation were also determined by scoring their abilities to survive on

different doses of UV radiation. Determination of percentages of viability showed no significant difference in the tolerance of UV radiation between the single mutants and the wild-type cells (Fig. 1C). These results suggest that the two paralogs HSP82 and HSC82 are redundant to each other. The temperature-sensitive iG170Dhsp82 strain (35) was used to investigate the effect of the abrogation of both Hsp82 and Hsc82 functions on DNA damage sensitivity. We incubated the iG170Dhsp82 strain at 25°C (permissive temperature) as well as at 37°C (restrictive temperature) for 2 h and 4 h and treated the cells with MMS. In the course of our studies, we noted that the iG170Dhsp82 strain, when preincubated at 37°C for a short interval (2 h), became significantly more sensitive to MMS than the strain grown at the permissive temperature (25°C). Prolonged incubation at 37°C (for 4 h) rendered the cells even more hypersensitive to MMS. However, the MMS sensitivity was not as drastic as that of the  $\Delta rad51$  strain (Fig. 1D). Measurement of the percentage of survivability of MMS-treated iG170Dhsp82 cells upon incubation for 4 h at 37°C showed a 62% decrement in survivability from that for cells grown at 25°C (Fig. 1E). In order to establish that the growth defect is due solely to MMS sensitivity and not to exposure to an increased temperature, the viability of isogenic wild-type cells (P82a) was monitored in parallel, where cells were preincubated at 37°C for 4 h prior to MMS treatment. We observed that such conditions were well tolerated by wild-type cells (data not shown). When the iG170Dhsp82 strain was grown at the restrictive temperature (37°C for 4 h), it showed significantly more sensitivity (measured by the percentage of viability) upon UV irradiation than when it was grown at 25°C (Fig. 1F). For wild-type cells, sensitivity to UV was also monitored after preincubation at 37°C (for 4 h). The percentage of survivability relative to that of cells grown at 30°C showed a similar trend (data not shown). Thus, our finding suggests that loss of both Hsp82 and Hsc82 functions makes cells hypersensitive to MMS- and UV-induced DNA damage. In contrast, single mutants behaved like the wild-type strain and were able to survive through both UV radiation and MMS treatment. Therefore, it is likely that the expression of either of the two isoforms of this chaperone (constitutively expressed Hsc82 and inducible Hsp82) is sufficient for the proper functioning of repair activity.

The reduced gene-targeting efficiency of the iG170Dhsp82 mutant at a nonpermissive temperature is correlated with decreased endogenous levels of Rad51 and Rad52. MMS treatment leads to single-strand breaks and subsequently results in DSBs during the S phase. UV radiation also causes DSBs, which are not restricted to any particular cell cycle phase. Thus, recovery from exposure to UV or MMS is a good measure of DNA repair activity. However, this method does not directly evaluate the efficiency of homologous recombination. On the other hand, gene targeting relies on the homologous-recombination machinery. Thus, we determined the gene-targeting efficiencies of the wild type and the Hsp82-inactivated mutant (the iG170Dhsp82 strain) at 37°C. To this end, we constructed an ADE2 cassette with flanking regions of ADH4 that was targeted at the ADH4 locus of chromosome VII-L. We measured the frequencies of targeted integration versus random integration by scoring the loss of the flanking KANMX marker (Fig. 2A). Gene-targeting efficiency was normalized by transforming equal amounts of an uncut replicating plasmid into the strains to account for any variation in the competence of DNA uptake between the strains. We observed that the gene-targeting

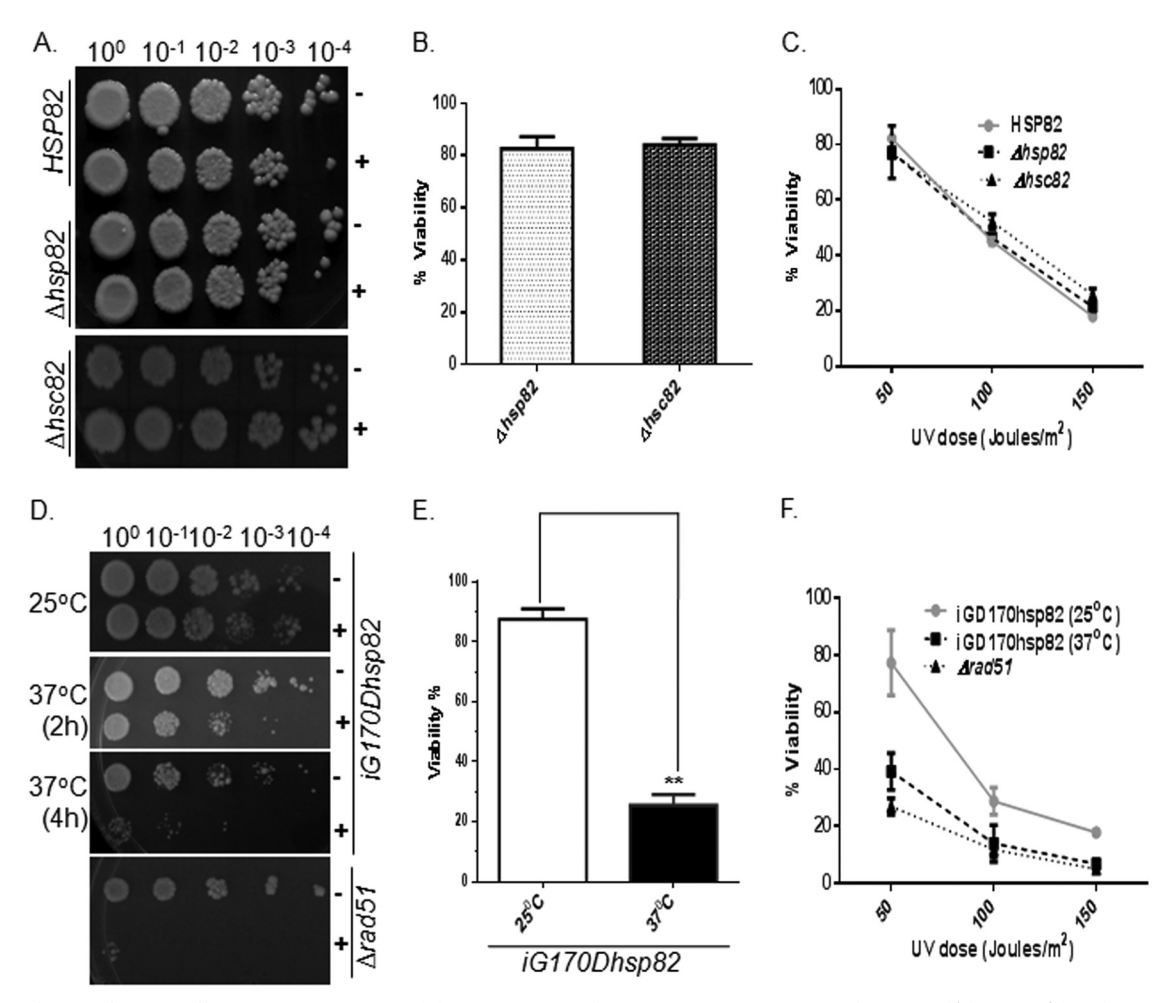


FIG 1 Loss of Hsp82 function affects DSB repair activity. (A) Return-to-growth experiments comparing single mutant ( $\Delta hsp82$  or  $\Delta hsc82$ ) strains with their isogenic wild-type (HSP82) control. For each strain, the upper row represents serial dilutions of untreated cells (-) and the lower row represents serial dilutions of cells treated with 0.03% MMS (+). (B) Percentages of survivability upon MMS treatment were plotted as the plating efficiencies of MMS-treated cells relative to that of untreated cells. Each treatment was repeated three times, and the mean value ( $\pm$ SD) was plotted. (C) Wild-type (HSP82),  $\Delta hsp82$ , and  $\Delta hsc82$  cells were irradiated with increasing doses of UV radiation. Percentages of viability were plotted as the plating efficiencies of irradiated cells relative to that of control cells. Mean values ( $\pm$ SD) from three independent experiments were plotted. (D) The iG170Dhsp82 strain ( $\Delta hsp82$   $\Delta hsc82$ ) at a permissive (25°C) or a restrictive (37°C) temperature (duration, 2 h or 4 h) was treated with 0.03% MMS, and return-to-growth analysis was performed. A  $\Delta rad51$  strain served as a negative control. (E) Percentages of survivability upon MMS treatment were plotted for the iG170Dhsp82 strain grown at 25°C or 37°C for 4 h. P values were calculated as 0.0032 using the two-tailed Student t test. (F) iG170Dhsp82 cells were grown at 25°C or 37°C for 4 h and were then exposed to increasing doses of UV radiation. Percentages of viability were calculated as described above. The experiment was repeated three times, and mean values ( $\pm$ SD) were plotted.

efficiency of the iG170Dhsp82 temperature-sensitive mutant was drastically lower at the nonpermissive temperature (37°C) than at the permissive temperature (25°C) (Fig. 2B). In order to rule out the possibility that the reduction did not result from exposure to a high temperature per se, we measured the gene-targeting efficiency of the isogenic wild-type strain after preincubation at 37°C for 4 h. Our results showed that the high temperature (37°C) did not cause any significant reduction in gene-targeting efficiency (Fig. 2B). We sought to determine the steady-state levels of two key HR proteins, namely, Rad51p and Rad52p, in order to explore the reason behind the dramatic loss of gene-targeting efficiency in the mutant cells at the nonpermissive temperature. Figure 2C shows slight decreases in the levels of Rad51p and Rad52p upon incubation at 37°C for 4 h. On the other hand, drastic reductions in both Rad51p and Rad52p levels were observed upon overnight incubation at 37°C. However, the amounts of Rad51p and Rad52p

were not reduced for the wild-type strain after 4 h of incubation at 37°C (Fig. 2C, lanes 4 and 5). Quantification of Rad51p and Rad52p levels after normalization with actin showed that there was about a 20% decrease in the Rad52p level after a 4-h incubation and that Rad52p was hardly visible after overnight incubation. Similarly, the level of Rad51p was also diminished by at least 80% after overnight incubation (Fig. 2D). In order to investigate whether the reductions in endogenous levels of Rad51p and Rad52p were occurring as part of a large transcriptional shift, we measured the transcript levels of RAD51 and RAD52 in the iG170Dhsp82 strain at both the permissive (25°C) and restrictive (overnight incubation at 37°C) temperatures. Our real-time RT-PCR data showed no significant change in the relative mRNA levels of the RAD51 or RAD52 transcript under those conditions (Fig. 2E). Thus, our work reveals that Hsp82 is involved in the maturation and stability of Rad52p and Rad51p.

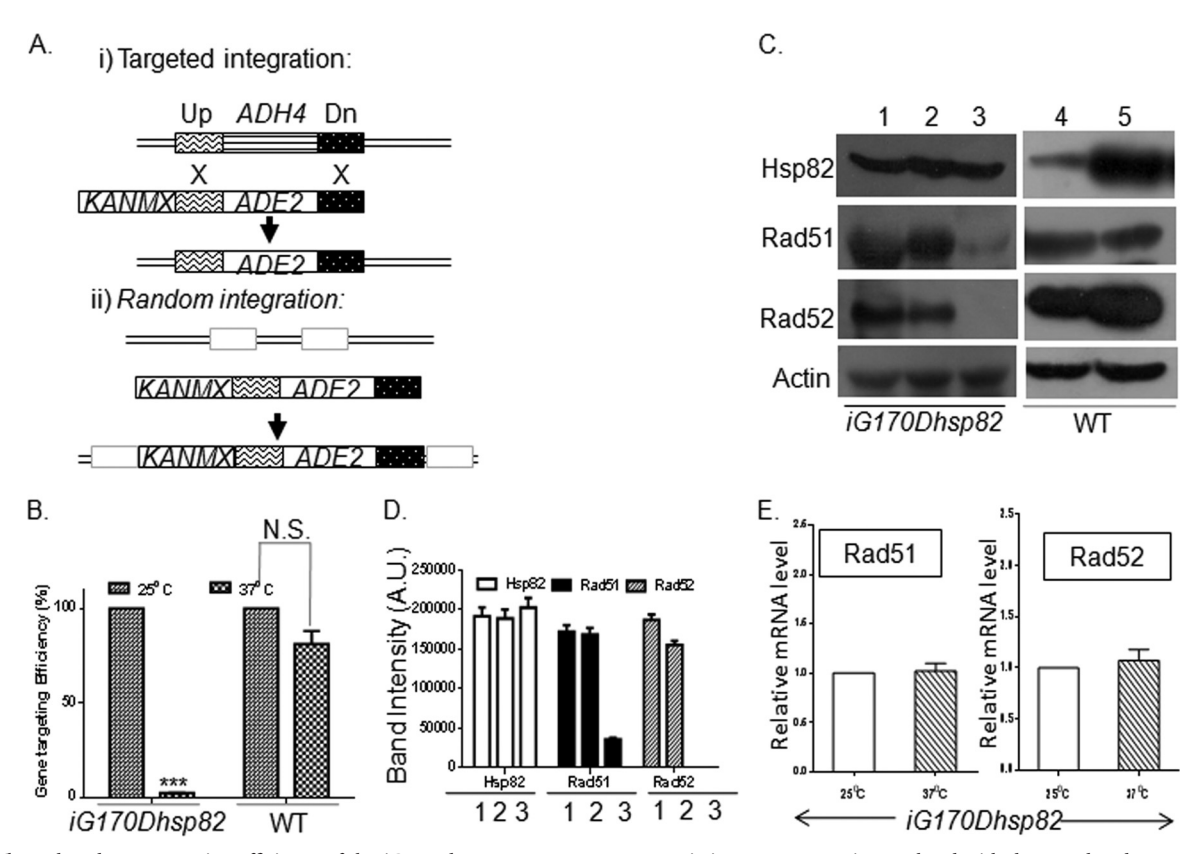


FIG 2 The reduced gene-targeting efficiency of the *iG170Dhsp82* mutant at a nonpermissive temperature is correlated with decreased endogenous levels of Rad51p and Rad52p. (A) Schematic representation of a gene-targeting cassette containing homologous stretches upstream (Up) and downstream (Dn) of *ADH4*, sequences flanking the *ADE2* gene, and a *KANMX6* selectable marker. Targeted insertion results in Ade<sup>+</sup> G418<sup>S</sup> colonies, whereas random integration produces Ade<sup>+</sup> G418<sup>R</sup> colonies. (B) Plots showing the percentage of gene-targeting efficiency, measured as the number of Ade<sup>+</sup> G418<sup>S</sup> colonies relative to the total number of Ade<sup>+</sup> colonies for the *iG170Dhsp82* strain at 25°C and 37°C. As a control, the gene-targeting efficiency of the isogenic wild-type (WT) strain was measured at 25°C and 37°C. Gene-targeting efficiency was normalized by transforming an equal amount of an uncut replicating plasmid into the strain grown at 25°C and 37°C to nullify the difference in competence for DNA uptake between strains. (C) Western blots showing the steady-state levels of Hsp82p, Rad51p, and Rad52p in *iG170Dhsp82* cells incubated at a permissive temperature (25°C) (lane 1) or a nonpermissive temperature (37°C) (lane 2) for 4 h or at the nonpermissive temperature overnight (lane 3). The levels of those proteins in isogenic WT cells are shown after growth at 25°C (lane 4) and after incubation at 37°C (lane 5) for 4 h. Actin serves as a loading control. The experiment was repeated three times, and one of the representative blots is presented. (D) Quantification of the Western blotting results showed a 4-fold reduction in the steady-state level of Rad51p and complete removal of Rad52p after growth of the *hsp82* temperature-sensitive mutant at the restrictive temperature overnight. Bars 1, 2, and 3 correspond to lanes 1, 2, and 3 of panel C. The data were normalized to the values for the loading control, actin. Each bar represents the mean density ± SD. (E) Real-time RT-PCR results showing the relative abundances of the

Rad51 is a client of Hsp82. To date, there has been no report that establishes Rad51 as a client of Hsp82. One of the primary requisites for clientage is a physical interaction between Hsp82 and its client (39). A genomewide chemical genetic screen had identified Rad51 as a putative interactive partner of Hsp82 (28). However, a physical interaction between Rad51 and Hsp82 had never been established. We performed a coimmunoprecipitation experiment that showed strong association between Rad51p and Hsp82 (Fig. 3A). The fraction that was immunoprecipitated using an irrelevant antibody IgG did not cross-react with the anti-Rad51 antibody (Fig. 3A). Additionally, the anti-Hsp82 antibody did not cross-react with Rad51 on a Western blot (data not shown), suggesting that such an interaction is specific in nature. Also, the control strain lacking rad51 showed no detectable background, although Hsp82 was immunoprecipitated from the cellular extract. It had been demonstrated earlier that degradation of Hsp90 clients upon treatment with 17-AAG is mediated via proteasomal pathway (40, 41). We were interested in exploring whether

Rad51p proceeded through proteasome-mediated degradation under conditions of *hsp82* inhibition. For that purpose, we treated a wild-type strain with 40 µM 17-AAG, which functionally inactivates *HSP82*. We used a  $\Delta pdr5$  strain, since deletion of the *PDR5* gene, which codes for a membrane-associated drug export pump, ensures the optimal entry of drugs (42). A fraction of that culture was supplemented with 50 µM MG132 (a proteasome inhibitor) along with 17-AAG. Total protein was isolated from those strains and was probed with an anti-Rad51 antibody. Western blot analysis showed that treatment with 17-AAG led to a considerable reduction in the Rad51p level, while MG132 treatment resulted in the restoration of Rad51p abundance, indicating the inhibition of proteasomal degradation of Rad51p (Fig. 3B and C). This experiment demonstrates that under conditions of hsp82 inhibition, Rad51p is processed via proteasomal degradation, supporting the conclusion that Rad51p is a direct client of Hsp82.

Mutational analysis of Hsp82 in DSB repair. Six *HSP82* point mutants with mutations (T22I, A41V, G81S, T101I, G313S, and

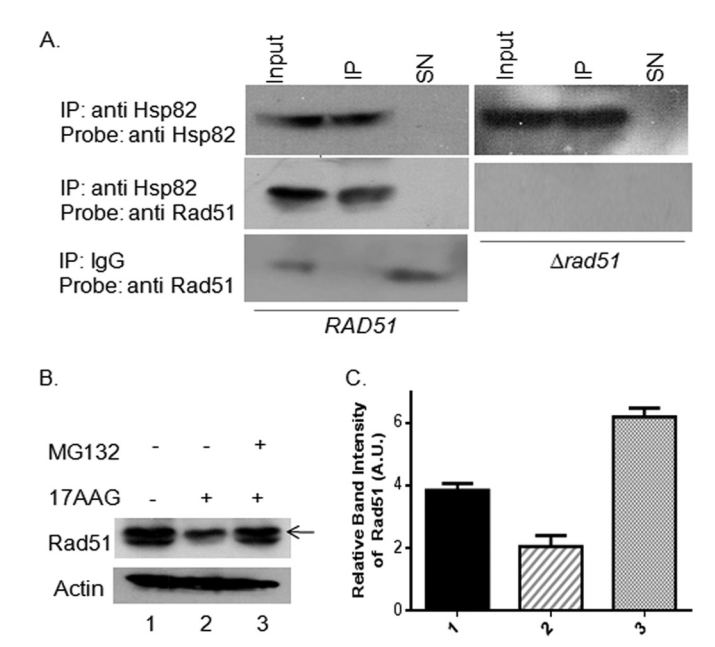


FIG 3 Rad51p is a client of Hsp82. (A) Western blot showing coimmunoprecipitation of Hsp82p and Rad51p from whole-cell extracts of a wild-type strain (RAD51) and a strain lacking Rad51p ( $\Delta rad51$ ). Immunoprecipitation (IP) was performed using an anti-Hsp82 antibody or an irrelevant antibody (IgG). An anti Rad51 antibody was used for Western blotting. Input, whole-cell extract; SN, supernatant; IP, pellet. (B) Western blot showing Rad51p levels in wild-type cells (lane 1), in cells treated with 40  $\mu$ M 17-AAG for 16 h (lane 2), and in cells treated with 40  $\mu$ M 17-AAG and 50  $\mu$ M MG132 for 16 h (lane 3). Actin is shown as a loading control. (C) Relative intensities of Rad51p bands in the Western blot. Bar numbers correspond to lane numbers in panel B.

iA587T) spanning its three domains, as well as the charged linker deletion mutant HH1a-p2HG/Hsp82(Δ211-259), were monitored for DSB repair activity (Fig. 4A). The charged linker region connects the N-terminal domain with the middle domain. It was previously demonstrated that removal of the charged linker had a distinct effect on glucocorticoid receptor activity and vSrc kinase phosphorylation (20). However, neither of these two clients is naturally present in Saccharomyces cerevisiae. This particular region of Hsp82 is evolutionarily conserved in all eukaryotes. However, its importance in yeast biology has remained elusive. To determine whether the missense mutants mentioned above as well as deletion mutants were able to recover efficiently from MMS treatment, they were all treated with 0.03% MMS and were subsequently spotted onto YPD plates at increasing dilutions, along with their isogenic control (Fig. 4B). We observed that five mutants, namely, the A41V, G81S, T101I, G313S, and  $hsp82(\Delta 211$ -259) mutants, were hypersensitive to MMS treatment, since they displayed 2-log-unit differences in their growth. In order to obtain more-quantitative comparisons between these strains, we also determined the percentage of viability of each mutant (Fig. 4C and D). Our results showed an 88% reduction in cell viability in the charged linker deletion mutant HH1a-p2HG/Hsp82(Δ211-259) relative to the strain carrying the wild-type *HSP82* allele (Fig. 4D). Three ATPase domain point mutants, the A41V, G81S, and T101I mutants, showed dramatic reductions in cell viability upon MMS treatment, indicating the importance of the ATPase domain in DNA repair. The G313S middle-domain mutant also displayed about a 50% reduction in survivability upon MMS treatment,

whereas the iA587T allele showed no sensitivity at all. The T22I mutant showed only a 10% decrease in survivability from that of the wild type (P82a). In another assay, all mutants were exposed to increasing doses of UV radiation, following which the percentage of survivability was analyzed. It was observed that the iA587T and T22I point mutants were marginally different in UV survivability from the control strain, P82a, while the G313S mutant was hypersensitive (Fig. 4E). On the other hand, the A41V, G81S, and T101I point mutants were significantly sensitive to UV treatment, reinforcing the importance of the ATPase domain in repairing UVmediated DNA damage. Also, the ability of the charged linker deletion mutant HH1a-p2HG/Hsp8 (Δ211-259) to survive after UV-induced damage was significantly different from that of its isogenic control (Fig. 4F). Thus, these results suggested that the charged linker region and residues A41, G81, T101, and G313 of Hsp82 are important for cell survival upon MMS- and UV-induced DNA damage.

Gene-targeting efficiencies of hsp82 point mutants and **charged linker deletion mutant.** We scored the gene-targeting efficiencies of all mutants to compare their homologous-recombination efficiencies. Gene-targeting efficiencies were found to be affected to various degrees by the mutations (Fig. 5A and B). Based on their DNA damage sensitivities and gene-targeting efficiencies, we categorized the mutants into three groups (Table 2). Group A consisted of the iA587T mutant, which had little effect on genetargeting efficiency (75% of activity retained). This correlates well with the previous result showing a negligible effect on MMS and UV survivability (Fig. 4). Group B included the A41V, T22I, G81S, and G313S mutants, which showed moderate effects on gene targeting (about a 66% reduction). Group C comprised mutants that were severely defective in gene targeting. In our study, the T101I mutant, the charged linker deletion mutant, and the Hsp82 temperature-sensitive mutant at the nonpermissive temperature fall into this category. Thus, mutational analysis revealed the specific regions of Hsp82 that were vital for the proper functioning of HR-mediated gene targeting. In order to understand the mechanism underlying the loss of HR function in these mutants, we determined the endogenous levels of Rad51p and Rad52p in the HR-dead T101I and  $hsp82(\Delta 211-259)$  mutants. To this end, for the detection of Rad52p, we attempted to tag the C-terminal end of RAD52 in these strains. Since the charged linker mutant is defective in gene targeting, we swapped the  $hsp82(\Delta 211-259)$  plasmid in the hsp82 T101I point mutant (which was RAD52-MYC tagged at the chromosomal locus) to create the RAD52-MYCtagged  $hsp82(\Delta 211-259)$  strain SLY65. Western blot analysis showed that the levels of Rad51p and Rad52p were significantly reduced in the T101I mutant, indicating the importance of the ATPase domain in the maturation of Rad51p and Rad52p (Fig. 5C). This conclusion was further supported by real-time RT-PCR analysis, which showed no change in the steady-state levels of RAD51 and RAD52 transcripts in the T101I mutant background (Fig. 5D). Additionally, we found that the levels of Rad51p and Rad52p were unaltered in the  $hsp82(\Delta 211-259)$  mutant (Fig. 5E and F). Quantification of band intensities showed a 4-fold reduction in the Rad51p level and a 2-fold reduction in the Rad52p level in the T101I mutant, whereas the levels of these proteins in the  $hsp82(\Delta 211-259)$  mutant remained unaltered (Fig. 5F). Taken together, the loss of gene-targeting efficiency in the ATPase-dead mutant can be correlated with the lower endogenous levels of Rad51p and Rad52p. On the other hand, the apparent lack of

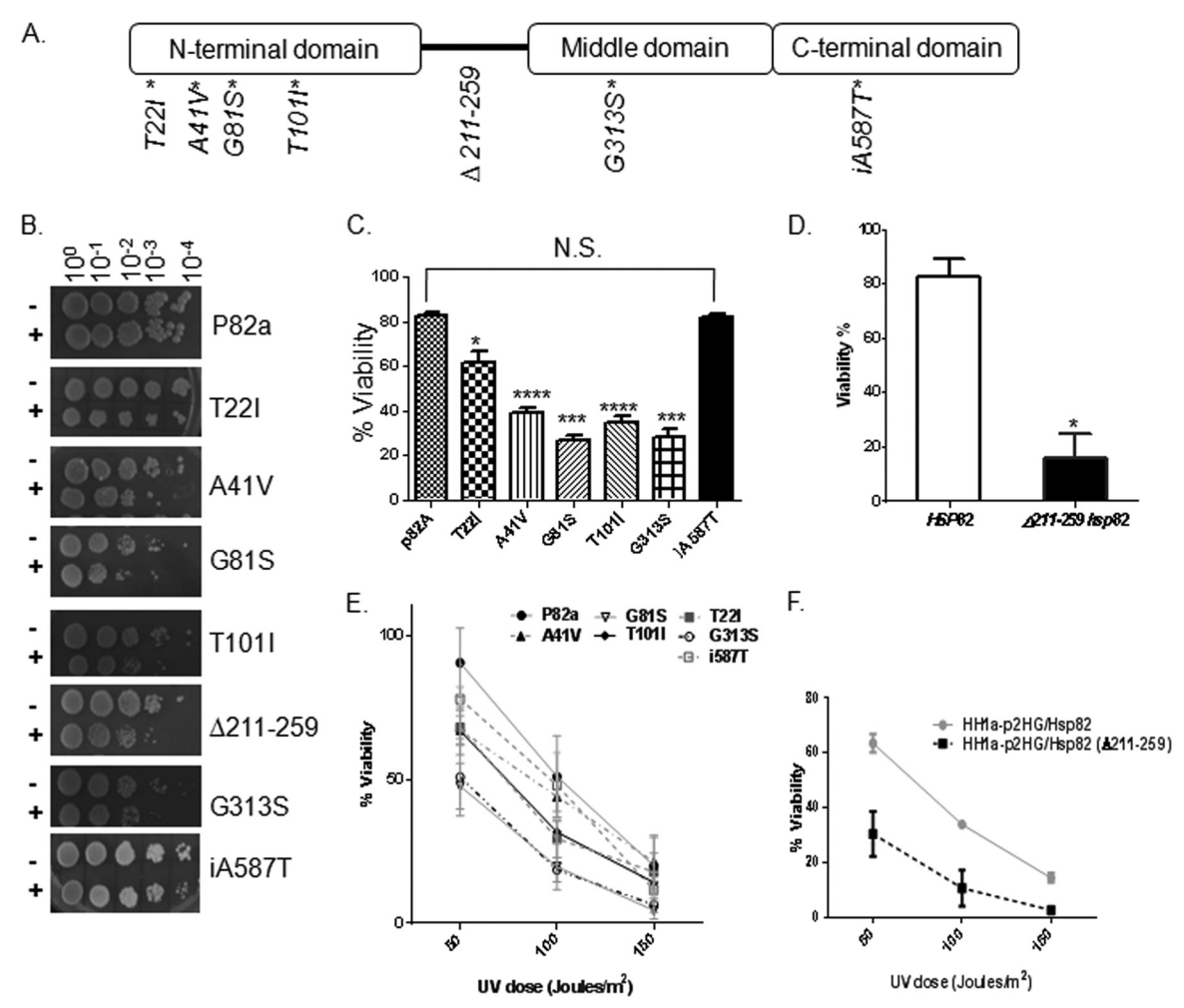


FIG 4 Mutational analysis of Hsp82 in DSB repair. (A) Schematic diagram of HSP82 gene structure showing the alterations in all the mutants used in this study. An asterisk indicates a point mutation, and a capital delta indicates a deletion mutation. (B) Return-to-growth analysis of the wild-type strain (P82a) along with seven different hsp82 mutant strains (identified on the right). In each panel, the upper row represents serial dilutions (indicated above the panels) of untreated cells (-) and the lower row represents serial dilutions of cells treated with 0.03% MMS (+). (C) The percentage of survivability with MMS is plotted for six hsp82 mutant strains (labeled on the x axis) and their isogenic wild-type control, P82a. The averages of results of four independent experiments  $\pm$  SD are plotted. \*\*\*\*, P < 0.001; \*\*\*, P < 0.001; \*\*, P < 0.001; \*\*, P < 0.005; N.S., not significant. (D) Percentage of survivability with MMS for the  $hsp82(\Delta 211-253)$  strain and its isogenic wild-type control. Error bars indicate SD; n = 3. (E) Percentages of viability of six hsp82 point mutant strains and their isogenic wild-type control, P82a, after exposure to increasing doses of UV radiation. The experiment was repeated three times, and mean values ( $\pm$ SD) are plotted. (F) Percentages of viability of wild-type (HH1a-p2HG/Hsp82) and charged linker deletion mutant [HH1a-p2HG/Hsp82( $\Delta 211-259$ )] strains after exposure to increasing doses of UV radiation. The experiment was repeated three times, and mean values ( $\pm$ SD) are plotted.

correlation between HR function and the abundance of recombinase proteins in the charged linker deletion mutant implies a complex interplay between the chaperone and these clients.

MMS-induced upregulation of Rad51p and Rad52p in the hsp82(Δ211-259) mutant. To understand the mechanism behind the drastic reduction in HR efficiency in the charged linker deletion mutant, we studied the MMS-induced upregulation of Rad51p and Rad52p. Wild-type and mutant strain were grown to an OD of 0.6 and were then separated into two groups, one of which was grown in the presence of MMS while the other was grown in its absence, and the Rad51p and Rad52p levels were estimated. Western blotting showed that the induction of Rad51p and Rad52p in the mutant strain was similar to that observed in the wild-type strain (Fig. 6A). Quantification of Rad51p from three independent harvests of cells showed a ~4-fold induction of Rad51p in the wild type and a ~2-fold induction in the charged

linker deletion mutant (Fig. 6B). We wanted to establish further that there is no difference in the transcriptional upregulation of RAD51 and RAD52 in the mutant upon MMS treatment. For that purpose, we isolated the total RNAs of the wild-type and mutant strains that had been left untreated or treated with MMS, and we measured the relative abundances of the RAD51 and RAD52 transcripts. Semiquantitative RT-PCR showed upregulation of RAD51 and RAD52 upon MMS treatment in both strains (Fig. 6C). Real-time RT-PCR quantification showed almost equal induction (4.7-fold) of RAD51 and RAD52 transcripts (2-fold) in MMS-treated and untreated samples in the wild type as well as in the  $hsp82(\Delta 211-259)$  mutant (Fig. 6D and E). Thus, our results revealed that the MMS-induced transcriptional upregulation of RAD51 and RAD52 was unaltered in the charged linker deletion mutant.

The extent of MMS-induced Rad51 focus formation is less in  $hsp82(\Delta 211-259)$  cells than in the wild-type control. Since MMS-

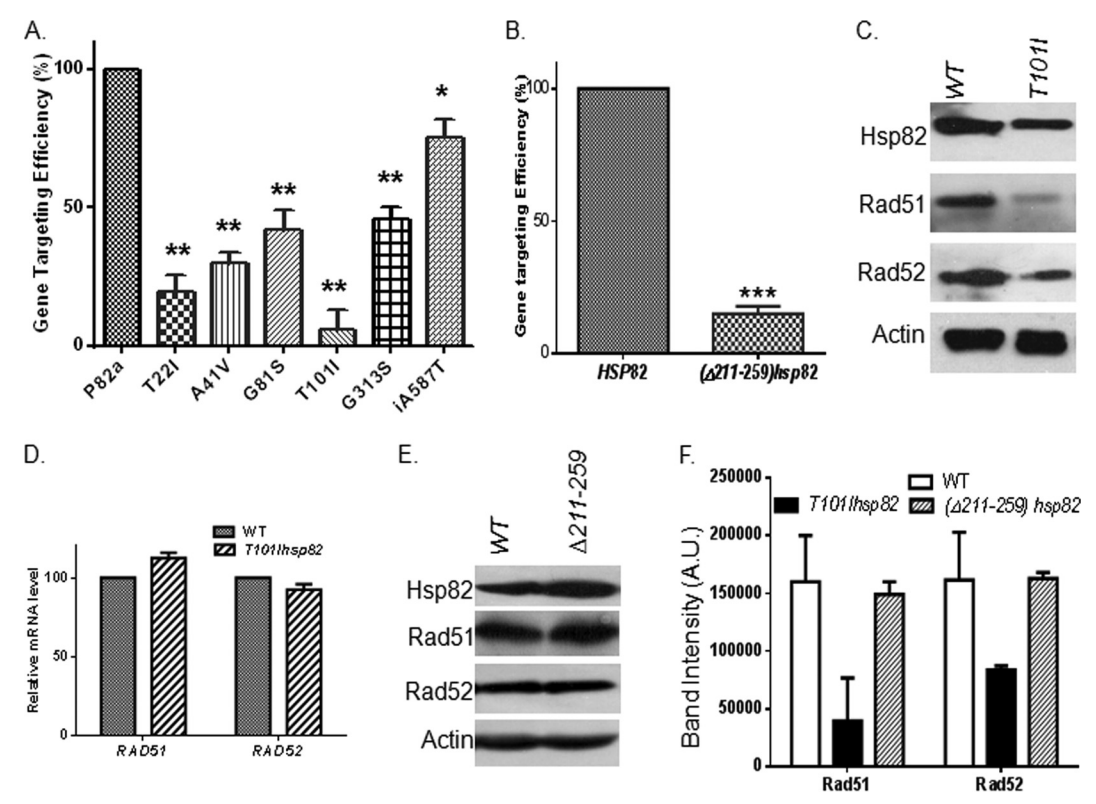


FIG 5 Gene-targeting efficiencies of hsp82 point mutants and charged linker deletion mutant. (A) Percentages of gene-targeting efficiency of six hsp82 point mutants and their wild-type control. The gene-targeting efficiency of the hsp82 T101I mutant is about 16-fold lower than that of the wild type strain P82a (HSP82). Error bars indicate SD; n=3. P values were calculated using the two-tailed Student t test (\*\*, P < 0.01; \*, P < 0.05). (B) Gene-targeting efficiency of the  $hsp82(\Delta 211-259)$  strain compared to that of its isogenic wild-type control. Error bars indicate SD; n=3. P values were calculated as 0.0010 (\*\*\*) using the two-tailed Student t test. (C) Western blots showing reductions in endogenous levels of Rad51p and Rad52p in the hsp82 T101I mutant. Actin acts as the loading control. WT, wild type (HSP82). (D) Real-time RT-PCR shows the relative mRNA levels of RAD51 and RAD52 in the hsp82 T101I mutant and its isogenic WT control. (E) Immunoblot showing no difference in the endogenous levels of Rad51p and Rad52p between the wild-type strain (HH1a-p2HG/Hsp82) and the charged linker deletion mutant [HH1a-p2HG/Hsp82)(2211-259)]. (F) Quantification of Western blots from three independent experiments for which results are shown in panels C and E. A 4-fold reduction in Rad51p levels and a 2-fold reduction in Rad52p levels were observed for the hsp82 T101I mutant. The band intensities in each lane were normalized against that of actin, and the mean densities  $\pm$  SD are plotted.

induced Rad51p upregulation is unaffected in the  $hsp82(\Delta 211-259)$  mutant, we sought to investigate whether the downstream function of Rad51 is affected in this mutant strain. For that purpose, we used an indirect immunofluorescence assay to investigate the ability to form MMS-induced Rad51 foci. We observed very bright fluores-

TABLE 2 Effects of hsp82 mutants on DNA damage sensitivity and gene-targeting efficiency

	hsp82 allele	Sensitivity <sup>a</sup> to:		Gene-targeting
Group		MMS	UV	efficiency
A	hsp82 iA587T	+	+	Little effect
В	hsp82 T22I hsp82 A41V hsp82 G81S hsp82 G313S	++	++	Moderate effect
С	hsp82(Δ211-259) iG170Dhsp82 hsp82 T101I	+++	+++	Severe effect

 $<sup>^</sup>a$  +, slightly sensitive; ++, moderately sensitive; +++, highly sensitive.

cent foci that were enriched with Rad51p in MMS-treated cells but not in untreated cells (Fig. 7A). We counted about 1,500 nuclei in each of the three independent harvests of cells in order to calculate the percentage of nuclei that had Rad51 foci. Our results demonstrated a ~20% reduction in Rad51 focus formation in  $hsp82(\Delta 211-259)$  cells from that in wild-type cells upon DNA damage (Fig. 7B). Next, we analyzed the distribution of foci in each nucleus. After analyzing a total of 4,500 MMS-treated nuclei of wild-type and mutant cells, we observed a striking, statistically significant difference in the distribution of foci. Our analysis revealed that mutant cells possessed primarily 1 focus per nucleus, and the total number was comparable to that for wild-type cells. However, the percentage of nuclei containing more than 1 focus was drastically lower in mutant cells than in wild-type cells. Our study showed 33% fewer nuclei with 2 foci, 42% fewer nuclei with 3 foci, and 77% fewer nuclei with 4 foci in mutant cells than in wild-type cells (Fig. 7C). Thus, we came to the conclusion that in the charged linker deletion mutant, the level of Rad51 focus formation, which is a prerequisite for repairing breaks in DNA, is significantly lower than that in the wild type, leading to greater MMS sensitivity.

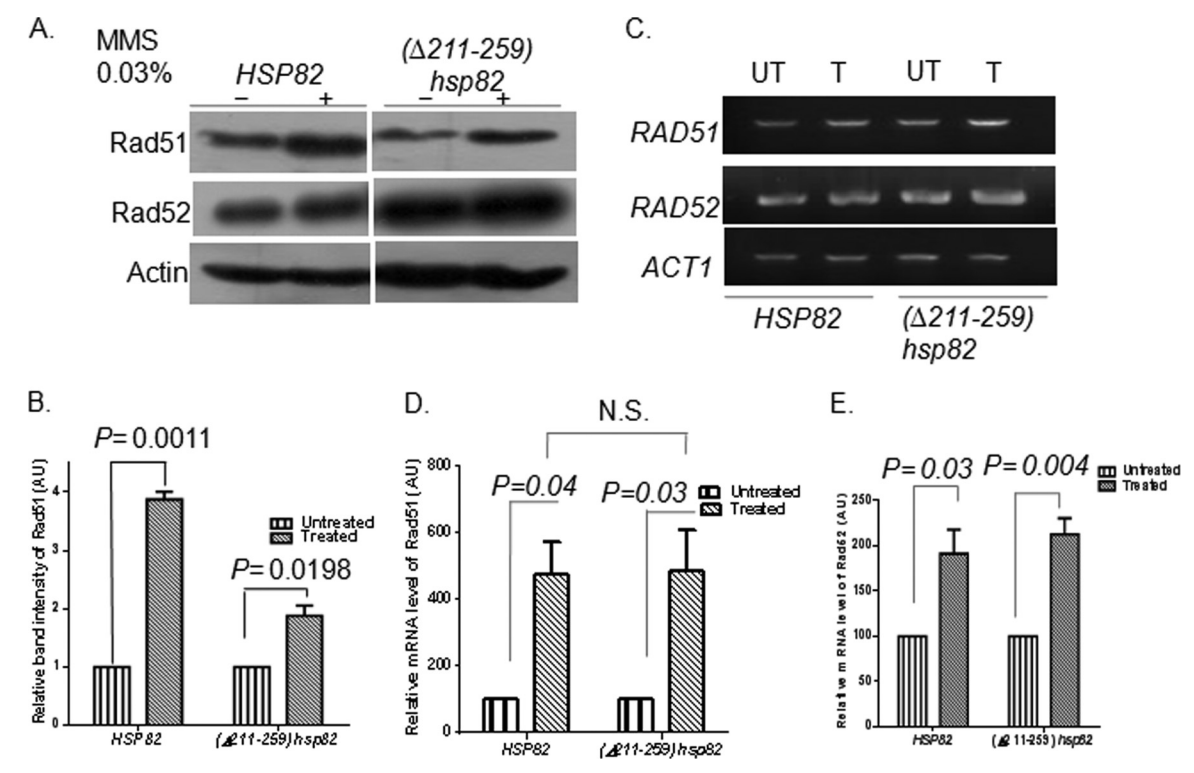


FIG 6 MMS-induced upregulation of Rad51p and Rad52p in the  $hsp82(\Delta 211-259)$  mutant. (A) Immunoblots showing Rad51p and Rad52p levels in wild-type (HSP82) and mutant [hsp82(\Delta 211-259)] strains in the presence and absence of 0.03% MMS. Actin is the loading control. (B) Quantification of Western blots from three independent experiments shows significant induction of Rad51p upon MMS treatment in both wild-type and mutant strains. The band intensity for each strain and condition was normalized against that of actin, and the mean densities  $\pm$  SD are plotted. The P values were calculated using the Student t test and are presented above the bars. (C) Semiquantitative RT-PCR shows relative levels of RAD51 and RAD52 transcripts in the mutant and the wild type upon MMS  $treatment.\ UT, untreated; T, 0.03\%\ MMS\ treated.\ ACT1\ serves\ as\ a\ control.\ (D\ and\ E)\ Real-time\ RT-PCR\ shows\ the\ quantitative\ abundances\ of\ RAD51\ (D)\ and\ Eq.\ (D)\$ RAD52 (E) transcripts upon 0.03% MMS treatment relative to those of untreated samples in both the wild-type and mutant strains.

Overexpression of Rad51 rescues MMS sensitivity and the defect in gene-targeting efficiency in the  $hsp82(\Delta 211-259)$  mutant. From Western blot analysis, it was apparent that the amount of Rad51p in the charged linker deletion mutant was similar to that in the wild type. However, the amount of active Rad51p may be limited, leading to decreased gene-targeting efficiency and increased MMS sensitivity. To establish that further, we overexpressed Rad51p in the mutant strain and investigated whether it could rescue MMS hypersensitivity and overcome the defect in gene-targeting efficiency. To this end, we transformed a 2µ expression vector harboring S. cerevisiae RAD51 into the  $hsp82(\Delta 211$ -259) and iG170Dhsp82 strains to generate strains TSY1 and SLY69, respectively. We exposed the cells to 0.03% MMS for 2 h and calculated the percentages of cell viability. We compared the viability of the strains with and without Rad51p overexpression (Fig. 8A) and observed a significant difference between the two alleles. In the iG170Dhsp82 strain grown at 37°C, overexpression of Rad51p could not rescue MMS sensitivity, as evidenced by the fact that the temperature-sensitive mutant at the restrictive temperature was unable to chaperone Rad51p folding. However, in the  $hsp82(\Delta 211-259)$  strain, overexpression of Rad51p can partially rescue MMS sensitivity. Our results showed that the percentage of cell viability increased 5-fold with Rad51p overexpression, but it was still 20% less than that of the wild type. In another assay, we studied the gene-targeting efficiency of mutant cells carrying pRAD51 and compared it with that of mutant cells carrying an

empty vector. We observed that Rad51p overexpression resulted in ~2.3-fold increased gene-targeting efficiency in the  $hsp82(\Delta 211-259)$  strain; however, this level of efficiency was still significantly less than that of the wild type (Fig. 8B). Western blotting confirmed the overexpression of Rad51p in these mutant strains (Fig. 8C).

## **DISCUSSION**

Our paper presents detailed work that helps in understanding whether the Hsp90 chaperone is responsible for the proper functioning of the DSB repair pathway in lower eukaryotes. Since these are unicellular organisms, failure to repair damaged DNA is lethal for them. Using various mutants with alterations throughout different domains of Hsp82, we have demonstrated that Hsp82 function is indispensable for the proper functioning of homologous-recombination-mediated DNA repair and have identified important residues as well as domains of Hsp82 that are absolutely critical for the proper functioning of the HR pathway.

Although previous studies have suggested a possible link between Hsp90 and DSB repair, the involvement of Hsp90 in HR has remained inconclusive due to conflicting findings. First, for tumor cells, it has been reported that Brca2p and Rad51p are destabilized upon prolonged incubation with the Hsp90 inhibitor 17-AAG. However, in normal cells, Hsp90 inhibitors do not affect survivability under DNA-damaging conditions (32). Thus, it is not clear whether the phenotype observed in tumor cell lines is a direct or

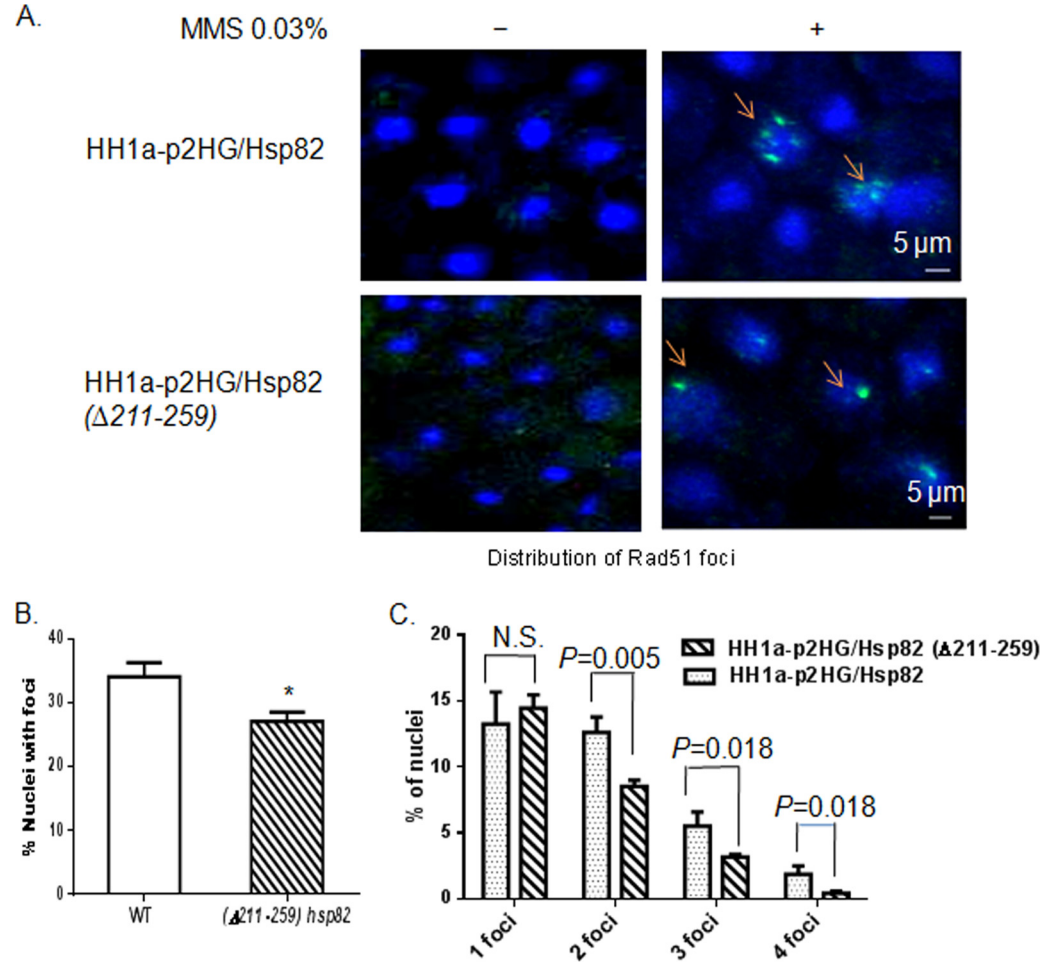


FIG 7 The extent of MMS-induced Rad51 focus formation is less in  $hsp82(\Delta 211-259)$  cells than in the wild-type control. (A) Wild-type (HH1a-p2HG/Hsp82) and mutant [HH1a-p2HG/Hsp82( $\Delta 211-259$ )] cells were treated with 0.03% MMS, and an indirect immunofluorescence assay was performed with anti-Rad51 to locate Rad51 foci. Nuclei were stained with DAPI. The arrows indicate Rad51 foci. The experiment was repeated three times, and representative data from one replicate are presented. (B) About 1,500 nuclei in each case were analyzed for the presence of Rad51 foci, and the percentages of nuclei with Rad51 foci were calculated for mutant and wild-type cells. The experiment was performed with three independent harvests of cells. The P value was calculated as 0.0103 using the two-tailed Student t test. (C) ImageJ software was used to analyze the image of each nucleus and to count the number of foci in it. A total of 4,500 wild-type and 4,500 mutant nuclei with 1, 2, 3, and 4 foci were counted, and the percentages of nuclei having 1, 2, 3, and 4 Rad51 foci were plotted for wild-type and mutant cells. An unpaired t test was performed using GraphPad Prism software, version 6. P values are indicated.

an indirect effect of Hsp90. Second, although a high-throughput in vitro study (with tandem affinity purification tagging) revealed an interaction between the Hsc82 N-terminal domain and Rad52p (27), no direct interaction of Rad51p with Hsp82 has been reported. Thus, it has remained ambiguous whether Rad51p is a physiological client of Hsp90. We report here, for the first time, evidence of physical interaction between Rad51p and Hsp82p. Our work establishes that under conditions of Hsp82 inhibition, Rad51p levels are drastically reduced in cells via proteasomal degradation. Also, in the iG170Dhsp82 strain (upon prolonged incubation at a restrictive temperature), the steady-state levels of both Rad51p and Rad52p proteins decrease dramatically, with substantial loss in gene-targeting efficiency. However, there is no change in the transcript levels of RAD51 and RAD52 in the iG170Dhsp82 strain. Taken together, these findings establish Rad51p as a client of Hsp82.

We performed detailed mutational analyses of several isogenic mutants of *hsp82* to monitor survivability upon MMS treatment

as a readout of repair activity. Our observations are that the Hsp82 temperature-sensitive mutant is hypersensitive to DNA damage at a nonpermissive temperature, while there is no significant reduction in cell survivability in either of the single knockout cells (the  $\Delta hsp82$  or  $\Delta hsc82$  mutant), implying that at least one copy of this chaperone is needed for survival under conditions of DNA damage. Our study reveals that most of the N-terminal domain mutants display severe defects in repairing MMS- and UV-induced DNA damage, suggesting the importance of the ATP hydrolysis function of Hsp82. The differential effects of many mutations across the three domains of Hsp82 suggest that in addition to the ATPase function, other functional domains of Hsp82 also contribute to the maturation/stability of DNA repair proteins. This claim is corroborated by the fact that the Hsp90-inactivated mutant (the iG170Dhsp82 strain at 37°C) shows a more dramatic phenotype than any of the point mutants. Since MMS sensitivity cannot be directly correlated with HR efficiency, we have measured the gene-targeting efficiencies of all the mutants. The results

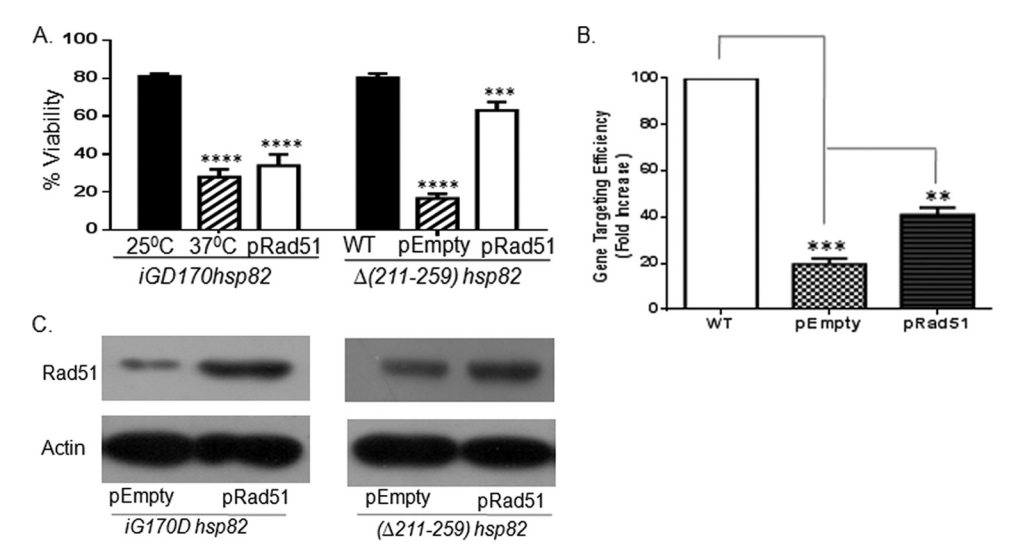


FIG 8 Overexpression of Rad51 partially rescues the MMS sensitivity and gene-targeting efficiency of the  $hsp82(\Delta 211-259)$  mutant. (A) The difference in the survivability of the iG170Dhsp82 strain treated with 0.03% MMS between 25°C and 37°C remained unaltered with Rad51p overexpression. However, the percentage of survivability of the  $hsp82(\Delta 211-259)$  mutant treated with MMS was partially rescued in the presence of Rad51p overexpression. Graphs show mean densities  $\pm$  SD from five independent experiments. \*\*\*\*, P < 0.0001; \*\*\*, P < 0.001. (B) The Rad51 overexpression plasmid and an empty expression vector were transformed individually into  $hsp82(\Delta 211-259)$  mutant cells. Gene-targeting efficiency was normalized by transforming equal amounts of an uncut replicating plasmid into both strains to nullify the difference in competence for DNA uptake between strains. Each bar represents the mean ( $\pm$ SD) for three independent experiments. Asterisks indicate values significantly different from that for the control (\*\*\*\*, P < 0.0001; \*\*\*, P < 0.001). (C) Immunoblot showing overexpression of Rad51p in the iG170Dhsp82 and  $hsp82(\Delta 211-259)$  strains. Actin serves as a loading control.

from the gene-targeting assay correspond well with the results from the DNA repair assay. Strikingly, three mutants exhibit severe reductions in HR-mediated gene targeting. One of them is the temperature-sensitive iG170Dhsp82 mutant, which was earlier reported to be nonfunctional at a restrictive temperature (35). The other two are the T101I and p2HG/Hsp82( $\Delta$ 211-259) mutants. Previous work revealed that the hsp82 T101I mutation causes a ≤90% reduction in ATPase activity, whereas the iA587T mutant possesses wild-type-like ATPase activity (43). Our work implies that the T101I point mutation may affect the structural stability of Rad51p and Rad52p relative to that for the wild type and that this defect in stability is correlated with a lessening of HR efficiency. Thus, it is tempting to suggest that the ATP hydrolysis activity of Hsp82 is essential for Rad51p stability. On the other hand, the iA587T mutant, which possesses wild-type-like ATPase activity and AMP-PNP (adenylylimidodiphosphate) binding (43), exhibits wild-type-like sensitivity to MMS and has a marginal effect on gene-targeting efficiency. The other ATPase domain mutants, such as the A41V, T22I, and G81S mutants, also show moderate effects on gene-targeting efficiency. It was demonstrated previously that though the T22I mutant possesses 6 times more ATPase activity than the wild-type, its affinity for AMP-PNP is less than that of the wild type. On the other hand, the A41V point mutant, with a mutation located at the rear end of the nucleotide binding pocket, also shows reduced affinity for AMP-PNP, which accounts for its moderate phenotype in HR efficiency.

The  $hsp82(\Delta 211-259)$  charged linker mutant presents an interesting scenario. It is the only mutant that shows a  $\sim$ 8-fold reduction in cell survivability upon MMS treatment as well as a >80% reduction in gene-targeting efficiency even though the levels of Rad51p and Rad52p remain unchanged. This mutant is so severely defective in HR function that it remains refractory to gene tagging and gene knockout despite several attempts. Previously, it was

reported that the  $hsp82(\Delta 211-259)$  mutant did not affect nucleotide binding to the N-terminal domain of Hsp90 and that its ATPase activity was also slightly higher (0.6 min<sup>-1</sup>) than that of the wild type  $(0.5 \,\mathrm{min}^{-1})$  (20). Our work indicates that though the structural stabilities of Rad51p and Rad52p in this mutant probably remain unaltered, Rad51p-mediated gene-targeting activity is drastically reduced. To account for this discrepancy, we propose that the ATPase activity of Hsp82p is necessary but not sufficient for the maturation of active Rad51p. Our hypothesis is supported by the significant reduction in the number of nuclei with multiple Rad51 foci, which accounts for the enormous reduction in cell viability. Thus, it is likely that in the absence of the charged linker region, only a fraction of the total Rad51p is active. We propose that a dynamic equilibrium might exist between the active and inactive forms of Rad51p in the cell. In the charged linker deletion mutant, the equilibrium is probably shifted toward the inactive state of Rad51p. Based on this hypothesis, one may predict that if the amount of Rad51p were increased artificially, the abundance of active Rad51p would increase, and this might rescue the phenotype. Our work showing a partial rescue of MMS sensitivity and gene-targeting efficiency supports this hypothesis.

Earlier work also showed that the charged linker deletion mutant possessed diminished chaperone function toward Hsp90 clients such as glucocorticoid receptor (GR) and vSrc, although their structural stability was unaltered (20). However, none of the clients documented above are required for *S. cerevisiae* biology. Although the charged linker region (amino acids 211 to 259) is evolutionarily conserved, the significance of such sequence conservation was not known. Previously, this region was reported to be dispensable for steroid hormone receptor regulation and the pheromone signaling pathway (19). Our work, for the first time, assigns a functional role in DSB repair to this charged linker region. Unlike steroid hormone signaling or pheromone signaling,

which is restricted to certain organisms, DSB repair pathways are conserved in all organisms. Thus, our finding that this evolutionarily conserved region of Hsp90 has an important role in a highly conserved cellular process such as DSB repair makes perfect sense.

Although yeast Hsp82 and its mammalian counterpart Hsp90 are widely viewed as cytoplasmic chaperones, more and more nuclear functions of Hsp82 have emerged in recent years. Its pivotal role in telomere capping and maintenance has been established (44). Recently, work on Sir2 protein dynamics as a function of Hsp82 activity has recognized a link between Hsp82 and telomere silencing (38). Two recent studies on Sba1 and Aha1, two important cochaperones of Hsp82, have unraveled an interesting connection with DNA repair proteins. In the first study, a highthroughput synthetic gene array (SGA) and network analysis revealed 11 DNA repair proteins (including Rad50) as putative clients of Sba1 (the yeast ortholog of p23). Overexpression of Sba1 has also been shown to enhance DNA repair activity (45). In another study, two major NHEJ proteins, Ku80 and DNA-PK<sub>c</sub>, have been found to be associated with human Aha1 (46). Our current work, along the same line, establishes a compelling link between the Hsp82 chaperone and HR-mediated DNA repair. Thus, uncovering such a nuclear clientele of Hsp82 establishes new and distinct functions of the multifaceted chaperone Hsp82.

#### **ACKNOWLEDGMENTS**

We are indebted to Didier Picard (University of Geneva) and Susan Lindquist (MIT) for the DP533 and *hsp82* mutant strains. We thank Meenu Babu and Meera Babu for critical reading of the manuscript.

This work is partly supported by grants from the Department of Biotechnology, Government of India (BT/PR11174/MED/29/98/2008), to M.K.B. and from the Council of Scientific and Industrial Research, Government of India [37(1549)/12/EMR-II], to S.B.

#### **REFERENCES**

- 1. Aylon Y, Kupiec M. 2004. DSB repair: the yeast paradigm. DNA Repair (Amst) 3:797–815. http://dx.doi.org/10.1016/j.dnarep.2004.04.013.
- Lin Y, Lukacsovich T, Waldman AS. 1999. Multiple pathways for repair of DNA double-strand breaks in mammalian chromosomes. Mol Cell Biol 19:8353–8360.
- 3. Niewolik D, Pannicke U, Lu H, Ma Y, Wang LC, Kulesza P, Zandi E, Lieber MR, Schwarz K. 2006. DNA-PKcs dependence of Artemis endonucleolytic activity: differences between hairpins and 5' or 3' overhangs. J Biol Chem 281:33900–33909. http://dx.doi.org/10.1074/jbc.M606023200.
- Stauffer ME, Chazin WJ. 2004. Physical interaction between replication protein A and Rad51 promotes exchange on single-stranded DNA. J Biol Chem 279:25638–25645. http://dx.doi.org/10.1074/jbc.M400029200.
- Baumann P, West SC. 1998. Role of the human RAD51 protein in homologous recombination and double-stranded-break repair. Trends Biochem Sci 23:247–251. http://dx.doi.org/10.1016/S0968-0004(98)01232-8.
- Liefshitz B, Kupiec M. 2011. Roles of RSC, Rad59, and cohesin in doublestrand break repair. Mol Cell Biol 31:3921–3923. http://dx.doi.org/10 .1128/MCB.05974-11.
- Picard D. 2006. Chaperoning steroid hormone action. Trends Endocrinol Metab 17:229–235. http://dx.doi.org/10.1016/j.tem.2006.06.003.
- Buchner J. 1999. Hsp90 & Co.—a holding for folding. Trends Biochem Sci 24:136–141. http://dx.doi.org/10.1016/S0968-0004(99)01373-0.
- 9. Young JC, Moarefi I, Hartl FU. 2001. Hsp90: a specialized but essential protein-folding tool. J Cell Biol 154:267–273. http://dx.doi.org/10.1083/icb.200104079.
- DeZwaan DC, Freeman BC. 2010. HSP90 manages the ends. Trends Biochem Sci 35:384–391. http://dx.doi.org/10.1016/j.tibs.2010.02.005.
- 11. Freeman BC, Morimoto RI. 1996. The human cytosolic molecular chaperones hsp90, hsp70 (hsc70) and hdj-1 have distinct roles in recognition of a non-native protein and protein refolding. EMBO J 15:2969–2979.
- 12. Borkovich KA, Farrelly FW, Finkelstein DB, Taulien J, Lindquist S.

- 1989. Hsp82 is an essential protein that is required in higher concentrations for growth of cells at higher temperatures. Mol Cell Biol 9:3919–3930.
- 13. **Donnelly A, Blagg BSJ.** 2008. Novobiocin and additional inhibitors of the Hsp90 C-terminal nucleotide-binding pocket. Curr Med Chem 15:2702–2717. http://dx.doi.org/10.2174/092986708786242895.
- Richter K, Muschler P, Hainzl O, Buchner J. 2001. Coordinated ATP hydrolysis by the Hsp90 dimer. J Biol Chem 276:33689–36696. http://dx .doi.org/10.1074/jbc.M103832200.
- 15. Panaretou B, Prodromou C, Roe SM, O'Brien R, Ladbury JE, Piper PW, Pearl LH. 1998. ATP binding and hydrolysis are essential to the function of the Hsp90 molecular chaperone *in vivo*. EMBO J 17:4829–4836. http://dx.doi.org/10.1093/emboj/17.16.4829.
- Ali MMU, Roe SM, Vaughan CK, Meyer P, Panaretou B, Piper PW, Prodromou C, Pearl LH. 2006. Crystal structure of an Hsp90-nucleotidep23/Sba1 closed chaperone complex. Nature 440:1013–1017. http://dx .doi.org/10.1038/nature04716.
- Richter K, Reinstein J, Bucher J. 2002. N-terminal residues regulate the catalytic efficiency of the Hsp90 ATPase cycle. J Biol Chem 277:44905– 44910. http://dx.doi.org/10.1074/jbc.M208457200.
- Obermann WMJ, Sondermann H, Russo AA, Pavletich NP, Hartl FUJ. 1998. In vivo function of Hsp90 is dependent on ATP binding and ATP hydrolysis. J Cell Biol 143:901–910. http://dx.doi.org/10.1083/jcb.143.4.901.
- Louvion JF, Abbas-Terki T, Picard D. 1998. Hsp90 is required for pheromone signaling in yeast. Mol Biol Cell 9:3071–3083. http://dx.doi.org/10.1091/mbc.9.11.3071.
- Hainzl O, Lapina MC, Buchner J, Richter K. 2009. The charged linker region is an important regulator of Hsp90 function. J Biol Chem 284: 22559–22567. http://dx.doi.org/10.1074/jbc.M109.031658.
- Meyer P, Prodromou C, Hu B, Vaughan C, Roe SM, Panaretou B, Piper PW, Pearl LH. 2003. Structural and functional analysis of the middle segment of hsp90: implications for ATP hydrolysis and client protein and cochaperone interactions. Mol Cell 11:647–658. http://dx.doi.org/10.1016/S1097-2765(03)00065-0.
- 22. Panaretou B, Siligardi G, Meyer P, Maloney A, Sullivan JK, Singh S, Millson SH, Clarke PA, Naaby-Hansen S, Stein R, Cramer R, Mollapour M, Workman P, Piper PW, Pearl LH, Prodromou C. 2002. Activation of the ATPase activity of hsp90 by the stress-regulated cochaperone Ahal. Mol Cell 10:1307–1318. http://dx.doi.org/10.1016/S1097-2765(02)00785-2.
- 23. Sato S, Fujita N, Tsuruo T. 2000. Modulation of Akt kinase activity by binding to Hsp90. Proc Natl Acad Sci U S A 97:10832–10837. http://dx.doi.org/10.1073/pnas.170276797.
- Soti C, Vermes A, Haystead TAJ, Csermely P. 2003. Comparative analysis of the ATP-binding sites of Hsp90 by nucleotide affinity cleavage: a distinct nucleotide specificity of the C-terminal ATP-binding site. Eur J Biochem 270: 2421–2428. http://dx.doi.org/10.1046/j.1432-1033.2003.03610.x.
- Prodromou C, Siligardi G, O'Brien R, Woolfson DN, Regan L, Panaretou B, Ladbury JE, Piper PW, Pearl LH. 1999. Regulation of Hsp90 ATPase activity by tetratricopeptide repeat (TPR)-domain co-chaperones. EMBO J 18:754–762. http://dx.doi.org/10.1093/emboj/18.3.754.
- Scheufler C, Brinker A, Bourenkov G, Pegoraro S, Moroder L, Bartunik H, Hartl FU, Moarefi I. 2000. Structure of TPR domain-peptide complexes: critical elements in the assembly of the Hsp70-Hsp90 multichaperone machine. Cell 101:199–210. http://dx.doi.org/10.1016/S0092-8674(00)80830-2.
- 27. Zhao R, Davey M, Hsu YC, Kaplanek P, Tong A, Parsons AB, Krogan N, Cagney G, Mai D, Greenblatt J, Boone C, Emili A, Houry WA. 2005. Navigating the chaperone network: an integrative map of physical and genetic interactions mediated by the HSP90 chaperone. Cell 120:715–727. http://dx.doi.org/10.1016/j.cell.2004.12.024.
- McClellan AJ, Xia Y, Deutschbauer AM, Davis RW, Gerstein M, Frydman J. 2007. Diverse cellular functions of the HSP90 molecular chaperone uncovered using systems approaches. Cell 131:121–135. http://dx.doi.org/10.1016/j.cell.2007.07.036.
- Dote H, Burgan WE, Camphausen K, Tofilon PJ. 2006. Inhibition of hsp90 compromises the DNA damage response to radiation. Cancer Res 66:9211–9220. http://dx.doi.org/10.1158/0008-5472.CAN-06-2181.
- 30. Quanz M, Herbette A, Sayarath M, de Koning L, Dubois T, Sun JS, Dutreix M. 2012. Heat shock protein 90α (Hsp90α) is phosphorylated in response to DNA damage and accumulates in repair foci. J Biol Chem 287:8803–8815. http://dx.doi.org/10.1074/jbc.M111.320887.
- 31. Zaidi S, McLaughlin M, Bhide SA, Eccles SA, Workman P, Nutting CM,

- Huddart RA, Harrington KJ. 2012. The HSP90 inhibitor NVP-AUY922 radiosensitizes by abrogation of homologous recombination resulting in mitotic entry with unresolved DNA damage. PLoS One 7:e35436. http://dx.doi.org/10.1371/journal.pone.0035436.
- 32. Noguchi M, Yu D, Hirayama R, Ninomiya Y, Sekine E, Kubota N, Ando K, Okayasu R. 2006. Inhibition of homologous recombination repair in irradiated tumor cells pretreated with Hsp90 inhibitor 17-allylamino-17-demethoxygeldanamycin. Biochem Biophys Res Commun 351:658–663. http://dx.doi.org/10.1016/j.bbrc.2006.10.094.
- Nathan DF, Vos MH, Lindquist S. 1997. In vivo functions of the Saccharomyces cerevisiae Hsp90 chaperone. Proc Natl Acad Sci U S A 94:12949– 12956. http://dx.doi.org/10.1073/pnas.94.24.12949.
- 34. Louvion JF, Warth R, Picard D. 1996. Two eukaryote-specific regions of Hsp82 are dispensable for its viability and signal transduction functions in yeast. Proc Natl Acad Sci U S A 93:13937–13942. http://dx.doi.org/10.1073/pnas.93.24.13937.
- Nathan DF, Lindquist S. 1995. Mutational analysis of Hsp90 function: interactions with a steroid receptor and a protein kinase. Mol Cell Biol 15:3917–3925.
- 36. Achanta SS, Varunan S, Bhattacharyya S, Bhattacharyya MK. 2012. Characterization of Rad51 from apicomplexan parasite *Toxoplasma gondii*: an implication for inefficient gene targeting. PLoS One 7:e41925. http://dx.doi.org/10.1371/journal.pone.0041925.
- Longtine MS, McKenzie A, III, Demarini DJ, Shah NG, Wach A, Brachat A, Philippsen P, Pringle JR. 1998. Additional modules for versatile and economical PCR-based gene deletion and modification in Saccharomyces cerevisiae. Yeast 14:953–961. http://dx.doi.org/10.1002/(SICI) 1097-0061(199807)14:10<953::AID-YEA293>3.0.CO;2-U.
- 38. Laskar S, Bhattacharyya MK, Shankar R, Bhattacharyya S. 2011. *HSP90* controls *SIR2* mediated gene silencing. PLoS One 6:e23406. http://dx.doi.org/10.1371/journal.pone.0023406.

- 39. Taipale M, Jarosz DF, Lindquist S. 2010. HSP90 at the hub of protein homeostasis: emerging mechanistic insights. Nat Rev Mol Cell Biol 11: 515–528. http://dx.doi.org/10.1038/nrm2918.
- Zhang H, Burrows F. 2004. Targeting multiple signal transduction pathways through inhibition of Hsp90. J Mol Med 82:488–499. http://dx.doi.org/10.1007/s00109-004-0549-9.
- 41. Mimnaugh EG, Xu W, Vos M, Yuan X, Isaacs JS, Bisht KS, Gius D, Neckers L. 2004. Simultaneous inhibition of hsp90 and the proteasome promotes protein ubiquitination, causes endoplasmic reticulum-derived cytosolic vacuolization, and enhances antitumor activity. Mol Cancer Ther 3:551–566. http://dx.doi.org/10.4161/cbt.3.6.846.
- 42. Ravid T, Hochstrasser M. 2007. Autoregulation of an E2 enzyme by ubiquitin–chain assembly on its catalytic residue. Nat Cell Biol 9:422–427. http://dx.doi.org/10.1038/ncb1558.
- 43. Prodromou C, Panaretou B, Chohan S, Siligardi G, O'Brien R, Ladbury JE, Roe SM, Piper PW, Pearl LH. 2000. The ATPase cycle of Hsp90 drives a molecular 'clamp' via transient dimerization of the N-terminal domains. EMBO J 19:4383–4392. http://dx.doi.org/10.1093/emboj/19.16.4383.
- 44. DeZwaan DC, Toogun OA, Echtenkamp FJ, Freeman BC. 2009. The Hsp82 molecular chaperone promotes a switch between unextendable and extendable telomere states. Nat Struct Mol Biol 16:711–716. http://dx.doi.org/10.1038/nsmb.1616.
- 45. Echtenkamp FJ, Zelin E, Oxelmark E, Woo JI, Andrews BJ, Garabedian M, Freeman BC. 2011. Global functional map of the p23 molecular chaperone reveals an extensive cellular network. Mol Cell 43:229–241. http://dx.doi.org/10.1016/j.molcel.2011.05.029.
- Sun L, Prince T, Manjarrez JR, Scroggins BT, Matts RL. 2012. Characterization of the interaction of Aha1 with components of the Hsp90 chaperone machine and client proteins. Biochim Biophys Acta 1823:1092–1101. http://dx.doi.org/10.1016/j.bbamcr.2012.03.014.

# Role of Hsp90 in Rad51 mediated DNA repair

## **ORIGINALITY REPORT**

SIMILARITY INDEX

17%

9%

2%

INTERNET SOURCES

**PUBLICATIONS** 

STUDENT PAPERS

## PRIMARY SOURCES

ec.asm.org Internet Source

Suhane, Tanvi, Shyamasree Laskar, Siddheshwari Advani, Nabamita Roy, Shalu Varunan, Dibyendu Bhattacharyya, Sunanda Bhattacharyya, and Mrinal Kanti Bhattacharyya. "Both the Charged Linker Region and ATPase Domain of Hsp90 Are Essential for Rad51-Dependent DNA Repair", Eukaryotic Cell, 2015. Publication

Submitted to University of East London Student Paper

bioinfopublication.org Internet Source

Pennisi, Rosa, Paolo Ascenzi, and Alessandra 5 di Masi. "Hsp90: A New Player in DNA Repair?", Biomolecules, 2015.

Publication

simms.library.sc.edu Internet Source

